DOCTOR OF PHILOSOPHY

The role of the BARD1 BRCT domains in the DNA damage response

Kaufmann, Aisling

Award date:
2014

DOCTOR OF PHILOSOPHY

The role of the BARD1 BRCT domains in the DNA damage response

Aisling Kaufmann

2014

University of Dundee

The role of the BARD1 BRCT domains in the DNA damage response

By

Aisling Kaufmann

Thesis submitted for the degree of

Doctor of Philosophy

University of Dundee

March 2014

Table of contents

List of figures

List of Tables

Abbreviations

53BP1;	Tumor suppressor p53-binding protein 1
ATM;	Ataxia telangiectasia mutated
ATP;	Adenosine triphosphate
BARD1;	BRCA1 Associated RING Domain 1
BIR;	Break Induced Replication
BLM;	Bloom Syndrome Protein
BRCA1;	Breast cancer type 1 susceptibility protein
BRCA2;	Breast cancer type 2 susceptibility protein
BRCC36;	BRCA1/BRCA2-containing complex subunit 36
BRCT;	BRCA1 C Terminus (domain)
BrdU;	Bromodeoxyuridine
BRE;	Brain And Reproductive Organ-Expressed Protein
CDK;	Cyclin-dependent kinase
CHD4;	Chromodomain-helicase-DNA-binding protein 4
CS;	Chicken Serum
CSR;	Class Switch Recombination
CstF;	Cleavage stimulation factor
CtIP;	CtBP-interacting protein
DDR;	DNA Damage Response
dHJ;	Double Holliday Junction
DMEM;	Dulbecco's Modified Eagle Medium
DNA;	Deoxyribonucleic acid
DSB;	Double-stranded Break
DSBR;	Double Strand Break Repair

DSP; Dithiobis[succinimidyl propionate]

DTT; Dithiothreitol

DUB; Deubiquitinating enzyme

EDTA; Ethylenediaminetetraacetic acid

EGTA; Ethylene glycol tetraacetic acid

ERCC1; DNA excision repair protein ERCC-1

FA; Fanconi Anaemia

FACS; Fluorescence-activated cell sorting

FANCJ; Fanconi anemia complementation group J

FANCM; Fanconi anemia complementation group M

FHA; Forkhead-associated (domain)

HCL; Hydrochloric acid

HECT; Homologous to the E6AP carboxyl terminus (domain)

HERC2; HECT And RLD Domain Containing E3 Ubiquitin Protein Ligase 2

HJ; Holliday Junction

HR; Homologous Recombination

HU; Hydroxy Urea

IR; Ionizing Radiation

IRIF; Ionizing Radiation Induced Foci

kDa; Kilo Dalton

LB; Lysogeny Broth

MCPH1; Microcephalin 1

MDC1; Mediator of DNA damage checkpoint protein 1

MERIT40; Mediator of RAP80 interactions and targeting subunit of 40 kDa

$MgCl_2$; Magnesium Chloride

MMEJ; Microhomology-Mediated End Joining

MPW; Millipore water

MRE11; Meiotic recombination 11 homolog 1

MRN; MRE11-RAD50-NBS1

NAOH; Sodium Hydroxide

NBS1; Nijmegen breakage syndrome protein 1

NES; Nuclear export Signal

Nf-kB; Nuclear factor of kappa light polypeptide gene enhancer in B-cells 1

NHEJ; Non-Homologous End Joining

NLS; Nuclear localisation signal

NSC; Non-Specific Control

o/n; over night

OD; Optical Density

P53; Cellular tumor antigen p53

PAGE; Polyacrylamide gel electrophoresis

PARG; Poly(ADP-ribose) glycohydrolase

PARP; Poly (ADP ribose) polymerase

PBS; Phosphate Buffered Saline

PCR; Polymerase Chain Reaction

PCV; Packed Cell Volume

PI; Propidium Iodide

PMSF; Phenylmethanesulfonyl fluoride

PTM; Post Translational Modification

PVDF; Polyvinylidene Difluoride

RAP80; Receptor-associated protein 80

RB;	Retinoblastoma
Rev1;	DNA repair protein REV1
RING;	Really Interesting New Gene
RNA pol II;	RNA polymerase II
RNA;	Ribonucleic acid
RNF168;	RING finger protein 168
RNF2;	RING finger protein 2
RNF8;	RING finger protein 8
ROI;	Region of Interest
RPA;	Replication Protein A
RPM;	Revolutions Per Minute
RT;	Room Temperature
SD;	Standard Deviation
SDSA;	Synthesis Dependent Strand Annealing
Spo11;	Sporulation-specific protein 11
SSA;	Single Strand Annealing
ssDNA;	single stranded DNA
STAT1;	Signal Transducer And Activator Of Transcription 1
TE;	Tris-EDTA
TopBP1;	DNA Topoisomerase II-Binding Protein 1
TOPOIIIα;	Topoisomerase IIIα
UIM;	Ubiquitin Interacting Motif
XP;	Xeroderma pigmentosum

Declaration

The work described here was undertaken in the Cancer division of the Medical Research Institute in the University of Dundee from October 2010 to September 2013, and was funded by the Dundee Cancer Campaign.

I hereby declare that this dissertation is based on results carried out by myself. Work other than my own is clearly indicated in the text by reference to the relevant researchers or to their publications. This dissertation has not in whole, or in part, been previously submitted for a higher degree.

Aisling Kaufmann

Prof. Kevin Hiom

Acknowledgements

I have received unrelenting advice and support from many people during my PhD and I would like to take this opportunity to thank them all.

First and foremost, I would like to thank Conor, Maggy and Anne for all the technical advice and help they have given me but also for being amazing people to work with. Thank you for brightening up my days and for all the laughs. A special thank you, for helping me through some difficult times and pushing me up the hill. I would also like to thank Jane for her support and humour.

To my family, thank you so much for always being there for me whether it was advice, support or just to listen. I might have some time soon to visit everyone. Thanks to all my friends in Ninewells, I couldn't have hoped for a nicer place to work.

I would like to acknowledge and thank Kevin for giving me the opportunity to carry out my PhD in his Lab. Your door was always open. Another thank you to Gareth for being a supportive second supervisor. I would also like to acknowledge the Mass spec and Microscopy departments in Ninewells and in the College of Life Sciences Dundee for providing great services and taking the time to help whenever needed.

Finally I would like to thank Chris. Thank you grounding me and making coming home after a hard day's work so enjoyable. Thank you for your belief, support and keeping me smiling.

Abstract

The DNA within a cell is damaged on a continuous basis by both endogenous and exogenous agents. One of the most dangerous types of damage a cell can incur are DNA Double stranded breaks (DSBs) as failure to repair these types of lesions can lead to mutations, cell death and cancer. In order to maintain genome integrity, cells have several different mechanisms to repair various types of DNA damage. BRCA1 is a tumour suppressor gene commonly mutated in many inherited breast and ovarian cancers. BRCA1 is fundamental to the repair to DNA damage especially the faithful repair of DSB by homologous recombination (HR) as loss of BRCA1 results in aberrant HR, chromosomal translocation and cancer. BRCA1 is almost always found in the nucleus bound to BARD1. BARD1 retains BRCA1 in the nucleus and enhances the E3 ubiquitin ligase function of BRCA1. The importance of BRCA1 in the repair of DNA DSBs has been extensively researched, however the role of BARD1 in repair remains unknown.

Similar to BRCA1, BARD1 contains tandem BRCT domains at its C-terminus which are important for binding phosphorylated proteins involved in DNA repair. Mutations in the BARD1 BRCT domains have been discovered in a few breast and ovarian cancers which suggested that BARD1 is important in the DNA damage response (DDR) independent of its function in stabilising BRCA1. Loss of the BARD1 BRCT domains also results in a decrease in the ability of cells to carry out HR. This thesis examines the contribution of the BARD1 BRCT domains to the repair of DNA DSBs. Using homologous recombination assays and colony survival assays, *Bard1* DT40 cells reconstituted with BARD1ΔBRCT showed a significant decrease in their ability to carry out HR and were also extremely sensitive to PARP inhibitors suggesting that the BARD1 BRCT domains do indeed play an important role in HR. Work carried out in this thesis suggests that BARD1 contributes to the stabilisation of the BRCA1-C complex which is important in the repair of DSBs. The BARD1 BRCT domains also showed defects in localisation and delayed recruitment to sites of damage. The defects

in HR and localisation seen in the absence of the BARD1 BRCT domains potentially implicate a functional role for the BARD1 BRCT domains in DSB repair. Potential BARD1 BRCT domain interacting proteins were also identified my Mass spec, which may shed some light onto the functional role of BARD1 in DNA repair.

Chapter 1 Introduction

1.1 Maintaining genome integrity and the DNA damage response.

Maintaining genome integrity is crucial to the function and survival of the cell. This concept refers to the ability of the cell to conserve and protect the information stored in its genome and to faithfully pass its genomic content on to daughter cells. DNA damage represents a continuous threat to genomic integrity. DNA can be damaged by a host of endogenous and exogenous agents such as metabolic by-products, errors in replication and toxins. Failure to repair DNA damage correctly can lead to cell death and mutations in the DNA which may result in the development of disease and cancer. Without an appropriate response to DNA damage, the survival of the cell and organism is under great threat.

In order to maintain genomic integrity cells carry out an intricate response to DNA damage termed the DNA damage response (DDR). The cellular response to DNA damage involves collaborative events which allow the repair of damage, cell cycle checkpoint control and apoptosis [1-3]. DNA repair pathways are responsible for maintaining genome integrity by actively repairing a variety of different types of lesions. The regulation of cell cycle progression is equally important in the DDR as inducing an arrest in the cell cycle allows the cell time to repair the damage and prevents replication of damaged DNA. Apoptosis is required to eliminate cells containing DNA damage which are beyond repair. Each of these processes relies on a large number of proteins which are involved in several molecular pathways and together they are known as the DDR. Defects in the DDR machinery contribute to a variety of diseases and cancer which highlights the importance of the DDR in the maintenance of genomic integrity [1]. Some of the best characterised diseases associated with DDR defects are Fanconi anaemia (FA) and Xeroderma Pigmentosum (XP).

1.2 DNA double strand break repair

DNA double strand breaks (DSBs) are one of the most dangerous types of lesions a cell can incur, potentially driving genetic instability leading to cell death or carcinomas. Even as little as one unrepaired DSB is sufficient to cause apoptosis [4] and is often associated with large chromosomal translocations and rearrangements [5]. DNA DSBs are lesions that occur when both strands of a DNA duplex are broken in close proximity to each other. Although DSB are commonly associated with normal reactions and processes that occur in the cell such as metabolic by products and collapsed replication forks [6, 7], they can also be induced by exogenous agents such as ionizing radiation and DNA crosslinking reagents. DSBs are also induced by the cell in a controlled manner in order to facilitate rearrangement of immunoglobulin loci in B-cell and T-cell receptors in process such as V(D)J and class switch recombination (CSR) in lymphocytes [8-11]. Moreover, failure to repair DSB is extremely toxic to cells and is considered to be a major driver in cancer [1].

In order to repair DSB, cells have evolved several pathways to repair these lesions. In eukaryotes, DSBs are repaired by two major pathways, Non-homologous end joining (NHEJ) and Homologous recombination (HR). These two repair processes are implemented at different stages in the cell cycle. NHEJ repairs the DNA DSB by the direct ligation of broken ends back together irrespective of their sequence. Although NHEJ is the more simplistic method of DSB repair, it is also error prone [12]. HR is an error free pathway used to repair DNA DSB. During the repair of a DSB a sister chromatid is used as a template to repair the damage. NHEJ can repair DSB at all stages throughout the cell cycle as it is not restricted by any particular cell cycle stage [12]. Although NHEJ is active throughout the cell cycle and favoured in G1, HR is more prevalent after DNA replication. HR is however restricted to late S and G2 phases of the cell cycle as this mechanism of repair requires the presence of a sister chromatid for repair. A schematic representation of the phases of the cell cycle where HR and NHEJ are active can be seen in figure 1.1.

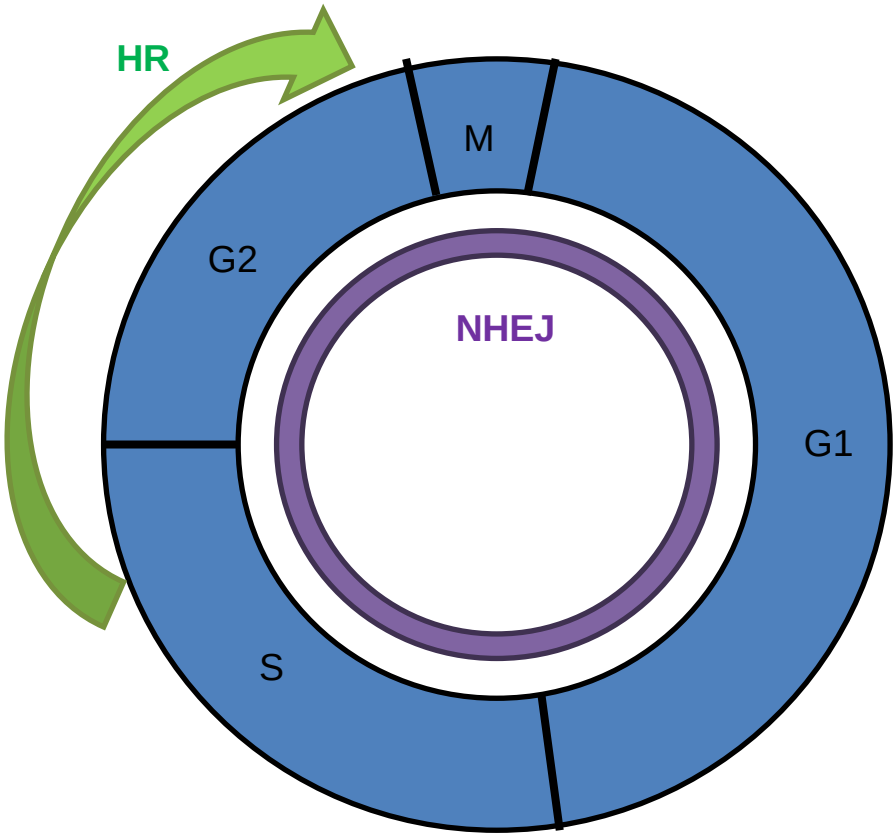

Figure 1.1 HR and NHEJ activity through the cell cycle
Representative image reflecting the type of repair carried out at different stages of the cell cycle. NHEJ is available for use throughout the cell cycle whereas HR is predominantly used in late S and G2 phase due to the requirement of a homologous template for repair, usually in the form of a sister chromatid.

1.2.1 DSB repair by NHEJ

The structure and base pair composition of DNA DSB ends vary depending on the method of damage and it is important for the cell to be able to process and repair diverse structural DSB ends to maintain genome stability. Unlike the majority of repair and recombination pathways, NHEJ evolved in both prokaryotic and eukaryotic cells in a manner which allowed mechanistic flexibility and enzyme multifunctionality [13-15]. These characteristics attributed to NHEJ repair, enables the repair of a DSB with a remarkable degree of structural tolerance to the diverse range of substrate DNA ends at DSBs. NHEJ requires a nuclease, to resect the damaged DNA, a polymerase, to synthesise nucleotides to bridge the gap at the break and a ligase to anneal the broken

strands together. The nucleases, polymerases and ligases which act in DSB repair by NHEJ are considered to be the most mechanistically flexible and multifunctional enzymes of their kind [15] as they can act in any order and can function independently at either side of the DSB.

NHEJ is active throughout the cell cycle and is favoured in G1 phase cells. NHEJ promotes the direct ligation of DSBs, in an error prone manner often leading to small insertions, deletions and chromosomal translocations if DSBs are joined from different parts of the genome [12]. As both HR and NHEJ are active during S and G2 phases of the cell cycle, the mechanisms which determine the choice of repair is still an active area of research. NHEJ is however very important in the repair of DSBs as NHEJ defective cells are extremely sensitive to IR [16] and exhibit severe combined immunodeficiency [17] due to its role in V(D)J and class switch recombination in lymphocytes. NHEJ is important for restoring molecular integrity to the cell after DNA damage but not sequence information.

NHEJ is conserved from bacteria to humans [18] and involves the recognition, end processing and ligation of a DSB. Although classical NHEJ is preferentially used when available, there is a second, back up, end joining pathway called Microhomology-mediated end joining (MMEJ) which has been shown to be active when cells are defective in both HR and NHEJ [19-21]. Mechanistically the binding of Ku to DSB is believed to initiate NHEJ in vertebrates [12]. Ku is predicted to be the initial protein to bind DSBs due to its abundance in the cell (estimated at 400,000 molecules/cell). Ku has also been shown to have the greatest affinity towards DNA ends in comparison to other DNA binding proteins in the cell [22]. Ku forms a toroidal heterodimer consisting of the Ku70 and Ku80 proteins which contains a hole large enough to encompass the DNA end [23]. *deVries et al* demonstrated that Ku can only load onto the DNA terminus and from there it can migrate to a more internal position on the DNA duplex [24]. The Ku heterodimer has no confirmed enzymatic activity and is predicted to provide a docking platform for NHEJ proteins, stabilising them and allowing them to carry out

their repair functions [25]. Once Ku is bound to the DNA it recruits the catalytic subunit of the DNA protein kinase (DNA-PKcs) to form an active DNA-PK holoenzyme [26]. This active kinase complex phosphorylates other proteins involved in the repair of DSB by NHEJ such as XLF, DNA ligase IV, XRCC4 and RPA2 as well as autophosphorlyating the DNA-PKcs [27-30]. The autophosphorylation of DNA-PKcs results in a structural change in the holoenzymes which is believed to facilitate DNA end processing [25]. In vertebrates, the majority of DNA end processing in NHEJ is carried out by Artemis, which forms a complex with the DNA-PKcs [31, 32]. Polymerisation or filling in the gap after end processing can be carried out by a variety of polymerases such as DNA polymerases X, theta and mu [33]. XRCC4, DNA ligase IV and XLF are the ligases responsible for covalently ligating the two DNA ends together [34, 35].

Recent findings implicated an alternative end joining pathway in the repair of DSBs [19, 21], called MMEJ. One of the most distinguishing properties of MMEJ is the use of short (5-25 base pairs) microhomologous sequences for aligning the broken strands before ligation of a DSB. This mechanism of end joining results in deletions around the DSB and has been associated with chromosome abnormalities such as translocations and rearrangements [20, 36-38]. Its mutagenic potential has also been demonstrated in disease and cancer [20, 39, 40]. Although there is very little understanding on the mechanism of MMEJ, it is proposed to involve strand resection and end processing to reveal small complimentary sequences followed by pairing of the microhomologous regions, flap removal and ligation. It is dependent on Mre11 and CtIP for end resection [41, 42], XPF and ERCC1 for cleaving the DNA flaps from the annealed intermediated [41, 43, 44]. DNA ligase I and III are involved in the ligation of DSBs by MMEJ in humans [45]. Due to the fact that MMEJ is exclusively mutagenic, it only occurs in very low frequencies in NHEJ competent cells. Although it is considered to be mainly a backup repair pathway there is evidence suggesting that MMEJ is

important for the repair of DSBs when HR is not active and the structure of the DSBs are not compatible with classical NHEJ [41].

Even with the potential to be error prone, both NHEJ and MMEJ pathways serve to protect the integrity of the genome by efficient and quick repair of hazardous DSBs. A representative image of the molecular mechanisms of both NHEJ and MMEJ can be seen in figure 1.2.

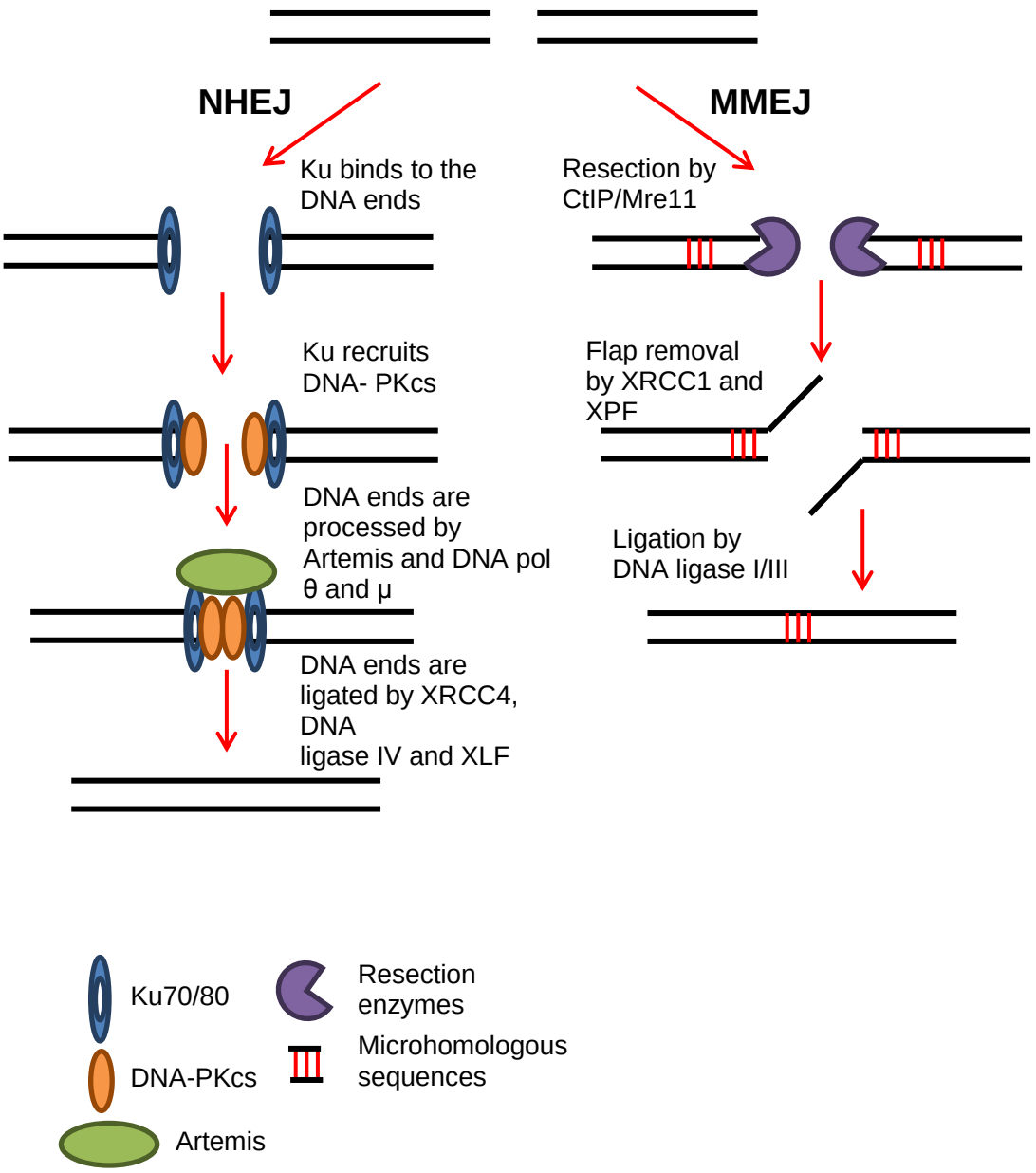

Figure 1.2 Mechanism of end-joining repair NHEJ and MMEJ
Representative illustration of the repair of a DSB by NHEJ and MMEJ. During NHEJ the Ku heterodimer binds the DSB and recruits DNA-PKcs. The DNA ends are processed by Artemis and DNA Polymerases and then ligated. Sequence is often lost during NHEJ making it an error prone process. In MMEJ the DSB ends are resected to reveal microhomologous sequences which are joined together. The overhanging DNA flaps are cleaved and the process is completed by ligation. MMEJ is exclusively mutagenic as a result.

1.2.2. DSB repair by HR

Homologous recombination is a more accurate DSB repair pathway which uses a homologous template to accurately repair damage. As previously mentioned, HR is only active during S and G2 phase of the cell cycle as it requires an identical template in the form of a sister chromatid to carry out faithful repair [16]. A sister chromatid is only available after replication during S and G2 phase. HR is not only vital for the repair of DSBs but also for interstrand crosslink repair, repair of DNA gaps, rescue of stalled or collapsed replication forks and meiotic chromosome segregation. The ultimate goal of HR repair is to retrieve information from an undamaged homologous DNA sequence to aid the repair of a DNA molecule which has lost sequence information as a result of a break in both strands of the DNA. This process requires the interaction of a damaged DNA sequence with a homologous undamaged DNA sequence. It has become evident that HR is a major contributor to the maintenance of genome stability as defects in the HR machinery can lead to disease, genome instability and cancer [8].

In 1964, Robin Holliday made a major breakthrough in the understanding of HR repair. He proposed a model to explain meiotic recombination which introduced the concept of the exchange of genetic material between homologous chromosomes through the formation of a Holliday junction (HJ) [46, 47]. Although the HJ model provided a basic understanding of recombination, it was unable to explain all HR scenarios and as a result, new adapted models of HR emerged. Several models have been proposed in the repair of DSB by HR: the synthesis dependent strand annealing (SDSA) model [48, 49], the Szostak model or more commonly known as the double strand break repair (DSBR) model [50] and the break induced replication (BIR) model [51] (figure 1.3). The process of HR can be divided into three main steps: pre-synapsis, synapsis and post-synapsis. The initial pre-synaptic phase involves the processing of the DNA ends and the loading of RAD51 onto the DNA. During synapsis, homology search and strand invasion is carried out resulting in the formation of a D-Loop intermediate. Post synapsis involves the synthesis of DNA from the template DNA at

the broken ends. All three HR models share the same pre-synaptic and synaptic mechanisms and only diverge during post-synapsis resulting in a variety of different crossover and non-crossover events.

Pre-Synapsis

Our current understanding of HR in higher eukaryotic cells indicates that HR is initiated by the formation of a DSB which is first recognised by the MRN complex. The MRN complex consists of the core proteins MRE11, RAD50 and NBS1 [52]. The MRN complex is involved in the initial processing of DNA DSBs. MRE11 and RAD50 are believed to be important for bridging two DNA ends through the coiled coil domain of RAD50 [53]. As well as the binding and bridging functions of the MRN complex, it also functions as an endonuclease and a 3'-5' exonuclease at DSBs. This function is attributed to the MRE11 protein (reviewed in [52]). The enzymatic activities of MRE11 have been shown to be stimulated by RAD50 and NBS1 in an ATP dependent manner [54]. The MRN complex also plays an important role in recruiting major HR repair proteins and signalling factors to sites of damage. In order to resect DNA and generate a 3' overhang which is required for HR, the MRN complex interacts with CtIP [55]. The MRN complex and CtIP are responsible for generating long range 5'-3' end resection which results in a 3' overhang, an essential intermediate in HR. The single stranded 3' overhangs are then coated with RPA (Replication protein A) [56] which initiates the next stage in HR called synapsis. The binding of RPA to ssDNA forms a nucleoprotein filament which stabilises and prevents the formation of DNA secondary structures which may interfere with the mechanism of HR.

Synapsis

During synapsis, the RAD51 protein carries out homology search and DNA strand invasion. In order for RAD51 to perform its function, it must first displace RPA from the ssDNA. RPA has been shown to have a higher affinity for ssDNA in comparison to RAD51 and RAD51 is unable to displace RPA *in vitro*. In order for HR to proceed,

recombination mediators help RAD51 displace RPA from the ssDNA. In yeast, RAD52 and RAD51 paralogues (RAD55 and RAD57) are recombination mediators which can overcome the inhibitory effects of RPA on RAD51 [57-60]. BRCA2 and RAD51 paralogues have been shown to play a similar recombination mediator role in vertebrates [61, 62]. Once RPA is displaced by RAD51, RAD51 forms long helical polymers which tightly wrap around the single stranded 3' overhang referred to as RAD51 nucleoprotein filament. This filament is responsible for binding to and invading a homologous DNA molecule ultimately forming a heteroduplex DNA (D-loop) structure. The ssDNA within the nucleoprotein filament is stretched which greatly facilitates fast and efficient homology search [63, 64]. The exact mechanism of homology search and strand invasion remains unclear. However when the D-loop is formed, a RAD51-dsDNA filament is formed which accommodates both the invading and donor DNA strands generating a template in which to repair the broken DNA end. DNA synthesis after D-loop formation extends the 3' annealed end using the homologous strand as a template. It is unclear which polymerases are responsible for D-loop extension. Post-synapsis will be discussed in relation to the three main subgroups of HR. It is important to note that resolution of D-loops forming non-crossover products is preferential in maintaining genome integrity.

Synthesis dependent strand annealing (SDSA) model

During the SDSA HR pathway the invading strand of the DSB is extended by repair synthesis. After repair synthesis, the invading strand is displaced from the homologous template. The invading strand then anneals to the 3' end of the original DSB. The repaired strand is then used as a further template to repair the second 3' resected DSB end. The process is completed by ligation. As a result, SDSA avoids the formation of crossovers products reducing the possibility of genomic rearrangements.

DNA Double strand break repair (DSBR) model

The DSBR branch of HR proceeds after the initial strand invasion by engaging the second end of the DSB. This can occur by either second end capture through DNA annealing or by invading the homologous template for a second time. Annealing of the second end of the DSB to the template DNA involves the protein RAD52 [65]. The DSBR model uses a two ended strand invasion mechanism which results in the formation of a double Holliday junction (dHJ). The dHJ is a substrate for both crossover and non-crossover products by BLM-TOPOIIIα and other structure specific endonucleases. Resolvase A activity, which has a similar specificity for HJ as bacterial RuvC, has been identified in mammalian cell extracts and appears to be responsible for cleaving HJ forming both crossover and non-crossover products [66]. On the other hand, the combined action of BLM DNA helicase and TOPOIIIα and their cofactor BLAP75/Rmi1 has been shown to process the dissolution of HJ into non-crossover products. BLM is believed to migrate the two junctions towards one another where TOPOIIIα separates them resulting in non-crossover products [67-69]. This in part explains why cells from patients with defective BLM helicase show an increase in sister chromatid exchange [67].

Break induced replication (BIR) model

The BIR pathway for HR repair of DSBs is employed when only one end of the DSB can engage in recombination. This can be as a direct result of a collapsed replication fork resulting in a single ended DSB, or if only one end of the DSB is homologous to the template [70, 71]. BIR is thought to be required to initiate replication at stalled and collapsed replication forks. As with both other models, BIR involves strand resection, invasion and homology search by RAD51, however the main difference is that only one strand is extended by DNA synthesis and the other strand is lost due to its absence or lack of homology with the template strand. The invading strand is postulated to form a replication fork, synthesising DNA until the end of the chromosome is reached [72].

This can often lead to loss of heterozygosity of any genetic information after the position of a DSB. Although BIR can involve large scale loss of genetic information, it does appear to be important in maintaining genomic integrity by alternative lengthening of telomeres and restarting collapsed replication forks. D-loops are resolved into non-crossover products in the BIR pathway.

1.2.3. DSB repair by Single strand annealing (SSA)

Single strand annealing of DSBs is considered to be an alternative mechanism in repairing DSB even though it technically is a form of HR. SSA repair occurs between direct repeats initiated by 5'-3' resection of a DSB end. During SSA the DSB ends are resected to expose complimentary repeats on both strands which are then ligated back together. Although this process shares similarities with MMEJ processing of DSB, resection during SSA can cover a large sequence to expose complimentary repeats. RAD52 is believed to be involved in the annealing of the repeats [73, 74]. ERCC1 and other SSA enzymes cleave the ssDNA flaps which form as a result of resection and annealing [74-76]. SSA results in deletions of sequence surrounding the DSB and is considered to be mutagenic in mammalian cells [72, 73]. However there is evidence suggesting that SSA is a frequent repair event between repetitive sequences which are abundant in the genome [77].

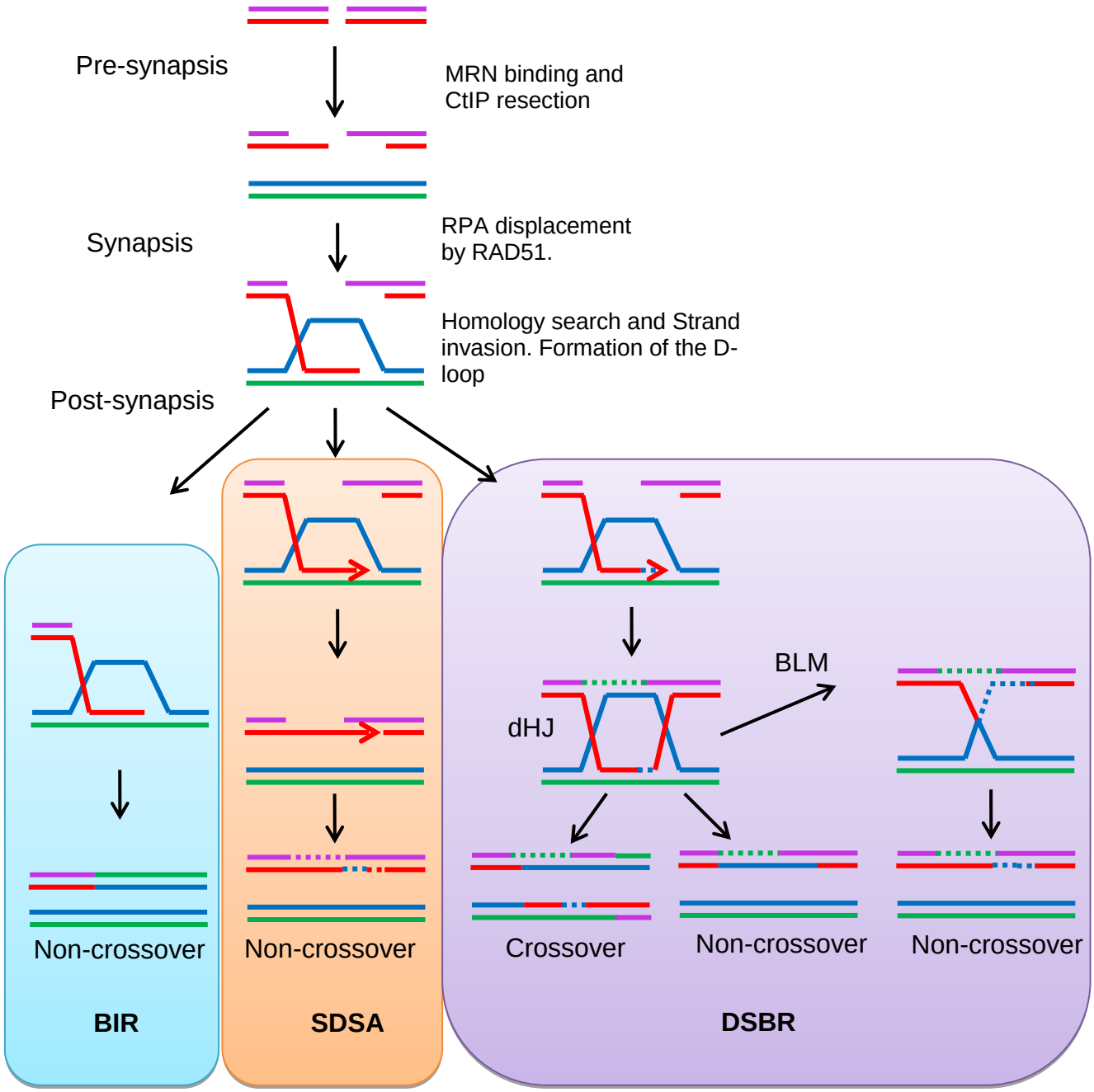

Figure 1.3 HR repair of DNA DSBs by BIR, SSDA and DSBR
Illustration of the repair of DSBs by different HR repair pathways. DSBs are recognised and resected by the MRN complex and CtIP. RPA binds with high affinity to the ssDNA. RAD51 displaces the RPA and carries out homology search and strand invasion in a homologous template leading to the formation of a D-loop. BIR, SSDA and DSBR pathways synthesize new DNA and resolve D-loop structures in different ways resulting in either crossover or non-crossover products after the repair of the DSBs. dHJ (double Holliday Junction), BLM (Blooms).

1.2.4 Regulation and DSB repair choice

The principle pathways to repair DNA DSBs are NHEJ, HR and SSA and the balance between them is highly dependent on cell type, species, cell cycle stage and the type of DNA damage. Regulation and the choice of DSB repair are fundamental to maintaining genome stability. Although NHEJ can lead to chromosomal translocations and loss of genomic information, it is important for B and T-cell development by class switch recombination and V(D)J recombination. When available, HR is the preferable repair pathway for DSB repair as it is considered to be error free. However tight regulation of HR is required as recombination can be harmful in certain situations like stalled replication forks where translesion synthesis is a safer method of repair. In certain genetic backgrounds, HR can generate nucleoprotein intermediates which results in a prolonged cell cycle arrest and even cell death [78-80]. It is also important to choose the correct type of HR repair in different circumstances and stages of the cell cycle. For example, HR repair by SDSA should be preferentially employed during mitosis to avoid crossover of genomic information and loss of heterozygosity.

One of the most evident types of regulation used in the choice of repair is demonstrated by the cell cycle. HR is restricted to the S and G2 phases of the cell cycle as a sister chromatid is required for repair and only available during the S and G2 phase. It has also become evident that transcription of HR genes and CDK mediated phosphorylation of HR proteins also restricts the HR process to the S and G2 phases of the cell cycle [81, 82]. Resection of DSB is required for the initiation of HR. CtIP is required for resection of DSB in mammalian cells and the protein levels of CtIP is reduced in G1 cells and greatly increased in S and G2 phases of the cell cycle which in turn regulates the amount of HR during the cell cycle [83].

Resection of a DNA DSB is fundamental to the commitment of repair by HR. DSB resection is highly regulated and low in G1 which favours NHEJ over HR repair at this stage in the cell cycle [84]. A major restriction point in the choice of repair in S and G2 phases of the cell cycle is the competition between end protection and resection

[85]. As previously mentioned the Ku heterodimer binds DNA ends with high affinity promoting NHEJ [12]. The combined action of the MRN complex and CtIP in humans and yeast is required for resection which promotes HR. DSB must be resected appropriately in the S and G2 stages of the cell cycle and cell cycle regulation of CtIP is paramount to the resection of DSB and initiation of HR. As well as CtIP protein degradation in G1, CDK phosphorylation of CtIP, which is required for MRN-CtIP complex formation, occurs in S/G2 phase [86, 87]. Resection is also negatively regulated by acetylation of CtIP [88, 89]. After DNA damage, CtIP is deactylated by SIRT6 as a means to promote HR [89]. The molecular mechanism by which MRN-CtIP displaces Ku from the DNA DSB end remains unclear. However recent studies of meiotic DSB repair in budding yeast has provided several insights into this process [90]. During meiotic recombination in yeast, Spo11 induces programmed DSB and remains covalently attached to the DSB. In order for 5'-3' resection to occur, Spo11 must be removed from the DSB end. Mre11 has been proposed to introduce an asymmetric endonucleolytic nick adjacent to Spo11 on the 5' DNA ends [90, 91] which is suggested to promote Exo1 dependent 5'-3' resection. Mre11 is responsible for 3'-5' degradation of the nicked strand to the DNA DSB end removing Spo11 [92]. It is possible that the same process is required in vertebrates using MRE11 and CtIP, however further evidence and study is required to investigate this possibility.

Regulation of RAD51 is another important factor in the control and choice of DSB repair. Regulation of RAD51 not only determines the type of repair used but it also prevents the use of HR when the effects may be detrimental to the cell as discussed earlier. Evidence from yeast suggests that Srs2 can counteract the function of RAD51 which is vital to the repair of DSB by HR. Biochemical studies revealed that Srs2 efficiently removes RAD51 filaments from DSB during pre-synapsis [93, 94]. The removal of RAD51 requires its interaction with Srs2 and is greatly enhanced in the presence of RPA preventing re-association of RAD51 with the DSB [93-97]. The interaction of Srs2 with RAD51 triggers the ATP hydrolysis of RAD51 which

destabilises the RAD51-DNA interaction [98]. To counteract this process and promote RAD51 filament formation on DSB ends, mediators of recombination, such as RAD55/RAD57, can suppress the action of Srs2 [99] and promote HR. There are no known human homologues of Srs2, however there are several human helicases predicted to have acquired a similar function. BLM and FANCJ have both been reported to contribute to the removal of RAD51 from DSBs [100, 101].

As discussed previously, BLM is important for resolving dHJ structures to prevent crossover events [67] during HR, maintaining genome integrity. The drosophila melanogaster BLM homologue, MUS-309, has also been shown to free the invading ssDNA tail from the D-loop promoting SDSA [102, 103]. In order to suppress crossovers in mitotic cells it is preferential to use SDSA over DSBR as SDSA results in non-crossover events. As well as BLM, FANCM in human cells has also been proposed to regulate HR by promoting SDSA [104].

RPA poses a major restriction to the implementation of HR as efficient displacement of RPA from ssDNA is required for RAD51 to bind and initiate strand invasion and homology search. RPA is an extra method of regulation of HR as it has a greater affinity for ssDNA than RAD51 and RAD51 can only displace RPA with the aid of recombination mediators triggered by DNA damage. It is also important to note that although regulation of DSB occurs through various mechanisms, signalling events which incorporate a vast amount of post-translational modifications such as phosphorylation, methylation and ubiquitylation, are responsible for the recruitment of key repair proteins at DSB. These PTM are reversible and are arguably the most important form of overall regulation of repair, not only contributing to the recruitment of repair proteins but also to the choice of repair of DSB. The involvement of signalling at DNA DSB will be discussed later in this chapter.

1.3 Signalling at DSBs

The eukaryotic cell employs a plethora of proteins involved in the detection and repair of DNA damage through a highly coordinated and complex signalling cascade. This signalling cascade, also known as the DDR, orchestrates a variety of processes including DNA repair, cell cycle checkpoint activation and transcriptional regulation in response to DNA damage. One of the main functions of the signalling cascade at DSBs is to recruit major repair proteins to the site of damage as well as regulating the type of repair carried out. The recruitment of repair protein involves an intricate cascade of posttranslational modifications including phosphorylation, ubiquitylation, actylation and sumoylation which actively recruit repair proteins and remodel the chromatin around a break to facilitate repair (figure 1.4). Signalling at DSB employs a variety of DDR proteins and various post-translational modifications which form sub nuclear foci at the DSB site known as ionizing radiation induced foci (IRIF) [105]. The IRIF arise due to extensive chromatin remodelling and accumulation of DDR proteins, which are paramount for mediating not only the signalling and repair of damaged DNA but also to activate cell cycle checkpoints or apoptosis. The importance of the proteins involved in signalling at DSB are highlighted in various disease phenotypes associated with defective DDR proteins such as developmental defects, immunodeficiency and neurodegenerative disorders [106-108].

The phosphorylation of histone variant H2A, H2AX, by ATM is one of the initial signals which allows the recruitment of other DDR proteins to accumulate at sites of DSBs [109, 110]. ATM is recruited and activated by the MRN complex which recognises DSB ends. ATM directly binds to the C-terminus of NSB1 [111, 112] and phosphorylates H2AX, on a conserved serine, within seconds of the induction of DSBs [113]. Phosphorylation of H2AX is an extremely important step early on in the signalling response to DSBs as it provides a docking platform for other DDR proteins. Many mediator and repair proteins fail to translocate to the nuclear foci when the ATM

phosphorylation site of H2AX is mutated [110, 114]. To further prove the importance of γH2AX, knockdown of H2AX in cells promotes genomic instability [110].

Mediator of DNA damage checkpoint 1 (MDC1) has been shown to bind the C-terminal phosphopeptide of γH2AX via its BRCT domains [115, 116]. MDC1 is recruited within seconds of a DNA DSB and appears to have several functions. Studies have shown that MDC1 may protect the C-terminus of γH2AX from premature dephosphorylation therefore allowing completion of DNA repair [116, 117]. It has also been proposed that MDC1 serves to amplify the DNA damage signal [115, 118] by interacting with ATM through its FHA domains causing further accumulation of ATM which leads to the propagation of γH2AX.

MDC1 also acts as an adaptor protein which leads to the recruitment of RNF8 through its FHA domain after phosphorylation by ATM. RNF8 is an E3 ubiquitin ligase which functions with UBC13, an E2 ubiquitin-conjugating enzyme, previously believed to mediate mono-ubiquitylation of histones H2A and H2AX at DSBs [119-122]. However recent studies have suggested that although RNF8 is recruited to DSBs before RNF168, RNF168 and not RNF8 is responsible for the initial monoubiquitylation of H2A [123]. *Mattiroli et al.* discovered that RNF8 is inactive towards H2A whereas RNF168 catalyses the monoubiquitylation of H2A at position K13/15 and RNF8 is more likely to extend the ubiquitin chain [123]. RNF168, another E3 ubiquitin ligase is recruited to DSBs in a RNF8 dependent manner which relies not only on the FHA domain of RNF8 but also its RING domain [124-126]. As a means to explain the requirement of the E3 ubiquitin ligase function of RNF8 in the recruitment of RNF168, *Mattiroli et al.* suggested that RNF8 ubiquitylates non-histone proteins which recruit RNF168 to the site of damage [123]. The recruitment of RNF8 and RNF168 is believed to further amplify the DSB signals by increasing K63-linked poly-ubiquitination on H2AX and H2A [124-126]. Cells lacking *RNF8* and *RNF168* have defective DSB repair [127] highlighting their importance in signalling at DSBs.

BRCA1, the tumour suppressor protein, is recruited to DSBs via the formation of the BRCA1-A complex. RAP80, an integral component of the BRCA1-A complex binds to K63 linked polyubiquitin chains on H2A catalysed by RNF8 and RNF168 [128]. This in turn tethers BRCA1 to the DSB via its interaction with Abraxas. RAP80 contains tandem ubiquitin binding motifs (UIMs) which recognise the ubiqitylated proteins at DSBs and facilitates BRCA1 localisation. RAP80 forms a complex with Abraxas, a scaffold protein, and three additional proteins, BRE, MERIT40 and a deubiquitylation protein called BRCC36 [128-133]. Phosphorylated Abraxas is recognised by the BRCT domains of BRCA1. BRCA1 is phosphorylated on serine 1386 and 1423 by ATM and phosphorylation at these sites are important for both S-phase and G2/M checkpoints after IR [134, 135]. The exact function of BRCA1 at DSB sites remains unclear.

P53 binding protein 1 (53BP1) is another checkpoint mediator protein recruited to DSBs. 53BP1 has been shown to interact with methylated histones H3 and H4. Foci formation of both BRCA1 and 53BP1 has been shown to be dependent on MDC1 and the RNF8 ubiquitin ligase [136] however the mechanism of recruitment of 53BP1 is still unknown as is the mechanism by which ubiquitin affects the interactions between the 53BP1 tudour domains and methylated histones. 53BP1 is a known activator of p53 [137] and is important in checkpoint signalling.

As mentioned earlier, repair of DSB by NHEJ may leave the cell subject to mutations. To date, the exact mechanism that allows preferential repair by HR has not yet been identified. Recently an interesting discovery was made in relation to 53BP1 and BRCA1 at DSBs. It is important to note that homozygous deletion of BRCA1 appears to be lethal during human and mouse development, primary cultured cell, MEFs and stem cells [138]. *BRCA1* null mice can be rescued by the deletion of one allele of *p53* however these mice exhibit an increase in spontaneous tumour formation [139]. BRCA1 deficient cells show a decrease in DSB repair by HR in the presence of 53BP1, however cells lacking both *BRCA1* and *53BP1* have a partially restored HR

pathway [140]. This new discovery leads us to believe that there may be a more complicated interplay between BRCA1 and 53BP1 at DSB sites.

The recruitment of a vast number of repair and signalling proteins to the site of damage is further complicated by the fact that repair does not take place on naked DNA, but instead on chromatin. Chromatin is the complex structure of DNA wrapped tightly around histone proteins which can be packed in a very tight complex known as heterochromatin or a more loosely packed euchromatin. Euchromatin is normally associated with a more open structure which is transcriptionally active as the DNA is easier to access whereas heterochromatin is considered to be transcriptionally silent due to the tight compaction of the DNA [141]. As a result the different packing of chromatin serves as an extra method of regulating key cellular process such as transcription, replication and repair due to the limitations imposed on proteins to access the DNA in heterochromatin [142, 143]. As a result, the modification of chromatin by chromatin remodelling factor plays an important role in the response to DSBs and many such factors have been shown to be recruited to sites of damage during the signalling cascade at DSBs [144].

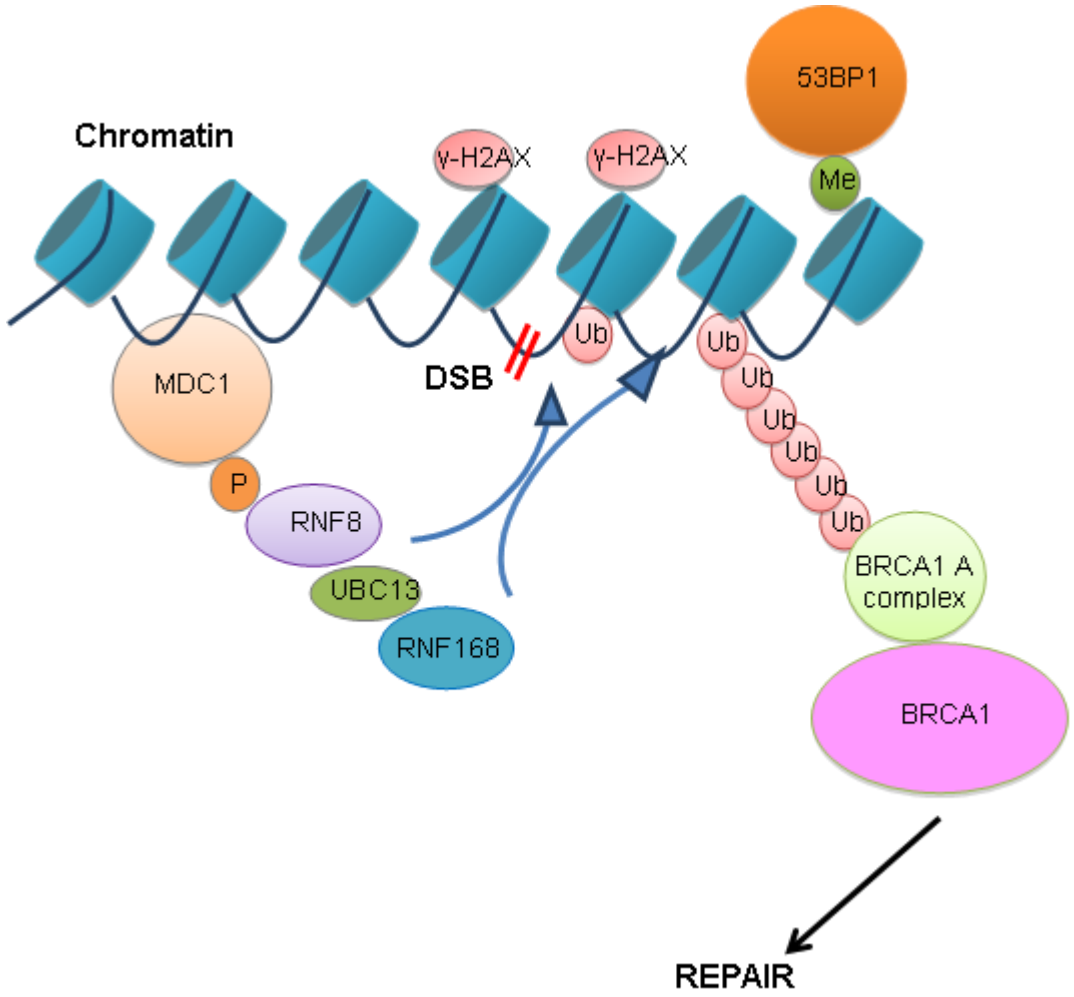

Figure 1.4 Signalling at DNA DSBs
Illustration of the signalling cascade after the induction of a DSB. The MRN (Mre11-RAD50-NBS1) complex recognises the DSB and activates and recruits ATM. ATM then phosphorylates the histone variant H2AX which initiates a complex signalling pathway involving several proteins important for repair. MDC1 binds γ-H2AX and recruits the ubiquitin ligase RNF8. RNF8 then recruits RNF168 which mono-ubiquitylates H2A and H2AX and together the concerted action of RNF8 and RNF168 extends the polyubiquitin chain. Poly-ubiquitin conjugated H2A/H2AX provides a docking platform for RAP80 which recruits BRCA1 through the BRCA1-A complex. As a result of the signalling cascade, repair proteins BRCA1 and 53BP1 are recruited to sites of damage.

1.3.1 Ubiquitin and signalling at DSBs

Although phosphorylation has long been known as a crucial post-translational modification in orchestrating several protein-protein interactions at DSBs, ubiquitylation has recently emerged as another key protein modification at sites of damage to ensure genome stability in response to damage. The ubiquitylation system is best characterised for its role in protein degradation however it is the non-degradative aspects of ubiquitylation known as the non-conventional signalling functions of ubiquitylation that appear to play the predominant role in the DDR. The signalling aspect of ubiquitin acts as a reversible post-translational modifier for proteins involved in the response to DNA damage. Shortly after its discovery, ubiquitylation and subsequent polyubiquitylation of proteins was found to target proteins for degradation in an ATP dependent manner by the 26S proteasome [145, 146]. Since then, ubiquitin modification has been associated with numerous non-degradative roles and is considered to be a signal similar to many other post-translational modifications.

Ubiquitylation of a substrate protein can occur by covalently attaching a single ubiquitin moiety onto a target protein known as mono-ubiquitylation or by extending the mono-ubiquitin chain forming a poly-ubiquitin chain. The mono-ubiquitylation of a protein can have several functional consequences such as intracellular vesicle transport, chromatin structure regulation, transcription and processing of DNA damage. However the intrinsic complexity of ubiquitin signalling arises from its ability to form poly-ubiquitin chains on its substrate. Ubiquitin is conjugated to a lysine residue on its substrate protein. Ubiquitin is a small 76 amino acid protein around 8.5 kDa and it contains seven lysine residues on the surface of the protein which can all be used for further ubiquitylation to form a ubiquitin chain [147]. Ubiquitin chains of different linkages can be formed on lysine's on the surface of ubiquitin which are associated with different functional outcomes [148]. For example, K48 linked poly-ubiquitin chains target the substrate protein for degradation, whereas K63 linked chains are more commonly associated with non-proteosomal signalling functions known to be involved

in endocytosis and the DDR [149]. The modification of a protein by the conjugation of ubiquitin is believed to create an additional interaction site on the substrate. Over twelve ubiquitin binding motifs have been identified in a variety of proteins such as the UIM in RAP80. Although most of these ubiquitin binding motifs are not selective for the type of ubiquitin modification, some are extremely selective and can distinguish between K63 linked ubiquitin chains and linear chains [150-152].

In response to DNA damage, especially DNA DSBs, a series of ubiquitin enzymes are recruited to sites of damage where they are involved in mediating a response to DNA damage serving to amplify the DNA damage signal and recruit major repair proteins. DNA checkpoint activation and repair relies on the recruitment of several E3 ubiquitin ligases. As a result many different E3 ligases are found at DNA DSBs including BRCA1, RNF8, RNF168, HERC2 and RNF2 among others. Although many questions about the regulation of ubiquitylation, substrates and functional relevance of ubiquitin chains remain unanswered, the importance of ubiquitin in the signalling at DNA DSBs is evident as loss of ubiquitylation abrogates the repair of DSBs.

1.3.2 Mechanism of protein ubiquitylation

Ubiquitin was first discovered by *Ciechanover et al* in the 1970s while studying the ATP-dependent degradation of the tyrosine aminotransferase enzyme. This group isolated a protein called ATP-dependent proteolysis factor 1 (APF-1) [145] which is now known as ubiquitin (ub). Since its discovery, the extensive research of several groups lead to the discovery of the process of ubiquitylation [153] (figure 1.5). Ubiquitylation involves the attachment of a ubiquitin moiety onto a substrate protein via the formation of an isopeptide bond between an amino group on a substrate protein and the c-terminus of the ubiquitin. Ubiquitylation is an ATP dependent process which involves the sequential action of three ubiquitin enzymes, the E1 activating enzyme, the E2 conjugating enzyme and the E3 ubiquitin ligase enzyme.

The initial step of ubiquitylation involves the activation of ubiquitin by the E1 enzyme. The E1 enzyme activates ubiquitin by displacing pyrophosphate from ATP generating a ubiquitin-adenylate intermediate [154-156]. As a result, a thioester bond forms between the thiol group of the cysteine in the active site of the E1 enzyme and a carboxyl group of a glycine in the C-terminus of ubiquitin. This process leads to the release of AMP. The active ubiquitin is then transferred to a cysteine in the active site of the E2 enzyme which is catalysed by a thioester transacylation process [157]. The final step on ubiquitylation involves the E3 ubiquitin ligase enzyme which catalyses the conjugation of the ubiquitin onto a lysine residue of the substrate protein via the formation of an isopeptide bond.

There are two main classes of E3 ubiquitin ligases which are categorised depending on the presence of either a HECT or RING domain and over 600 such proteins have been identified in mammalian cells [158]. RING domain containing E3 enzymes act as scaffolds to facilitate the conjugation of the ubiquitin on the E2 enzyme onto the substrate bringing the E2, ubiquitin and substrate in close proximity to each other. On the other hand, HECT domain containing proteins have direct catalytic activity forming an extra thioester bond between the catalytic cysteine residue and the ubiquitin [159]. In humans there are only two known E1 enzymes, Ube1 and Uba6. There are around 40 E2 enzymes in humans all containing a conserved catalytic conjugating domain [160]. The E3 enzymes have been shown to possess substrate specificity from structural studies [161-163] and it is believed that the combination of E2 and E3 enzymes ultimately determines not only the target substrate but also the type of ubiquitylation.

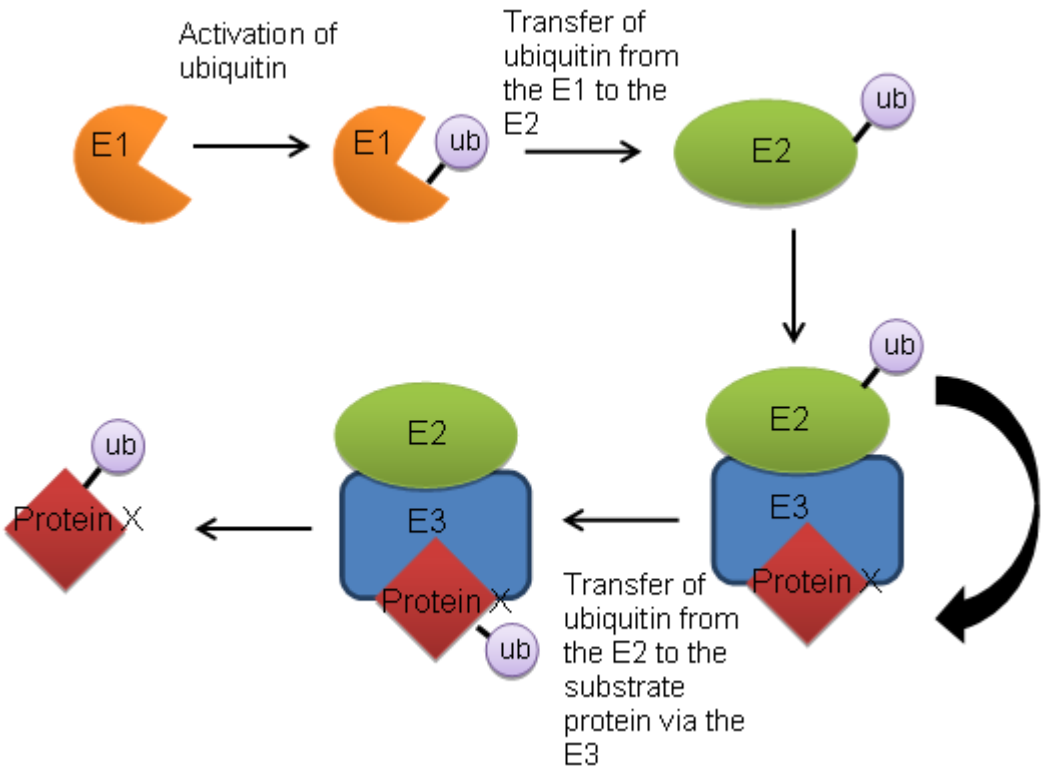

Figure 1.5 Mechanism of Ubiquitylation
Diagram of the process of conjugating ubiquitin onto a substrate protein. Ubiquitin is first activated by an E1 enzyme in a process requiring ATP. The active ubiquitin is then attached onto the E1 enzyme via a thioester bond. The ubiquitin is then transferred onto the conjugating E2 enzyme catalysed by a thioester transacylation process. The final stage of ubiquitylatiuon requires an E3 enzyme to transfer the ubiquitin to a lysine residue on the substrate protein forming an isopeptide bond. After mono-ubiquitylating the protein further ubiquitylation can occur to create a poly-ubiquitin chain.

1.3.3 Ubiquitin ligases and their role in the DDR

Ubiquitylation of proteins involved in the DDR is fundamental for efficient DSB repair and signalling at sites of damage [164, 165]. As a result, several E3 ubiquitin ligases are recruited to sites of DNA damage such as BRCA1/BARD1, RNF8, RNF168, HERC2, RAD18 and RNF4 and loss of these proteins results in impaired DSB repair ,signalling and an increase in sensitivity to DNA damaging agents [119-122, 124, 126, 166-168]. Although the BRCA1 BARD1 heterodimer is a well characterised ubiquitin ligase, the relevance of the E3 activity of these proteins in the repair of DNA damage remains unclear. Several breast cancers contain mutations in the BRCA1 RING

domain which abrogates its E3 ubiquitin ligase activity [169-171]. This suggested that the E3 ligase activity of BRCA1 is required for tumour suppression, however most of the breast cancer BRCA1 RING mutations not only abrogated its E3 ligase activity but also disrupted the BRCA1 BARD1 interaction suggesting that the phenotypes observed with these mutations were as a result of a complete loss of BRCA1 function in the absence of BARD1 rather than a requirement for the ubiquitin ligase activity of BRCA1. The hypothesis that the BRCA1 E3 ligase activity is not fundamental to the DDR was further strengthened when *Reid et al*, observed that the RING domain of BRCA1 was not required for DSB repair or cell viability [172]. The group introduced a point mutation (I26A) into the BRCA1 RING domain which abrogated the ubiquitin ligase activity of BRCA1 whilst still enabling its interaction with BARD1. The BRCA1I26A mutant was HR competent and showed no increased sensitivity to DNA damaging agents suggesting that the BRCA1 RING domain is not required for HR.

RNF8 is a 485 amino acid E3 ubiquitin ligase enzyme first discovered in 1998 by *Seki et al* [173]. RNF8 contains an N-terminal forkhead-associated (FHA) domain which is responsible for binding to phospho-threonine residues and also a C-terminal RING domain which attributes its E3 ubiquitin ligase function [174, 175]. Research over the past few years have highlighted the importance of RNF8 in response to DNA damage. Loss of RNF8 in cells has been shown to lead to defective HR especially in heterochromatin [176]. Recently *Oestergaard et al.* demonstrated that *Rnf8* DT40 cells were sensitive to DNA damaging agents and required for ubiquitylation at DNA DSBs to facilitate the recruitment of BRCA1 and 53BP1 to sites of damage [177]. The analysis of *Rnf8* deficient mice revealed a mild phenotype. These *Rnf8* mice were sensitive to IR and also exhibited subtle defects in V(D)J recombination and CSR [178-180].

Following DNA damage, RNF8 is recruited to sites of damage by interacting with the phosphorylated MDC1 through its FHA domain [119-121]. RNF8 has been elucidated as an important factor in the recruitment of both BRCA1 and 53BP1 to sites

of damage which is dependent on its E3 ligase function [119-122] . RNF8 is also responsible for the recruitment of another E3 ubiquitin ligase, RNF168, to sites of damage [124, 126]. This recruitment is dependent on both the FHA and RING domain of RNF8. Interestingly the ubiquitin ligase activity of RNF8 is not sufficient to retain BRCA1 and 53BP1 at sites of damage and the concerted action of RNF8 and RNF168 has been shown to be required for this stabilisation. Due to the recruitment order of RNF8 and RNF168, it was originally predicted that RNF8 mono-ubiquitylated H2A and RNF168 extended the ubiquitin chain in the form of K63-linked poly ubiquitin chains, however recent evidence has demonstrated that although RNF8 can ubiquitylate free H2A *in vitro* it does not have any activity towards H2A in the context of chromatin. Instead it was shown that RNF168 mono-ubiquitylated H2A and together RNF8 and RNF168 extended the poly-ubiquitin chains [123]. Given that RNF8 acts on H2A after RNF168 yet the ubiquitin ligase function is required to recruit RNF168, it has been suggested that RNF8 ubiquitylates non-histone proteins which may lead to the recruitment of RNF168 [123]. However these potential RNF8 substrates have not yet been identified.

RNF168 is another E3 ubiquitin ligase enzyme important in mediating the response to DNA damage and recruiting repair proteins to DNA damage sites. RNF168 contains an N-terminal RING domain and two UIMs (ubiquitin interacting motif). Similar to RNF8, RNF168 has been implicated in HR, as loss of the protein leads to defective HR and sensitises cells to DNA damaging agents [176, 177]. Mutations in RNF168 are also associated with the human RIDDLE syndrome which is characterised by radiosensitivity and immunodeficiency among other clinical features [126]. RNF168 is recruited to DNA damage via its UIM domains in a manner dependent on RNF8 and is responsible for the mono-ubiquitylation of H2A, ultimately leading to the recruitment of BRCA1 and 53BP1 [123]. K63, non-degrading, ubiquitin chains are essential for the recruitment of repair proteins BRCA1 and 53BP1 to DSBs [2, 181, 182], Both RNF8 and RNF168 are required for ubiquitylation at sites of damage and loss of either

proteins severely impedes the recruitment of BRCA1 and 53BP1 to DSBs [122, 124, 126, 177].

RNF8 and RNF168 are important in the recruitment of BRCA1 and 53BP1 to DSBs, however these two proteins are predicted to have contrasting functions in terms of repair. BRCA1 is thought to stimulate repair of DSBs via HR in a faithful manner whereas 53BP1 promotes the more error prone pathway on repair, NHEJ. It has become evident over the last few years that signalling at DSBs mediates and regulates the decision to repair DSB either by HR or by NHEJ and much further work is needed to address the function of RNF8 and RNF168 in the decision of repair. The exact function and biological relevance of these two ubiquitin ligases in relation to the repair of DSB remains unclear.

1.4 BRCA1 and BARD1

1.4.1 Introduction to the tumour suppressor gene BRCA1

A tumour suppressor gene is defined as a genetic factor in which loss of heterozygosity can lead to the development of a tumour. Breast cancer is one of the most common cancer affecting 1in 9/12 women throughout their life time. Although there are many factors that contribute to the development of breast cancer including hormonal imbalance and obesity, the most prominent factor is family history. The genetic basis underlying common forms of inherited breast and ovarian cancers was discovered to be due to germ line mutations in the Breast cancer type 1 susceptibility protein (BRCA1) and BRCA2 [183, 184]. BRCA1 and BRCA2 are the most commonly mutated genes in hereditary breast and ovarian cancer [185] Although germ line mutations of BRCA1 are only associated with a small percentage of total breast and ovarian cancers, it is estimated that around 10% of hereditary breast and ovarian cancer arise due to germ line BRCA1 mutations [186]. There has also been some recent evidence that BRCA1 is responsible for the development of some sporadic breast cancers [187].

BRCA1 mutation carriers inherit one mutated copy of the BRCA1 gene and loss of heterozygosity of the Wild type gene is commonly associated with tumours. Although patients do not display any apparent phenotypic abnormalities, they have an increased risk of 80% in developing either breast or ovarian tumours throughout their life time [188]. BRCA1 is involved in many important cellular processes including cell cycle checkpoint control, repair and chromatin remodelling. However its role in the repair of DSB by HR is considered to be its most important function in tumour suppression.

1.4.2 The BRCA1 gene

The BRCA1 gene was identified in 1990 and subsequently cloned in 1994 [184, 189]. BRCA1 is a relatively large gene of 1863 amino acids encoded in 24 exons. Orthologues of BRCA1 can be found in many vertebrates including mice, chicken and zebra fish. BRCA1 homologues and several BRCA1 complex members have also been discovered in plants [190-192] however, to date there is no clear BRCA1 homologue in either *Saccharomyces cerevisea* or *Schizosaccharomyces pombe*. Many functions of BRCA1 can be attributed to functional domains encoded in the gene. BRCA1 contains a really interesting new gene (RING) domain at its N-terminus which contributes to the E3 ubiquitin ligase function of the protein [193, 194]. The C-terminus of the protein contains a tandem BRCA1 C-terminal (BRCT) repeat which is known to bind phosphorylated proteins important for repair [193]. BRCA1 also harbours a nuclear export signal (NES) at its C-terminus and two central Nuclear localisation signals (NLS) [193, 195]. BRCA1 interacts with a variety of proteins attributing several functional roles for BRCA1 in DNA repair, cell cycle regulation and transcriptional regulation [196, 197] (figure 1.6)

1.4.3 The BARD1 gene

BRCA1 associated RING domain protein 1 (BARD1) was identified in a yeast two hybrid screen of BRCA1 RING domain interactors [194]. BARD1 is encoded by 777 amino acids [194] and shares many structural similarities with BRCA1 (figure1.6).

BARD1 has a RING domain in its N-terminus which has been shown to interact with the BRCA1 RING domain forming a stable heterodimer both *in vitro* and *in vivo* [170, 198]. Similar to BRCA1, BARD1 also contains tandem BRCT domains at its C-terminus. Furthermore BARD1 also has three tandem ankyrin repeats [199] not present in BRCA1. It has been suggested that all three functional domains of BARD1 (RING, BRCT and ankyrin repeats) are essential for its role in the DDR.

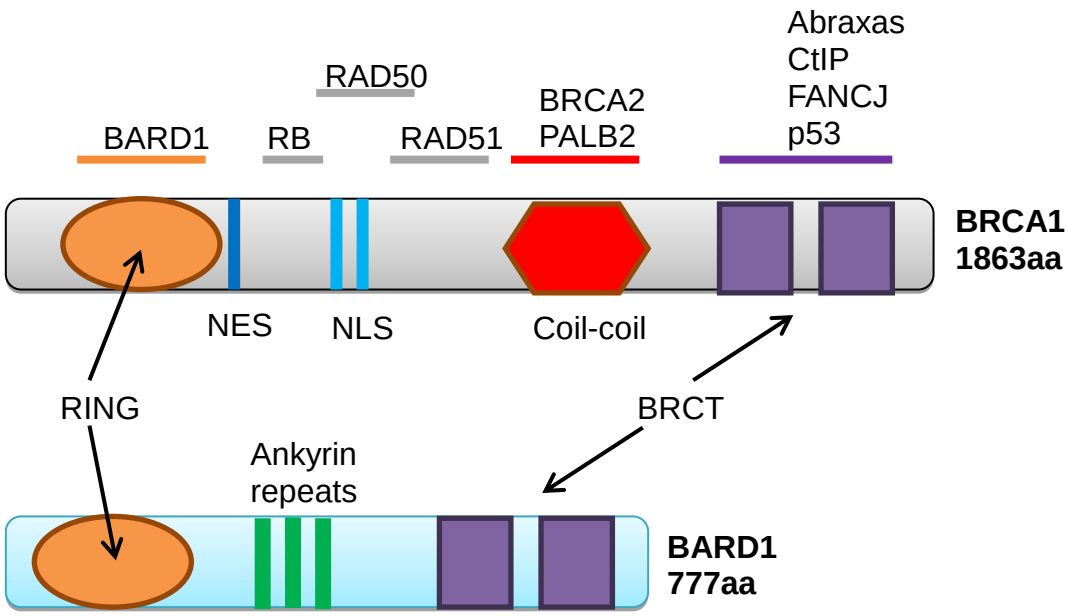

Figure 1.6 BRCA1 and BARD1 functional domains and BRCA1 interacting proteins
Representative image of the BRCA1 and BARD1 genes illustrating common functional domains, the RING and BRCT domains. BRCA1 also contains NES and NLS motifs and BARD1 harbours ankyrin repeats. The proteins above BRCA1 represent BRCA1 interacting proteins and their position corresponds to the region of BRCA1 with which they interact.

1.4.4 The role of BRCA1/BARD1 in the DNA damage response

In order to maintain genome stability the cell must implement an efficient response to DNA damage. BRCA1 has been shown to be important in the response to DNA damage as defects or loss of BRCA1 in cells results in gross genome instability. This

phenotype is strikingly evident in the karyotyping of BRCA1 null cells as they demonstrate extensive chromosomal translocations, aberrant fusion events and duplications [200-202]. The genome instability phenotype associated with loss of BRCA1 is associated with several diseases such as Fanconi anaemia, Blooms syndrome and cancer [203, 204]. BRCA1 is associated with numerous complexes [184, 196, 205] resulting in a variety of distinct functions. These BRCA1 complexes have several functions in DNA repair, cell cycle checkpoint activation and transcriptional regulation [196, 197].

BRCA1 is found almost exclusively in the nucleus bound to its interacting protein BARD1 [194]. The BRCA1-BARD1 heterodimer is formed by the interaction of four alpha helices flanking their RING domains [198, 206]. The interaction of BRCA1 with BARD1 is paramount to the DDR functions of BRCA1 and is heavily supported by both *in vivo* and *in vitro* evidence. Abolishing the BRCA1 BARD1 interaction results in defective HR and point mutations preventing the BRCA1 BARD1 interaction are often seen in breast cancers [172, 207]. Binding of BARD1 masks the nuclear export signal of BRCA1 allowing its retention in the nucleus where it has its function. Heterodimerization of BRCA1 and BARD1 has also been shown to greatly increase the ubiquitin ligase activity of BRCA1 and it considered to be important for the stabilisation of both proteins [170, 208, 209]. Both *Bard1* and *Brca1* knockout mice are embryonic lethal and almost phenotypically indistinguishable. The loss or mutation of either proteins in cells has been demonstrated to severely increase sensitivity to DNA damaging agents indicating that both BRCA1 and BARD1 share similar function in response to DNA damage [201, 207, 210]. The importance of the BRCA1 BARD1 interaction in genome stability is further demonstrated by BRCA1 mutations found in cancers which abrogate its binding to BARD1[211]. The frequency of BARD1 mutations found in cancers is very low in comparison to those found in BRCA1, however a number of BARD1 mutations in cancers have been discovered [212-214].

As previously mentioned, BRCA1 interacts with a variety of proteins attributing several unique functions to BRCA1 in response to DNA damage (figure 1.6). The importance of these interactions will be discussed in relation to three major functions of BRCA1 in DNA repair, cell cycle checkpoint activation and regulation and transcriptional regulation. Unless otherwise stated, all these interactions and functions of BRCA1 are dependent on the formation of the BRCA1 BARD1 heterodimer.

The role of BRCA1 in DNA repair

Initial clues that BRCA1 is important for the repair of DSBs via HR came from a study carried out by *Scully et al* in 1997 demonstrating that BRCA1 colocalised with RAD51 at sites of damage [215]. Since then a vast number of studies have implicated BRCA1 in the repair of DSB via HR. Loss of BRCA1 or partial loss of BRCA1 function has been shown to decrease HR [201, 202, 216, 217] in cells and sensitises the cell to various DNA damaging agents [218]. BRCA1 null cells have also been shown to be extremely sensitive to PARP inhibitors [219]. The recruitment of BRCA1 to DSBs remains to be one of the most convincing pieces of evidence suggesting a role for BRCA1 in HR. Upon DNA damage, BRCA1 is activated and recruited to DSBs. This recruitment is initiated by the MRN complex which recognises the break and recruits ATM. The key role of ATM is to recruit repair proteins by phosphorylating histone H2AX [113, 220]. BRCA1 localises to DSBs through its interaction with Abraxas, which forms a stable complex at sites of damage. The relevance and importance of this interaction will be discussed later on in this chapter.

Although the exact molecular mechanism by which BRCA1 contributes to the repair of DSB via HR remains unknown, the interaction of BRCA1 with certain repair proteins has provided potential mechanisms of action. Evidence suggests that BRCA1 interacts with the MRN complex through its interaction with CtIP forming the BRCA1-C complex [221]. The MRN complex, which is fundamental to the recruitment of repair proteins to sites of damage and also in the initiation of HR, is thought to directly recruit BRCA1-CtIP by binding phosphorylated CtIP [221]. The MRN-CtIP-BRCA1 complex mediates

extensive resection at DSBs generating ssDNA, a prerequisite for HR [55, 222]. 53BP1 is believed to inhibit DSB resection promoted by CtIP and BRCA1 is required to overcome this inhibition [223]. Although both CtIP and the MRN complex are required for resection and HR, the direct interaction between CtIP and BRCA1 appears to be less important [166, 224, 225] suggesting that BRCA1 may be more important in preventing the inhibition of resection by 53BP1and therefore promoting HR.

DNA strand invasion and homology search during HR is carried out by the recombinase protein RAD51 [226]. After DNA end resection by MRN-CtIP, RAD51 displaces RPA from the ssDNA with the help of recombination mediators. BRCA2 has been shown to be important in the formation of the RAD51 filament [227]. BRCA1 is essential for the retention of both RAD51 and BRCA2 at sites of damage [228]. It is believed that this is one of BRCA1s fundamental roles in DSB repair by HR. Whether BRCA1 interacts with RAD51 in a direct or indirect manner remains unclear. BRCA1 has been suggested to recruit BRCA2 to DSBs via PALB2 which acts as a linker protein between BRCA1 and BRCA2 [229, 230]. Indirectly, BRCA1 is considered to be vital for the recruitment of the RAD51 to DSBs through the recruitment of BRCA2 via PALB2. In confirmation of this functional role of BRCA1, BRCA1 is known to colocalise with RAD51 at sites of damage and loss of BRCA1 results in a reduction of BRCA2, PALB2 and RAD51 foci formation after DNA damage and abrogates HR [229, 230].

Over the last few years a novel role for BRCA1 in DNA repair has emerged. Recent evidence suggests that BRCA1 plays an important role in the regulation and choice of repair at DSBs. BRCA1 localises to DSBs via its interaction with Abraxas, however the recruitment of BRCA1 to DSBs can also be facilitated by the DNA damaged induced interaction of BRCA1 N-terminus with the NHEJ protein Ku80 [231]. Rather than promoting NHEJ, the recruitment of BRCA1 to DSB by Ku80 is predicted to facilitate HR by removal of NHEJ repair proteins such as 53BP1 from the DSB [223]. This function is suggested to prevent aberrant end joining and to regulate the choice of NHEJ and HR. Contrary to expectations, the depletion of RAP80 and Abraxas, which

are responsible for recruiting BRCA1 to DSBs, resulted in an increase in DNA end resection and HR [224, 232](unpublished results). Loss of RAP80 also correlates with an increase of RAD51 and CtIP at DSB resulting in excessive resection at DSB and gross chromosomal rearrangements [224]. This suggests that BRCA1 plays an important role in regulating the amount of HR that occurs at a DSB preventing genome instability.

All the known interactors of BRCA1 which are important in DNA repair, such as Abraxas, CtIP, PALB2 and RAD51, interact with the C-terminal BRCT domains of BRCA1 or in the case of RAD51, it is predicted to bind to a more central region of BRCA1. Although the RING domain of BRCA1 is important in DNA repair as it interacts with BARD1, the ubiquitin ligase function of BRCA1 appears to be dispensable for HR. As previously mentioned, the introduction of an I26A point mutation into the RING domain of BRCA1, which disrupts its E3 ubiquitin ligase function, had no effect on HR efficiency [172]. Although the ubiquitylation targets of BRCA1 BARD1 remain elusive, it has been suggested that H2A is a target. *Chen et al*. demonstrated that the N-terminus of BRCA1 containing its RING domain is required for the ubiquitylation of H2A and several groups have reported that loss of BRCA1 results in a decrease in ubiquitylated H2A [233-235]. CtIP has also been shown to be ubiquitylated by BRCA1 BARD1 both *in vivo* and *in vitro* and suggested that ubiquitylation of CtIP was required for its retention at DSB [236]. Earlier reports also demonstrated that the loss of BRCA1 resulted in a reduction in ubiquitylation at DSB, suggesting a role for the BRCA1 ubiquitin ligase function in the signalling cascade at sites of damage [121]. It would appear that although BRCA1s ubiquitin ligase function may contribute to ubiquitylation events at DSBs, its function is not vital to the repair process as defects in HR are not seen in the absence of BRCA1 ubiquitin ligase activity [172] and the majority of BRCA1 function in HR can be attributed to its BRCT domains.

The role of BRCA1 in cell cycle checkpoint activation and regulation.

In order to ensure that the cell proceeds through the cell cycle without any DNA lesions or mutations, cell cycle checkpoints are used to monitor the chromatin and DNA status during various stages during the cell cycle [237]. After DNA damage it is important for the cell to activate cell cycle checkpoints to allow the cell time to repair the damage and also to prevent unrepaired damage being replicated resulting in the loss of genomic information or mutations in daughter cells [238]. Defects in cell cycle checkpoint proteins often results in developmental abnormalities, genome instability and cancer [239]. Cell cycle checkpoints can be classified as G1/S, S and G2/M checkpoints and BRCA1 is suggested to play a role in all checkpoints to maintain genome integrity in response to DNA damage.

Following DNA damage cells are arrested at the G1/S boundary by the G1/S checkpoint. This checkpoint prevents damaged DNA progressing into S phase and subsequent replication of damaged DNA. *Fabbro et al* demonstrated the importance of BRCA1 in the G1/S checkpoint as the loss of BRCA1 failed to arrest cells in on the G1/S phase boundary after DNA damage [240]. In this study it was demonstrated that in response to IR damage, BRCA1 was required for the phosphorylation of p53 by ATM which in turn lead to the G1/S checkpoint activation via p21 [240]. The tumour suppressor protein p53 plays a vital role in the G1/S checkpoint by regulating the transcription of p21, a cyclin inhibitor [241-243]. Shortly after the cloning of BRCA1, it was discovered that inhibition of BRCA1 resulted in the acceleration of growth in both WT and malignant cells [244]. It was believed that this was as a result of cell cycle control via BRCA1 and it was later established that the interaction between RB and BRCA1 was required to induce a G1/S arrest [245]. *Aprelikova et al.* demonstrated that BRCA1 BRCT domains interact with hypophosphorylated RB and that hypophosphorylated RB interacts with E2F inhibiting cell proliferation [245]. They suggested that the binding of BRCA1 to RB maintained RB in a hypophosphorylated state allowing it to interact with E2F.

The S phase checkpoint is another cell cycle checkpoint which prevents S phase progression and replication directly in response to DNA damage [246]. *Xu et al* highlighted the involvement of BRCA1 in the S phase checkpoint after IR induced DNA damage. They showed that the S phase checkpoint was defective in the BRCA1 mutant cell line HCC1937, and the introduction of functional BRCA1 restored the S phase checkpoint defect [134]. Defects in the S phase checkpoint are a common characteristic associated with defects in many DDR proteins such as ATM, ATR, Chk1 and Chk2 [247-250]. After DNA damage, ATM and ATR are activated and are involved in regulating Chk1 and Chk2 activity which in turn leads to the regulation of cyclins and cyclin-dependent kinases (CDKs) [251]. Cyclins and CDKs are essential in the regulation of cell cycle progression. Although the exact mechanism of BRCA1 function in S phase checkpoint is not clear, it has been suggested that BRCA1 regulates the Chk1 kinase activity and that BRCA1 phosphorylation by ATM /ATR is required for this function [252]. Phosphorylation of Ser1387 on BRCA1 by ATM is required for the S phase checkpoint [134]

The final checkpoint is the G2/M checkpoint which serves as a barrier to prevent damaged cells from entering mitosis and passing their damage on to a daughter cell. Late S and G2 phases of the cell cycle are also responsible for the most accurate type of DSB repair during the cell cycle. Arresting the cell in G2 phase allows the cell time to faithfully repair its damage before cell cycle progression. As with the G1/S and S phase checkpoints, the G2/M checkpoint is also activated in response to IR damage. Loss of functional BRCA1 has also been shown to abrogate the G2/M checkpoint [202]. As previously mentioned Chk1 and Chk2 are activated by ATM and ATR in response to damage which leads to the activation of the G2/M checkpoint by suppressing cyclin B and Cdc2 activity [253-256]. Similarly to S phase, BRCA1 regulates the activity of Chk1 during the G2/M checkpoint [86]. In contrast to S phase checkpoint control, the ATM mediated phosphorylation of Ser1423 on BRCA1 is

required for G2/M checkpoint activation [86] suggesting that phosphorylation on different sites of BRCA1 may be key to the activation of different cell cycle checkpoints.

The role of BRCA1 in transcriptional activation.

Monteiro et al. discovered that BRCA1 could activate transcription in both yeast and mammalian cells [257]. They showed that the transcriptional activity of BRCA1 depended on a region in its C-terminus (BRCT domains) which, when bound to a GAL4 DNA binding domain, activated transcription. It was also demonstrated that the transcriptional role of BRCA1 was a key aspect of its tumour suppressor function as a point mutation associated with the BRCT domains of BRCA1, was commonly found in patients with early onset breast and ovarian cancer and were deficient in transcriptional activation [257]. Further evidence of the importance of BRCA1 transcriptional regulation in the prevention of cancer came from a study demonstrating that cancer prone point mutations in the BRCT domains of BRCA1 were often defective for both transcriptional regulation and growth control whereas neutral BRCA1 polymorphisms did not show the same defects [258].

It is believed that the transcriptional role of BRCA1 is mainly due to its interaction with RNA polymerase II (RNA polII). BRCA1 was found to co-immunoprecipitate with RNA polII holoenzyme complex via its association with RNA helicase A [259]. Cancer associated point mutation of BRCA1 were found to prevent the BRCA1-RNA polII interaction strengthening the belief that this interaction is important for tumour suppression [260]. As well as BRCA1s interaction with RNA polII, it has been demonstrated that BRCA1 regulates the phosphorylation of RNA polII by negatively regulating the phosphorylation of Cdk-activating kinase [261]. This function is believed to regulate cell cycle progression in response to DNA damage. Although BRCA1 has been shown to interact with RNA polII, it is not required for basal transcriptional function and it also doesn't appear to be an essential component in the RNA polII holoenzyme complex. The biological relevance of BRCA1 and transcriptional

regulation remains unclear, however it is possible that it is only required in response to DNA damage.

As previously mentioned, BRCA1 interacts with the growth suppressor RB [262] under non-damaging conditions preventing the activation of p21. It is thought that in the presence of DNA damage, this interaction is abrogated which in turn allows the transactivation of p21mediated by BRCA1 [262]. p21 plays an important role in the arrest of cells during the cell cycle in response to DNA damage allowing the cell time to repair its damage. As well as its interaction with RNA polII and RB, BRCA1 has also been shown to interact with a variety of transcription factors such as estrogen receptor α, p53 and STATI [263-265]. Through these interactions, BRCA1 is predicted to modulate transcription activation in response to DNA damage.

The role of BARD1 in the DDR.

Very little is known about the role of BARD1 in response to DNA damage apart from its functional role in stabilising BRCA1 in the nucleus and enhancing the E3 ubiquitin function of BRCA1. It is believed that all the tumour suppressor and DDR functions of BRCA1 depend on its interaction with BARD1. However there is evidence that BARD1 may play a functional role in DNA repair independent of its role in stabilising BRCA1 as mutations in BARD1 independent of BRCA1 mutations have been discovered in a few breast and ovarian cancers [213, 214, 266]. Furthermore, another mechanism by which BARD1 is suggested to contribute to the tumour suppressor function of BRCA1 is through its interaction with the cleavage stimulation factor (CstF) [267]. It was discovered that CstF is required for 3'-terminal endonucleolytic cleavage of pre-mRNA a process fundamental to transcription [268]. BARD1 interacts with CstF via its ankyrin repeats and it has been speculated that this interaction is involved in DNA repair by preventing mRNA processing[267].

Although there are no known proteins which interact with the BARD1 BRCT domains, studies revealed that the BRCT domains of BARD1 are important for the

repair of DNA DSBs via HR [266, 269] as the loss of the BARD1 BRCT domains resulted in defects in HR efficiency. It is evident that BARD1 contributes to genome stability and has a functional role in HR, however more research is needed to understand its contribution to the DDR and repair of DNA DSBs independent of its role in stabilising BRCA1.

1.4.5 The role of PARP and PARP inhibitors in the repair of DSBs.

The clinical relevance of PARP and PARP inhibitors in relation to BRCA1 and BRCA2 defective breast and ovarian cancers came from the discovery that PARP inhibitors were selectively lethal to cells harbouring mutations or loss of BRCA1 and BRCA2 due to synthetic lethality [219, 270-272]. The potential of PARP inhibitors to kill BRCA1 and BRCA2 deficient cells arose from the rationale that cells with a defective HR repair pathway rely on single stranded break repair pathway to repair single stranded breaks which is dependent on PARP. However with the inhibition of PARP, single stranded breaks are not repaired and can lead to DSB through replication. Cells which are defective in HR and treated with PARP inhibitors are unable to repair damage efficiently resulting in cell death [270, 273]. As a result of this phenomenon, PARP inhibitors are commonly used as a research tool to assess the ability of a cell to carry out efficient HR.

Research over the past decade has illustrated the importance of Poly(ADP-ribosyl)ation catalysed by the PARP1 enzyme as a fundamental post translational modification involved in the signalling, detection and repair of ssDNA breaks as well as DSBs. PARP1 catalyses the covalent attachment of PAR polymers onto histones, repair proteins and chromatin modulators as well as auto Poly(ADP-ribosyl)ation [274, 275]. Parylation is a rapidly reversible process catalysed by PARG [276]. PARP1 plays an important role in DNA repair and binds to damaged DNA under conditions of genotoxic stress [274]. The main role of PARP1 in response to DNA damage is in the repair of single stranded breaks via both the base excision repair (BER) and single stranded break repair (SSBR) pathways after oxidative stress. PARP1 catalyses the

formation of long branched PAR chains on repair proteins involved in ssDNA breaks and these negatively charged polymers form a scaffold recruiting other critical repair proteins such as XRCC1 to sites of damage [277, 278].

Although PARP1 is historically considered to be involved in the SSBR and BER repair pathways of ssDNA breaks, evidence is continuing to emerge on the importance of PARP1 in the repair of DSBs. PARP1 has since been shown to interact and cooperate with several key DSB repair proteins, namely ATM, DNA-Pkcs, Ku80 and the MRN complex [279-282]. Studied have revealed that loss of PARP1 results in a hyper-recombination phenotype leading to an increase in spontaneous sister chromatid exchange suggesting a regulational role for PARP1 in DSB repair [283, 284]. *Bryant et al.* have also contributed to the understanding of the role of PARP1 in DSB repair suggesting that PARP1 plays an important role in HR at HU induced collapsed replication forks [285]. Although the function of PARP and PARylation in DSBs is unclear, recent crystal structure analysis of PARP1 suggests that PARP1 can recognise and potentially bind DSBs [286]. *Li et al* proposed that PARylation at DSBs is required for the early recruitment of BRCA1 via the BARD1 BRCT domains to sites of damage [287] however the biological relevance of this observation is not known as BRCA1 still recruits to DSB independent of PARP1 later on in a γH2AX dependent manner [287]. Interestingly, PARP1 has also been recently shown to be involved in recruiting several chromatin remodelling proteins, such as CHD4 and MTA1 involved in DSB repair, to sites of damage [288].

The collective evidence of the function of PARP1 clearly demonstrates that it plays many important roles in the repair of DNA damage, especially DSB repair, however more research is required to elucidate its mechanism and function in DSB repair.

1.5 The role of BRCT domains in DSB repair

The BRCT domain was originally identified in BRCA1 and mutations in the BRCA1 BRCT domains are associated with many breast and ovarian cancers [183, 184, 193]. Since their discovery, BRCT domains have been discovered in over 50 proteins, the majority of which are associated with DNA damage repair [289, 290]. Mutations in the BRCT domains of several other proteins apart from BRCA1, such as NBS1, NBN and MCPH1 have been found in cancer [291-293] which further highlight the importance of the BRCT domains in the DDR. BRCT domains are conserved and found in species ranging from bacteria to humans [289, 290]. Although they don't have any intrinsic enzymatic activity, BRCT domains play a pivotal role in mediating phosphorylation dependent protein-protein interactions essential for DNA repair and cell cycle checkpoint activation [291, 294-297].

The BRCT domains of BRCA1 and BARD1 appear to play an important role in HR. Loss of either the BARD1 or BRCA1 BRCT domains has been shown to abrogate HR indicating that [269, 298], at least for these two proteins, the BRCT domains are extremely important for faithfully repairing DSB.

1.5.1 The structure and function of BRCT domains.

The BRCT domains were first identified as a structural domain in the C-terminus of BRCA1 and the structural fold of a BRCT domain was revealed from crystallography studies carried out in XRCC1 [299]. The BRCT domain is relatively small containing between 90 and 100 amino acids [193]. BRCT domains are present in many scaffold proteins involved in DNA repair and cell cycle checkpoint control. BRCT domains are found as both single units and multiple units in proteins and the ability of BRCT domains to bind phosphorylated proteins has been shown in both single and tandem BRCT domains [300, 301]. For example, the tandem BRCT domains in BRCA1 recognise the phosphorylated peptide motif pS-P-T-F found in three BRCA1 interacting proteins; Abraxas, FANCJ and CtIP [86, 133, 300-303]. It is believed that BRCA1s

ability to recognise and interact with different proteins involved in the DDR is fundamental to its function in DNA repair and is responsible for BRCA1 recruitment to sites of damage. The relevance and function of BRCA1 BRCT interacting proteins will be further discussed latter on in this chapter.

Although the main attribute of BRCT domains is their ability to bind phosphorylated proteins, it has recently become evident that their function is not exclusive to phospho-binding. BRCT domains have been shown to interact with proteins in a phospho-independent manner, bind DNA and also interact with PAR [304]. This highlights the diverse function and specificity of BRCT domains. The structure of a BRCT domain is a globular α/β fold. The fold contains a central 4-stranded β-sheet flanked by a single α-helix on one side and 2 α-helices on the opposite side. This fold is conserved amongst the majority of BRCT domains and deviations in sequence and structure mainly occur in the connecting loops and linkers between BRCT domains. The most highly conserved regions within BRCT domains are found within regions responsible for binding a phospho-peptide and a hydrophobic core [291, 305].

Although the core structure of BRCT domains are well conserved between proteins, the domain architecture can be very varied. As well as the identification of single and tandem BRCTs in proteins, BRCT domains have also been shown to interact with other functional domains increasing their functional capacity and specificity. Single or isolated BRCT domains have been discovered in proteins such as PARP1 and DNA ligase III which contain only one BRCT domain. XRCC1 also contains single BRCT domains as the two BRCT domains in XRCC1 are separated by a long stretch of amino acids making both BRCT domains isolated from each other [299]. The ability of tandem BRCT domains to bind to phosphorylated proteins has been well established in terms of both structure and function however the phospho-binding ability of single BRCT domains remains unclear. Initial evidence that single BRCT domains can interact with phosphorylated peptides came from an *in vitro* study by *Yu et al.*

demonstrating that the single BRCT domains of yeast REV1 and Lig3 preferentially interacted with a phospho ligand library in comparison to a non-phosphorylated counterparts [301]. Crystal structure evidence from TopBP1 BRCT6 protein containing single BRCT domains, revealed that it lacked a functional phospho-binding pocket and therefore it was suggested that it could not bind phospho-peptides on its own [306]. Given the smaller surface area available for binding on a single BRCT compared to that of a tandem BRCT domain it is highly plausible that tandem BRCT domains are more efficient in their capacity to bind phosphorylated proteins.

The canonical structure and packing of tandem BRCT domains was revealed through the crystallisation of the BRCA1 BRCT domains [307]. This study revealed that the packing of the tandem BRCT domain occurred through a hydrophobic interface involving the α2 helix from the N-terminal BRCT domain and the α1' and α3' helices located in the C-terminal BRCT domain. Since then, the conserved configuration of BRCT-BRCT domains has been observed in many other tandem BRCT containing proteins such as BARD1, MDC1 and the 7/8th BRCT domains in TopBP1 [308-311]. Their role in phospho-binding has been well established in comparison to single BRCT domains. Interestingly, variations within tandem BRCT domains also exist as in the tandem BRCT domains of DNA ligase IV which do not fold together as the linker arm between the BRCT domains is distinctively longer than normal tandem BRCT domains. However it is due to this variation in structure that DNA ligase IV is able to bind its partner XRCC4 [297, 312]. In the case of NBS1, its tandem BRCT domains are coupled to its FHA domain which is suggested to attribute a higher level of complexity and specificity to the protein [221, 313].

The crystal structure of tandem BRCT containing proteins such as BRCA1 and MDC1 bound to their phospho-ligands uncovered a bipartite recognition method conserved within the tandem BRCT domains required for phospho-ligand binding. The two regions responsible for binding were described as a pSer/pThr binding pocket in the N-terminal BRCT domain and a hydrophobic binding pocket in the interface of the

two BRCT domains (figure 1.7). The pSer pocket is believed to bind the phosphorylated Ser/Thr residue on the ligand whereas the hydrophobic pocket is expected to bind the peptide at the +3 position in respect to the pSer [116, 291, 310, 314, 315]. The minimal requirement for recognition of a peptide by tandem BRCT domains is a pS/pT-X-X-X motif whereby the amino acid in position +3 dictates the majority of the binding specificity [316].

As well as binding phospho-ligands, the tandem BRCT domains of BRCA1 and TopBP1 have been shown to bind DNA strand breaks and ends *in vitro* [317, 318]. The implication that proteins involved in the repair of DNA damage containing BRCT domains may be able to directly bind DNA ends offers the possibility that BRCT domain proteins may act as damage sensors as well as signal transduces.

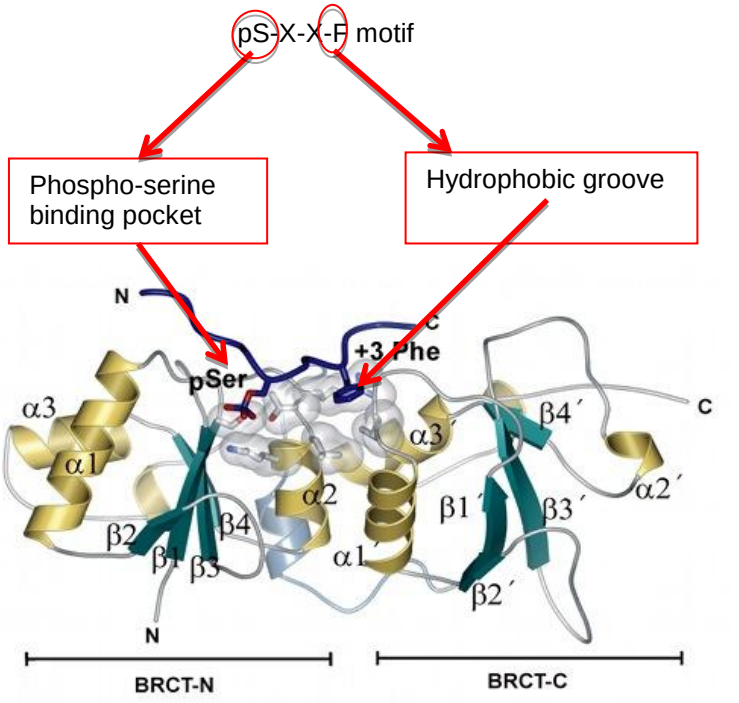

Figure 1.7 BRCT domain phospho-binding pockets
Representative image of the two areas within the BRCA1 tandem BRCT domains which recognise a phosphorylated peptide. The phospho-serine binding pocket binds the pSer whereas the hydrophobic groove is responsible for binding the amino acid residue at position +3 in relation to the pSer. Figure adapted from Williams et al 2004.

1.5.2 The BRCA1 BRCT domains.

Truncations and missense mutations in the BRCT domains of BRCA1 are commonly associated with both breast and ovarian cancers highlighting their importance in the tumour suppressor function of BRCA1 [183, 184]. BRCA1 contains tandem BRCT domains in the C-terminus of the protein. As in most BRCT domains, the structure of the BRCA1 BRCT repeats consist of a central four stranded β-sheet flanked by three α-helices [307, 319]. The two BRCA1 BRCT domains pack together in a head to tail manner to form one domain involving the α1 and α3 of the C-terminal BRCT domain and α2 of the N-terminal BRCT domain [307, 320]. Only the tandem BRCT domains of BRCA1 can bind phosphorylated peptides but not the singly isolated BRCT domains suggesting that the packing of the two BRCT domains is extremely important for binding. The hydrophobic interface between the two tandem BRCT domains is highly conserved in tandem BRCT domain containing proteins and has been shown to be extremely important in binding phospho-ligands. In agreement with this, several breast and ovarian cancers have been identified which contain the M1775R point mutation in the hydrobhobic interface of the tandem BRCT domains of BRCA1 [183, 184]. The phospho-binding pocket of BRCA1 is selective for pSer and is believed to interact with two side chains; S1655 and K1702 in the BRCA1 BRCT domains. The BRCA1 BRCT domains have been shown to selectively bind phosphorylated peptides containing a pS-P-T-F motif. BRCA1 interacts with pS-P-T-F motifs within Abraxas, CtIP and FANCJ and it is thought that the ability of BRCA1 to recognise and bind several different proteins involved in the DDR contributes to BRCA1 function in DNA damage and repair [86, 133, 300, 301, 303]. The M1775 residue within the hydrophobic binding pocket at the interface of the two BRCT domains of BRCA1 is believed to bind the phosphorylated peptide at position +3 in relation to the pSer.

BRCA1 BRCT domains interact with Abraxas, FANCJ and CtIP which are known to be important in the signalling and repair of DSBs. The interaction of BRCA1 as part of the BRCA1 BARD1 heterodimer forms three mutually exclusive complexes

with these proteins called the BRCA1-A,-B and –C complex and the disruption of these complexes has been shown to increase sensitivity to IR and cause genome instability [321] (figure 1.8). Mutations in the BRCT domains of BRCA1, which are known to disrupt phospho-peptide interactions, have been shown to result in both hyper-recombination by *Dever et al.* [321] and defects in HR by *Shakya et al*. [298]. Although the interaction between the BRCA1 BRCT domains and Abraxas, CtIP and FANCJ appear to be fundamental to the repair of DSBs and BRCA1 functions in the DDR and tumour suppression it remains unclear how these complexes function in the DDR. The BRCA1 complexes will now be discussed in terms of their potential function in the DDR and DSB repair.

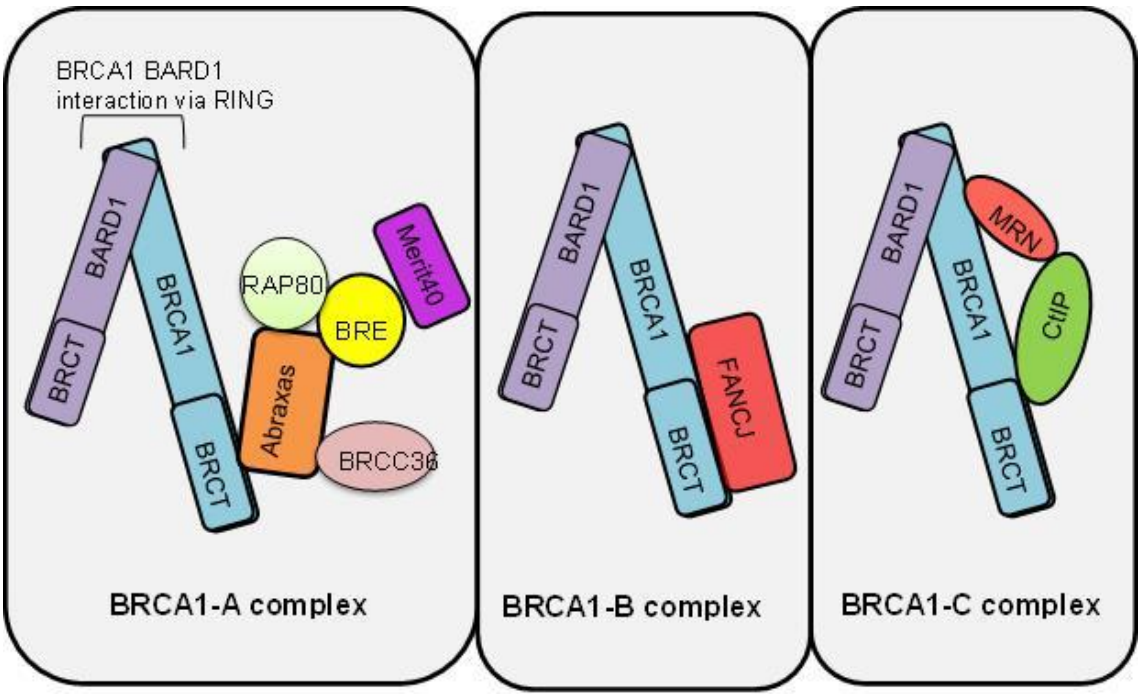

Figure 1.8 The BRCA1 -A, -B and –C complexes
Graphic representation of the different components of the BRCA1 complexes. The BRCA1 BARD1 heterodimer forms the integral core of all three complexes. Abraxas is the main protein to interact with BRCA1 in the BRCA1-A complex whereas FANCJ and CtIP interact with BRCA1 to form the BRCA1-B and –C complexes.

The BRCA1-Abraxas interaction in the DDR.

The BRCA1-A complex is known to contain at least five proteins including RAP80, Abraxas, MERIT40, BRE and BRCC36 [128-130, 132, 133, 302, 303]. Abraxas has been shown to interact with the BRCA1 BRCT domains through a phospho-Serine group in its C-terminus. The residue in Abraxas responsible for binding to BRCA1 is S406 [302]. Abraxas functions as an adapter protein which mediates the interaction of BRCA1 with the BRCA1-A complex and participates in recruiting BRCA1 to sites of damage. It appears that most of the BRCA1 complex members are important for maintaining BRCA1 at DSBs as a decrease in MERIT40 or BRE leads to a reduction in many BRCA1-A complex members and severely reduces the number of BRCA1 foci at sites of damage [322]. BRCA1 is recruited to sites of damage through the BRCA1-A complex as RAP80 recognises K63 ubiquitin chains covalently attached to histone H2AX [2, 323]. It is believed that one of the main functions of the interaction of BRCA1 and Abraxas is to recruit BRCA1 to DSBs. It has been suggested that the function of the BRCA1-A complex at DSB is to regulate the amount of HR at sites of damage as loss of RAP80 and Abraxas results in aberrant hyper-recombination [224, 232].

Ubiquitylation is a key regulatory mechanism in many cellular processes including the DDR [324, 325]. Ubiquitylation is a reversible process and de-ubiquitylation at DNA DSBs is crucial to the regulation of signalling in the DDR. [326-329]. Deubiquitinating enzymes (DUBs) catalyse the removal of ubiquitin from modified proteins. BRCC36 is a DUB found in the BRCA1-A complex and it has deubiquitylating activity specifically towards K63 linked chains [128, 330]. It is important to note that four members of the BRCA1-A complex have ubiquitin binding motifs. Although RAP80 is the only UIM containing protein in this complex with the ability to bind K63 ubiquitin chains, Abraxas, BRCC36 and BRE also contain MPN and UBC domains which can bind long poly ubiquitin chains [132]. Hence it is likely that the BRCA1-A complex is structured in a way which facilitates the DUB activity of BRCC36 attributing a possible regulatory role for the BRCA1-A complex in the repair of DSBs.

The BRCA1-FANCJ interaction in the DDR.

FANCJ is a DNA helicase which interacts with the BRCA1 BRCT domains in a cell cycle dependent manner. During S-phase the C-terminal region of FANCJ, Ser990, becomes phosphorylated and interacts with BRCA1 [294, 301, 331]. It has previously been demonstrated that FANCJ is required for progression through S-phase and for the checkpoint accumulation of cells in G2 in response to DNA damage [86, 301, 332]. FANCJ is involved in the replication stress induced checkpoint via its interaction with TopBP1 [333]. As well as interacting with BRCA1, FANCJ has also been shown to be a member of the Fanconi anaemia complex. Loss of any of the Fanconi anaemia proteins results in the genetic disorder Fanconi anaemia which is associated with several developmental defects and an increased risk of malignancies due to an increased sensitivity to crosslinking agents [331, 334-338].

In vitro studies have shown that FANCJ is an ATP dependent helicase which preferentially unwinds DNA in a 5'-3' direction. FANCJ binds and unwinds DNA substrates that share great similarities with an intermediate step during HR [339, 340]. FANCJ has been shown to be required for HR in human cells as loss of FANCJ results in defective HR and chromosome instability after damage by intercrosslinking agents [331]. DT40 cells lacking FANCJ are extremely sensitive to intercrosslinking agent and show genome instability after damage, however they do not exhibit the same HR defects seen in human cells with the loss of FANCJ [331, 341]. This may be partially due to the fact that avian FANCJ lacks the Ser990 residue which interacts with BRCA1 hence in DT40 cells, BRCA1 and FANCJ do not interact (Sequence alignment in PubMed). Although the exact function and mechanism remains unclear, it is believed that BRCA1-FANCJ are essential for DNA repair especially during replication repair, checkpoint activation and tumour suppression [301, 342, 343].

The BRCA1-CtIP interaction in the DDR.

The BRCA1-C complex contains the MRN complex as well as CtIP. The formation of this complex is cell cycle dependent and interacts during S and G2 phase where the BRCT domains of BRCA1 interact with the phosphorylated Ser327 residue on CtIP [86, 87]. As previously discussed, CtIP plays a crucial role in the end resection at DSBs, an early requirement for HR [55, 222]. By interacting and stimulating the nuclease activity of the MRN complex, CtIP promotes HR by end resection. The requirement of BRCA1 to interact with CtIP for efficient repair of DSBs by HR remains controversial. Work carried out by *Yun et al*, in DT40 cells harbouring a CtIP mutant unable to interact with BRCA1 suggested that this interaction was necessary for HR [344]. However further studies carried out *by Reczek et al*, and *Nakamura et al*, suggests that this interaction is not required for HR repair [225, 345]. Much further research is required to investigate the functional relevance of the BRCA1-CtIP interaction.

The biological and functional relevance of the BRCA1 complexes remains somewhat unclear in relation to the function of BRCA1 in the repair of DSBs via HR. However, the fact that many breast and ovarian cancers contain point mutations in the BRCA1 BRCT domains preventing phospho-protein binding clearly highlights the importance of these interactions as there are no other proteins known to interact with the BRCA1 BRCT domains. Evidence suggesting that loss or point mutations in the BRCT domains of BRCA1 show defects in HR augments the importance of the BRCA1 BRCT domains in DSB repair.

1.5.3 The BARD1 BRCT domains.

The crystal structure of BARD1 BRCT domains were elucidated by *Birrane et al*. in 2007 [311]. The BRCA1 and BARD1 BRCT domains are structurally very similar. BARD1 also contains tandem BRCT domains at the C-terminus of the protein which are predicted to bind phospho-peptides. The crystal structure of BARD1 BRCT domains revealed a very similar fold with those of BRCA1 and MDC1 with a central

four stranded β-sheet flanked by three α-helix. As in the tandem BRCA1 BRCT domains the two BRCT domains are linked by a central α-helix [311]. It is of note that no phosphorylated peptides are known to interact with the BARD1 BRCT domains however, using a synthetic peptide library it was predicted that the BARD1 BRCT domains recognise ligands with the following motif; pSer-D/E-D/E-E [346] which is different to that of BRCA1. The two BRCT domains are closely packed revealing a potential phospho-protein interacting pocket and a hydrophobic pocket suggested to bind a ligand at the +3 position. The phospho-binding pocket is formed from Ser575, Gly576, Thr617 and Lys619 residues which structurally conform to the standard binding pocket in BRCA1. The hydrophobic pocket at the interface of the two BARD1 BRCT domains is lined with Ser616, Met621, His685, His686, and Ile764 residues. His686 in the BARD1 BRCT domains corresponds with Met1775 in the BRCA1 BRCT domains and is predicted to be responsible for interacting with the ligand at the +3 position in relation to the pSer. Interestingly the hydrophobic pocket has a negative electrostatical potential at neutral pH and requires a more acidic environment to protonate His686 and positively charge the hydrophobic pocket. This suggests that the potential of BARD1 BRCT domains to bind a ligand may be greatly influenced by local changes in pH [311].

Although the BARD1 BRCT domains have not been shown to interact with any proteins to date, the importance of the BARD1 BRCT domains is highlighted in several breast and ovarian cancers which carry mutations and truncations in the BARD1 BRCT domains [213, 214, 266]. Further evidence of the importance of the BARD1 BRCT domains in the DDR was evident from studies carried out by *Westermark et al.* and *Laufer et al*. which demonstrated that in the absence of the BARD1 BRCT domains HR was severely compromised [266, 269]. Interestingly *Li et al* have very recently shown that the BARD1 BRCT domains are important for the very early recruitment of BRCA1 and BARD1 to DSBs initiated by the interaction of the BARD1 BRCT domains with PAR [287]. This work suggests a functional role for the BARD1 BRCT domains in

recruitment at DSBs. However, the functional relevance of this process remains to be determined. Very little is known about the BARD1 BRCT domains or their function in the DDR however this evidence strongly implicates a role for the BARD1 BRCT domains in the faithful repair of DSBs via HR.

1.6 Aims

The aim of this thesis is to investigate the contribution of the BARD1 BRCT domains in the DDR. Using *Bard1* DT40 cell lines reconstituted with BARD1ΔBRCT, the first aim is to confirm their role in HR using Homologous recombination assays and assess their sensitivity to DNA damaging agents. As BARD1 is bound to BRCA1 in the BRCA1 complexes, the contribution of the BARD1 BRCT domains in the formation of the BRCA1 complexes will be investigated. Recent evidence suggests that the BARD1 BRCT domains are important for the early recruitment of BRCA1 to DNA damage sites, this suggests that the BARD1 BRCT domains may be important for localisation to DSBs. The function of the BARD1 BRCT domains in relation to localisation to DSBs within the cell will be studied using both live microscopy recruitment to sites of damage and fixed cell microscopy. BRCT domains serve as phospho-interacting domains, however there are no known proteins which interact with the BARD1 BRCT domains. This thesis will also attempt to elucidate any potential BARD1 BRCT domain interacting proteins which could implicate a functional role for BARD1 in response to DNA damage.

In the final results chapter of this thesis the functional role of the ubiquitin ligases RNF8 and RNF168 in the signalling at DNA DSBs will be investigated. This will be carried out by identifying point mutations in the RING domains of RNF8 and RNF168, which render the proteins ubiquitin ligase dead, and assessing the contribution of the ubiquitin ligase activity of both proteins to the DDR.

Chapter 2 Materials and Methods

Materials

2.1 General reagents and Buffers

2.1.1 General Reagents

Company	Catalogue #	Product
VWR UK	A1493.0010	Kanamycin [10g]
Melford	A0104	Ampicillin [25g]
SIGMA	C0378-25G	Chloramphenicol [25g]
In house	Core reagent	Lysogeny broth (LB)
UK VWR	28029.260	di-Sodium hydrogen phosphate 2.H_2O
UK VWR	103156X	Tris Base
UK VWR	27810.295	Sodium Chloride
UK VWR	443852A	Dithiothreitol (DTT)
UK VWR	436992S	Magnesium Chloride
UK VWR	24387.292	Glycerol
UK VWR	20302.260	EDTA disodium salt 2.H2O
Melford Labs	E1102	EGTA
UK VWR	28829.296	Tween 20
UK VWR	28244.262	Sodium Hydroxide Pellets
UK VWR	20821.330	ethanol
UK VWR	20104.334	Acetic acid (glacial) 100% (17.4M)
SIGMA	09830-500G	Ammonium hydrogen carbonate
UK VWR	22317.26	Calcium Chloride 2.H2O
UK VWR	22711.244	Chloroform
Melford Labs	B2001	HEPES
UK VWR	20254.401	Hydrochloric acid 32 % (10.2M)
Sigma Aldrich	I8896-100ML	Igepal CA630 (NP40)
Melford Labs	B2004	PIPES
UK VWR	26764.260	Potassium Chloride
UK VWR	20842.330	2-Propanol (iso-propanol)
UK VWR	27727.231	di-Sodium tetraborate decahydrate
UK VWR	27778.260	Sodium Bicarbonate
UK VWR	441514A	Tris Hydrochloride

UK VWR	28817.295	Triton X 100
SIGMA	B5002-100MG	BrdU
Qiagen	19101	RNase A (100mg/ml)
Melford Labs	Y1333	Yeast Extract [500g]
Melford Labs	T1332	Tryptone
Roche Applied Science	05892970001	c0mplete ULTRA, mini, EASYpack [30 tablets]
Roche Applied Science	04906837001	PhosStop [20 tablets]
Fisher	PN87785	Halt Protease Inhibitor Cocktail, EDTA-Free (100X) [1ml]
Fisher	PN78420	Halt Phosphatase Inhibitor Cocktail (100X) [1ml]
UK VWR	70746-3	Benzonase [10K Units]
Fisher	PN88701	Universal Nuclease for Cell Lysis
SIGMA	T1895	Thymidine

2.1.2 General Buffers

Binding Buffer	**40mM Imidazole, 20mM HNa_2PO_4, 500mM NaCl.**
Elution buffer	500mM Imidazole, 20mM HNa_2PO_4, 500mM NaCl
Dialysis Buffer	500mM NaCl, 50mM Tris-CL, 2mM DTT
MOPS Buffer	50 mM MOPS, 50 mM Tris Base, 0.1% SDS, 1 mM EDTA, pH 7.7
Transfer Buffer	1x NuPAGE® Transfer Buffer, 10-20% Methanol, 1x Antioxidant
TEA ubiquitin ligase buffer	Triethanolamine
50X TAE buffer	2M Tris-Base, 1M Acetic acid, 50mM EDTA
SOC	0.5% Yeast Extract, 2% Tryptone, 10 mM NaCl, 2.5 mM KCl, 10 mM MgCl2, 10 mM MgSO4, 20 mM Glucose
Lysis Buffer	20mM Tris-Base (pH 7.5), 0.14M NaCl, 10% v/v glycerol, 0.01% v/v NP40, 2mM $MgCl_2$, 1X protease and phosphotases, Benzonase 50U/ml
Wash Buffer	50mM Tris-Base (pH 7.5), 0.5M NaCl, 20mM EGTA, 1% v/v Triton X, 1X protease and phosphotases.
Isotonic lysis buffer	10 mM Tris HCl pH7.5, 2 mM MgCl2, 3 mM CaCl2, 320 mM sucrose, 1 mM DTT, 1x protease inhibitor cocktail
Extraction	20 mM HEPES pH 7.7, 1.5 mM MgCl2, 420 mM NaCl , 0.2 mM EDTA,

buffer	25% glycerol, 1 mM DTT, 1x protease inhibitor cocktail
Ce buffer	10mM HEPES, 60mM KCl, 1mM EDTA, 0.075% NP40, 1mM DTT, 1X protease and phosphotases
NE buffer	20mM Tris-Base, 420mM NaCl, 1.5mM $MgCl_2$, 0.2mM EDTA, 25% v/v glycerol, 1X protease and phosphotases
Blocking Buffer	0.5% v/v Tween, 1% w/v BSA in PBS
CSK Buffer	0.1M NaCl, 0.3M Sucrose, 10mM PIPES (pH7), 3mM $MgCl_2$, 1mM EGTA

2.2 Molecular Biology Methods

2.2.1 DNA extraction and purification

UK VWR	**VWRID6943-02**	**E.Z.N.A. Plasmid Miniprep Kit I (V-Spin)**
UK VWR	VWRID6942-02	E.Z.N.A. Plasmid Miniprep Kit I (Q-Spin)
UK VWR	VWRID6905-03	E.Z.N.A. Fastfilter Plasmid Midiprep Kit
UK VWR	VWRID6915-03	E.Z.N.A. Fastfilter Endo-free Midiprep Kit
UK VWR	VWRID6924-03	E.Z.N.A. Fastfilter Plasmid Maxiprep Kit
UK VWR	VWRID5032-03	EZNA SQ Blood DNA Purification Kit
UK VWR	VWRID2500-01	EZNA Gel Extraction Kit (V-Spin)
UK VWR	VWRID6294-01	EZNA MicroElute Gel Extraction Kit (V-Spin)
UK VWR	VWRID6492-01	EZNA Cycle Pure Kit (V-Spin)
UK VWR	VWRID6293-01	EZNA MicroElute Cycle Pure Kit (V-Spin)
UK VWR	VWRID6296-01	EZNA MciroElute DNA Clean-up Kit (V-Spin)
Qiagen	12163	QIAGEN Plasmid Maxi Kit

2.2.2 Restriction endonuclease digests.

DNA digestions were carried out using either New England Biolabs digestion enzymes or Fermentas Fast digest enzymes.

2.2.3 DNA Ligations

Fisher	FQ-K1422	Rapid DNA Ligation Kit

2.2.4 Bacterial *Transformations*

Invitrogen	18265-017	Subcloning Efficiency DH5α Competent Cells

2.2.5 Plasmids and primers used

Plasmids

Plasmid name	**Source**
pcDNA5 FRT TO N GFP	John Rouse
pcDNA5 FRT TO delBRCT hBARD N GFP	John Rouse
pcDNA5 FRT TO hBARD N GFP	John Rouse
pOG44	John Rouse
pSV2-Fok1mCherryLacI	Rodger Greenberg
pSV2-Fok1D450AmCherryLacI	Rodger Greenberg
pEYFP C1-ggRNF168	Vibe Oestergaard
pEGFP C1-hsRNF8	Vibe Oestergaard
PcB/His BARD1 K619M	Created in Lab
PcB/His BARD1 S575F	Created in Lab
PcB/His BARD1 S575F/K619M/H686R	Created in Lab
PcB/His BARD1 del BRCT	Created in Lab
PcB/His BARD1 FL	Created in Lab
PcB/His BRCA1 M1775R	Created in Lab
PcB/His BRCA1 K1702M	Created in Lab
PcB/His BRCA1 S1655F	Created in Lab
PcB/His BRCA1 del BRCT	Created in Lab

PcB/His BRCA1 FL	Created in Lab
PcB/His BARD1 H686R	Created in Lab
pcDNA5 FRT TO hBARDS575F/K619M/H686R N GFP	Created in Lab
pcDNA5 FRT TO hBARDS575F N GFP	Created in Lab
pcDNA5 FRT TO hBARDK619M N GFP	Created in Lab
pcDNA5 FRT TO hBARDH686R N GFP	Created in Lab
pcDNA5 FRT TO hBARDS575F/H686R N GFP	Created in Lab
pcDNA5 FRT TO hBARDS575F/K619M N GFP	Created in Lab
pcDNA5 FRT TO hBARDK619M/H686R N GFP	Created in Lab
pcDNA5 FRT TO hBARDL107P N GFP	Created in Lab
pM3Not hBARDdeltaBRCT	Created in Lab
pM3Not hBARDS575F/K619M/H686R	Created in Lab
pM3Not hBARDS575F	Created in Lab
pM3Not hBARDK619M	Created in Lab
pM3Not hBARDH686R	Created in Lab
pM3Not hBARDL107P	Created in Lab
pM3Not hBRCA1S1655F/K1702M/M1775R	Created in Lab
pM3Not hBRCA1S1655F	Created in Lab
pM3Not hBRCA1K1702M	Created in Lab
pM3Not hBRCA1M1775R	Created in Lab
pM3Not hBRCA1S1655F/M1775R	Created in Lab
pM3Not hBRCA1K1702M/M1775R	Created in Lab
pM3Not hBRCA1S1655F/K1702M	Created in Lab
pVP16 Abraxas	Created in Lab
pVP16 Abraxass406a	Created in Lab
eGFP-hsRNF8i405a	Created in Lab
eYFP-ggRNF168i18a	Created in Lab
POPTH RNF8	Created in Lab

POPTH RNF8i405a	Created in Lab
POPTH RNF168	Created in Lab
POPTH RNF168i18a	Created in Lab
pM3 Not	Clontech
pVP16	Clontech
pM3Not - hs BARD1	Created in Lab
pM3Not - hs BRCA1 BRCT (4585-5589)	Created in Lab
pM3Not - hs BARD1 (aa 1-119)	Created in Lab
pVP16- Y3Not - hs BRCA1 (aa 1-109)	Created in Lab
pVP16-Y3Not - hs BACH1 aa 888- 1249	Created in Lab
pVP16-Y3Not - hs BRCA1 big RING (aa 1- 250)	Created in Lab
pM3Not - hs BARD1 big RING (aa 14- 186)	Created in Lab
pVP16-Y3Not - hs FANCJ S990D	Created in Lab
pVP16 -Y3 - hs CtIP	Created in Lab
pVP16- Y3 - A hs CtIP S327A	Created in Lab
pVP16-Y3Not - hs FANCJ	Created in Lab
p- ISce I expression vector	Created in Lab

Table 2.1 Plasmids generated and used.

Primers

EcoRI miBrca1 R	TACAGAATTCAGCCTTTTCTACATTCATTCTG
BRCA2R EcoRV	GATCGATATCTTAGAGCTCCTCTTGAGATGGGTAGTT
BRCA1R EcoRV	GATCGATATCTCAGTAGTGGCTGTGGGGGAT
BRCA1F Acc651	GATCGGTACCGCCACCATGGATTTATCTGCTCTTCG
BRCA1F BsiWI	GATCCGTACGGCCACCATGGATTTATCTGCTCTTCG
BARD1 Kpn1 1R	ATAGGTACCTCAGCTGTCAAGAGGAAGCAACTC
BARD1delpm3f	ATCTGTCGACCATGCCGGATAATCGGCAGCCG

BARD1delpm4R	ATCTCTAGAATCAATCCCTACGCTGCCCAGTGTTC
delta BARD1 1R	ATACCCGGGTCAATCCCTACGCTGCCCAGTGTT
ggBARD1 1R	CTGGCAATTGGGTTACTACCAGGG
ggBARD 1F	GGTGCAAGACATGCAGATAAACCG
hsBARD1 1R	TTCACAGCCATATTGGGCAACAG
hs BARD1 1F	TGTGGTTTAGCCCTCGAAGTAAGAA
BRCA1 S1655F	AAAGAATGTCCATGGTGGTGTTTGGCCTGACCC
BRCA1 M1775R	GCTATGGGCCCTTCACCAACAGGCCCACAGATC
BRCA1 K1702M	TGTGTGTGAACGGACACTGATGTATTTTCTAGGAATTGCGGG
BARD1 H686R	GGGAACCTTCAAACACCGTCCAAAGGACAACCTTA
BARD1 S575F	GACCTCTTGTACTTATAGGCTTTGGGCTGTCTTCAGAACAAC
BARD1 K619M	GCAGTTCAAAGTACCTTGATGTGTATGCTTGGGATTCTC
BARD1L107P R	CAAATTTCGAAGCTTACTACAAGGTTGAATCATGCTGTCCAGTTG
BARD1L107P F	CAACTGGACAGCATGATTCAACCTTGTAGTAAGCTTCGAAATTTG
VO233	TTAGGCATTGCTCTGCTGAGGTTTTGC
VO230	CCTCTTTTTCCCACGTTCCTGTCTCC
VO231	GAATTACAGATGGTATGGTTGCACGGC
VO232	ACACGCTCTCTGGTGCTGGATAACTGC
ggRNF168 cD 1R	CAAGAACCTTTCCGACCCTTGTGG
ggRNF168 cD 2F	GAGGTCTTTGTGGAGCCCGTGAC
RNF8 2R cD	GCAATTGTCCAGAACCAAAGAGTACGT
RNF8 cD 1F	TCTGCCCCCTGATGATTTCTCGA
mutIggRNF168 1R	AGGAATCTACTGACGGAGACGGTTCGAACGTACCTCCAG
mutIggRNF168 1F	TCCTTAGATGACTGCCTCTGCCAAGCTTGCATGGAGGTC
ABRAs406a 1R	CCGCTCAAAATGTAGGAGCCCGTGAATATTCACCAAA
ABRAs406a 1F	TTTGGTGAATATTCACGGGCTCCTACATTTTGAGCGG
hRNF8 1F	CATAGATCTGGGGAGCCCGGCTTCTTCG
hRNF8 1R	GATGGTACCCGGTCTTCAGAACAATCTCTTTGC

hRNF8dI-1R(mut)	TGAAGTATTCTGAACAAGCAATACATTGGAGCTCATTCTCTAGCACATCAT
hRNF8dI-1F(mut)	ATGATGTGCTAGAGAATGAGCTCCAATGTATTGCTTGTTCAGAATACTTCA

Table 2.2 List of Primers used

2.2.6 RNA and cDNA preparation and amplification

AMS Bio	**CS-104B**	**RNA Bee [100ml]**
UK VWR	VWRIPR032	DEPC Treated Water (RNase free)
Fermentas	K1631	RevertAidTM H Minus First Strand cDNA Syntheis Kit
Fermentas	K1651	Maxima H Minus First Strand cDNA Synthesis Kit
UK VWR	22711.244	Chloroform

2.2.7 Polymerase Chain reaction (PCR)

Fermentas	**R0192**	**dNTP Mix, 10mM each**
Fermentas	EP0702	DreamTaqTM DNA Polymerase (5u/µl)
Fermentas	EP0712	DreamTaqTM Green DNA Polymerase (5u/µl)
Fermentas	F-530S	Phusion® High Fidelity DNA Polymerase
Star Lab UK	A1402-3700	8 Strip PCR Tube (0.2ml)

2.2.8 Site directed mutagenesis

Agilent (Stratagene)	**210518**	**QuikChange Lightening Mutagenesis Kit**
Agilent (Stratagene)	210515	QuikChange Lightening Multi Mutagenesis Kit

2.2.9 DNA Agarose gels electrophoresis

UK VWR	**730-2961**	**GelGreen Nucleic Acid Stain in water (10,000x)**
Fermentas	SM0242	GeneRulerTM 100bp DNA Ladder
Fermentas	SM0311	GeneRulerTM 1kb DNA Ladder
Melford	MB1200	Agarose

2.3 Protein methods and Biochemical Materials

2.3.1 Protein quantification by Bradford assay

Perbio Science	**23200**	**Coomassie (Bradford) Protein Assay Kit**
VWR UK	634-2501	1.5-3.0 ml Semi Micro Cuvettes (PS) - 340-900 nm

2.3.2 Polyacrylamide gel electrophoresis (PAGE)

Invitrogen	**NP0335BOX**	**NuPAGE® Novex® 4-12% Bis-Tris Gel 1.5 mm, 10 well**
Invitrogen	NP0004	NuPAGE® Sample Reducing Agent (10X)
Invitrogen	NP00061	NuPAGE® Transfer Buffer (20X)
Invitrogen	NP0005	NuPAGE® Antioxidant
Invitrogen	NP0008	NuPAGE® LDS 4X LDS Sample Buffer
Fisher Scientific	PN26634	SpectraTM Multicolor Broad Range Protein Ladder
Perbio Science	26625	SpectraTM Multicolor High Range Protein Ladder
Perbio Science	26628	SpectraTM Multicolor Low Range Protein Ladder
Fermentas	R0571	PageBlueTM Protein Staining Solution
Perbio Science	26616	PageRulerTM Prestained Protein Ladder
Perbio Science	26614	PageRulerTM Unstained Protein Ladder
UK VWR	0670-500G	MOPS

2.3.3 PAGE staining

Perbio Science	**24612**	**GelCode SilverSNAP Stain Kit II**
Thermo	24620	PageBlue Protein Staining Solution

2.3.4 Western Blotting

SevernBiotech	**40-2010-01**	**10% Sodium Azide**
Perbio Science	23228	BCA Protein Assay Reagent A
Perbio Science	23224	BCA Protein Assay Reagent B
Perbio Science	32106	Pierce ECL Western Blotting Substrate
Konica Minolta	A9KN	A Plus Medical Film - 18x24cm
UK VWR	730-3230	Kodak Biomax MS-1 X ray Film
UK VWR	730-3241	Kodak BioMax MR-1 X ray film
Labtech Ltd.	CAXOSGK01824	Type B X ray Cassette - 18 x 24 cm
Labtech Ltd.	1212604	Pure Nitrocellulose Supported - 0.45µm
Millipore	IPFL00010	Immobilon-FL PVDF Transfer Membrane
Insight Biotechnology	sc-2955	Chicken anti-rabbit IgG-HRP
Insight Biotechnology	sc-2371	Bovine anti-mouse IgG-HRP
Insight Biotechnology	sc-2313	Donkey anti-Rabbit IgG-HRP
Insight Biotechnology	sc-2005	Goat anti-Mouse IgG-HRP
Insight Biotechnology	sc-2020	Donkey anti-goat IgG-HRP
Insight Biotechnology	sc-2064	Goat anti-mouse IgM-HRP
LI-COR	926-68071	IRDye 680RD Goat anti-Rabbit IgG
LI-COR	926-32210	IRDye 800CW Goat anti-Mouse IgG
LI-COR	926-68074	IRDye® 680RD Donkey anti-Goat IgG

Anitodies for Western blot and microscopy

Antibody	Dilution	Source
CHD4 (Mouse)	1:1000	Abcam (ab54603)
HUWEI (Rabbit)	1:1000	Bethyl (A300-486A)
Abraxas (Rabbit)	1:500	Bethyl (A302-180A)
RbBP7 (Rabbit)	1:1000	Bethyl (A300-959A)
MTA2 (Rabbit)	1:1000	Bethyl (A300-395A)
UBC9 (Rabbit)	1:200-500	Abgent (AP1064a)
LSD1 (Rabbit)	1:1000	Abcam (ab17721)
ARF1 (Rabbit)	1:1000	Abcam (ab32524)
GAPDH (Mouse)	1:2000	Gene Tex (GTX627408)
CtIP (Goat)	1:500	Santa Cruz (sc-5970)
CtIP (Rabbit)	1:500	Bethyl (A300-488A)
FLAG® M2 (Mouse)	1:1000	Sigma (F1804-1MG)
Fancj (Mouse)	1:1000	R&D systems (MAB6496)
BRCA1 (Rabbit)	1:500	Santa Cruz (sc-642)
BRCA1 (Mouse)	1:200	Calbiochem (OP92-100UG)
BARD1 (Rabbit)	1:500	Santa Cruz (sc-11438)
GFP (Mouse)	1:1000	Santa Cruz (sc-53882)
Histone H2A (Rabbit)	1:1000	Abcam (ab13923)
P84 (Mouse)	1:1000	GeneTex (GTX70220)
His-probe (Rabbit)	1:1000	Santa Cruz (sc-803)
RAD51 (Ab-1) (Rabbit)	1:300	Calbiochem (PC130)
RPA (Ab-2) (Mouse)	1:300	Calbiochem (NA18)
Phospho H2AX (Mouse)	1:500	Millipore (05-636)
Phospho H2AX (Rabbit)	1:500	Millipore (07-164)

Table 2.3 List of Antibodies

2.3.5 Protein Purification

GE Healthcare	**17-5286-01**	**HisTrap FF crude column 5mls**
Life Technologies	C6000-03	**BL21(DE3) Chemically Competent *E. coli***
Fermentas	R0391	**IPTG [1g]**
UK VWR	286874D	Imidazole
Fisher	PN87785	Halt Protease Inhibitor Cocktail, EDTA-Free
Perbio Science	87731	Slide-A-Lyzer G2 Dialysis Cassettes, 10K MWCO, 15mL

2.3.6 Ubiquitin ligase activity assay

Perkin Elmer	**NEX404010UC**	**I-125 Ubiquitin [10µCi/100µl]**
GE Healthcare	27-1006-01	ATP
Sigma	U5507-1MG	Ubiquitin
New England Biolabs	M2502S	Histone H2A Human (1mg/ml)
New England Biolabs	M2505S	Histone H2B Human (1mg/ml)
New England Biolabs	M2503S	Histone H3.1 Human (1mg/ml)
New England Biolabs	M2504S	Histone H4 Human (1mg/ml)
Boston Biochem	U-100H	Human Recombinant Ubiquitin
Boston Biochem	E-305	Ubiquitin Activating Enzyme (UBE1)
Boston Biochem	E2-616	UbcH5a/UBE2D1

2.3.7 Mammalian two hybrid analysis

Dual-Luciferase® Reporter Assay System

Promega	E1910	Dual-Luciferase® Reporter Assay System

2.3.8 GFP Pull down

Thermo scientific	**22585**	**DSP(Dithiobis[succinimidyl propionate])**
Chromotek	gta-20	GFP-Trap® coupled to **agarose beads**
Cambio	CA-1713-2105	Agarose beads 2% cross-linked
SIGMA	T7660-5G	Tetracycline HCl [5g]

2.4 Cell Culture Materials

2.4.1 Tissue Culture

SIGMA	**C5405-500ML**	**Chicken Serum**
BIOSERA	S07859S180T/500	FBS, Tet Free, EU Approved
BIOSERA	FBS-6911-BRI10700	FBS, EU Approved
BIOSERA	FBS-8033-BRI10700	FBS, EU Approved
SIGMA	D2650-100ML	DMSO - Tissue Culture Grade
SIGMA	T4049-500ML	1 x Trypsin-EDTA
Invitrogen	15070063	Penicillin-Streptomycin, liquid (5000U/ml)
Invitrogen	31985047	Opti-MEM® I Reduced Serum Medium
Invitrogen	41966029	DMEM media
Invitrogen	21875034	RPMI
UK VWR	479-3200	Mr Frosty [1/box]
Roche Diagnostics	05651786001	CASY Clean [3 x 500ml]
UK VWR	HECH1102/1	Medicine Cup - 30ml Clear [800]
UK VWR	HECH1102/15	Medicine Cup Lid [1000]
Roche Diagnostics	05651808001	Casyton [10l]
UK VWR	391-8845	10 Cryovials [200/box]
SOURCE BIOSCIENCE	ant-gn-1	G418 (Neo) [10mls (100mg/ml)]

2.4.2 DT40 Transient transfection

LONZA	VCA-1002	Amaxa Nucleofection Kit T (DT40) [25 rxn]

Equipment; Lonza; Nucleofector™ 2b Device

2.4.3 DT40 Stable transfection

UK VWR	732-2269	Electroporation Cuvette - 4mm [50]

Equipment; Bio-rad; Gene Pulser® II

2.4.4 Transient and stable transfection of adherent cells (human)

Roche Applied Science	**06366236001**	**X-tremeGENE HP Transfection Reagent**
Roche Applied Science	06365779001	X-tremeGENE 9 Transfection Reagent
SIGMA	C7983-50EA	Cloning Cylinder - 4.5mm
SIGMA	Z273554-1EA	Dow Corning® high-vacuum silicone grease
SIGMA	Z374458-100EA	Cloning Discs - 5mm [100/pkt]
SOURCE BIOSCIENCE	ant-hg-1	Hygromycin B (☠) [10mls (100mg/ml)]

2.4.5 Colony survival assay

Invitrogen	**32500043**	**DMEM/F-12 Powder with Glutamine**
SIGMA	M0512-500G	Methylcellulose 4000cP
Life Technologies	25080060	Sodium Bicarbonate 7.5% solution
Axon Medchem	Axon 1464	Olaparib
UK VWR	400046-5	Hydroxyurea

2.4.6 siRNA knockdown in human cells

Thermo Scientific	T-2001-02	DharmaFECT 1 Transfection Reagent
Thermo Scientific	L-003461-00-0005	ON-TARGETplus Human BRCA1 (672) siRNA - SMARTpool

2.5 Flow cytometry methods

2.5.1 Flow cytometry and FACS

BD Pharmingen	**555627**	**Anti-BrdU (Mouse) antibody**
BD Pharmingen	554001	Goat anti-mouse FITC antibody
UK VWR	734-0000	5ml round bottom tubes (FACS) (BD 352008) [1000/box]
Sigma	P4170-10MG	Propidium Iodide [10MG]

2.6 Microscopy methods

2.6.1 Immunocytochemistry

VWR UK	**631-1580**	**Round Coverslip - 18mm ø [10 x 100]**
VWR UK	631-1582	Round Coverslip - 22mm ø [10 x 100]
VWR UK	631-0107	Polysine Slide [72]
VWR UK	631-1578	Round Coverslip - 13mm ø [10 x 100]
Science Services Gmbh	157-8-100	8% Paraformaldehyde [100mls]
Invitrogen	D3571	DAPI dilactate [10mg]
Invitrogen	P36930	ProLong® Gold antifade reagent [10mls]
UK VWR	631-1507	Microscope Slide Box for 25 slides
Invitrogen	A-11001	Alexa Fluor® 488 Goat Anti-Mouse IgG
Invitrogen	A-21042	Alexa Fluor® 488 Goat anti-Mouse IgM
Invitrogen	A-11008	Alexa Fluor® 488 Goat Anti-Rabbit IgG

Invitrogen	A-11078	Alexa Fluor® 488 Rabbit Anti-Goat IgG
Invitrogen	A-11004	Alexa Fluor® 568 Goat Anti-Mouse IgG
Invitrogen	A-11079	Alexa Fluor® 568 Rabbit Anti-Goat IgG
Invitrogen	A-11011	Alexa Fluor® 568 Goat Anti-Rabbit IgG
Invitrogen	A-11012	Alexa Fluor® 594 Goat Anti-Rabbit IgG
Invitrogen	A-21238	Alexa Fluor® 647 Goat anti-Mouse IgM
Invitrogen	A-21244	Alexa Fluor® 647 Goat Anti-Rabbit IgG
Invitrogen	A-21235	Alexa Fluor® 647 Goat Anti-Mouse IgG
Grace Biolabs	664204	Silicone isolators
Ibidi	81166	Micro 35mm dish Grid 500
Invitrogen	21063-029	DMEM, HEPES, no phenol red
Invitrogen	C10388	Click-iT® EdU Alexa Fluor® 555 Imaging Kit

Methods

2.7 Molecular Biology Methods

2.7.1 DNA extraction and purification

All purification of circular plasmids was performed using E.Z.N.A. Miniprep kit, Midiprep kit and Maxiprep kit. The Qiagen Plasmid Maxi kit was used solely in the purification of the ISce1 plasmid as the ISce1 plasmid could not be purified using E.Z.N.A Maxiprep kit. Linearised plasmid DNA was purified using either E.Z.N.A PCR purification or gel extraction kits.

Genomic DNA from DT40 cells purified using EZNA SQ BLOOD DNA PURIFICATION KIT, 3-5x10^6 cells were pelleted by centrifugation at 300g for 5mins and the medium was aspirated leaving behind 30µl. The pelleted cells were resuspended in the residual liquid. 600µl of WTL buffer was added to the cell suspension and mixed by pipetting. 3µl of RNAse A was added to the mix and inverted 20 times, then incubated at 37° for10mins. Once the lysate cooled to RT 200µl of PCP buffer was added, vortexed for 30sec and incubated on ice for 5mins. The lysate was then centrifuged at 14000g for 3mins. The supernatant was transferred to a new 1.5ml eppendorf and 600µl of isopropanol was added and mixed by inverting. The lysate was then centrifuged at 14,000g for 1min, the supernatant was aspirated and the DNA pellet was washed twice with 70% ethanol. After the wash step the DNA pellet was allowed to dry before resuspension with 30-50µl 8mM Sodium Hydroxide to aid the solubility of the DNA.

2.7.2 Restriction endonuclease digests

Restriction endonuclease digests were carried out using either New England Biolab endonucleases or Fast digest Fermentas endonucleases. Digestions were carried out according to manufacturer's protocols. Generally reactions were carried out in a final volume of 30µl. For diagnostic digestions 1µl of miniprep DNA was digested for 1hr at 37°C. For cloning purposes, 5-7µg of DNA was digested o/n at 37°C. 1 unit of alkaline

phosphatase per 1µg of DNA was added to vectors for the same duration as the endonuclease digestion.

2.7.3 DNA Ligations

DNA ligations were performed using Rapid DNA Ligation Kit from Fisher, according to manufactures guidelines. Generally 50ng of vector DNA and sufficient insert DNA to give a 3:1 molar ratio of insert to vector were used per reaction. Reactions were incubated at room temperature for 30mins.

2.7.4 Bacterial Transformations

Bacterial transformations were performed using Subcloning Efficiency DH5α Competent Cells (Invitrogen) as follows; 100µl of ice cold chemically competent *Escherischia coli* suspension was mixed in a 1.5 ml eppendorf with 10-20µl ligation reaction or 300ng uncut plasmid DNA, incubated on ice for 20 min, incubated at 42°C for 45 s to heat-shock and transferred immediately to ice. After 1min, 700µl SOC media (2% tryptone, 0.5% yeast extract, 10 mM NaCl, 2.5 mM KCl, 10 mM MgCl2, 10 mM MgSO4, and 20 mM glucose) was added to the transformation and it was incubated at 37°C for 1 h with shaking at 220 rpm. 200-700µl was then plated on LB agar plus antibiotic selection plates and incubated overnight at 37°C.

2.7.5 DNA Sequencing and sequence analysis

Plasmid DNA was sequenced by the DNA sequencing services in the MRC department of the University of Dundee. For a single reaction, 600ng of DNA in 30µl of elution buffer (from Miniprep kit) was sent to the sequencing services. Primers provided by the sequencing services were used, or own primers at a concentration of 3.2µM were also sent with the plasmid DNA.

Sequence files were received as a ".zip" file and analysed using vector NTI software. Sequences were compared to reference sequences obtained from Pubmed. DNA constructs and oligonucleotide were all designed using Vector NTI software.

2.7.6 RNA and cDNA preparation and amplification

RNA was extracted from cells using RNA-Bee from Amsbio. For adherent human cells, a confluent 10cm plate was trypsinised and the cells were pelleted (300g 5mins), for DT40 cells, roughly $6x10^6$ cells were pelleted. The cell pellets were washed in PBS and resuspended in 50µl of PBS. 1ml of RNA-Bee and 200µl of chloroform was added to the cells and shaken vigorously for 30sec, then incubated on ice for 5mins. The lysates were spun down at 12,000g for 15mins at 4°C. The upper aqueous phase was transferred to a new eppendorf and 500µl of isopropanol was added and left for 5-10mins at RT. The sample was centrifuged at 12,000g for 5mins at 4°C. The supernatant was carefully removed and the RNA pellet was washed x2 in 70% ethanol and centrifuged at 7,500g for 5mins. After allowing the pellet to dry, it was resuspended in 200µl RNase-free water and the concentration of the RNA was measured using a spectrometer.

Reverse transcription PCR (RT-PCR) was carried out using either RevertAid H Minus First Strand cDNA Synthesis Kit or Maxima H Minus Reverse Transcriptase according to manufacturer's guidelines (see below). cDNA was diluted to 2µg in 100µl of Millipore Water (MPW).

Reaction (RevertAid)	
RNA	2µg
Oligo$(dt)_{18}$ primer	1µl
Random hexamer primer	1µl
5x reaction buffer	5µl
Ribolock RNase inhibitor	1µl
10mM dNTP mix	2µl
RevertAid H reverse transcriptase	1µl

Reaction (Maxima)	
RNA	2µg
Oligo$(dt)_{18}$ / Random hexamer primer	1µl
5x reaction buffer	4µl
10mM dNTP mix	1µl
Maxima H Minus Enzyme Mix	1µl

Table 2.4 RevertAid and Maxima RT-PCR reactions.

2.7.7 Polymerase Chain reaction (PCR)

PCRs were carried out as follows for the different PCR enzymes

Phusion high fidelity DNA polymerase

Reaction

5X Phusion HF or GC Buffer	10µl
10 mM dNTPs	1µl
Forward Primer (10µM)	2µl (0.4µM)
Reverse Primer (10µM)	2µl (0.4µM)
Template DNA	20ng
Phusion DNA Polymerase	0.5µl
MPW	Up to 50µl

Cycle

Temperature	Time	Cycles
98°C	3mins	1
98°C	20sec	35
Annealing temp	30sec	
72°C	15-30 seconds/kb of DNA	
72°C	10 mins	1
4°C	∞	1

Dream Taq Green DNA polymerase

10X DreamTaqGreen Buffer	5µl
10 mM dNTPs	1µl
Forward Primer (10µM)	2µl (0.4µM)
Reverse Primer (10µM)	2µl (0.4µM)
Template DNA	20ng
DreamTaq DNA Polymerase	0.5µl
MPW	Up to 50µl

Cycle

Temperature	Time	Cycles
95°C	3mins	1
95°C	30sec	35
Annealing temp -5°C	30sec	
72°C	1min/kb of DNA	
72°C	10 mins	1
4°C	∞	1

Table 2.5 PCR reactions and PCR cycle for Phusion and Dream Taq polymerases.

2.7.8 Site directed mutagenesis

Site directed mutagenesis was performed using QuikChange Lightening Mutagenesis Kit from Agilent. Primers were designed using the Quick change primer design tool on the Agilent website to mutate a single amino acid. Mutagenesis of plasmid DNA was confirmed by sequencing. The reaction was carried out as follows;

Plasmid DNA	50ng
10× QuikChange Lightning Buffer	5µl (1x)
Forward primer	125ng
Reverse Primer	125ng
dNTPs (10mM)	1µl
Quick solution	1.5µl
QuikChange Lightning Enzyme	1µl
MPW	Top up to a final volume of 50µl

PCR cycle;

Temperature	Time	Cycles
95°C	2mins	1
95°C	20sec	18
60°C	10sec	
68°C	30 seconds/kb of plasmid DNA	
68°C	5 mins	1
4°C	∞	1

Table 2.6 PCR reactions and PCR cycle for Site directed mutagenesis.

Directly after the PCR, 2µl of DpnI restriction enzyme was added to the reaction and incubated for 30mins at 37°C to digest the parental non-mutated DNA. The mutated plasmids were then transformed using XL10-Gold ultracompetent cells according to manufacturer's guidelines.

Multi-Site directed mutagenesis was performed using QuikChange Lightening Multi Mutagenesis Kit from Agilent. Primers were designed using the Quick change primer design tool on the Agilent website to mutate a single amino acid. In order to mutate 3 amino acids, three separate forward primers were generated. No reverse primers are needed for this reaction. The reaction was carried out as follows;

Plasmid DNA	300ng
10× QuikChange Multi Lightning Buffer	5µl (1x)
Forward primer	175ng in total (see below)
dNTPs (mM)	2µl
Quick solution	0.5µl
QuikChange Lightning Enzyme	2µl
MPW	Top up to a final volume of 50µl

Primers

Primers	1	2	3
Reaction 1	100ng	50ng	25ng
Reaction 2	25ng	100ng	50ng
Reaction 3	50ng	25ng	100ng

This primer mix was used to increase the likelihood of obtaining all the different mutation combinations possible.

PCR cycle

Temperature	Time	Cycles
95°C	2mins	1
95°C	20sec	30
55°C	30sec	
65°C	30 seconds/kb of plasmid DNA	
65°C	5 mins	1
4°C	∞	1

Table 2.7 PCR reaction, primers and PCR cycle for multi-Site directed mutagenesis.

2.7.9 Ethanol precipitation of DNA

1/10 Volumes of 3M Sodium acetate (pH 5.2) was added to the DNA to be precipitated. 2 volumes of 100% ethanol was added to the mix and inverted a few times to insure mixing. The mixture was incubated at -20°C for at least 1hr and then the DNA was pelleted by centrifugation at 20000 x g for 20mins. The DNA pellet was then washed twice with 70% ethanol and spun down at 15000 x g for 5mins between washes. The DNA pellet was allowed to air dry before resuspension in an appropriate buffer.

2.7.10 DNA Agarose gel electrophoresis

DNA was run on Agarose gels ranging from a 0.5-1.5%. Agarose gels were made by dissolving agarose in 1x TAE buffer. Once the TAE buffer was added to the agarose powder the solution was weighed and then microwaved to dissolve the agarose. The solution was weighed again after boiling and the volume of the solution was compensated for by adding MPW to bring it back to its original volume. Ethidium bromide or gel green (concentration according to manufacturing protocol) was added to the melted agarose once it had cooled down to around 60°C and poured into a casting tray with a suitable comb. Once the gel had set, DNA plus loading buffer was added to the wells and run at 110Volts for around 1hr in 1xTAE buffer. The DNA was imaged using an Alpha Innotech FluorChem® Imaging system.

2.8 Protein methods and Biochemical techniques

2.8.1 Preparation of whole cell extracts

1.5 x10^7 DT40 cells, or a confluent 10cm dish of human adherent cells were pelleted at 300g for 5mins and washed twice in 10mls of PBS. The cell pellet was resuspended in 200µl lysis buffer and incubated at RT for 10mins to allow the nuclease to work. Lysates were then incubated on ice for 20-30mins. The lysates were then centrifuged at 20000 x g for 20mins at 4°C to pellet debris and insoluable protein and the soluble protein was transferred to a fresh 1.5ml eppendorf. Protein concentration was measured by Bradford assay (as described in section 2.2.5) and stored at -80°C.

2.8.2 DT40 cellular fractionation

Cellular fractionation was performed essentially according to (Wang and Caldwell, 2006). All buffers were ice cold and all incubation steps were performed on ice. Briefly, 1.5 x 10^8 DT40 cells were pelleted, washed 2x in 100ml ice-cold PBS, resuspended gently in 5x the packed cell volume (PCV) of isotonic lysis buffer. The PCV was taken as being 1 µl per 1x10^6 cells, i.e. for 2.0 x10^8 cells the PCV was 200 µl. The resuspended cells were transferred to a 1.5ml eppendorf on ice and incubated for 15 min. 10% NP-40 was added to a final concentration of 0.3% and the cell suspensions mixed gently by inversion then immediately centrifuged for 30 sec at 3000 x g. The supernatant (cytoplasmic fraction) was transferred to a fresh tube. The pellet was resuspended in 5x PCV isotonic lysis buffer, mixed gently and pelleted at 1500 rpm for 5min. The supernatant was removed and the pellet resuspended in 3x PCV extraction buffer. Tubes were vortexed at medium speed for 15 min followed by vortexing at high speed for 15 min. Insoluble material was pelleted by centrifugation at 20000 x g for 15 min and the supernatant was moved into a fresh tube (soluble nuclear fraction). Samples were either used for PAGE Western blot or stored at -20°C.

2.8.3 Human adherent cellular fractionation

Confluent 15cm plates of HEK cells were washed twice with cold PBS, scraped off and spun down. Supernatant was aspirated off and the pellet was resuspended in 5PV Ce buffer and incubated on ice for 3mins. The lysate was centrifuged at 1,300 x g for 10mins and the supernatant was collected (cytoplasmic fraction). The nuclear pellet was washed in Ce buffer minus NP40. Nuclear pellet was then resuspended in 1 pellet volume NE buffer and the salt concentration was adjusted to 400mM using 5M NaCl. An additional pellet volume of NE buffer was added to the pellet and mixed. Incubate on ice for 10mins, vortexing the sample from time to time. Spin down the nuclear and cytoplasmic lysates at 14000 x g for 15mins.

2.8.4 Acid histone extraction

1.5 x 10^7 DT40 cells were harvested and washed twice with PBS. The cells were then lysed in isotonic lysis buffer as described in 2.2.2. The nuclei were pelleted and the supernatant was discarded (cytoplasmic fraction). The nuclei were washed in isotonic lysis buffer before adding 60µl of 0.2M HCL solution. The suspension was gently mixed and incubated o/n at 4°C. The debris was then pelleted at 10,000 x g and the supernatant histone fraction was transferred to a clean tube and neutralised (pH 7) with 0.2 M NaOH before Western blot analysis.

2.8.5 Protein quantification by Bradford assay

1-10µL of the protein solution to be assayed was added to a cuvette and lysis buffer was added to a final volume of 10µL. Bradford reagent was diluted 1:1 with MPW and 1ml dispensed into the cuvette. Absorbance at 595 nm was measured and protein concentrations were calculated by comparison to a standard curve of 595 nm absorbance's made using a range of known concentrations of bovine serum albumin in the Bradford assay.

2.8.6 Polyacrylamide gel electrophoresis (PAGE)

Polyacrylamide gel electrophoresis (PAGE) was carried out using 4-12% pre-cast Bis-tris mini-gels. 50mg of protein in 1xLDS sample buffer and 50mM DTT were boiled for 5mins prior to gel loading. 10µL of protein marker was used, unless otherwise stated. Gels were run at 180V for 1hr with 1X Mops buffer using Novex gel electrophoresis tanks.

2.8.7 PAGE staining

After PAGE, gels were either coomasie or silver stained using PAGE-blue or Pierce silver staining. Both staining were carried out according to manufacturer's guidelines.

2.8.8 Western Blotting

Western blotting was performed using the Xcell IIBlot module in the Novex minigel tanks. Either Nitrocellulose or PVDF membranes were used for transfer. Nitrocellulose membrane was used for all conventional Western blots and PVDF membranes were used for Licor Western blot analysis. PVDF membrane was pre-treated with methanol for 1min, water for 2mins and then 1xTransfer buffer for a further 2-5mins. Nitrocellulose membrane was briefly incubated in 1xTransfer buffer prior to transfer. The transfer buffer was composed of 1x transfer buffer, 10% (nitrocellulose membrane) or 20% (PVDF membrane) methanol and 1x antioxidant. Transfer was set up according to manufacturer's protocol. Samples were transferred for 1hr 30mins – 2hrs at room temperature at 35Volts.

Post transfer, membranes were rinsed in PBS-T (PBS with 1% Tween 20) and blocked for 1hr in PBS-T with 5% marvel. The membrane was incubated with the primary antibody in PBS-T marvel o/n at 4°C shaking. The membrane was washed 3x 5mins in PBS-T. The membrane was then incubated with the secondary antibody in PBS-T with 5% marvel for 1hr at RT, washed 3x 5mins in PBS-T and incubated with ECL (1;1 detection regent1;2) for 3mins before exposure to x-ray film and developed.

For quantification of relative protein levels, the Licor system was employed. Low background immunofluorescence PVDF membrane was used for transfer. Membrane was treated the same as aforementioned. Fluorescent secondary antibodies were used to detect the protein of interest. After the secondary antibody was washed off with PBS-T x3, the membrane was incubated in water and then imaged using the Licor.

2.8.9 Protein Purification

Full length RNF8, RNF168 and point mutants RNF8, RNF168 were purified via a His-trap column. His-tagged proteins were expressed in BL21(LysE3) *E-coli* cells.

Culture growth and protein expression

A single colony was inoculated into 10mls of LB plus ampicillin (100µg/ml) and chloramphenicol (37µg/ml). The cultures were incubated o/n at 37°C. 7mls of culture was then inoculated into 400mls of LB plus ampicillin (100µg/ml) and incubated at 37°C until the O.D. reached 0.6. 0.4mM IPTG was then added to the culture to induce protein expression. RNF8 and mutant RNF8 were incubated for 2hrs at 37°C before harvesting. RNF168 and mutant RNF168 were incubated at 18°C o/n before harvesting. Cultures were spun down and pellets were either frozen until needed or lysed.

Cell lysis

10mls of binding buffer was added per gram of bacterial pellet and resuspended. The following was added to the resuspended pellets and allowed to rock at RT for 30mins;

- 1mM $MgCl_2$
- 1mMPMSF
- 0.2mg/ml lysozyme
- 5mM DTT
- Protease inhibitor cocktail

Samples were freeze-thawed (incubation at -80°C then thawed at RT) 2-3 times to ensure lysis. Lysates were sonicated at 60% output for 5mins until they were no longer viscous. Lysates were centrifuged at 38,000g for 20mins. Supernatant was filtered through a 0.22μM PES membrane.

Loading lysate onto column

The His-trap crude FF 5ml columns were washed with 5-10 column volumes of MPW and then with 10 column volumes of binding buffer. Lysate was loaded on to the column in a loop manner using an electrical pump o/n at 4°C.

Column purification and dialysis

Proteins were purified using the Akta explorer. His columns were washed with 75mls binding buffer and then eluted in 1.5ml fractions using the elution buffer. Samples were collected according to the elution peak.

Slida lyzers were incubated in dialysis buffer before sample was applied. 15ml slida lyzers were used in the dialysis process. Protein sample was injected into the cassette. The buffer was changed twice throughout the day and once more before leaving o/n. The dialysis process occurred at RT and gentle stirring via a magnetic stirrer. With every buffer change, the NaCl content was reduced by 100mM. The final concentration of NaCl was 300mM. The dialysed samples were aliquoted into 1ml volumes and the insoluble fractions were pelleted. A Bradford assay was carried out to check the protein concentration of the samples. The protein samples were then frozen down with 10% glycerol at -80°C.

Note

All proteins apart from mutant RNF168 were eluted from the column in a one-step elution process by adding 500mM imidazole buffer. Mutant RNF168 was eluted using a gradient elution buffer from 50mM up to 500mM imidazole. This was carried out to

clean up the elution process, however no difference was observed between the one-step and gradient elution process

2.8.10 Ubiquitin ligase activity assay

Ubiquitin ligase activity assays were carried out as follows, first by pre-incubating the enzymes with cold ubiquitin before adding ^{125}I labelled ubiquitin to the mix.

10x buffer	1µl
ATP (20mM)	1µl
E1 enzyme	1µl
E2 enzyme	1µl
E3 enzyme	2µl
Ubiquitin (1mg/ml)	1µl
Top up to 10µl of MPW	-

The reaction was incubated for 1hr at 37°C, the following was then added to the mix

10x buffer	1µl
ATP (20mM)	1µl
^{125}I labelled ubiquitin	1µl
Histones	2µl
Top up to 10µl of MPW	-

Table 2.8 Ubiquitin ligase activity assay reaction

The reaction was incubated for a further 1hr at 37°C before samples were run on 4-12% gradient Bis-Tris gel. The gel was then dried and exposed to either X-ray film imaged via a phosphoimager, from 1hr to 24hr at -80°C before developing.

2.8.11 Mammalian two hybrid analysis

Genes of interest were cloned into the pM3-Not and pVP3-Not plasmids resulting in their fusion to either the GAL4 DNA binding or activation domains respectively (pM3-

Not expresses the bait, pVP3-Not expresses the prey). Hek-293 or HeLa cells were seeded in 24 well plates and transfected with xtremegene 9 when 70-90% confluent. Cells were transfected with 125ng of each vector, 125ng of pG5-Luc (GAL4 driven firefly luciferase vector) and 12.5ng of an internal control vector (pRL-CMV, expressing renilla luciferase). 24hrs after transfection cells were washed x2 with PBS and lysed using 100µl 1xPLB buffer by rocking at RT for 20-30mins. 20µl of lysate was loaded onto a 96 well plate and a dual luciferase assay was used to calculate the ratios of firefly/renilla luciferase activity for each sample according to manufacturer's guidelines. The fold induction is the ratio for a given interacting pair of proteins divided by the same ratio for the empty vectors.

2.8.12 GFP Pull down

GFP tagged proteins were pulled down using chromotek GFP-trap beads. HEK 293 cells were grown in 15cm plates and induced with 2.5ng/ml (GFP, GFP- BARD1) or 7.5ng/ml (GFP -BARD1ΔBRCT) tetracycline o/n before lysis. Cells were washed x2 PBS and scraped from their dishes. The cells were pelleted at 300g for 5mins and resuspended in 500µl lysis buffer/15 cm dish and incubated at RT for 10mins (Nuclease enzyme activity) and then on ice for a further 20mins. The crosslinker in the lysis buffer was then quenched by adding 200mM TRIS-HCL to the mix and allowed to incubate on ice for a further 30mins. The insoluble fraction and debris was then pelleted by centrifugation at 20000 x g at 4°C for 20mins. Protein concentration was measured using the Bradford assay.

GFP trap beads and the agarose beads were washed twice with PBS followed by a single wash with lysis buffer before suspension in a 50% slurry with lysis buffer. For pull downs with less than 5mg of protein, 20µl of GFP-trap slurry was used, otherwise for every 1mg of protein 4µl of GFP-trap slurry was used. 10 times the volume of agarose beads were used in comparison to GFP-trap per pull down. Pelleting of beads was carried out at 4°C for 2mins at 3,200 x g.

Following protein quantification, equal amounts of comparative GFP-proteins were added to agarose beads to remove any unspecific protein binding to the beads. The lysates were gently mixed on a rotating wheel at 4°C for 1hr 30mins. The beads were then pelleted and the lysate was then transferred to a new tube and incubated with the GFP-trap beads. The lysates were gently mixed again on a rotating wheel at 4°C for 1hr 30mins. The GFP and agarose beads were pelleted and washed x3 with wash buffer. After adding the wash buffer, the beads were gently mixed by inverting the tubes 10 times before pelleting. After the washing step, beads were resuspended in 2x Sample buffer containing 50mM DTT (roughly 40µl/2mg of protein used in the pull down) and boiled for 20-30mins. Boiling in sample buffer removed the crosslinks and also striped the protein from the beads. The beads were pelleted and 40µl of sample was loaded per gel for western blotting. 50µg of input was used for western blotting. Concentration of input was determined as in section 2.2.5.

2.8.13 Mass spectrometry

Tandem Mass spectrometry (MS/MS) was performed by the Mass spectrometry facility at the college of life sciences Dundee according to standard protocols. Samples were processed as part of the service. Proteins were digested with trypsin. An Orbitrap Velos machine was used to carry out the Mass Spec. Data was used to search the IPI human database using Mascot (Matrix Science, UK). Mascot output was validated using Scaffold 3 (Proteome Software, USA). Peptide identifications were accepted if they could be established at greater than 85.0% probability as specified by the Peptide Prophet algorithm (Keller et al., 2002). Protein identifications were accepted if they could be established at greater than 99.0% probability and contained at least 2 identified peptides. Protein probabilities were assigned by the Protein Prophet algorithm (Nesvizhskii et al., 2003). Proteins that contained similar peptides and could not be differentiated based on MS/MS analysis alone were grouped to satisfy the principles of parsimony.

Mass Spectrometry of a second set of samples (no crosslinker) were carried out in the Ninewells Mass spectrometry facility using an orbitrap machine. Data was analysed by PEAKs software adhering to the same stringency factors as mentioned above. The sample preparation was carried out in house as follows; Samples were run around 1cm into a 4-12% Bis-Tris gel via PAGE. After the initial running of the samples in a gel, all further preparation and processing was carried in in a laminar flow hood. The protein bands were cut from the gel into very small pieces. 100µl of 100mM ammonium bicarbonate in a 50% acetonitrile solution was added to the gel pieces and incubated at RT for 30mins. 500µl of acetonitrile was then added to the samples and incubated at RT until the gel slices were visibly white and shrunken. Samples were then spun down and liquid was removed from the samples. After destaining the gel slices, the samples were reduced and alkylated. 50µl of 10mM DTT in 100mM ammonium bicarbonate was added to the samples and incubated at 56°C for 30mins and then allowed to cool. 500µl acetonitrite was then added to the samples for 10mins before removing. 50µl of a 55mM iodacetamide solution in 100mM ammonium bicarbonate was added to the sample and incubated in the dark for 20mins. The gel slices were finally shrunk with the addition of 500µl acetonitrile which was removed after dehydrating the samples. The next stage of processing the samples for Mass spectrometry involved the trypsin digestion of the peptides within the gel slices. The samples were covered with trypsin (13ng/µl trypsin in 10mM ammonium bicarbonate containing 10% v/v acetonitrile) and sonicated for 1hr at 37°C before incubation o/n at 37°C. Extraction of the digested peptides was then employed by the addition of 100µl extraction buffer (1:2 v/v 5% formic acid/acetonitrile) for 15mins at 37°C. The liquid was then removed and the samples were dried using a speedy-vacuum and stored at -20°C until Mass spectrometry analysis.

2.9 Cell Culture Methods

2.9.1 Culture of DT40

DT40 cells were grown in suspension at concentrations ranging between $3x10^4$ cell/ml and $1x10^6$ cells/ml. Cells were grown in RPMI medium supplemented with 10% FBS, 3% CS and 5mls Penn/strp at 37°C with 5% CO_2. CS was heat inactivated for 30mins at 56°C prior to addition to RPMI medium. Complete medium was preheated at 37°C before use. DT40 cells were generally split every second day to $1x10^5$ cells/ml. the day before the use of DT40 cells in an experiment, the cells were split to $2x10^5$ cells/ml to ensure logarithmic growth.

2.9.2 Culture of human adherent cell lines

Adherent HeLa, Hek 293 and U2OS cells were grown in DMEM medium supplemented with 10% FBS at 37°C with 5% CO_2. Tetracycline inducible cell lines were grown in tetracycline free medium. To Split adherent cells, plates with adherent cells were washed twice with PBS-EDTA and incubated with TE for 3-5mins at 37°C until the cells detached from the plate. They were then seeded in new plates with fresh medium at a lower density. Cells were generally split 1 in 4 every second day.

2.9.3 Freezing and storage of cells

For freezing, $3x10^6$ DT40 cells were pelleted at 300g for 5mins and frozen in aliquots of 500µL freezing media. Confluent 10cm plates containing human cell lines were trysinised and pelleted then frozen in aliquots of 500µL freezing media. All cells were frozen in cryovials and stored in Mr. Frosties at -80°C for the first 24hrs. The cells were then transferred to liquid nitrogen for long term storage.

2.9.4 DT40 Transient transfection

Transient transfection of DT40 cells was performed using the Amaxa Nucleofector II and the Nucleofector T kit (Lonza). For each transfection, $3x10^6$ cells were pelleted at 300g for 5mins and resuspended in 82µl of room temperature nucleofector plus 18µl

supplement. 30µg of plasmid DNA dissolved in 1-10 µl of TE buffer was added and the suspension thoroughly mixed by gentle pipetting. This was transferred to the supplied 2 mm electroporation cuvette and electroporated in the Amaxa Nucleofector II using program B-023. The transfected cells were then transferred to 5ml of media in a labelled 6-well plate and cultured for 24 hours at 37°C and 5% CO_2 in complete RPMI in a humidified environment.

2.9.5 DT40 Stable transfection

50µg of plasmid DNA containing genes of interest was linearized o/n using suitable restriction enzyme. After linearization, the DNA was then ethanol precipitated and resuspended in 50µl sterile PBS. $1x10^7$ subconfluent DT40 cells were pelleted, washed in 25ml ice-cold PBS, resuspended in 600 µl ice-cold PBS and gently mixed with DNA. The cell/DNA mixture was transferred to 4mm electroporation cuvettes and incubated on ice for 20 min. The cell/DNA mixture was again gently mixed before electroporation. Electroporation was performed using a Gene Pulsar II (Bio-rad) and the following settings: 250V (volts), 950µF (capacitance).

Cells were placed on ice for 5 min to recover, then added to 50 ml complete RPMI in a 125 cm^2 flask. The cells were then incubated at 37°C at 5% CO_2. 24hrs after transfection 50 ml 2x selection media was made up by adding antibiotics to 50 ml complete RPMI. 2x selective media was added to the transfected cells and mixed well (total volume 100mls). Cells in selective media were plated out into flat-bottomed 96-well plates in 200µl aliquots, and were incubated at 37°C/5% CO2 for 7-10 days until clones were apparent. G418 was used as a selective agent at a concentration of 2mg/ml.

2.9.6 Transient transfection of adherent cells (human)

HeLa and HEK-293 cells were transfected with X-tremeGENE 9 transfection reagent and U2OS cells were transfected with X-tremeGENE HP transfection reagent. Cells were seeded the day before transfection so that they were 70-90% confluent on day of

transfection. On the day of transfection, Optimem was added to a sterile tube, the transfection reagent was then added to the tube as well as the DNA. The mix was vortexed briefly and then spun down and incubated at RT for 15-20mins. The mixture was added to the cells in a drop wise manner and incubated for 24hrs at 37°C, 5% CO_2 before analysis.

X-tremeGENE 9

	Total volume for transfection (µl)	DNA (µg)	XtremeGENE reagent 3:1 (µl)
24 well plate(1 well)	25	0.25	0.75
12 well plate(1 well)	50	0.5	1.5
6 well plate (1 well)	100	1	3
10cm plate	500	5	15

X-tremeGENE HP

	Total volume for transfection (µl)	DNA (µg)	XtremeGENE reagent 1:1 (µl)
24 well plate(1 well)	50	0.5	0.5
12 well plate(1 well)	100	1	1
6 well plate (1 well)	200	2	2
10cm plate	1000	10	10

Table 2.9 X-tremeGENE 9/HP transfection reaction

2.9.7 Stable transfection of Human Adherent cells

HEK-FRT-Flp-In cells were stably transfected using Invitrogens Flp-In system. This DNA recombination system uses a recombinase (Flp) and site-specific recombination to facilitate integration of the gene of interest into a specific site in the genome of mammalian cells. In summary, a Flp Recombination Target (FRT) site is first integrated into your cell line. The FRT plasmid also confers zeocin resistance allowing positive cells to be selected for. Once the FRT site is stably integrated into a locus in the

genome, pcDNA5 (an expression plasmid containing an FRT site linked to a hygromycin resistant gene) containing your gene of interest is then transfected into the zeocin resistence cells. A Flp recombinase expression plasmid, pOG44, for expression of the Flp recombinase under the control of the human CMV promoter is cotransfected with pcDNA5. Upon co-transfection, the Flp recombinase expressed from pOG44 mediates a homologous recombination event between the FRT sites (integrated into the genome and on pcDNATM5/FRT) such that the pcDNA5/FRT construct is inserted into the genome at the integrated FRT site.

The HEK and U2OS cells used were already stably transfected with pFRT/lacZeo. HEK-FRT-Flp-In cells were transfected with xtremegene 9 and U2OS-FRT-Flp-In cells were transfected with xtremegene HP according to manufacturer's guidelines.

Transfections were as follows in 10cm plates;

	Total volume for transfection (µl)	**DNA (µg) 9;1 (pOG44;pcDNA5)**	**XtremeGENE reagent 3:1 (µl)**
HEK-FRT-Flp-In cells	500	4.5 ; 0.5	15

Table 2.10 Reactions for stable transfection of HEK-FRT-Flp-In cells

24hrs post transfection, cells were given fresh medium. 48hrs post transfection cells were trysinised and seeded 1 in 4, 1 in 8, and neat in media containing 100µg/ml Hygromycin for selection. Selective media was changed every 3-4days. Single clones were picked using cloning discs or cylinder between 12-20days. Clones were expanded and confirmed positive by Western blot.

2.9.8 Colony survival assay

Media containing methylcellulose is used in this assay. Due to its viscous consistency, it provides an optimal semi solid matrix where in single cells producing colonies can form without easy disruption. Methylcellulose media is made up before cells are treated

and is used up to four weeks after preparation. The methylcellulose media is made as following:

10g of methylcellulose is autoclaved in a 1L glass bottle with a magnetic stir bar.

- 200mls of MPW water, at 55°C, is added to the autoclaved methylcellulose and shaken vigorously until all the powder is mixed with the MPW and not stuck to the walls of the bottle.
- 500mls of DMEM containing sodium bicarbonate in filter sterilised and added to the methylcellulose mix and shaken vigorously.
- *DMEM media*; 11.99g of DMEM plus 32.5mls of 7.5% sodium bicarbonate dissolved in 500mls of MPW.
- Allow to stir overnight at 4°C. *(Note; methylcellulose only becomes fully soluble when temperature is below 8*°C)
- 100mls of FBS, 30mls of CS and 10 mls of penn/strep are added to the solution. MPW is then added to bring the final volume to 1L. The media is then stirred over night at 4°C and then stored at 4-8°C until use*. (Note; The methylcellulose media is stirred at room temperature for a few hours before on the day of use.)*

5mls of methylcellulose media is added to each well in a 6 well plate.

Treatment of cell lines with Olaparib was carried out in 24 well plates. $2x10^5$ cells were seeded in a 24 well plate with media and treated with the following concentrations of Olaparib; 0µM, 0.25µM, 0.5µM, 1µM, 1.5µM and 3µM. Cells were treated in a final volume of 1ml per well for 24hrs. 24hrs following treatment cells were serially diluted 1;10, 1;100 and 1;500 (approximately $2x10^4$, $2x10^3$ and $4x10^2$ cells/ml). $2x10^3$, $2x10^2$ and 40 cells were dropped onto the prepared 6 well plates containing methylcellulose in technical duplicate for each drug concentration (ie 100µL of diluted cells). Once cells were plated, the 6 well plates were mixed gently in an 8-shape motion, 5 times

forwards and backwards. MPW was then added between the wells in a plate for humidity and the plates were placed undisturbed in a 37°C incubator for 10-14 days.

Chronic treatment of cells with Hydroxy Urea (HU) was carried out much the same as with Olaparib. Cells were serially diluted as before and then added drop-wise to methylcellulose media containing the following concentrations of HU; 0µM, 100µM, 150µM and 200µM.

10-14 days after plating, colonies formed were counted and an average of the technical duplicates was taken and used as a single result. Colonies formed in each cell line were compared to untreated cell and percentage survival was plotted using a logarithmic scale. Each experiment was completed at least 3 times. The IC50 values were calculated from log dose response curves using GraphPad Prism 6 software.

2.9.9 siRNA knockdown in human cells

siRNA knockdown of proteins in cells was carried out using Thermo Scientific Dharmafect transfection reagent. 1 x 10^5 HeLa cells were plated in 6 well dishes in antibiotic free media and incubated o/n at at 37°C, 5% CO_2. A 5µM stock solution of siRNAs was prepared in 1X siRNA buffer (Provided with Dharmafect). In one tube 10µl of the 5µM siRNA stock was diluted in 190µl of optimum. In the second tube 4µl of Dharmafect was added to 196µl optimum. Both tubes were incubated at RT for 5mins before adding the content of both tubes together and incubating the mixture for a further 20mins at RT. 1.6mls of complete media was added to the siRNA/Dharmafect solution after the incubation. The culture media was aspirated from the cells in 6-well plates and the transfection mixture was added to the cells. The final concentration of siRNA used was 25nM. Cells were incubated at 37°C, 5% CO_2 for up to 72hrs before harvesting and analysis. When cells were required for further experiments the transfection media was removed after 24hrs and replaced with complete media after re-seeding.

2.9.10 Cell synchronisation; Double thymidine block

In order to synchronize HEK cells in late G1/S phase for analysis of cell cycle progression via BrdU/PI FACScan analysis cells were seeded in 10cm dishes at 20% confluency in the morning of the start of the experiment. That evening cells were treated with 2.5mM thymidine and incubated at 37°C, 5% CO_2 for 16hrs to arrest the majority of cells in early S-phase. The media containing thymidine was then aspirated from the cells and they were allowed to recover for 6hrs. After recovery, the cells were treated with a further 2.5mM thymidine for 16hrs at 37°C, 5% CO_2. The thymidine containing media was then aspirated from the cells and fresh media was applied to release the cells from the arrest. Cells were harvested between 0 and 10hrs in 2hr intervals after the final release before fixation and analysis by PI/BrdU FACScan. Cells were pulse labelled with 10µM BrdU for 30 mins before harvesting to incorporate BrdU into replicating S-phase cells.

2.10 Flow cytometry methods

2.10.1 Flow cytometry and FACS

Samples were analysed by Becton Dickinson FACScan using Cell quest. Post analysis was carried out using WinMDI 2.9 software.

Propidium iodide/BrdUcell cycle assay

6 X 10^6 HEK 293 cells were harvested from culture using trypsin. The cells were washed twice with PBS and resuspended in 200µL PBS. The cells were then fixed by adding 2mls of 70% ice cold ethanol dropwise to the cells while gently vortexing the cells. Cells were fixed for at least 16hrs at -20°C. After fixation, the samples were washed twice with PBS and resuspended in 1ml 2M HCL/0.5% Triton X and incubated at RT for 30mins. The samples were then centrifuged at 300 x g and resuspended in 1ml of 0.1M Sodiumtetraborate (pH8.5) and incubated for 1min at RT. The cells were washed a further two times in Blocking buffer before incubating the samples in 1;500 anti-BrdU in 100µl blocking buffer. The cells were incubated with the BrdU antibody for

1hr30mins at RT. Following primary antibody incubation, the samples were washed with blocking buffer and then resuspended in 100µl of 1;100 FITC anti-BrdU conjugated secondary antibody in blocking buffer and incubated in the dark for 30mins. The samples were then washed in PBS and resuspended in 500µl PBS with 25 µg/ml propidium iodide (PI) and 1;400 RNAse roughly 15mins before FACS analysis. Flow cytometry was performed on a Becton Dickinson FACScan with excitation at 488 nm. Complete cells were gated by forward and side scatter, singlets were gated by PI area vs events and the percentage of cells at different stages of the cell cycle was deduced by plotting PI vs BrdU (FL2-A vs FL1-H). 10,000 gated cells were counted.

2.10.2 Homologous recombination efficiency assay (HRE assay)

3 x 10^6 DTDR17 DT40 cells were transiently transfected with 30µg of pIsce-I plasmid using the Amaxa nucleofection system. Programme B-23 was used. Directly after transfection, cells were incubated in 6 well plates containing 5mls of media and incubated at 37°C for 24 hours. Cells were then spun down at 300g for 5mins and washed twice with PBS before re-suspension in 500µL of PBS. The cells were analysed for green fluorescence using the FACScan fluorescence activated cell sorter. A live population of cells was gated for using forward and side scatter and the percentage of green fluorescent cells per 10,000 cells within this population were counted and compared to no DNA transfected cells and plotted on a bar chart.

2.11 Microscopy methods

2.11.1 Immunocytochemistry

Pre-extraction (Adherent cell)

Before fixation cells growing on cover slips (70% confluent) or in dishes (70% confluent) were washed twice with CSK buffer, incubated for 5mins with CSK buffer containing 0.5% Triton X, then washed a further two times with CSK buffer. All steps were carried out on ice.

Fixation, permeabilisation and staining

Cells were fixed with either 4% paraformaldehyde at RT or 100% cold methanol at -20°C for 10mins. Cells fixed with paraformaldehyde were then permeabilised, 3 x 3mins, with PBS and 0.5% triton X. there is no need to permeabilise methanol fixed cells.

The cells were then blocked in IF blocking buffer for 20mins to 1hour at 37°C. Blocking buffer was then removed and the primary antibody was added in blocking buffer to the cells. These were incubated at 37°C for 1 hour. The primary antibody was removed and the cells were washed 3 times with PBS. A solution containing a 1:1000 dilution secondary Alexa antibody and 1µg/ml Dapi in blocking buffer was then added to the cells for 30 mins at 37°C. The cells were washed a further 3 times with PBS and mounted on slides with 15µl of prolong gold.

EdU staining was carried out using the Invitrogen Click-it EdU imaging Kit using alexa fluor 555 azide. This was carried out according to manufacturer's guidelines.

The slides were kept in the dark o/n and the following day the coverslips were sealed with clear nail varnish. Slides were kept at 4°C in the dark until imaged.

Note for DT40 cells (suspension cells)

Dt40 cells were pre-extracted in 15ml falcon tubes. $3x10^6$ cells were used per slide. After pre-extraction the cells were resuspended in 200µl PBS and pipetted onto polylysine coated slides. They were left to settle and attach to the slides for 15mins before fixation, permeabilisation and staining. Silicone isolators were sealed onto the slides before cells were added, maintaining a sealed area to fix and stain the cells.

All immunocytochemistry experiments were imaged using a DeltaVision Spectris Restoration Microscope built around an Olympus IX70 stand, with a 60 x/100 x/1.4NA lens (Applied Precision, LLC, WA). Optical sections were recorded every 0.2 µm, and 3D data sets were deconvolved using the constrained iterative algorithm implemented in SoftWoRx software (Applied Precision LLC). Image data were quantified using SoftWoRx software.

2.11.2 Live cell monitoring and laser induced DNA damage

HEK 293 and U2OS cells were plated in 35mm ibidi µ-Dishes with a Grid-500 at a density of 1-2 x 10^5 cells and incubated o/n at 37°C in 5% CO_2. The following morning cells were pre-sensitized with 10µM BrdU (in complete DMEM) for 24hrs before laser striping. When required, cells were treated with 1µg/ml doxycycline/tetracycline to induce expression of proteins in a tetracycline inducible system. One hour before laser striping the culture media was aspirated from the cells and replaced with 1ml HEPES buffered DMEM in the absence of phenol red to prevent a potential interference of the phenol red in complete media with the laser absorption. The cells were then allowed to equilibrate with the temperature of the microscope platform for at least 20mins before the induction of a laser induced damage stripe. The microscope and platform was maintained at 37°C throughout the experiment. Before beginning, the laser focus was calibrated. All photoactivation experiments were conducted using a DeltaVision Spectris (as above) fitted with a 10 mW 405 nm solid-state laser. The laser was focused to diffraction-limited spots in the shape of a single line and spot bleaching

performed with a single 2sec stationary pulse at 100% laser power. A pattern spacing of 10 was adopted to create a line of spot bleaching. The cells were subsequently imaged every 30sec after laser induced damage to monitor the accumulation of the fluorescent tagged protein to the site of damage. The 60X lens was used to induce the photobleaching and to image the cells.

2.11.3 Laser induced DNA damage

In order to analyse the recruitment of non-fluorescently tagged proteins to laser induced damage stripes a different system was adopted in comparison to 2.5.2. Cells were prepared using the same mechanism as in 2.5.2. A Leica TCS SPSII was used to induce a laser stripe damage in the live cells. Using the FRAP Wizard, a 405nm laser was adopted to induce the stripe of damage. The laser was focused to a line (ROI) across the nucleus of two cells at a time and the width of the ROI rectangle used was 4 pixels. Using the 60X lens, a stripe of damage was induced with 100% laser power and 200 iterations. The position of the cells damaged within the grid system on the ibidi dishes was recorded and the cells were allowed to recover at 37°C in 5% CO_2 for 1hr post damage to allow the recruitment of repair proteins of interest to the laser induced stripe of damage. After recovery, the cells were pre-extracted, fixed and stained using the desired immuno-fluorescent antibodies and imaged using the DeltaVision Spectris Restoration Microscope.

Note; when HEK 293 cells were used for methods 2.5.2/2.5.3 The ibidi dishes were pretreated with polylysine for 24hrs at 4°C before seeding the cells. This was done to allow the cells to adhere more tightly to the dish and prevent the loss of the cells during striping and processing as HEK 293 cells are semi-adherent.

2.11.4 γ-irradiation of DT40 cells and foci counting

In order to quantify the number of RAD51, RPA and CtIP foci induced in different DT40 cell lines after DNA damage, cells were γ-irradiated, fixed and stained and then the damage induced foci were counted. DT40 cells were seeded 2 x 10^5 cells/ml 24hrs

before irradiation. A cesium source of γ-irradiation was used to induce 4GY of damage to the cells. After irradiation the cells were allowed to recover at 37°C in 5% CO_2 for 1-4hrs. After recovery the cells were pre-extracted, fixed and stained with the appropriate antibodies as in 2.5.1. The cells were imaged using a 60X lens on the DeltaVision Spectris Restoration Microscope. The images were deconvoluted as previously described and the damage induced foci were counted using Imaris software. The foci were counted in relation to quality and foci of non-damaged cells were compared to damaged cells. The experiment was repeated in triplicate counting between 100-300 cells per experiment.

2.12 Statistics

Standard deviation(S.D)

Error bars were calculated using Standard deviation in all cases when the experiment was repeated at least three times. S.D was calculated as follows;

$$s = \sqrt{\frac{\sum(x - \bar{x})^2}{n - 1}}$$

S=SD

X=each value in the data set

$\bar{X}$=mean of all values in data set

N=number of data points

Paired student t-test

The paired student t-test was used to calculate the statistical significance between two data sets ie HRE assay. It was calculated as follows;

$$t = \frac{M_1 - M_2}{\sqrt{\frac{SD_1^2}{n_1} + \frac{SD_2^2}{n_2}}}$$

M_1/M_2=data set 1 and 2 means

SD_1/SD_2=Standard deviation of data set 1 and 2.

N=number of data points

Once the t value was calculated the corresponding p value was elucidated from a maths table. The degrees of freedom were taken to be n-1.

IC_{50} values

In order to determine the inhibitory effect of Parp inhibitor Olaparib on the survival of DTDR17 cells using a colony survival assay, an IC_{50} value was calculated. IC50 value is defined as the concentration of a test compound required to achieve half maximal inhibition with Olaparib. The IC50 values were calculated from log dose response curves using GraphPad Prism 6 software.

Chapter 3 The role of the BARD1 BRCT domains in the stabilisation of the BRCA1 complexes.

3.1 Introduction

BARD1 was discovered in a yeast two-hybrid screen identifying BRCA1 interacting proteins [194]. The heterodimer formed between BRCA1 and BARD1 is obligatory for their function in the DNA damage response (DDR). Loss of either proteins leads to indistinguishable phenotypes. Both *Brca1*- and *Bard1*- null mice are embryonic lethal [207], and cell lines derived from these mice exhibit severe chromosomal abnormalities and defects in HR.

One of the main functions of BARD1 is to bind to BRCA1, stabilising and enhancing BRCA1 activity [169, 209, 347]. However more recently, it has become evident that the BRCT domains of BARD1 contribute to the maintenance of genome stability [266, 269]. The BARD1 BRCT domains are not required to bind BRCA1, revealing a novel role for BARD1 in HR independent of its requirements to stabilise and retain BRCA1 in the nucleus. The mechanism and function by which the BRCT domains of BARD1 contribute to the DDR remain unknown.

In this chapter, genetic and biochemical assays are deployed to investigate whether the BARD1 BRCT domains contribute to the stabilisation of the BRCA1-A, B and C complexes.

3.2 Results

3.2.1 The BARD1 BRCT domains are required for HR

Current evidence supporting that the BARD1 BRCT domains are important for efficient HR has been carried out in model systems using transient expression or transient knockdown of BARD1 as opposed to stable expression or knockout [266] which would allow a more in-depth and long-term study of the functional importance of the BARD1 BRCT domains in the DDR. In order to clarify the importance of the BARD1 BRCT

domains in HR, DT40 cell lines with a complete *Bard1* knock-out status were used (gift from C. Vanderberg). DT40 have been shown to be a good model system to study the DDR and have been used in numerous studies of DNA repair. Loss or mutation of DDR proteins in DT40 cells have a strong phenotypic resemblance to their murine counterpart [348]. DT40 show a high rate of targeted integration of transfected DNA [348, 349] allowing facile gene knockout and stable integration of a gene of interest. The *Bard1* cells were stably reconstituted with either *HsBARD1* or *HsBARD1ΔBRCT*.

DT40 cell lines used throughout chapters 3-5 are derived from a modified version of DT40 (known as DTDR17). DTDR17 cells are genetically modified to allow the measurement of homologous recombination efficiency *in vivo*. This cell line contains a single copy the pDR-GFP construct, previously described by *Pierce et al* [350]. The construct contains two inactive copies of the *GFP* gene. One *GFP* gene contains two stop codons at the 5' end and a restriction site recognised by the restriction enzyme Isce-I. The second *GFP* gene only consists of an internal fragment of the gene, lacking both the 5' and the 3' end. Once the restriction enzyme Isce-I is introduced into the cell line it generates a staggered DSB. Efficient HR is measured by the relative expression of GFP by FACs. Once Isce-I creates a staggered DSB in the non-functional GFP, only cells which are proficient in HR can express a functional GFP thereby efficient HR can be measured by the relative GFP expression of mutant cell lines in comparison to WT cells. The repair of an Isce-I induced DSB by homologous recombination can be measured in the DTDR17 cell line.

In order to confirm that the BRCT domains of BARD1 are required for efficient HR the homologous recombination efficiency (HRE) assay was used. *Bard1* cells reconstituted with either full length *HsBARD1* or *HsBARD1ΔBRCT* were transfected with the Isce-I plasmid to generate a DSB. The level of GFP expression was analysed by FACs 24hrs after transfection. Consistent with previous studies, the loss of the BRCT domains of BARD1 greatly reduces the ability of the cells to carry out efficient HR (figure 3.1(b). Importantly the decrease in GFP expression, which correlates with a

decrease in HRE, seen in the absence of the BARD1 BRCT domains was fully corrected with the expression of full length HsBARD1. This suggests that the human and chicken *BARD1* genes are interchangeable fully functional orthologues. The stable expression levels of reconstituted *BARD1* cells with either HsBARD1 or HsBARD1ΔBRCT can be found in figure 3.14.

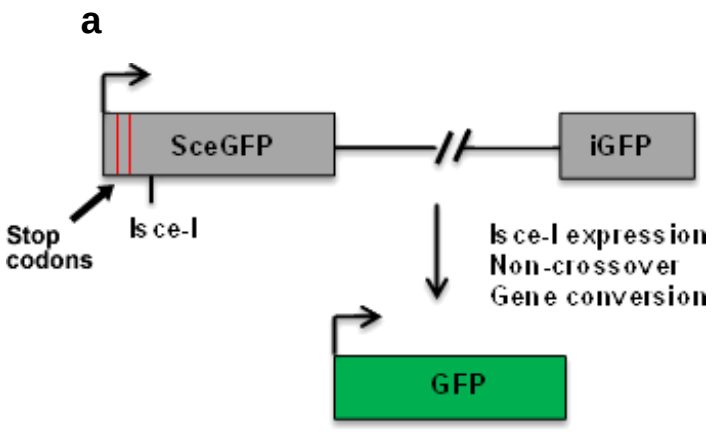

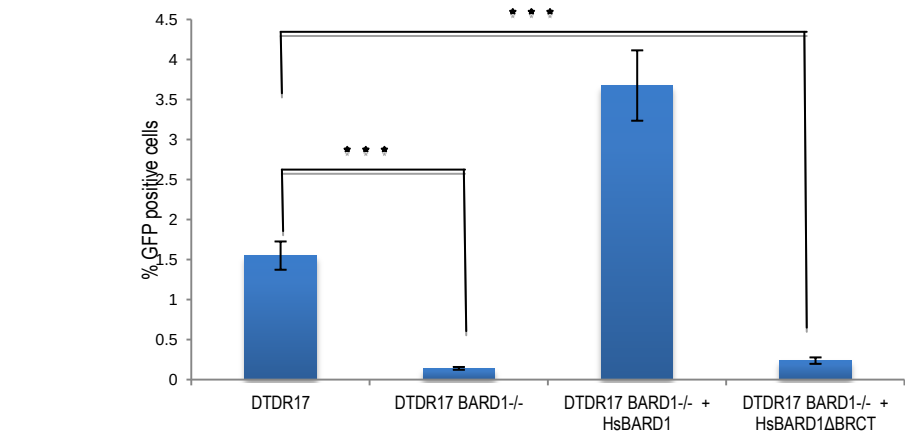

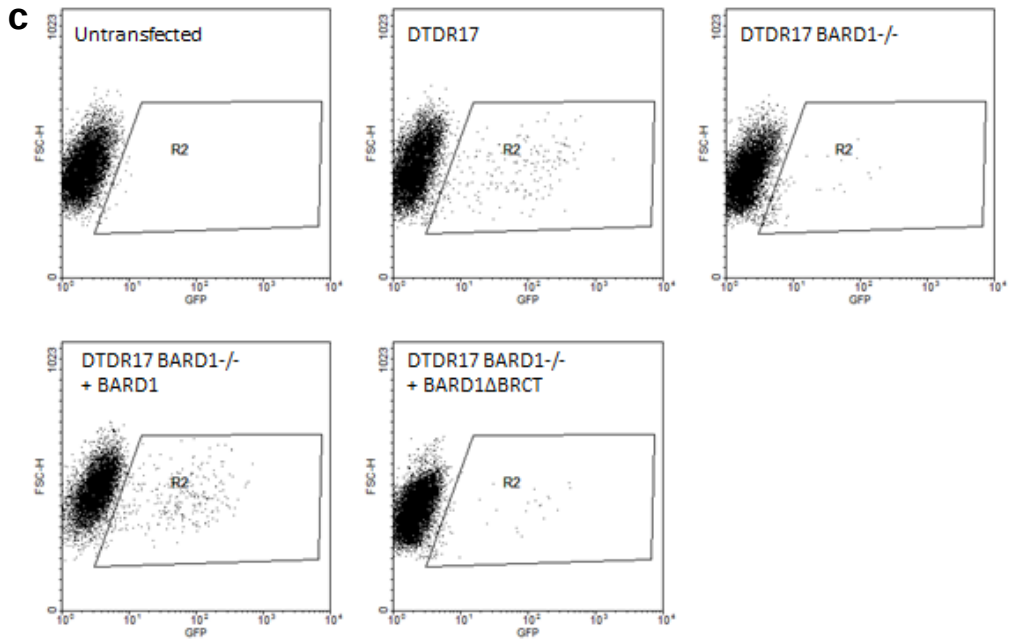

Figure 3.1 The BARD1 BRCT domains are required for efficient HR
(a) Schematic representation of the pDR-GFP construct which is stably integrated into a single site of the DT40 genome in the DTDR17 cell line. The pDR-GFP contains a SceGFP gene which has two in frame stop codons and also an Isce-I restriction site. A functional GFP is only produced when the Isce-I induced DSB is repaired by short tract non-crossover gene conversion, using the internal GFP fragment as a template for repair.
(b) HRE assay illustrating the percentage of cells expressing GFP 24hrs after transfection with the Isce-I expressing plasmid. Results were normalised to untransfected cells. Data shown are the mean of at least 3 independent experiments. Error bars, s.d. *** indicates a statistical significance p value of ≤ 0.001. P value derived from the student t-test.
(c) Representive dot plot of raw data from figure (b) Cells expressing GFP were identified by FACS analysis. GFP positive cells were gated for relative to their GFP status and size (FSC-H) and seen in the box R2.

DTDR17 cells lacking the BRCT domains of BARD1 showed a decrease in their ability to carry out efficient HR in comparison to WT cells according to the HRE assay in figure 3.1(b,c). *Bard1* cells reconstituted with *HsBARD1* appear to express double the level of GFP in comparison to WT, however this is commonly seen throughout this chapter in HRE assays. It is believed to be due to the overexpression of BARD1, however the endogenous level of BARD1 could not be analysed due to the lack of chicken BARD1 antibodies. The defects in HR seen in figure 3.1 in the absence of the BARD1 BRCT domains is not believed to be due to an expression difference between reconstituted HsBARD1 and HsBARD1ΔBRCT as the expression of both proteins appear to be very similar as seen in figure 3.14(a).

Bard1 cells reconstituted with *HsBARD1ΔBRCT* were also sensitive to the PARP inhibitor, Olaparib (figure3.2 (b). In comparison to WT cells, *Bard1* cells and cells reconstituted with *HsBARD1ΔBRCT* showed a 10 to 20 fold decrease in the amount of colonies formed when treated with a PARP inhibitor at 3μM and around a four fold decrease in IC_{50} value. PARP is an important factor in the repair of single stranded breaks and it is generally accepted that cells lacking both PARP-dependent SSB repair and also key proteins required for the repair of DNA DSBs are inviable [219, 351, 352]. *Brca1* null cells have been shown to be extremely sensitive to PARP inhibitors. Experimental studies suggest that in the absence of PARP, unrepaired SSB form DSB during replication and only cells which are competent in repairing DSB can survive.

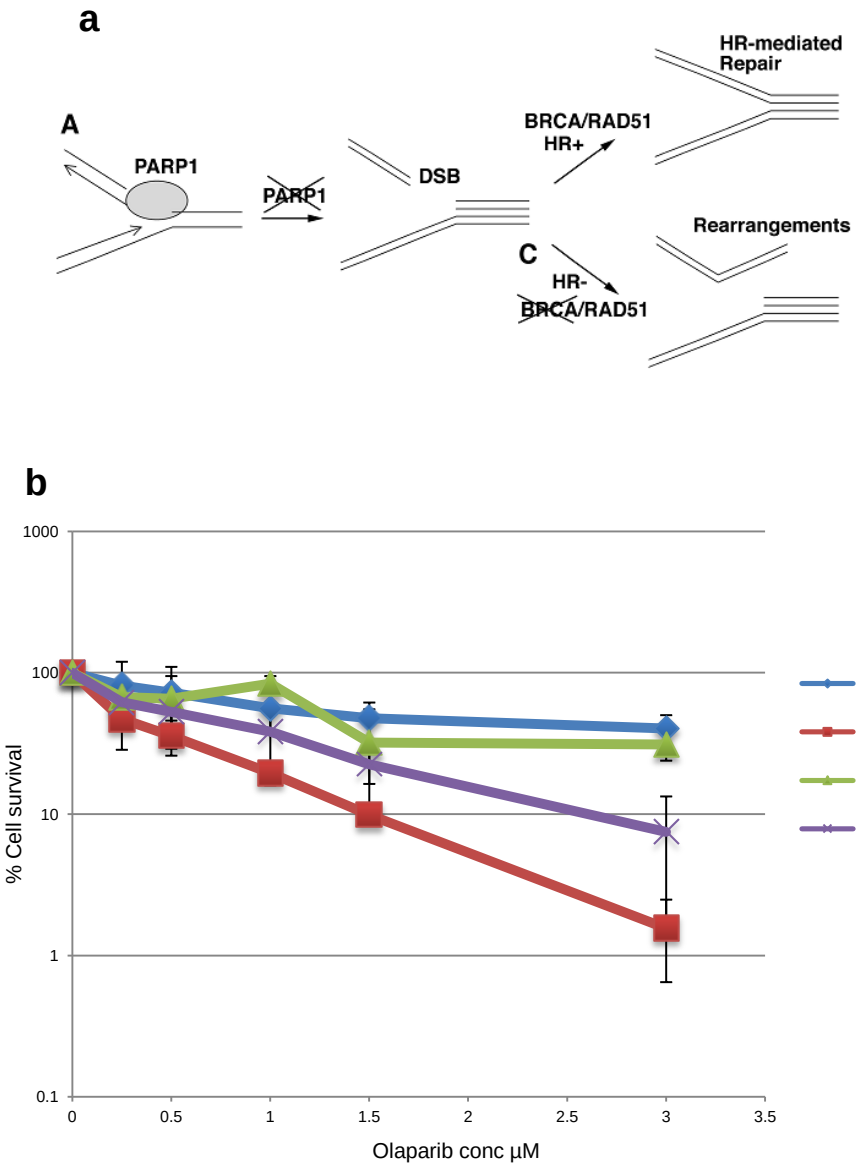

Cell Line	IC_{50} Value(µM)	IC_{50} Fold increase over DTDR17
DTDR17	2.059	1
DTDR17 BARD1-/-	0.4885	4.2
DTDR17 BARD1-/- (+) hsBARD1	1.883	1.1
DTDR17 BARD1-/- (+) hsBARD1ΔBRCT	0.8744	2.36

Figure 3.2 Loss of the BRCT domains of BARD1 sensitises cells to Olaparib
(a) Schematic representation of how PARP inhibitors sensitise HR deficient cells. Adapted from *Joseph A. De Sot and Chu-Xia Deng 2006.*
(b) Colony survival assay illustrating the sensitivity of *Bard1* and HsBARD1ΔBRCT cells to PARP inhibitor, Olaparib. Wild type, *Bard1* and mutant cells expressing either HsBARD1 or HsBARD1ΔBRCT were treated for 24hrs with 0-3µM Olaparib before being plated on methylcellulose cellulose media, as described in the Methods and materials section. Surviving colonies were counted 9-12 days after plating and plotted relative to untreated cells. Data shown are the mean of at least 3 independent experiments. The IC50 values were calculated from log dose response curves from at least 3 independent experiments.

As shown in figures 3.1 and 3.2, *Bard1* cells are extremely sensitive to PARP inhibitors and also have severely impeded HR according to the HRE assay in comparison to WT cells. *Bard1* cells expressing HsBARD1ΔBRCT also appear to be less efficient in repairing DNA DSBs. The loss of the BRCT domains alone doesn't demonstrate the same level of sensitivity as a complete *BARD1* Knock-out. The loss of the BARD1 BRCT domains does not affect the formation of the BRCA1 BARD1 heterodimer allowing BRCA1 to play its role in repairing the DSB [194] whereas complete loss of BARD1 prevents the retention of BRCA1 in the nucleus where it has its DDR function. This may partly explain the difference in sensitivity to DNA DSBs, between *BARD1* knockout cells and those which lack the BARD1 BRCT domains. Results so far in this chapter suggest that the loss of the BARD1 BRCT domains decreases the efficiency of HR in cells and sensitises these cells to PARP inhibitors indicating that the BRCT domains of BARD1 contribute to the efficient repair of DNA DSBs.

To confirm that the decrease in HR efficiency and sensitivity to PARP inhibitors shown in cells lacking the BARD1 BRCT domains cannot be accounted for by the potential mislocalisation of the protein, the localisation of HsBARD1 and HsBARD1ΔBRCT in *Bard1* cells was analysed by Western blot. Lysates from *Bard1* cells reconstituted with either *HsBARD1* or *HsBARD1ΔBRCT* were separated into their nuclear and cytoplasmic fractions and the localisation of BARD1 was investigated by Western blot. Fractionations of cell extracts confirm that HsBARD1 and HsBARD1ΔBRCT are proficient in localising to the nucleus (figure 3.3). The BARD1 antibody used recognises only human BARD1 and does not recognise chicken BARD1, therefore a direct comparison between Wild type cells and mutant reconstituted cell lines was not possible. α-GAPDH was used as a cytoplasmic marker and α-P84 was used as a nuclear indicator to assure that the method of fractionation used was proficient in separating the nuclear and cytoplasmic fractions. It is important to note that figure 3.3 is not an accurate depiction of the overall expression of HsBARD1 and HsBARD1ΔBRCT as the "whole" expression of HsBARD1 is relatively low. A more

accurate representation of the total expression of BARD1 and HsBARD1ΔBRCT can be seen in figure 3.14(a) and figure 3.3 should only be referenced in relation to the cytoplasmic and nuclear localisations as the whole lysates appear to not have transferred correctly.

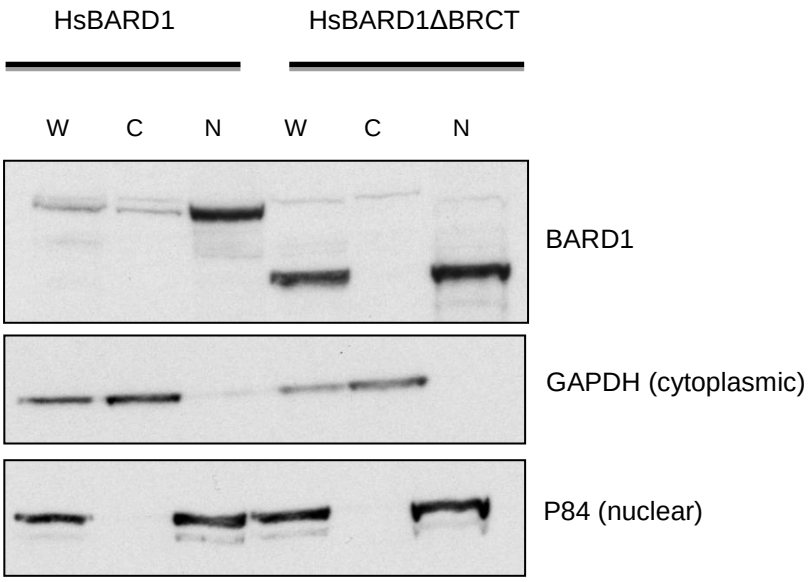

Figure 3.3 Fractionation of DTDR17 *Bard1* reconstituted cells.
Cell lysates were fractioned into their cytoplasmic and nuclear fractions as described in the Methods and Materials chapter. W(whole), C(cytoplasmic) and N(nuclear) Fractions were analysed by Western blotting. The majority of BARD1 is located in the nuclear fractions for both reconstituted mutant cell lines.

During the analysis of the Homologous recombination efficiency of *Bard1* cells and reconstituted cells in figures 3.1(b), 3.12(a) and 3.15(a) it became clear that the difference in the expression level of reconstituted proteins corresponded to a variation in the results of the assay. To investigate the impact this had on the results observed with the loss of the BRCT domains, a number of different unique clones from the same DTDR17 *Bard1* cell line reconstituted with *HsBARD1ΔBRCT* were analysed using the HRE assay. As shown in figure 3.4(b) there is a variation in the expression of HsBARD1ΔBRCT. Consistent with the results in figure 3.1, all unique clones in figure

3.4 show a decrease in efficient repair of DSBs by HR. It appears that the expression of level of HsBARD1ΔBRCT does impact the level of GFP expression in the HRE assay however the overall result remains clear in comparison to either Wild type cells or *Bard1* cells reconstituted with full length *HsBARD1*. The difference of clonal expression was calculated by band density using ImageJ. The % expression of the HsBARD1ΔBRCT clones were normalised relative to the expression of GAPDH compared to the highest expressing clone (13).

a

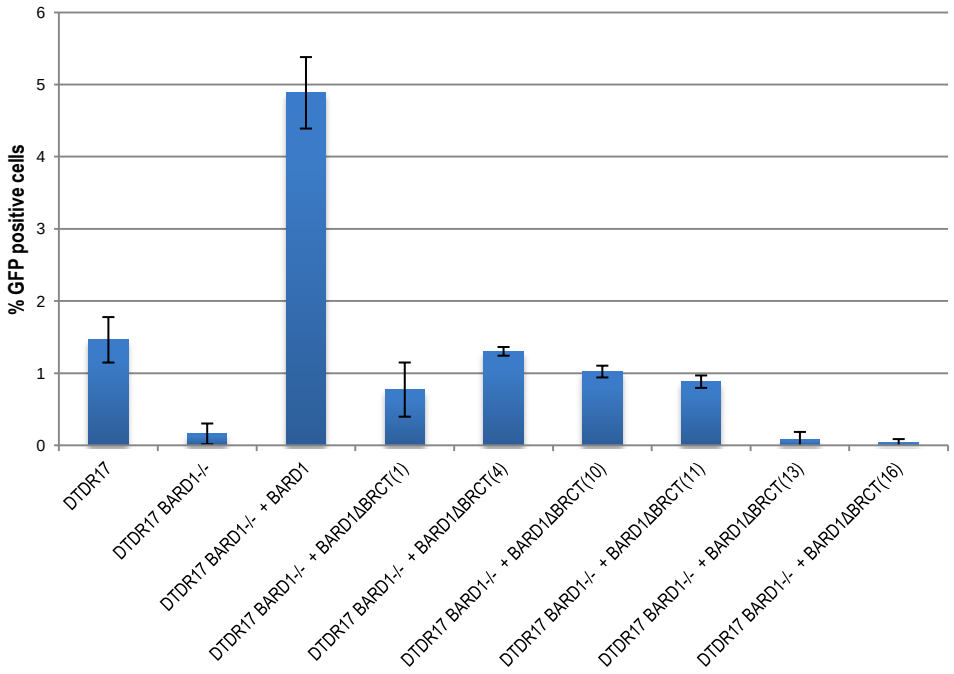

b

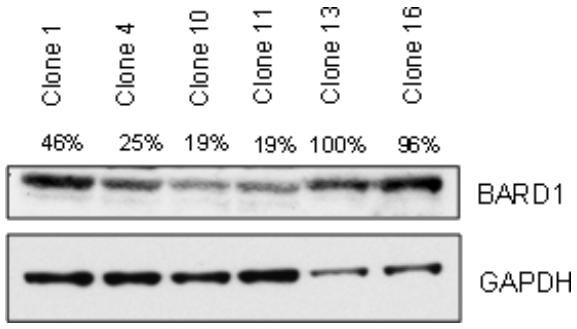

c

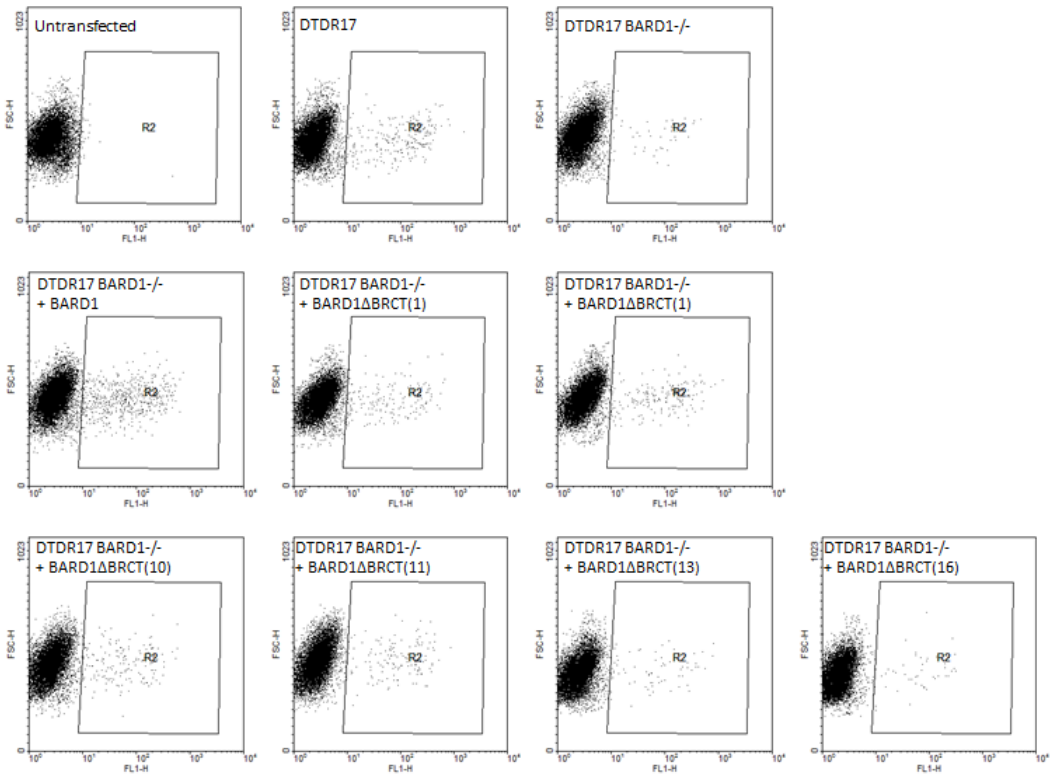

Figure 3.4 HRE assay comparing DTDR17 BARD1-/- + HsBARD1ΔBRCT clones.
(a) HRE assay illustrating the percentage of cells expressing GFP 24hrs after transfection with the Isce-I expressing plasmid. Results were normalised to untransfected cells. Data shown are the mean of at least 3 independent experiments. Error bars, s.d.
(b) Western blot illustrating the expression of the different unique clones. % expressing compared to highest expressing clone and band density calculated using imageJ.
(c) Representative dot plot of raw data from figure (a) Cells expressing GFP were identified by FACS analysis. GFP positive cells were gated for relative to their GFP status and size (FSC-H) and seen in the box R2.

The results in figures 3.1(b), 3.2(b) and 3.4(a) strongly suggest that the BARD1 BRCT domains are important in the repair of DNA DSBs. Figures 3.1(b) and 3.4(a) shows that the loss of the BARD1 BRCT domains results in a decrease in efficient HR compared to WT cells and figure 3.2(b) indicates that the loss of the BRCT domains of BARD1 sensitises the cells to PARP inhibitors. The defects seen in cell lines lacking the BARD1 BRCT domains appears not to be due to mislocalisation of the protein to the nucleus (figure 3.3). As sensitivity to PARP inhibitors is common in cells with aberrant HR, these results firmly implicate a functional role for the BARD1 BRCT in the repair of DNA DSBs.

3.2.2 The BARD1 BRCT domains help stabilise CtIP in the BRCA1-C complex.

Several years ago three different proteins were discovered to form complexes with the BRCA1 BARD1 heterodimer. These proteins were identified as Abraxas, FANCJ and CtIP and they form three different complexes referred to as the BRCA1-A, BRCA1-B and BRCA1-C respectively [133, 228, 346]. All three proteins bind to the BRCA1 BRCT domains in a phosphorylation dependent manner and are important in the DDR [353]. To date the main function of BARD1 in these complexes is to bind BRCA1, allowing its nuclear retention and greatly increasing BRCA1s E3 ligase activity. With the recent knowledge that the BRCT domains of BARD1 are also important for HR, it is possible that they contribute to the formation and/or stabilisation of the BRCA1 complexes.

As previously mentioned, Abraxas, FANCJ and CtIP bind to the BRCA1 BRCT domains in a phosphorylation dependent manner. The BARD1 BRCT domains have also been shown to be capable of binding a synthetic phospho-peptide containing a pSer-D/E-D/E-E motif, however there are no known phospho-proteins which specifically interact with the BARD1 BRCT domains [346]. Although BRCA1 is known to form the main phospho-dependent interaction with Abraxas, FANCJ and CtIP it has never been shown if BARD1 can contribute to these interactions. To determine if the BARD1 BRCT domains contribute to the formation of the BRCA1 complexes, Flp-In HEK 293 cells stably expressing either GFP-BARD1 or GFP-BARD1ΔBRCT were generated.

Flp-In HEK 293 cells were used to generate stable cell lines expressing GFP-BARD1 and GFP-BARD1ΔBRCT as they are designed to allow tetracycline inducible expression of the stably integrated gene. This cell line also allows facile targeted integration of a Flp-In expression vector containing your gene of interest into a single stably integrated FRT site at a transcriptionally active genomic locus within the cell line.

A pull down of GFP-BARD1ΔBRCT was compared to GFP-BARD1 in their ability to form the BRCA1 complexes. Using the same conditions. GFP-BARD1ΔBRCT and GFP-BARD1 were immunoprecipitated and the amount of Abraxas, CtIP and FANCJ pulled down with GFP-BARD1ΔBRCT and GFP-BARD1 was analysed by Western blot to determine any differences in their ability to form the BRCA1 complexes. BARD1ΔBRCT was not as efficient at forming the BRCA1-C complex which binds CtIP (figure 3.5). The decrease in the amount of CtIP found to co-immunoprecipitate with GFP-BARD1ΔBRCT in comparison to GFP-BARD1 was statistically significant according to the student t-test. This suggests that the BRCT domains of BARD1 may help stabilise the BRCA1-C complex and could potentially clarify their role in promoting genome stability.

HEK 293 cells stably expressing GFP alone were used as a control. As previously stated, the expression GFP-BARD1 and GFP-BARD1ΔBRCT was induced and regulated by tetracycline. For this experiment, it was important to keep the levels of expression of GFP-BARD1 and GFP-BARD1ΔBRCT as close to endogenous levels of BARD1 as possible to avoid potential dominant negative effects associated with overexpression of proteins. In order to maintain a 3 fold over endogenous BARD1 expression GFP-BARD1 was induced with 2.5ng tetracycline and GFP-BARD1ΔBRCT was induced with 7.5ng tetracycline over night before harvesting cells (figure 3.5(a).

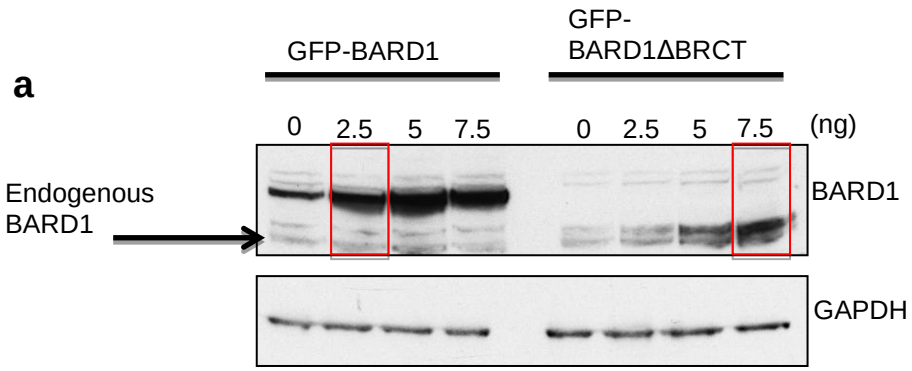
a
GFP-BARD1
GFP-BARD1ΔBRCT
0 2.5 5 7.5 0 2.5 5 7.5 (ng)
Endogenous BARD1
BARD1
GAPDH

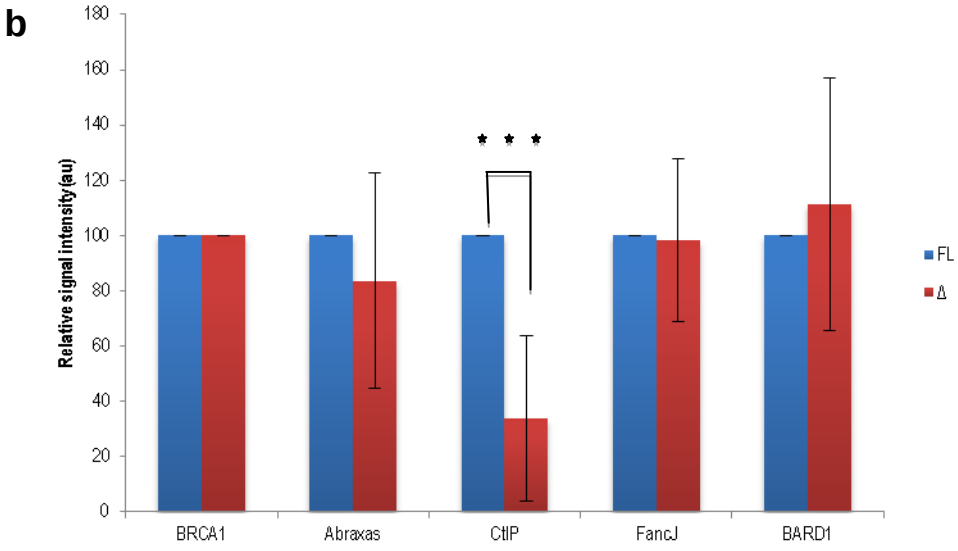
b
Relative signal intensity(au)
180
160
140
120
100
80
60
40
20
0
BRCA1
Abraxas
CtIP
FancJ
BARD1
FL
Δ

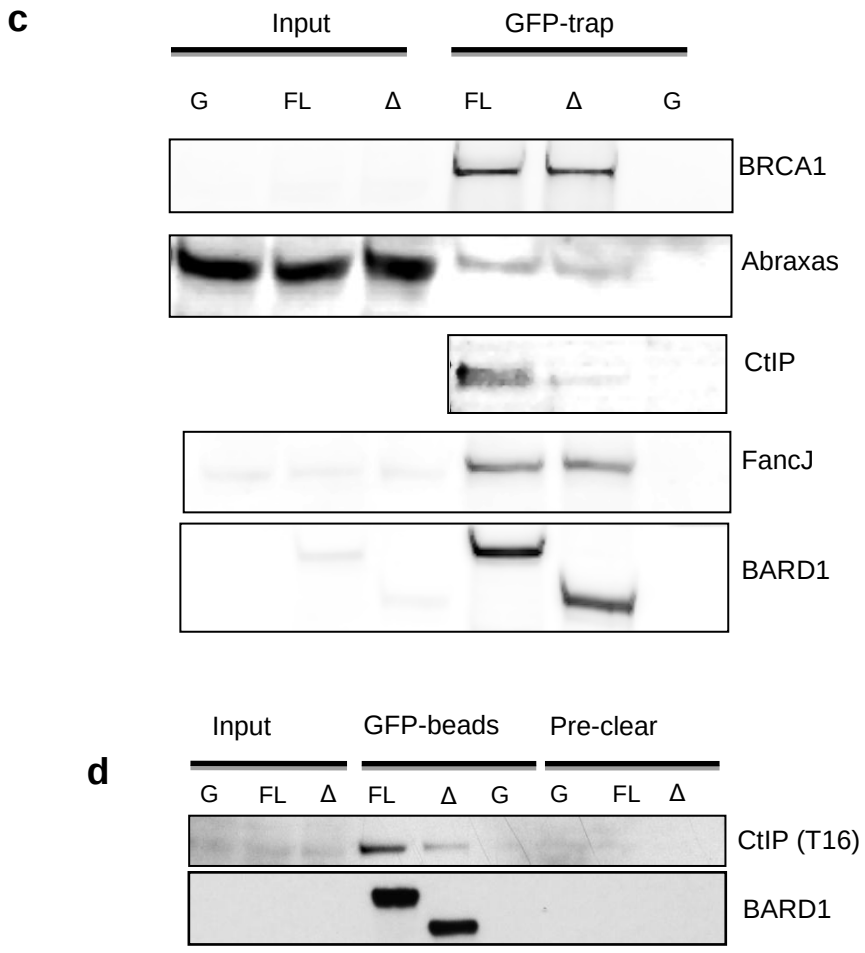

Figure 3.5 The BRCT domains of BARD1 are important in stabilising the BRCA1-C complex
(a) Western blot illustrating the concentration of tet required to induce the expression GFP-BARD1 and GFP-BARD1ΔBRCT to 3 times the endogenous BARD1 level. Cells were induced o/n with different tet concentration and harvested the following morning before analysis by Western blot.
(b)Licor quantification of a GFT-trap pull down. GFP-BARD1 and GFP-BARD1ΔBRCT were pulled down and immunopercipitated proteins were analysed by licor Western blotting. Each protein band was quantified by Licor software and figures were normalised to amount of BRCA1 present. FL(GFP-BARD1), Δ (GFP-BARD1ΔBRCT). *** indicates a statistical significance p value of ≤ 0.001. P value derived from the student t-test. Data shown are the mean of at least 6 independent experiments. Error bars, s.d.
(c) A representative Licor Western blot from which the graph in figure (a) was generated. FL (GFP-BARD1), Δ (GFP-BARD1ΔBRCT), G(GFP)
(d) Duplicate Western blot from experiment in figure (b) using a different CtIP (T-16) antibody.

The pull downs were carried out under crosslinked conditions to ensure that all potential BRCA1 complex members could be co-immunoprecipitated with BARD1. The GFP-BARD1 and GFP-BARD1ΔBRCT lysates were crosslinked with DSP, an amine reactive crosslinker, before the pull down was carried out. The amount of Abraxas,

FANCJ and CtIP found to co-immunoprecipitate with GFP-BARD1 and GFP-BARD1ΔBRCT was plotted in figure 3.5(b) relative to the amount of BRCA1 pulled down. As BRCA1 is known to be responsible for binding Abraxas, FANCJ and CtIP, the difference in the ability of either GFP-BARD1 or GFP-BARD1ΔBRCT to pull down the BRCA1 complex members is illustrated relative to the amount BRCA1 pulled down (figure 3.5(b). The CtIP antibody (T-16) normally used for traditional Western blotting was not compatible with the Licor system so another CtIP antibody (bethyl) was used, however the same result was observed with the T-16 antibody using a traditional Western blot method and X-ray film as seen in figure 3.5 (d). The CtIP antibody used in figure 3.5 (c) shows extremely high background signal, therefore no input was shown. This antibody was only suitable for use after imunnoprecipitation as the majority of unspecific bands are lost. There was very little variation in the levels of FANCJ pulled down with both GFP-BARD1 and GFP-BARD1ΔBRCT through each experiment and no difference was observed in the amount of FANCJ co-immunoprecipitated with GFP-BARD1 in comparison to GFP-BARD1ΔBRCT. However on several occasions the amount of Abraxas pulled down appeared to be less in the case of GFP-BARD1ΔBRCT in comparison to GFP-BARD1. This was not consistently reproducible to make any conclusive deductions.

Similar to DTDR17 cells, GFP-BARD1 and GFP-BARD1ΔBRCT expressed in the FLP-In HEK 293 cells are proficient at localising to the nucleus (figure 3.6 (a). GFP-BARD1 and GFP-BARD1ΔBRCT and the control cell line containing just GFP also progress through the cell cycle at the same rate (figure 3.6 (b,c,). This evidence suggest that the decrease in the amount of CtIP bound to the BRCA1-C complex in the absence of the BARD1 BRCT domains is not due to defects in the progression through the cell cycle. BRCA1 is known to have important roles in the regulation of the cell cycle as a heterodimer with BARD1 [134]. Although the HEK 293 cell lines contain endogenous BARD1 it still important to rule out any possible dominant negative effects that the overexpression of GFP-BARD1 and GFP-BARD1ΔBRCT may have on the cell

cycle. The expression levels of Abraxas, FANCJ and CtIP do not change significantly between the different cell lines during the cell cycle (figure 3.6(d).

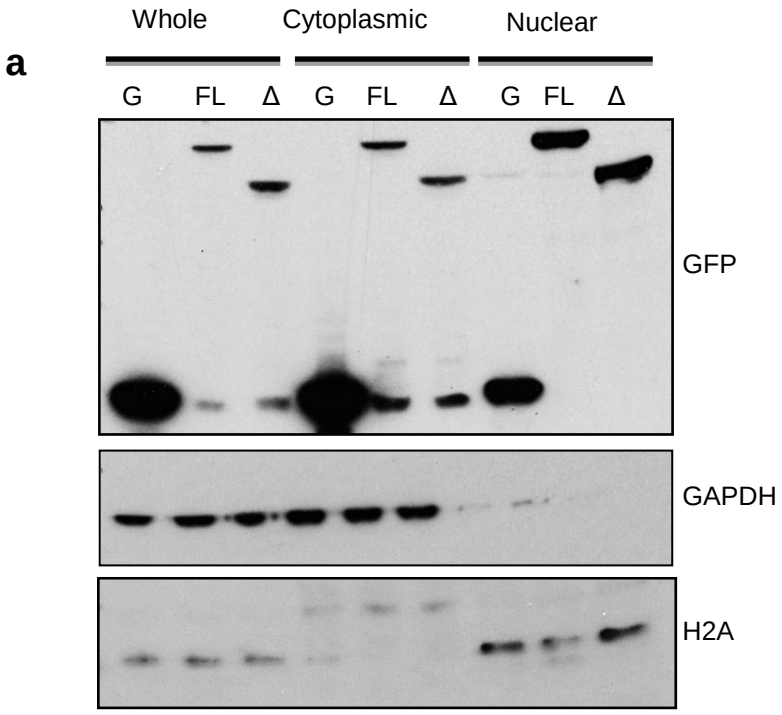

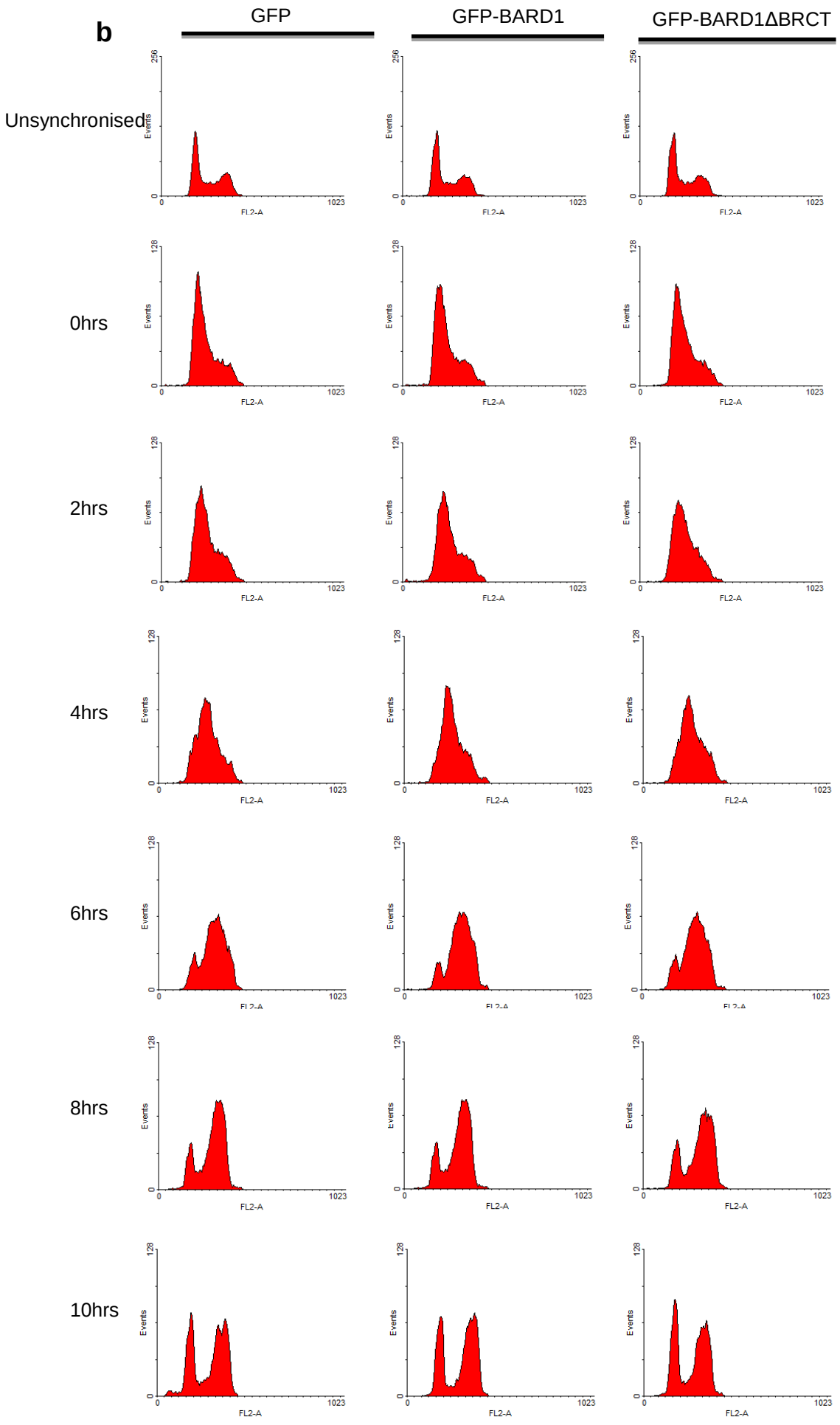
b
GFP
GFP-BARD1
GFP-BARD1ΔBRCT
Unsynchronised
0hrs
2hrs
4hrs
6hrs
8hrs
10hrs
Events
FL2-A
0
1023

c

		GFP	GFP BARD1	GFP BARD1ΔBRCT
Unsychronised	G1	30.81	35.15	33.5
	S	48.92	41.7	47.17
	G2	14.65	14.34	14.23
0hrs	G1	58.86	59.48	54.57
	S	0.74	0.85	0.57
	G2	21.33	21.27	21.52
2hrs	G1	11.07	6.82	9.43
	S	76.72	77.09	76.53
	G2	7.81	9.2	6.96
4hrs	G1	10.54	7.23	7.97
	S	75.57	77	76.08
	G2	8.07	8.21	10.16
6hrs	G1	10.21	8.29	9.96
	S	66.58	65.91	65.84
	G2	15.07	18.26	16.13
8hrs	G1	14.18	15.8	16.2
	S	49.93	47.1	47.6
	G2	25.38	24.6	29.28
10hrs	G1	27.83	30.05	29.83
	S	25.98	26.94	26.63
	G2	37.48	29.69	36.13

d

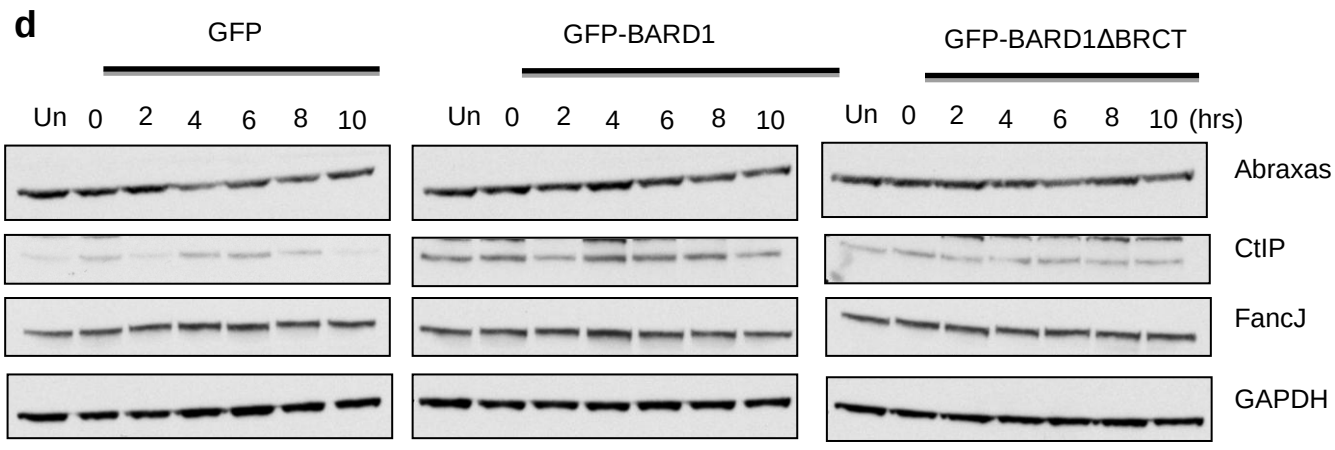

Figure 3.6 GFP-BARD1 and GFP-BARD1ΔBRCT cell lines are not hindered through the cell cycle.
(a) Western blot of the localisation of HEK reconstituted cell lines. GFP (G), GFP-BARD1 (FL) and GFP-BARD1ΔBRCT (Δ)
(b) Representative FACS analysis for cell cycle profiles of cells stained with propidium iodide (PI).Cells were arrested in late G1 phase by a double thymidine block and released. Samples were taken up to 10hrs after release.
(c) Representative table of the amount of cells in the different stages of the cell cycle obtained from the FACS analysis of cell cycle profiles, as in (a), of cells stained with PI and BrdU .Cells were pulse labelled with BrdU 20 minutes before fixing and staining.
(d) Western blot of the lysates collected at each time point after release from the double thymidine block. Unsynchronised (Un).

The results shown in this chapter so far strongly suggest that the BARD1 BRCT domains have an important functional role in the repair of DNA DSBs as loss of the BRCT domains of BARD1 results in a decrease of HR efficiency and also sensitises cells to PARP inhibitors. Evidence from figure 3.5(b) shows that the loss of the BRCT domains of BARD1 may abrogate the formation of the BRCA1-C complex as less CtIP is found to co-immunoprecipitate with the BARD1 BRCA1 heterodimer in the absence of the BARD1 BRCT domains. This result potentially implicates a functional role for the BARD1 BRCT domains in the stabilisation of the BRCA1-C complex.

3.2.3 Designing BARD1 BRCT point mutants to disrupt the potential binding of phosphorylated proteins.

It has become evident that the BARD1 BRCT domains play an important role in the DNA damage response and, according to figure 3.5(b), may help stabilise CtIP to the BRCA1-C complex. The BRCT domain is an evolutionary conserved module which is found in many prokaryotic and eukaryotic proteins. BRCT domains have been shown to bind proteins in a phosphorylation dependent manner. Several BRCT domain containing proteins have been associated with processes that are essential for cell cycle regulation and DNA repair [290]. It is possible that the DDR function of the BARD1 BRCT domains may depend on their potential interaction with a phospho-protein. In order to investigate this hypothesis, single point mutations, which are predicted to disrupt potential phospho-protein binding, were generated in the BARD1 BRCT domains.

BRCT domains were first discovered in the C-terminus of the BRCA1 protein which contains two tandem repeat BRCT domains [193]. Although several BRCT domain containing proteins commonly have two copies of a BRCT sequence, however proteins containing between one and eight units have been identified [193, 289, 290, 304]. The method by which the BRCT domains of BRCA1 bind phosphorylated proteins has been described by three independent crystallographic studies [314, 315, 354]. The BRCA1 BRCT domains recognise pSer-X-X-Phe motifs such as those found in Abraxas, FANCJ and CtIP and BRCA1 has been shown to interact with these three proteins in a phosphorylation dependent manner. Mutations in the pSer-X-X-Phe motifs of Abraxas, FANCJ and CtIP prevent their binding to BRCA1 (figure 3.7(a). The phospho-peptide binds in a groove which involves both the BRCT domains. The crystal structure of the BRCA1 BRCT domains revealed that there is a phospho-binding pocket in the N-terminal BRCT domain which binds the phosphate oxygen atom. The phenylalanine residue is recognised by a hydrophobic pocket found at the interface of the N- and C-terminal BRCT interface reviewed in [291].

BRCA1 and BARD1 are structurally very similar, especially in relation to the formation and location of their BRCT domains. Both proteins contain tandem BRCT domains in the C-terminus of the protein. However in contrast to the BRCA1 BRCT domains, there are no known phospho-binding proteins known to interact with the BARD1 BRCT domains. The recent elucidation of the crystal structure of the BARD1 BRCT domains identified Ser575 and Lys619 as two key residues for binding pSer peptides. His686 was considered to be favoured as the main residue responsible for forming the hydrophobic groove according to the BARD1 BRCT crystal structure, similar to M1775R in BRCA1 [311]. Consistent with previous studies, point mutations in the BRCT domains of BRCA1, equivalent to Ser575 and Lys619 in BARD1, prevent phosphorylated Abraxas, FANCJ and CtIP binding to the BRCA1 BRCT domains (figure 3.7(b) Taking into consideration the crystal structure of BARD1 BRCT domains and comparing them to known point mutations affecting the binding of phospho-

proteins to the BRCA1 BRCT domains (figure 3.8(a), three separate point mutation were generated in the BARD1 BRCT domains which are predicted to abrogate the binding of a potential phospho-peptide. As an extra measure of assurance, the BRCT domains of BARD1 were compared in different species revealing highly conserved regions where the phospho-protein interactions are thought to occur (figure 3.8(d).

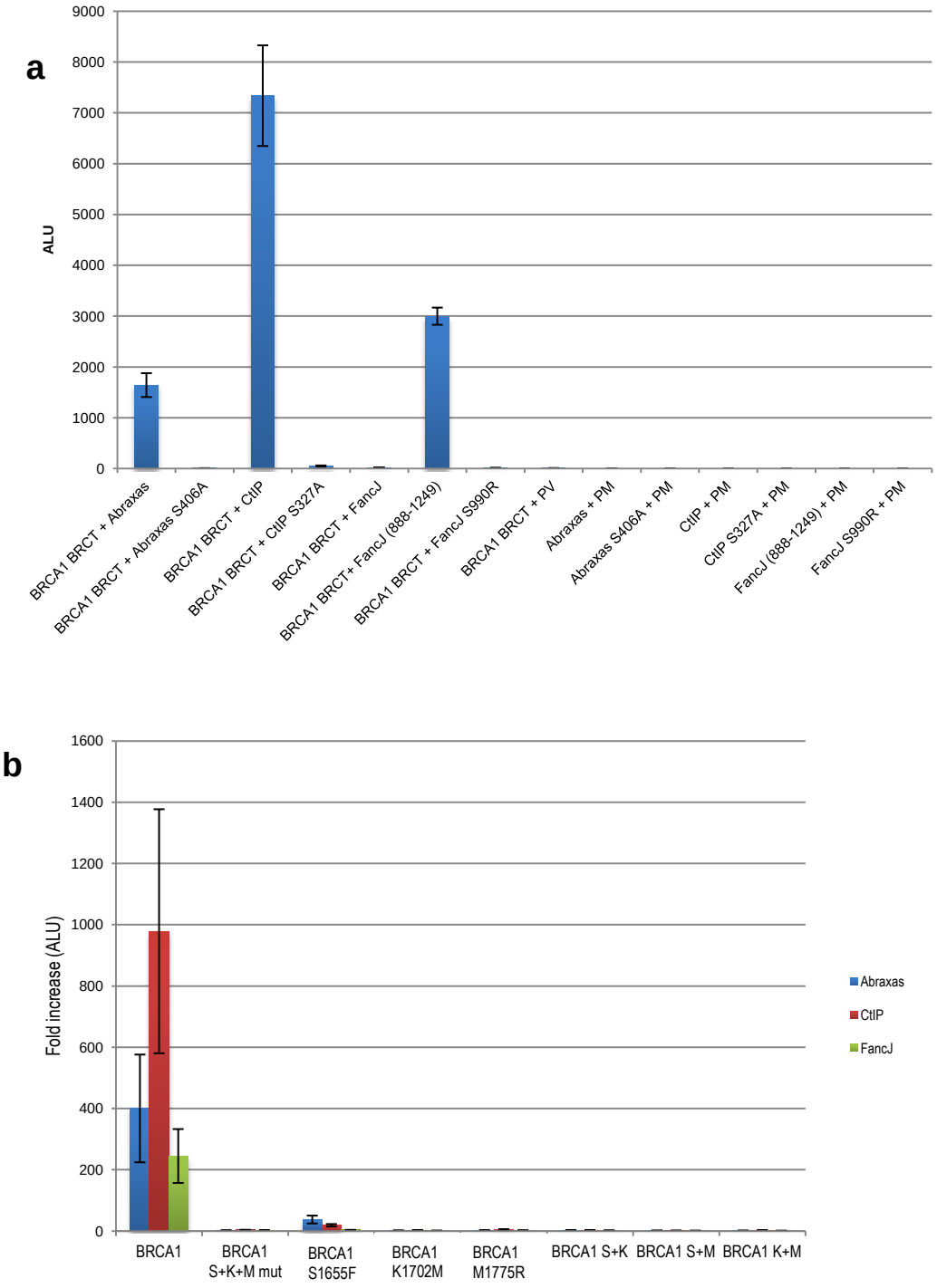

Figure 3.7 BRCA1 binds Abraxas, FANCJ and CtIP is a phospho-dependent manner.
(a) Mammalian two-Hybrid assay between BRCA1 and its binding partners. The intensity of the luciferase read out (ALU) indicated binding between the bait and prey proteins. PM and PV are the empty vectors used as a binding control..The BRCA1 BRCT domains interact with Abraxas, FANCJ and CtIP but not with their mutant counterparts which prevent phosphorylation. . Data shown are the mean of at least 3 independent experiments. Error bars, s.d.
(b) Mammalian two-Hybrid analysis indicating that BRCA1S1665F, BRCA1K1702M, BRCA1M1775R and the triple mutant prevent interaction with the known phoshpo-binding protein interactors. FANCJ (888-1249) was used as full length FANCJ does not interact with BRCA1 in this Mammalian two-hybrid. Data shown are the mean of at least 3 independent experiments. Error bars, s.d.

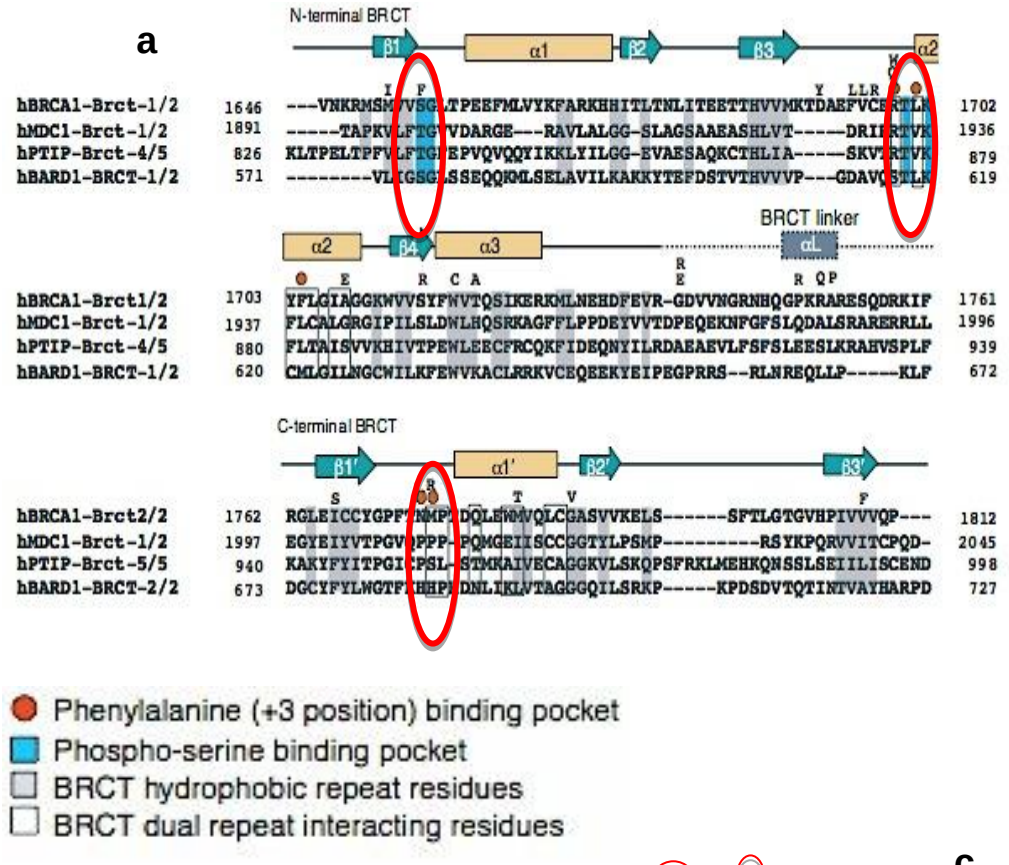

Phenylalanine (+3 position) binding pocket
Phospho-serine binding pocket
BRCT hydrophobic repeat residues
BRCT dual repeat interacting residues

b

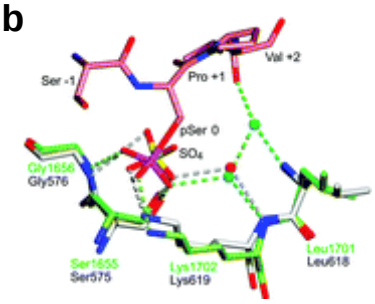

c

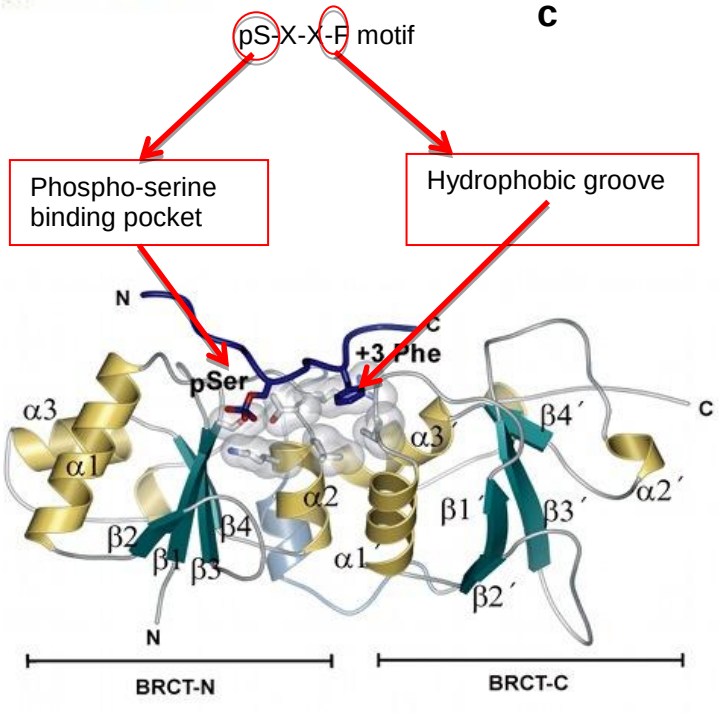

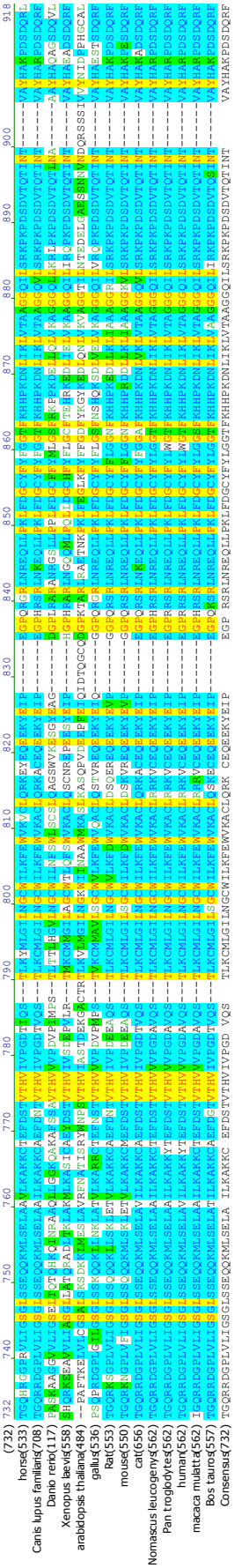
732
740
750
760
770
780
790
800
810
820
830
840
850
860
870
880
890
900
918
(732)
horse(533)
Canis lupus familaris(708)
Danio rerio(117)
Xenopus laevis(558)
arabidopsis thaliana(484)
gallus(536)
Rat(553)
mouse(550)
cat(656)
Nomascus leucogenys(562)
Pan troglodytes(562)
human(562)
macaca mulatta(562)
Bos taurus(557)
Consensus(732)

Figure 3.8 BARD1 BRCT point mutants
(a) Amino acid sequence alignment of the BRCT domains of BARD1, BRCA1, MDC1 and MCPH1. Mutated sites are circled in red, regions highlighted blue are highly conserved and responsible for the phosho-serine binding pocket. Figure adapted from *Williams et al 2004*
(b) Stick model of the phospho-binding pocket of BRCA1(green) and binding of CtIP ligand (pink) BARD1 phosho binding pocket is superimposed onto BRCA1s in grey. Figure adapted from *Birrane et al. 2007*
(c) Illustration of the BRCT binding pockets. Figure adapted from *Williams et al 2004.*
(d) Sequence alignment of BARD1 BRCT from a variety of species.

The point mutants generated in the BRCT domains of BARD1 were, S575F, K619M and H686R. The S575F and K619M mutation are predicted to disrupt the phospho-binding groove whereas the H686R is predicted to disrupt the hydrophobic binding pocket. A triple mutant was also generated as there has been evidence suggesting that a single point mutation in the BRCT domain of another protein (XRCC1) is not enough to prevent binding of a phospho-protein to the BRCT domains (correspondence with Keith Caldecott).

3.2.4 BARD1 binds CtIP and potentially Abraxas not in a phosphorylation dependent manner.

Previous results in this chapter indicated that BARD1 potentially stabilises CtIP to the BRCA1-C complex. Full length BARD1 interacts with CtIP and to a lesser extent Abraxas in a Mammalian two-Hybrid system (figure 3.9(a). This interaction appears to be dependent on the phosphorylation of CtIP and Abraxas as their phospho-mutant counterparts do not interact with BARD1 in the Mammalian two-hybrid (figure 3.9). The BRCT domains of BARD1 alone are not sufficient to form these interactions. The BARD1 BRCT domains do not interact with Abraxas and CtIP (figure 3.9(a). However, it has often been observed in the lab that large full length proteins such as BRCA1 and FANCJ do not interact in a Mammalian two-Hybrid. In a mammalian two-Hybrid system the prey and bait proteins are fused to an activating domain and a binding domain. Only when the activation domain and binding domain are brought into close contact, by the interaction of the bait and prey proteins, do they form a functional transcription

factor. This leads to the significant increase of the expression of a reporter gene, which is GFP in this case, which is measured and relates to the interaction between the bait and prey proteins. In the case of full length BRCA1 and FANCJ, it is possible that the lack of interaction seen in a mammalian two-hybrid is due to the structural confirmation of the proteins preventing the interaction between their fused binding and activation domains. In the case of BRCA1, only the BRCT domains are used and similarly only the region around the pSer-X-X-Phe of FANCJ can be used in this system.

Figure 3.9(b) reveals that the BARD1 BRCT domains containing point mutations also interact with CtIP and Abraxas suggesting that the interaction is not dependent on the phospho-binding potential of BARD1 BRCT domains. Loss of the BARD1 BRCT domains shows a greater interaction with CtIP than observed with the full length protein. Figure 3.9 illustrates that BARD1 interacts with CtIP and to a lesser extent Abraxas even in the absence of its BRCT domains. In both figures the relative signal obtained is a lot lower than those seen with BRCA1 interactions, this may indicate that the BARD1 binding seen is of a weaker or more transient nature.

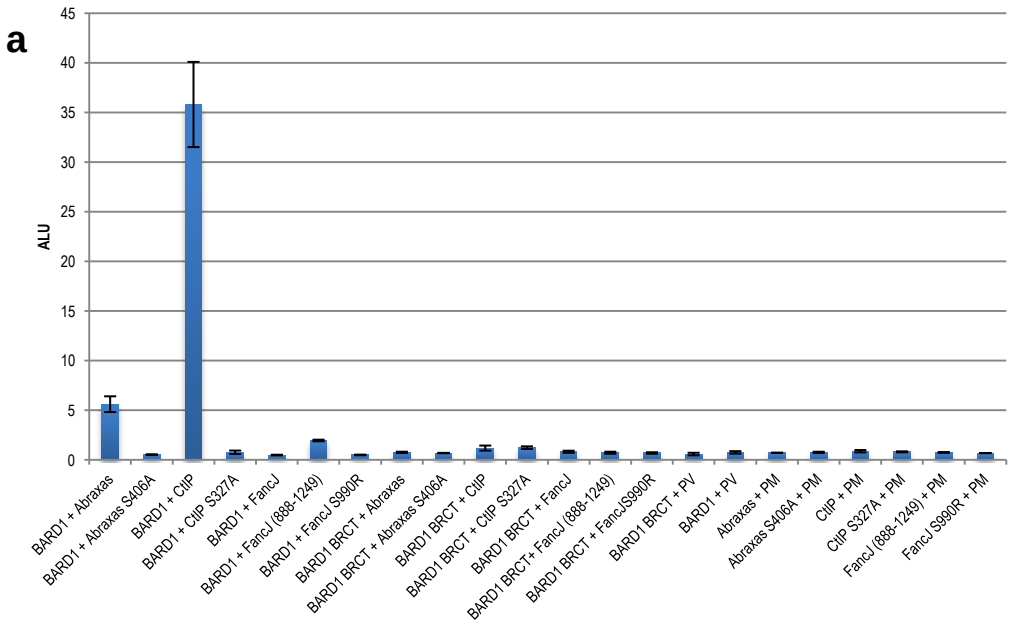

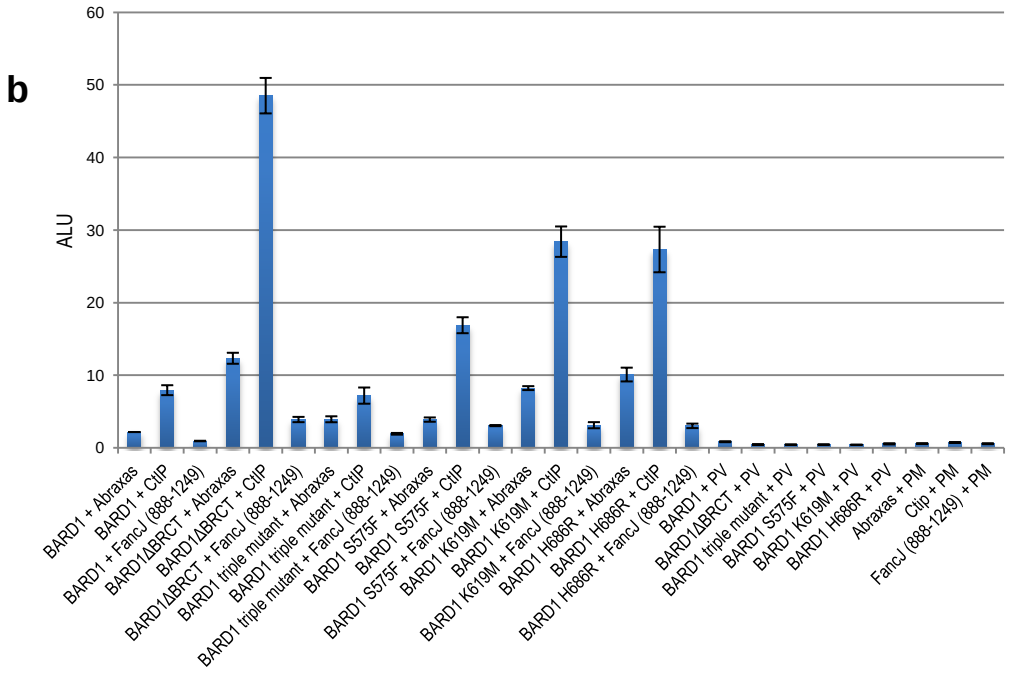

Figure 3.9 BARD1 interacts with CtIP and to a lesser extent Abraxas.
(a) Mammalian two-Hybrid assay between BARD1 and the BRCA1 binding partners. The intensity of the luciferase read out (ALU) indicated binding between the bait and prey proteins. PM and PV are the empty vectors used as a binding control.BARD1 interact CtIP and to a lesser extent Abraxas but not with their mutant counterparts which prevent phosphorylation. . Data shown are the mean of at least 3 independent experiments. Error bars, s.d.
(b) Mammalian two-Hybrid analysis indicating that BARD1S575F, BARD1K619M, BARD1H686R and the triple mutant do not prevent interaction with the known BRCA1 interacters. Data shown are the mean of at least 3 independent experiments. Error bars, s.d.

3.2.5 The binding of BARD1 to CtIP it dependent on BRCA1.

To determine whether BARD1 can directly bind to CtIP, a point mutant in the ring domain of BARD1 (BARD1L107P) was generated to prevent the formation of the BRCA1 BARD1 heterodimer. BRCA1 and BARD1 bind via α-helices flanking their RING domains [206]. BARD1L107P has been previously shown to abrogate the binding of BRCA1 to BARD1 by disrupting one of the α-helices at the interface of binding [269]. BARD1L107P does indeed prevent BRCA1 binding (figure 3.10(b). In the absence of BRCA1, BARD1 cannot bind to CtIP as shown in figure 3.10(a). To confirm this result the interaction between BARD1 and the BRCA1 interacting partners were examined in cells treated with a BRCA1 siRNA. As expected similar results were seen in both experiments when BRCA1 was knocked down or prevented from binding to BARD1.

a

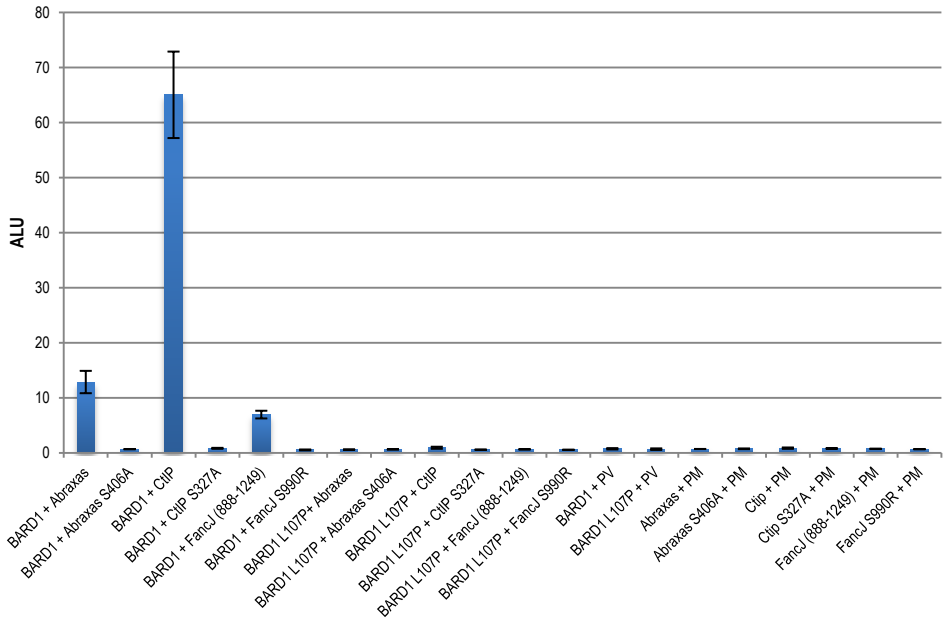
ALU
80
70
60
50
40
30
20
10
0
BARD1 + Abraxas
BARD1 + Abraxas S406A
BARD1 + CtIP
BARD1 + CtIP S327A
BARD1 + FancJ (888-1249)
BARD1 + FancJ S990R
BARD1 L107P+ Abraxas
BARD1 L107P + Abraxas S406A
BARD1 L107P + CtIP
BARD1 L107P + CtIP S327A
BARD1 L107P + FancJ (888-1249)
BARD1 L107P + FancJ S990R
BARD1 + PV
BARD1 L107P + PV
Abraxas + PM
Abraxas S406A + PM
Ctip + PM
Ctip S327A + PM
FancJ (888-1249) + PM
FancJ S990R + PM

b

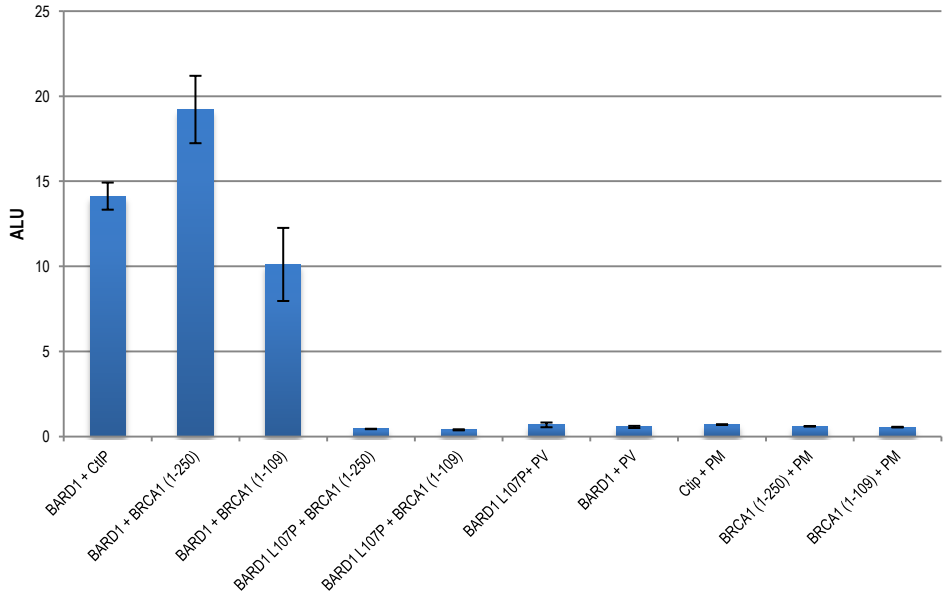
ALU
25
20
15
10
5
0
BARD1 + CtIP
BARD1 + BRCA1 (1-250)
BARD1 + BRCA1 (1-109)
BARD1 L107P + BRCA1 (1-250)
BARD1 L107P + BRCA1 (1-109)
BARD1 L107P+ PV
BARD1 + PV
Ctip + PM
BRCA1 (1-250) + PM
BRCA1 (1-109) + PM

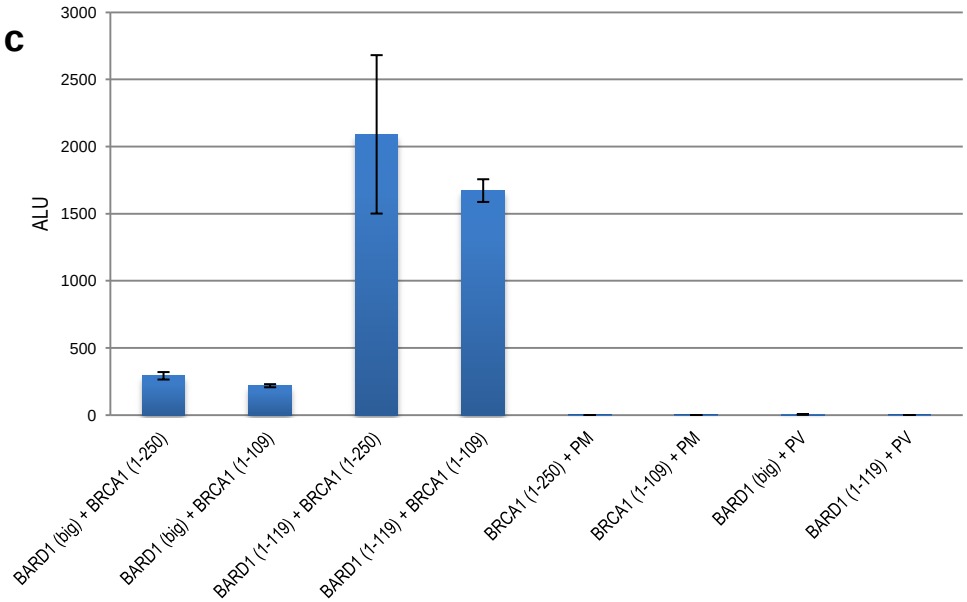
c
3000
2500
2000
1500
1000
500
0
ALU
BARD1 (big) + BRCA1 (1-250)
BARD1 (big) + BRCA1 (1-109)
BARD1 (1-119) + BRCA1 (1-250)
BARD1 (1-119) + BRCA1 (1-109)
BRCA1 (1-250) + PM
BRCA1 (1-109) + PM
BARD1 (big) + PV
BARD1 (1-119) + PV

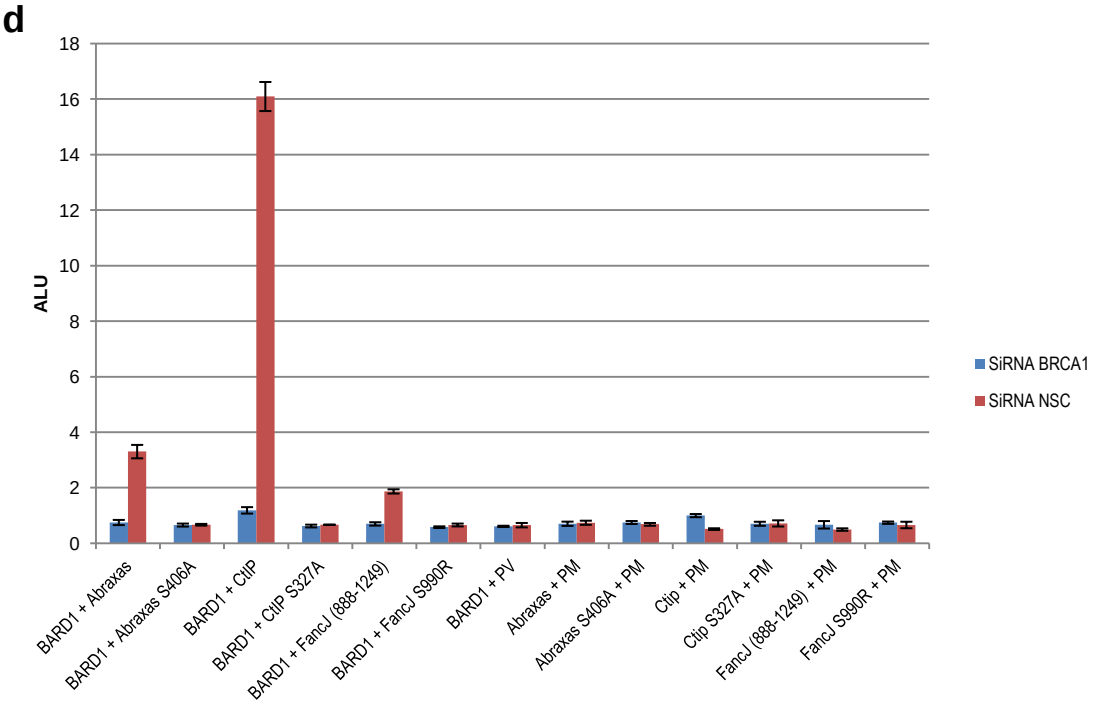
d
18
16
14
12
10
8
6
4
2
0
ALU
BARD1 + Abraxas
BARD1 + Abraxas S406A
BARD1 + CtIP
BARD1 + CtIP S327A
BARD1 + FancJ (888-1249)
BARD1 + FancJ S990R
BARD1 + PV
Abraxas + PM
Abraxas S406A + PM
Ctip + PM
Ctip S327A + PM
FancJ (888-1249) + PM
FancJ S990R + PM
SiRNA BRCA1
SiRNA NSC

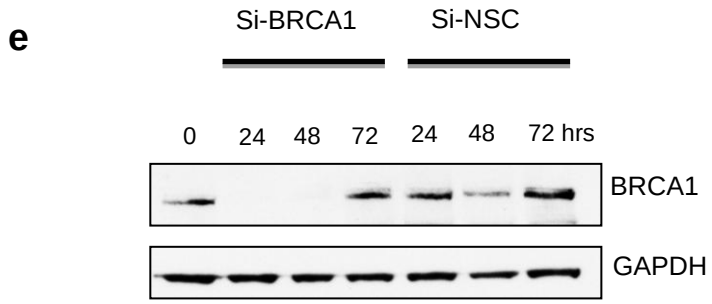

Figure 3.10 BARD1 and CtIP binding it dependent on BRCA1
(a) Mammalian two-Hybrid assay between BARD1L107P and the BRCA1 binding partners. The intensity of the luciferase read out (ALU) indicated binding between the bait and prey proteins. PM and PV are the empty vectors used as a binding control.BARD1L107P does not form any interactions. Data shown are the mean of at least 3 independent experiments. Error bars, s.d.
(b) Mammalian two-Hybrid analysis indicating that BARD1 can interact with both the large and small ring domains of BRCA1. Data shown are the mean of at least 3 independent experiments. Error bars, s.d.
(c) Mammalian two-Hybrid analysis indicating that BARD1L107P prevents the Ring domain of BRCA1 binding. Data shown are the mean of at least 3 independent experiments. Error bars, s.d.
(d) Mammalian two-Hybrid analysis showing that in the absence of BRCA1 BARD1 cannot interact with Abraxas, FANCJ or CtIP. Experiment was carried out 48 hrs after siRNA transfection. Data shown are the mean of at least 3 independent experiments. Error bars, s.d.
(e) Western blot of lysates harvested between 24 and 72hrs after siRNA treatment. BRCA1 knockdown is clearly present after 24 and 48hrs. Whereas the non-specific control (NSC) does not appear to affect the levels of BRCA1 expression.

The results in figure 3.10 indicate that the interaction between BARD1 and CtIP, shown earlier in a Mammalian two-Hybrid assay, depends on BRCA1. The Mammalian two-Hybrid assay can indicate a direct or an indirect interaction between a bait and a prey protein. It appears that for this experiment the formation of the BRCA1 BARD1 heterodimer is necessary for CtIP to bind. With this result in mind, the overall weaker signals observed in figure 3.9 of BARD1 and the BRCA1 complex members in comparison to the signal obtained with BRCA1 and its interacting partners may be partially explained by an indirect interaction between BARD1 and CtIP. It appears that the interaction between BARD1 and CtIP seen in a Mammalian two-hybrid may be completely dependent on the presence of BRCA1 as BARD1 BRCT domains alone cannot bind CtIP (figure 3.9a). It is possible that the interaction seen between BARD1 and CtIP in the Mammalian two-hybrid is in fact an interaction between BRCA1 and CtIP.

3.2.6 The predicted Phospho-binding residues within the BARD1 BRCT domains are not responsible for stabilising CtIP to the BRCA1-C complex.

The BARD1 BRCT domains appear to play a role in the stabilisation of CtIP to the BRCA1-C complex (figure 3.5b). As discussed previously, the best characterised function of BRCT domains are their ability to bind phosphorylated proteins. In order to elucidate whether the potential phospho-binding function of the BARD1 BRCT domains are responsible for this stabilisation, stable inducible HEK Flp-In cell lines containing GFP-BARD1S575F, GFP-BARD1K619M, GFP-BARD1H686R and GFP-BARD1 triple mutant were generated. Tetracycline was used to induce the expression of the BARD1 mutants to near endogenous levels (figure 3.11(a). Using a GFP-trap pull down system as previously described, it became clear that point mutations in the BRCT domains of BARD1 disrupting potential phospho-protein interaction domains, had no effect on stabilising the BRCA1 complexes as the same levels of Abraxas, FANCJ and CtIP were co-immunoprecipitated with GFP-BARD1 and the BARD1 point mutants (figure 3.11(b) As shown previously by a Mammalian two-Hybrid analysis, the presence of BRCA1 is not only vital to the formation of the BRCA1 complexes but also necessary to see any interaction between BARD1 and CtIP. This is evident in figure 3.11(d) as no Abraxas, FANCJ or CtIP can be pulled down with BARD1 in the absence of BRCA1.

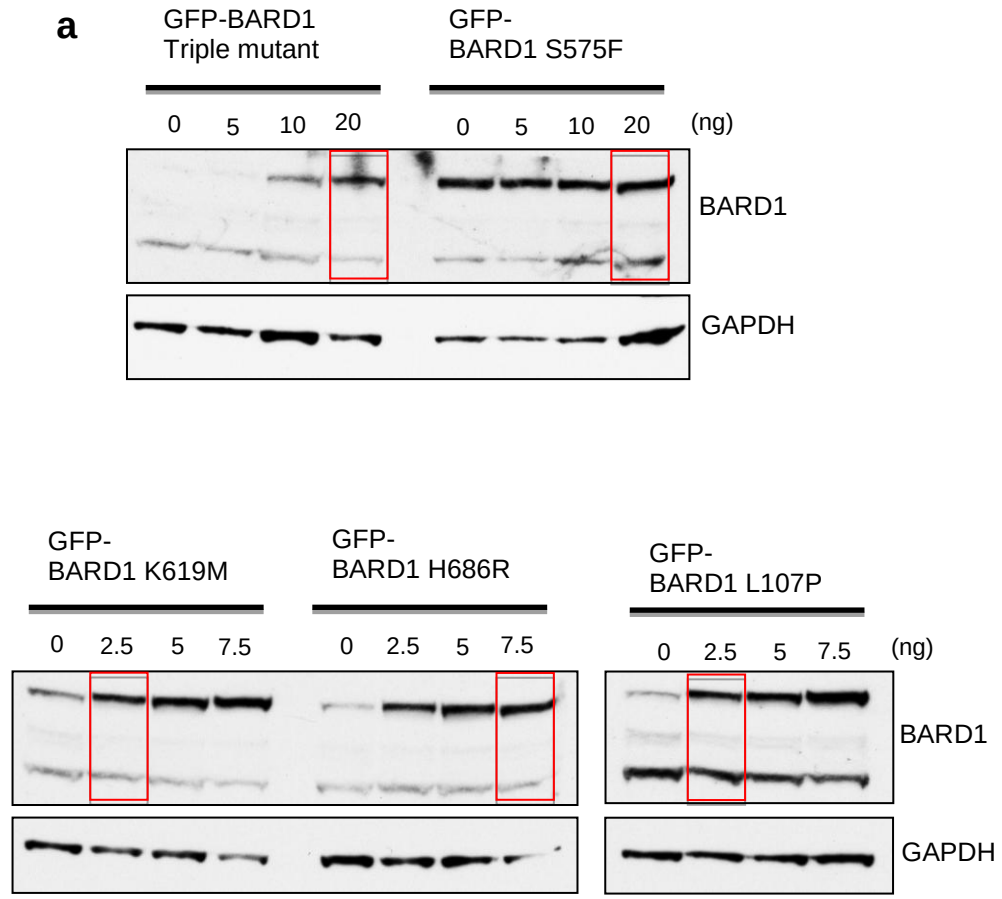
a
GFP-BARD1
Triple mutant
GFP-
BARD1 S575F
0 5 10 20
0 5 10 20
(ng)
BARD1
GAPDH
GFP-
BARD1 K619M
GFP-
BARD1 H686R
GFP-
BARD1 L107P
0 2.5 5 7.5
0 2.5 5 7.5
0 2.5 5 7.5
(ng)
BARD1
GAPDH

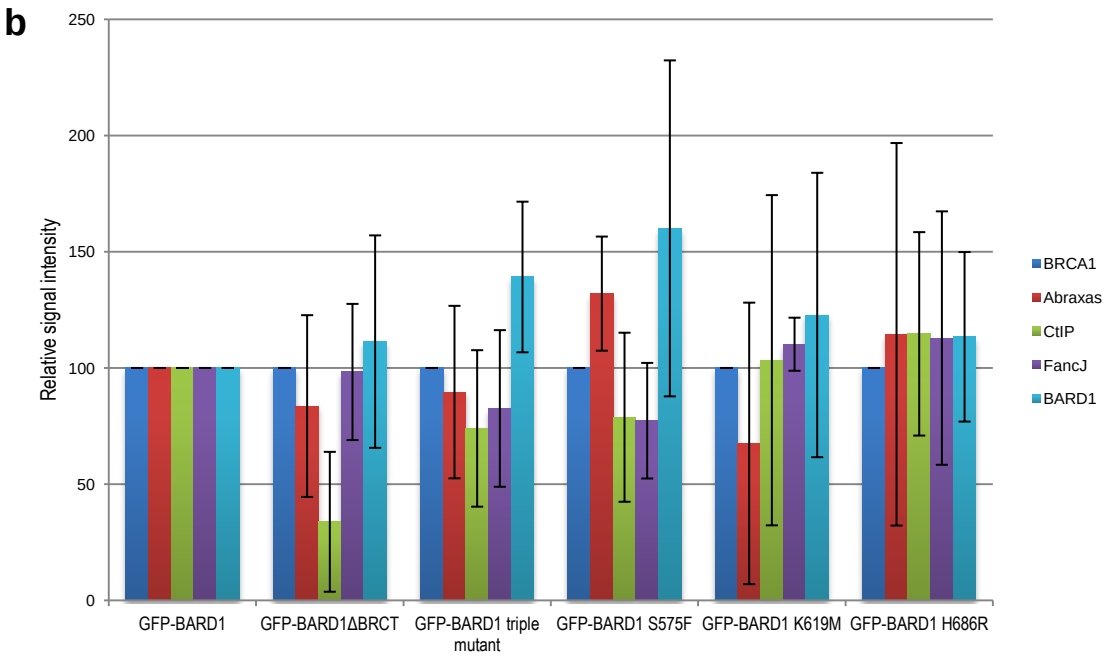
b
Relative signal intensity
250
200
150
100
50
0
GFP-BARD1
GFP-BARD1ΔBRCT
GFP-BARD1 triple mutant
GFP-BARD1 S575F
GFP-BARD1 K619M
GFP-BARD1 H686R
BRCA1
Abraxas
CtIP
FancJ
BARD1

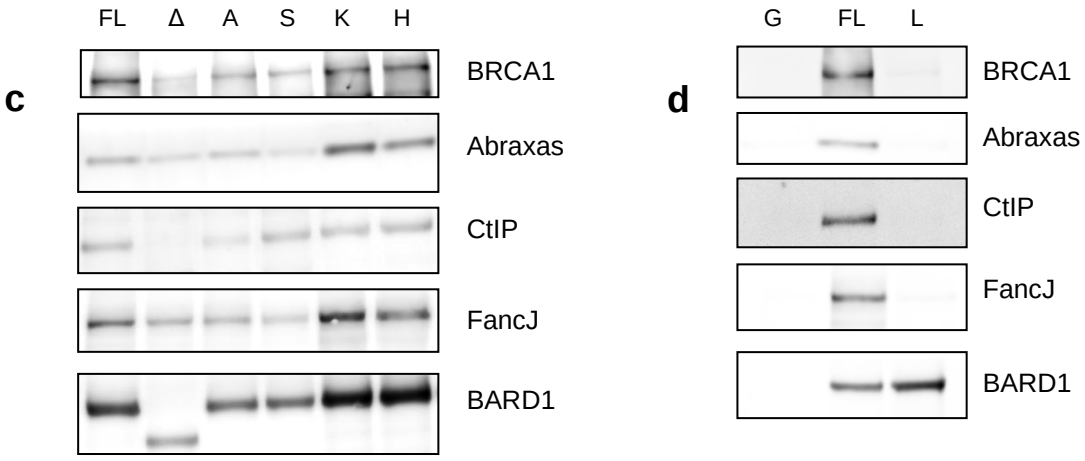

Figure 3.11 BARD1 phospho-mutants to not contribute to the stabilisation of the BRCA1 complexes
(a) Tet induced expression of the BARD1 mutant HEK cell lines. Concentration of tet used for each cell line is circled in red.
(b) Licor quantification of a GFT-trap pull down. GFP-BARD1 and mutant forms were pulled down and immunopercipitated proteins were anylised by licor Western blot. Each protein band was quantified by Licor software and protein values were normalised to amount of BRCA1 present. Data shown are the mean of at least 3 independent experiments. Error bars, s.d.
(c) A representative Licor Western blot from which the graph in figure (a) was generated. FL(GFP-BARD1), Δ (GFP-BARD1ΔBRCT) A (GFP-BARD1 triple mutant), S(GFP-BARD1S575F), K (GFP-BARD1K619M), H(GFP-BARD1H686R)
(d) Pull down comparing GFP-BARD1 to GFP-BARD1L107P, Analysed by Western blot. GFP-BARD1L107P does not co-immunopercipitate with BRCA1, Abraxas, FANCJ or CtIP.

3.2.7 BRCA1 BRCT point mutants have a HR defect

The BRCT domains of BRCA1 are crucial in the repair of DNA DSBs. Loss of the BRCT domains of BRCA1 impairs the efficient repair of DNA DSB, leading to a HR phenotype. There are several conflicting findings in the literature regarding the HR status of cells containing point mutations in the phospho-binding regions of BRCA1. *Valerie et al* see an increase in HR while *Baer et al* see a reduction [298, 321]. However these experiments were carried out in cell lines transiently expressing BRCA1. In order to compare the effects of the point mutations generated in BARD1 BRCT domains to those in the BRCA1 BRCT domains on a biological level, DTDR17 BRCA1-/- cells were reconstituted with either a complete HsBRCA1 BRCT delete

mutant or with the BRCA1 point mutants previously discussed. *Brca1* cells reconstituted with BRCA1 BRCT domain point mutants, known to disrupt the binding of phosphoproteins, showed a decrease in HR efficiency by the HRE assay (figure 3.12(a). Consistent with this result, BRCA1 mutant cell lines were also sensitive to PARP inhibitors demonstrated in the colony survival assay in figure 3.12(c).

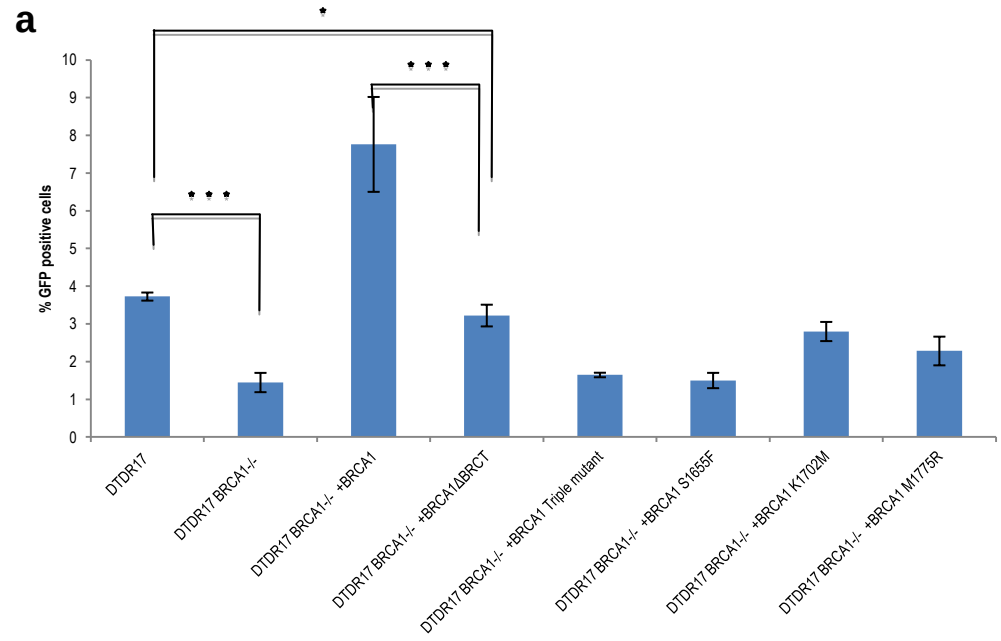

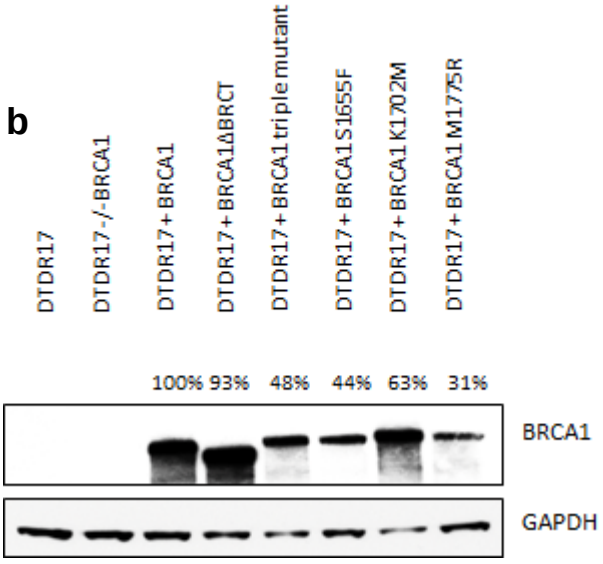

c

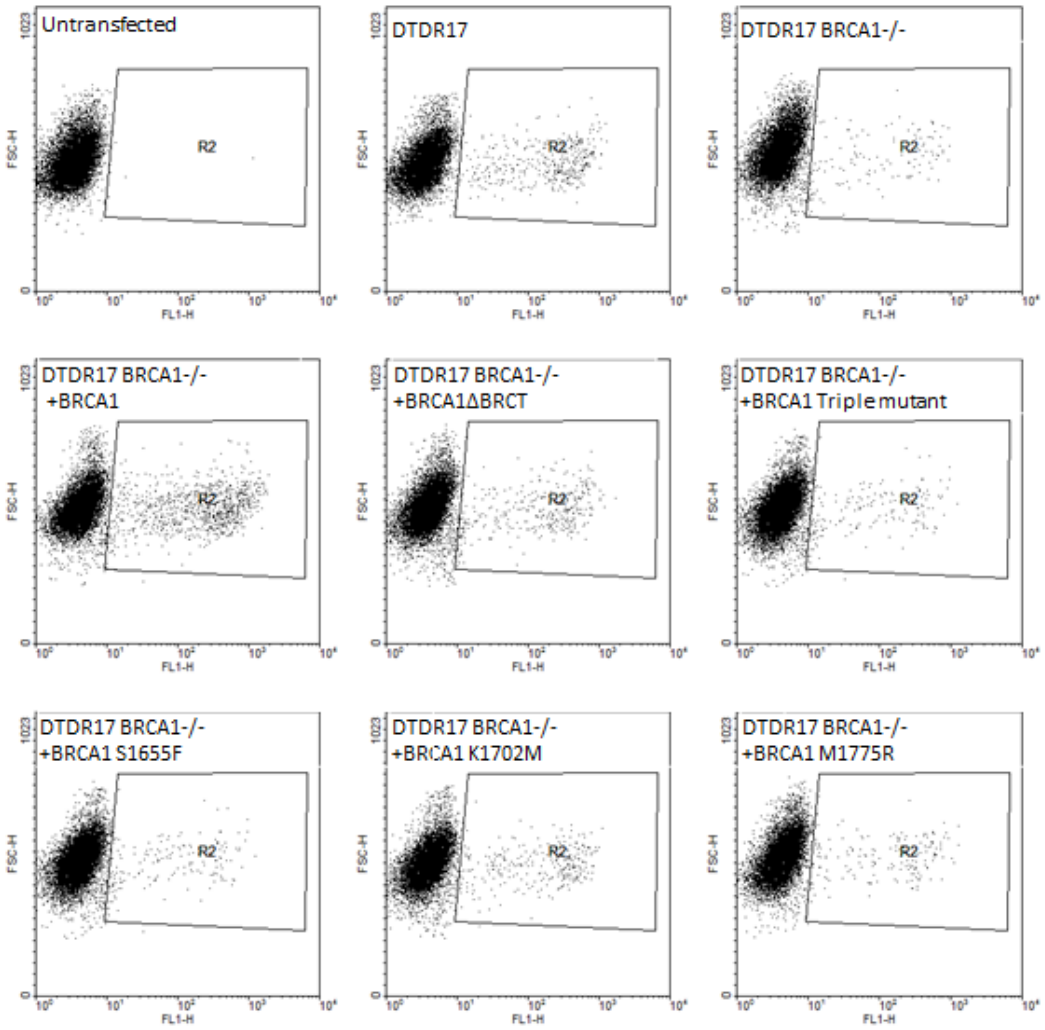
Untransfected
DTDR17
DTDR17 BRCA1-/-
DTDR17 BRCA1-/- +BRCA1
DTDR17 BRCA1-/- +BRCA1ΔBRCT
DTDR17 BRCA1-/- +BRCA1 Triple mutant
DTDR17 BRCA1-/- +BRCA1 S1655F
DTDR17 BRCA1-/- +BRCA1 K1702M
DTDR17 BRCA1-/- +BRCA1 M1775R
R2
FSC-H
FL1-H

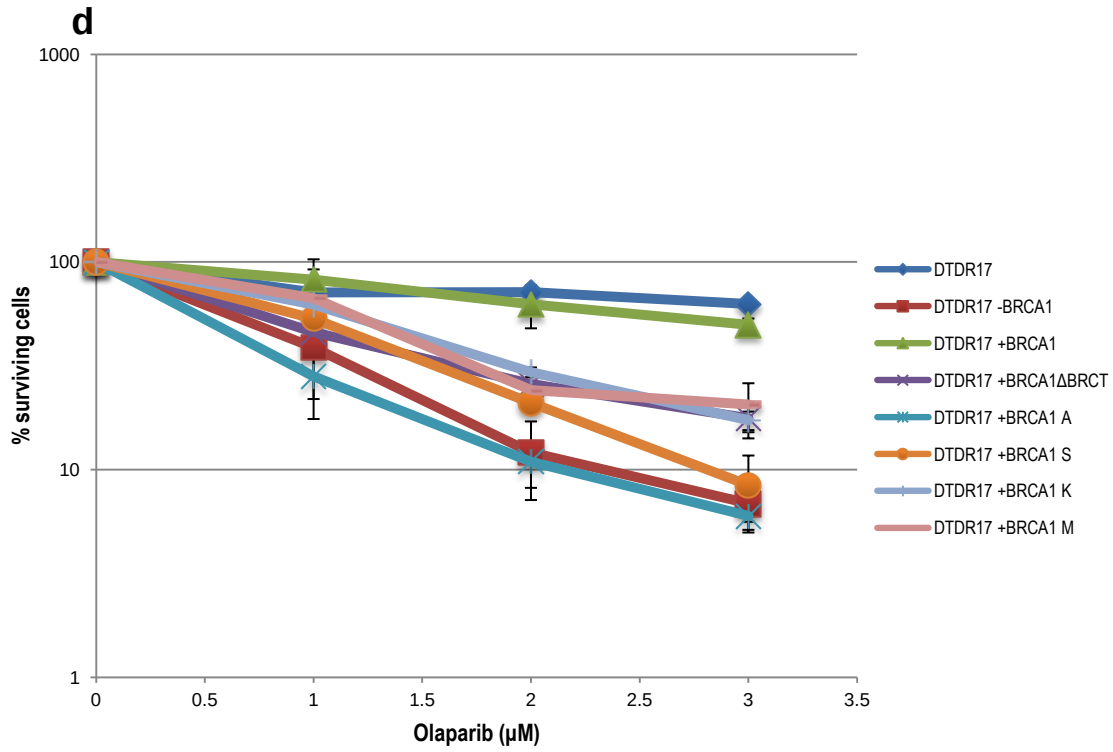

Cell Line	IC_{50} Value(μM)	IC_{50} Fold increase over DTDR17
DTDR17	5.268	1
DTDR17 -BRCA1	1.066	4.9
DTDR17 +BRCA1	4.21	1.25
DTDR17 +BRCA1ΔBRCT	1.418	3.56
DTDR17 +BRCA1 A	0.939	5.61
DTDR17 +BRCA1 S	1.346	3.9
DTDR17 +BRCA1 K	1.702	3.1
DTDR17 +BRCA1 M	1.737	3.04

Figure 3.12 Point mutations in the BRCA1 BRCT domains abrogates HR efficiency

(a) HRE assay illustrating the percentage of cells expressing GFP 24hrs after transfection with the Isce-I expressing plasmid. Results were normalised to untransfected cells.
*** indicates a statistical significance p value of ≤ 0.001 and * represents a p value of ≤ 0.05 P value derived from the student t-test Data shown are the mean of at least 3 independent experiments. Error bars, s.d.
(b) Western blot illustrating the expression of the different reconstituted *Brca1* cell lines. % expression compared to the expression of reconstituted *Brca1* cell line expressing full length BRCA1. Band density calculated using imageJ.
(c) Representive dot plot of raw data from figure (a) Cells expressing GFP were identified by FACS analysis. GFP positive cells were gated for relative to their GFP status and size (FSC-H) and seen in the box R2.
(d) Colony survival assay illustrating the sensitivity of *Brca1* and reconstituted mutant cell lines to PARP inhibitor, Olaparib. Cells were treated for 24hrs with 0-3μM Olaparib before being plated on methylcellulose cellulose media, as described in the Methods and materials section. Surviving colonies were counted 9-12 days after plating and plotted relative to untreated cells.
Data shown are the mean of at least 3 independent experiments. Error bars, s.d. The IC_{50} values were calculated from log dose response curves of at least 3 independent experiments.

It is evident from the results in figure 3.12(a), that in comparison to *Brca1* cells reconstituted with full length human BRCA1, reconstituted mutant BRCA1 variants show defects in HR. The BRCA1 antibody used to detect the expression of reconstituted BRCA1 in figure 3.12(b) only detects human BRCA1 hence endogenous chicken BRCA1 cannot be detected. The same cell lines are also significantly more sensitive to PARP inhibitors in comparison to Wild type cells. The phenotype of these cells cannot be explained by a localisation failure as BRCA1 in all the reconstituted cell lines localises to the nucleus (figure 3.13).

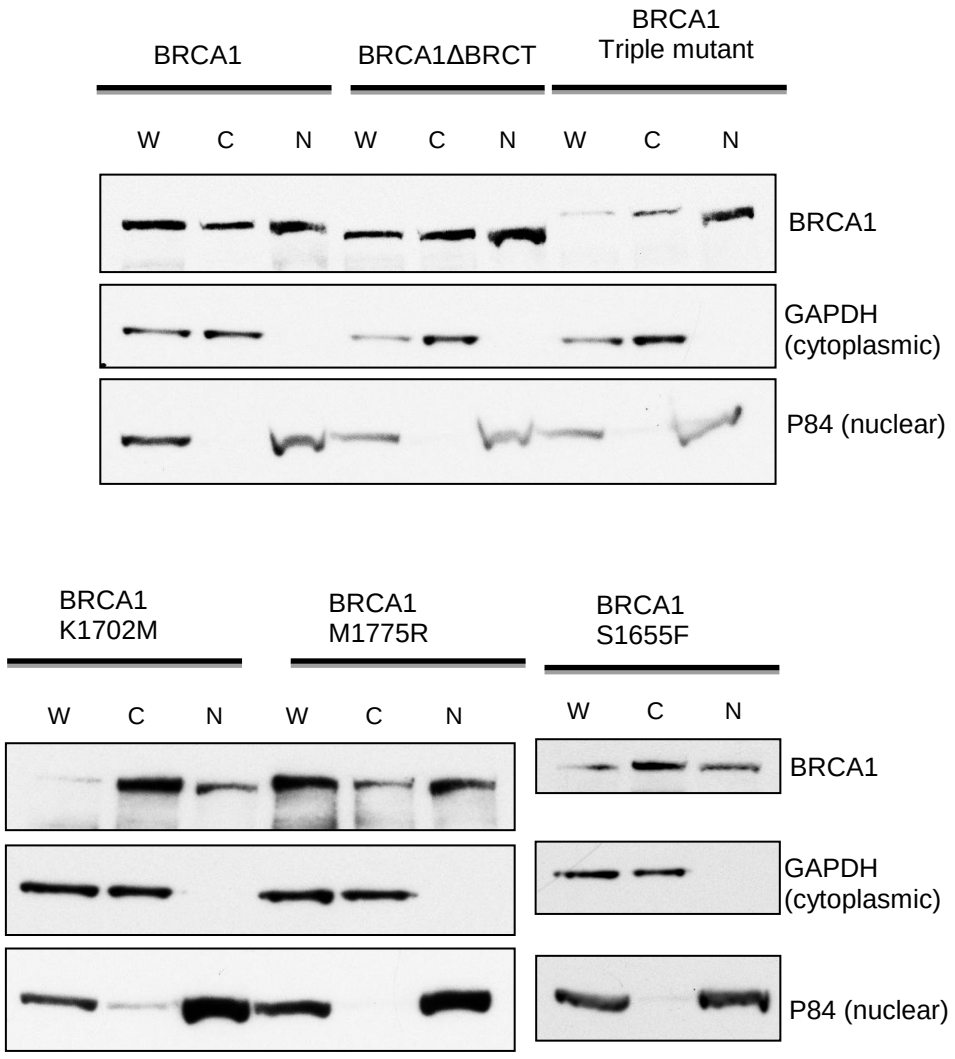

Figure 3.13 Fractionation of DTDR17 *Brca1* reconstituted cells.
Cell lysates were fractioned into their cytoplasmic and nuclear fractions as described in the Methods and Materials chapter. W(whole), C(cytoplasmic) and N(nuclear) Fractions were analysed by Western blotting. The majority of BRCA1 is located in the nuclear fractions for both reconstituted mutant cell lines.

3.2.8 BARD1 BRCT point mutants do not have a HR phenotype.

Point mutations in the BRCT domains of BARD1 which are predicted to disrupt potential phosphorylated proteins binding appear not to be important in the formation of the BRCA1 complexes. The loss of the BRCT domains of BARD1 greatly impairs the cells ability to carry out efficient repair of DNA DSBs. In order to elucidate whether these particular point mutants also show defects in the HRE assay and are sensitive to PARP inhibitors, the DTDR17 *Bard1* cell line was stably reconstituted with the respective BARD1 point mutants. The expression of reconstituted BARD1 and the BARD1 point mutants are illustrated in figure 3.14,

Interestingly, although the equivalent point mutants in BRCA1 show clear defects in HR, the point mutations in the BARD1 BRCT domains appear to behave like Wild type cells. In both the HRE assay (figure 3.15(a), and the colony survival assay with PARP inhibitors (figure 3.15(b), the mutant cell lines do not seem to have any complications in faithfully repairing DNA DSBs.

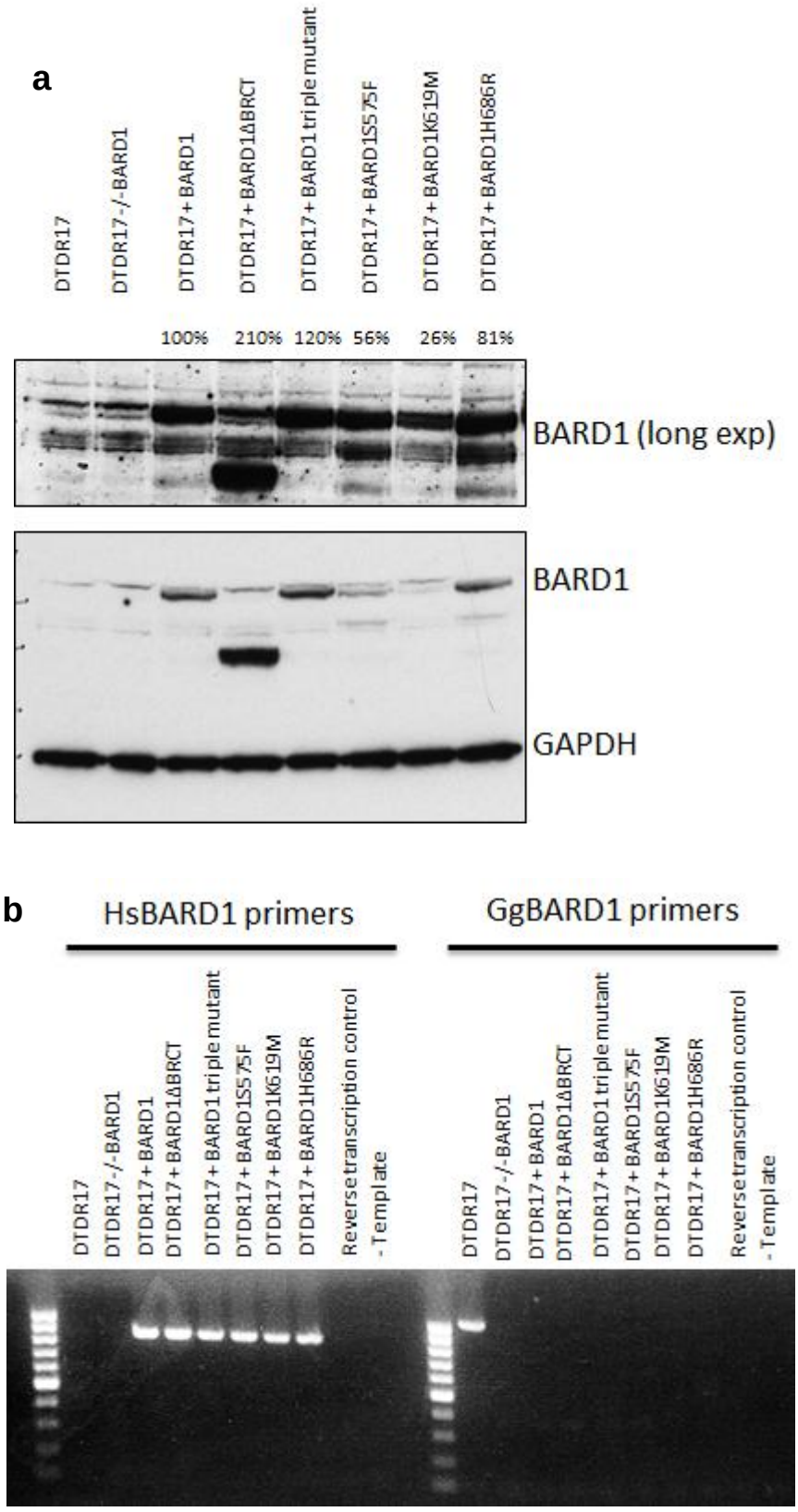

Figure 3.14 Generation of DTDR17 *Bard1* mutant cell lines
(a) Western blot of reconstituted DTDR17 *Bard1* cell lines. Upper band seen is unspecific in DT40 cells. % expression above blot was calculated using imageJ densitometry and is relative to the expression of reconstituted full length hsBARD1.
(b) PCR of cDNA extracted from the respective cell lines. Human and chicken BARD1 primers were used to amplify a small internal region of BARD1.

The reconstituted cell lines generated in figure 3.14(a) show a variation in expression which may contribute to a variation in the HRE assay results as previously discussed. It is clear from the PCR analysis in figure 3.14(b) that the cell lines have indeed been reconstituted correctly as the human BARD1 primers only detect reconstituted human BARD1. The BARD1 chicken primers fail to detect any template cDNA in either the parental or reconstituted cell lines as wild type BARD1 is completely absent. The primers were designed to be exclusive to either human or chicken BARD1.

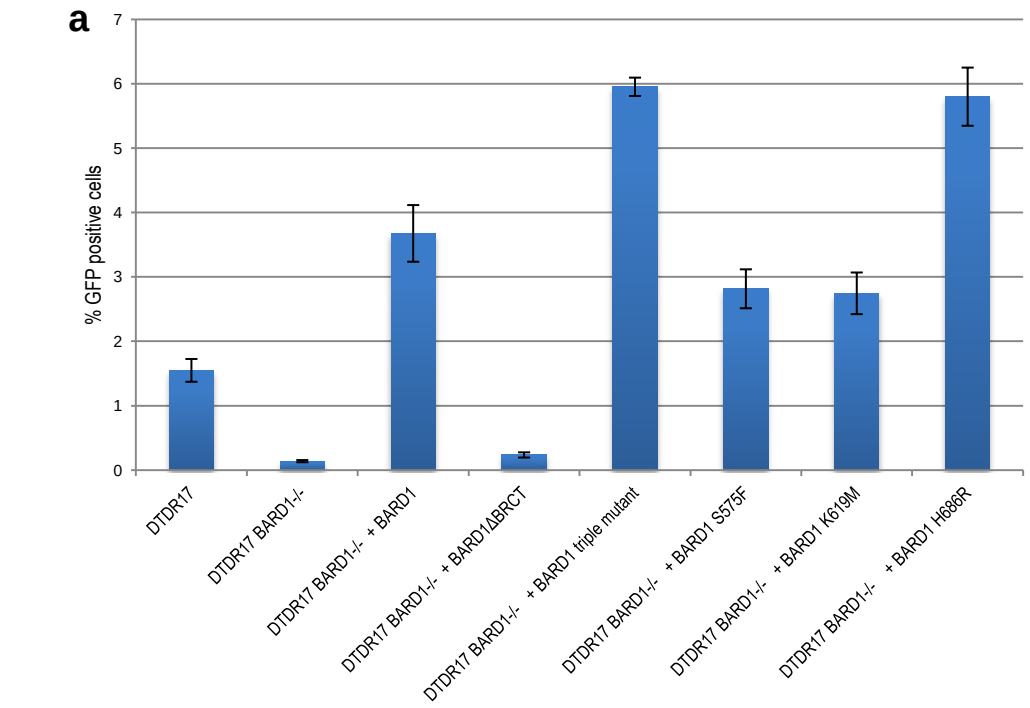
a
% GFP positive cells
0
1
2
3
4
5
6
7
DTDR17
DTDR17 BARD1-/-
DTDR17 BARD1-/- + BARD1
DTDR17 BARD1-/- + BARD1ΔBRCT
DTDR17 BARD1-/- + BARD1 triple mutant
DTDR17 BARD1-/- + BARD1 S575F
DTDR17 BARD1-/- + BARD1 K619M
DTDR17 BARD1-/- + BARD1 H686R

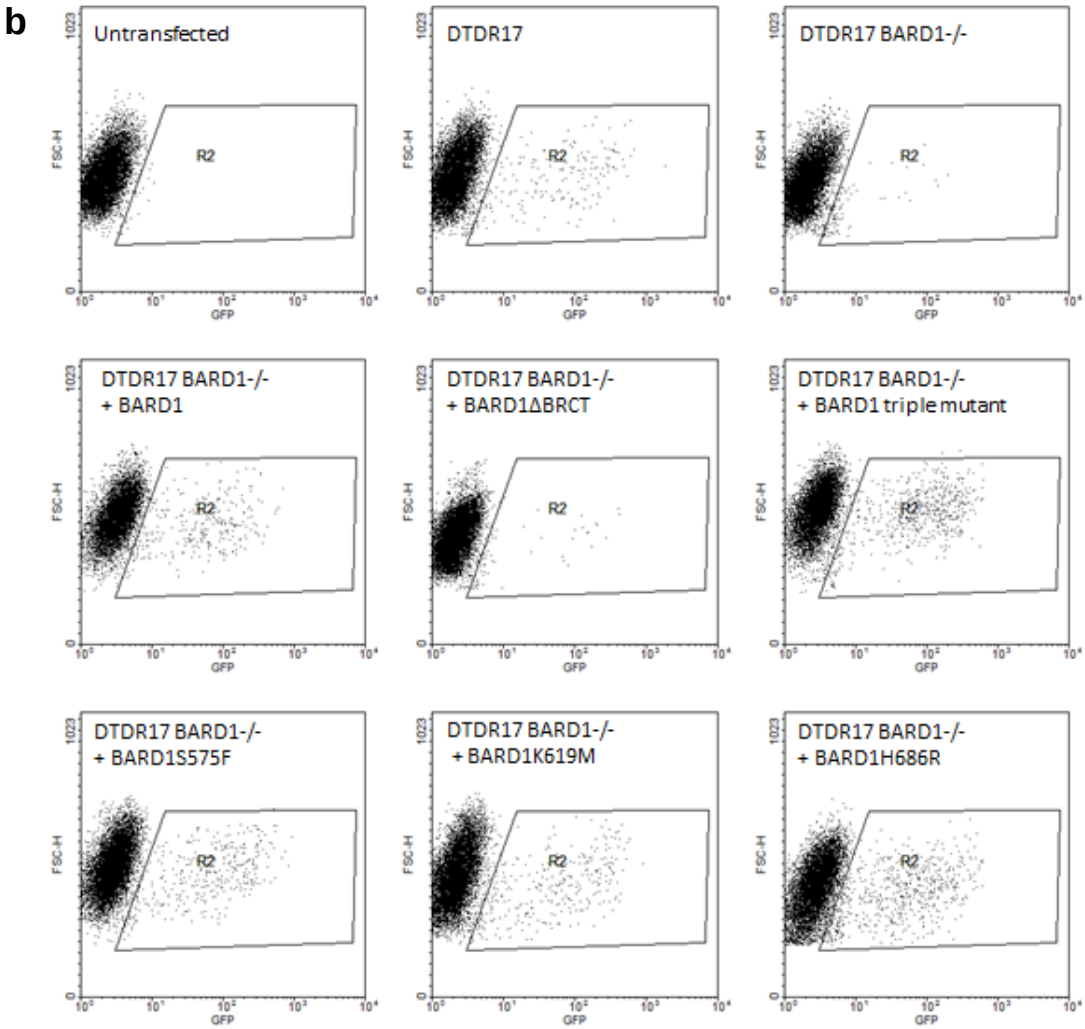
b
Untransfected
DTDR17
DTDR17 BARD1-/-
DTDR17 BARD1-/- + BARD1
DTDR17 BARD1-/- + BARD1ΔBRCT
DTDR17 BARD1-/- + BARD1 triple mutant
DTDR17 BARD1-/- + BARD1S575F
DTDR17 BARD1-/- + BARD1K619M
DTDR17 BARD1-/- + BARD1H686R
R2
FSC-H
GFP

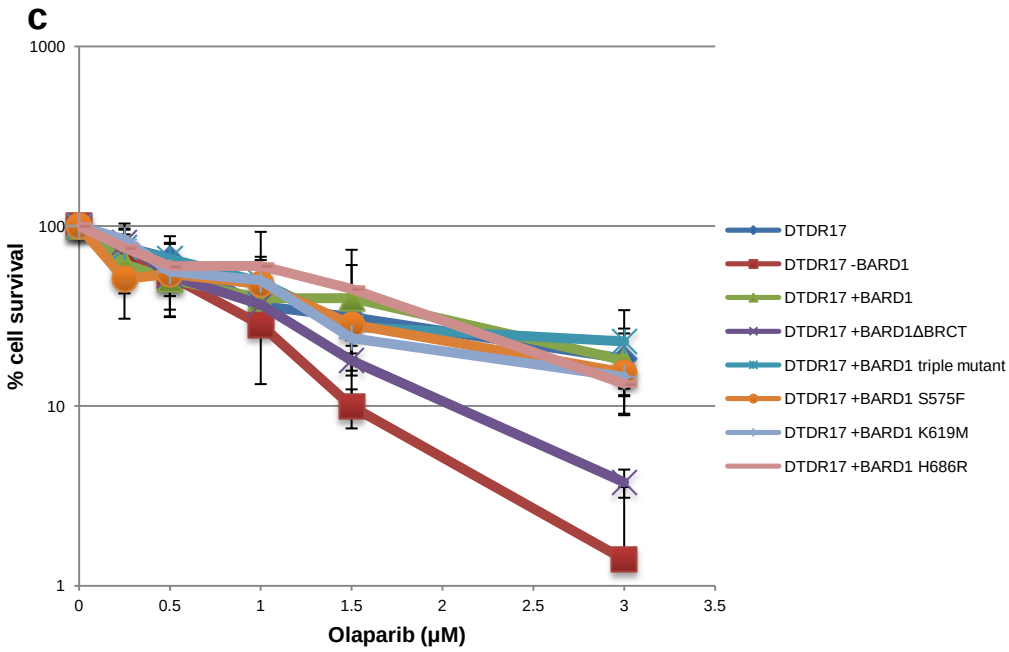

Figure 3.15 BARD1 point mutant do not have a HR phenotype
(a) HRE assay illustrating the percentage of cells expressing GFP 24hrs after transfection with the Isce-I expressing plasmid. Results were normalised to untransfected cells. Data shown are the mean of at least 3 independent experiments. Error bars, s.d.
(b) Representive dot plot of raw data from figure (a) Cells expressing GFP were identified by FACS analysis. GFP positive cells were gated for relative to their GFP status and size (FSC-H) and seen in the box R2.
(c) Colony survival assay illustrating the sensitivity of *Bard1* and reconstituted mutant cell lines to PARP inhibitor, Olaparib. Cells were treated for 24hrs with 0-3μM Olaparib before being plated on methylcellulose cellulose media, as described in the Methods and materials section. Surviving colonies were counted 9-12 days after plating and plotted relative to untreated cells. Data shown are the mean of at least 3 independent experiments. Error bars, s.d.

As previously mentioned, point mutants in the BRCT domains of BARD1 do not show any defects in HR. Although the levels of HRE are not as high in BARD1S575F and BARD1K619M compared to the other mutant cell lines, they are still higher than Wild type levels. This may also be partly due to their expression levels as demonstrated in figure 3.4. All the point mutants show almost no sensitivity to PARP inhibitors unlike cells without the BRCT domains of BARD1. These results clearly indicate that the HR phenotype seen with the loss of the BARD1 BRCT domains is not due to the potential phospho-binding ability of the BRCT domains.

As expected the point mutations generated in BARD1 do not affect the localisation of BARD1 as it localises to the nucleus as seen in figure 3.16.

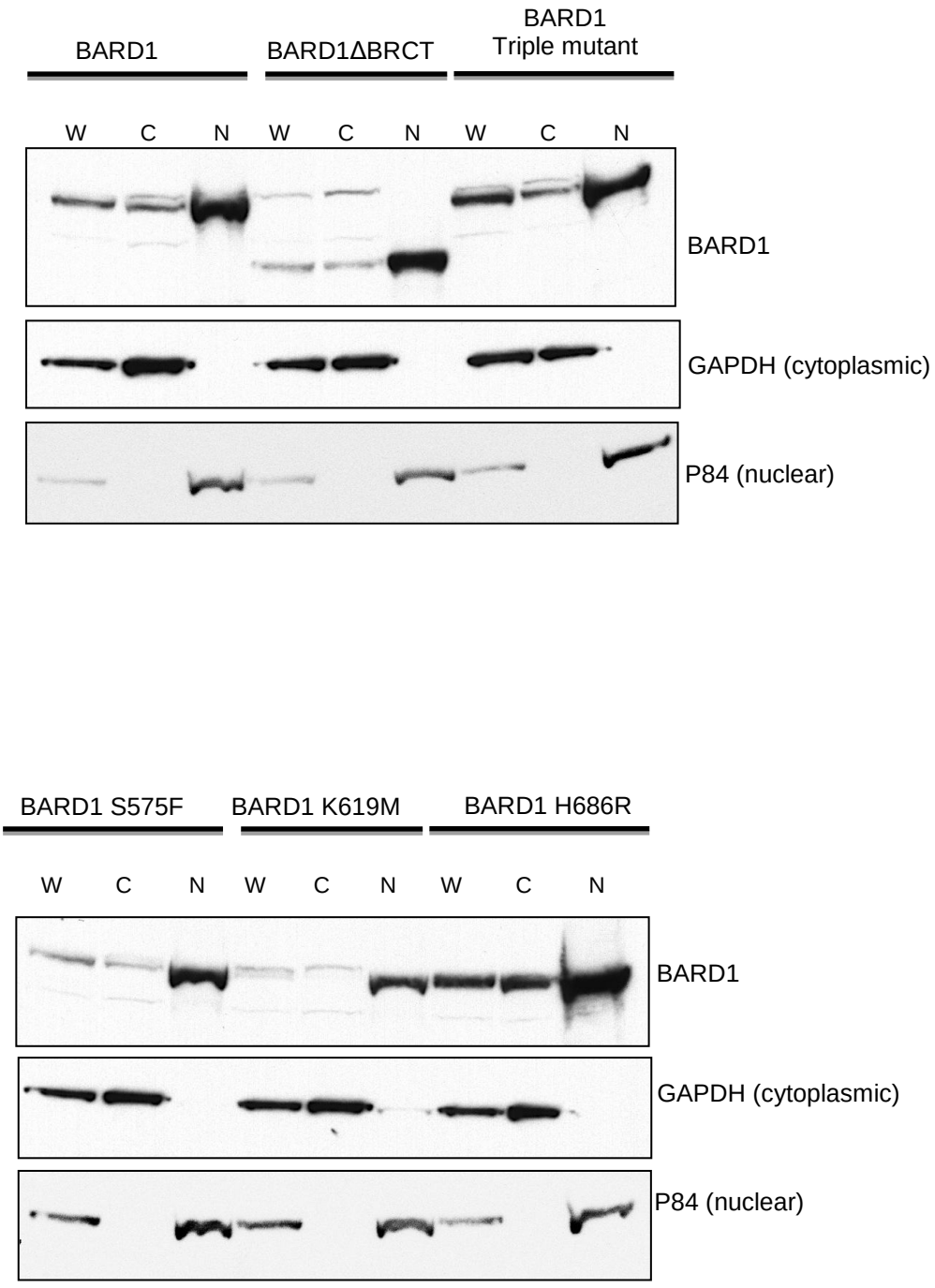

Figure 3.16 Localisation of *Bard1* reconstituted cell lines
Cell lysates were fractioned into their cytoplasmic and nuclear fractions as described in the Methods and Materials chapter. W(whole), C(cytoplasmic) and N(nuclear) Fractions were analysed by Western blot. The majority of BARD1 is located in the nuclear fractions for both reconstituted mutant cell lines.

3.3 Summary

The BARD1 BRCT domains are important for HR and potentially help stabilise the BRCA1-C complex.

BARD1 interacts with CtIP in a BRCA1 dependent manner.

Potential phospho-binding sites of the BARD1 BRCT domains do not contribute to the stabilisation of the BRCA1 complexes.

Potential phospho-binding sites of the BARD1 BRCT domains appear not to be important for HR, whereas disruption of the phospho-binding sites of the BRCA1 BRCT domains impedes the efficient repair of DNA DSBs.

Chapter 4 The role of the BARD1 BRCT domains in recruitment to DNA Damage

4.1 Introduction

The localisation of the BRCA1 BARD1 heterodimer to sites of DNA damage is vital for the repair of DNA lesions, specifically DNA DSBs. Using molecular biology techniques it has become evident that the BARD1 BRCT domains play an important role in HR. In order to gain a more functional understanding of the role of the BARD1 BRCT domains in HR, this chapter will attempt to address the relevance of the BARD1 BRCT domains in terms of localisation and recruitment to sites of Damage.

4.2 Results

4.2.1 Localisation of BARD1ΔBRCT is different to BARD1.

The BRCA1 BARD1 heterodimer has long been known to localise to sites of damage [208] and this recruitment is fundamental to the repair of damaged DNA. The recruitment of BRCA1 to lesions is mediated by γH2AX and MDC1[323]. More recently a complex ubiquitylation signalling pathway initiated by the phosphorylation of H2AX is thought to ultimately recruit BRCA1 via the RAP80 complex and Abraxas [128, 130, 133].

Yu et al published a paper recently which highlighted the importance of the BARD1 BRCT domains as they localise BRCA1 to sites of damage very shortly after damage in a PAR dependent manner [287]. In order to further investigate the functional role the BARD1 BRCT domains have in recruitment to DSBs, Tet inducible HEK 293 cell lines were used as described in chapter 3. As previously mentioned, these cell lines stably express either GFP-BARD1 or GFP-BARD1ΔBRCT. A HEK cell line expressing just GFP alone was used a control for most experiments.

During the initial characterisation of the cell line, there was a striking difference between the localisation of GFP-BARD1 and GFP-BARD1ΔBRCT (figure 4.1). GFP protein on its own appears to localise to both the cytoplasm and the nucleus whereas GFP-BARD1 and GFP-BARD1ΔBRCT can be found mainly in the nucleus. Interestingly GFP-BARD1 appears to form discrete nuclear foci unlike GFP-BARD1ΔBRCT whose nuclear localisation is more scattered.

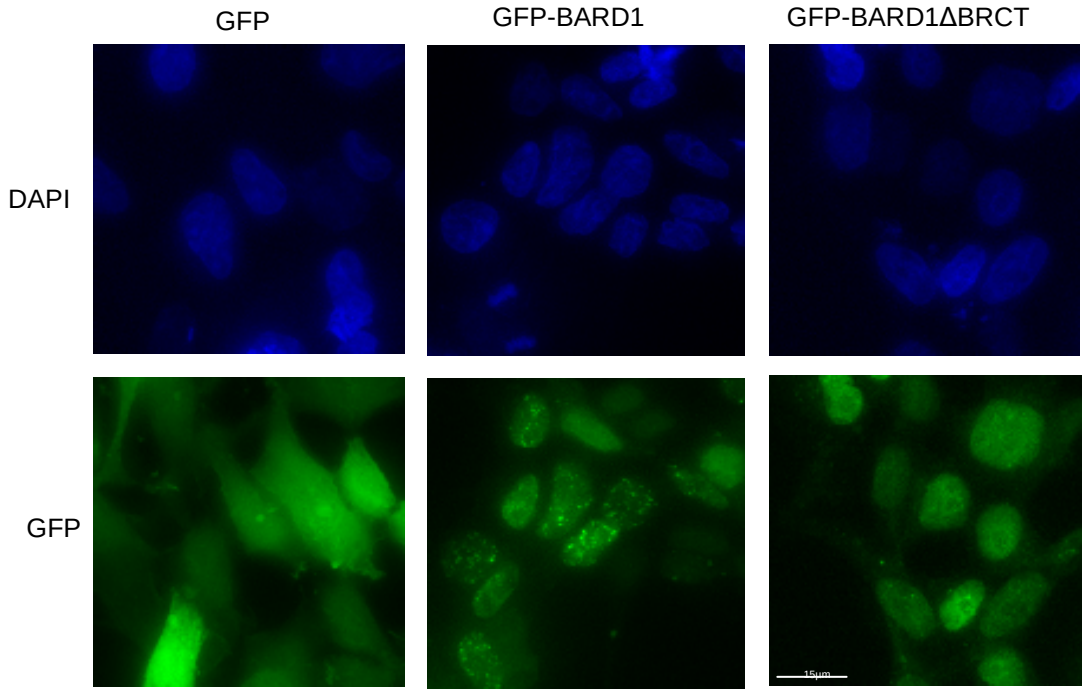

Figure 4.1 Localisation of GFP-BARD1 and GFP-BARD1ΔBRCT
Immunofluorescent microscopy illustrating the localisation of GFP-BARD1, GFP-BARD1ΔBRCT and GFP alone. X-axis indicated the cell lines used and Y-axis shows nuclear stain (DAPI) and GFP. Images were taken by DeltaVision Spectris Restoration Microscope using a 60X objective. A similar supplementary figure (S1) can be seen in the supplementary data on disc at the end of the appendix.

4.2.2 GFP-BARD1ΔBRCT cannot efficiently form S-phase foci.

Figure 4.1 illustrates that BARD1 forms discrete nuclear foci however these foci are absent in the cell line expressing BARD1ΔBRCT. *Baer et al* described similar discrete nuclear foci termed “BRCA1 nuclear dots” [355]. These foci are S-phase dependent, and both BRCA1 and BARD1 have been shown to localise to these foci. According to figure 4.2 it appears that the foci seen in figure 4.1 are also S-phase related. The number of cells with more than 10 foci/cell is equivalent to the amount of cells in S-

phase according to EDU and PCNA staining. Interestingly even the predicted phospho-binding point mutants of the BARD1 BRCT domains, described in the previous chapter, also form these nuclear foci. GFP-BARD1L107P, which cannot interact with BRCA1, also forms nuclear foci indicating that the recruitment of BARD1 to these S-phase associated foci is not dependent on its interaction with BRCA1. Only the complete loss of the BRCT domains appear to disrupt the ability of BARD1 to localise to the “BRCA1 Nuclear dots”

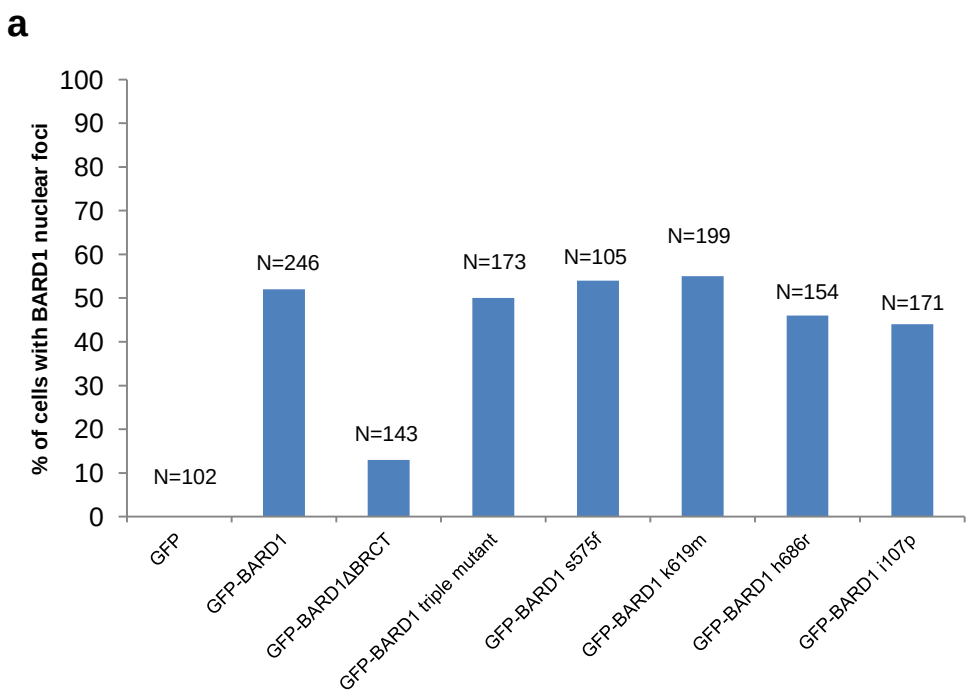

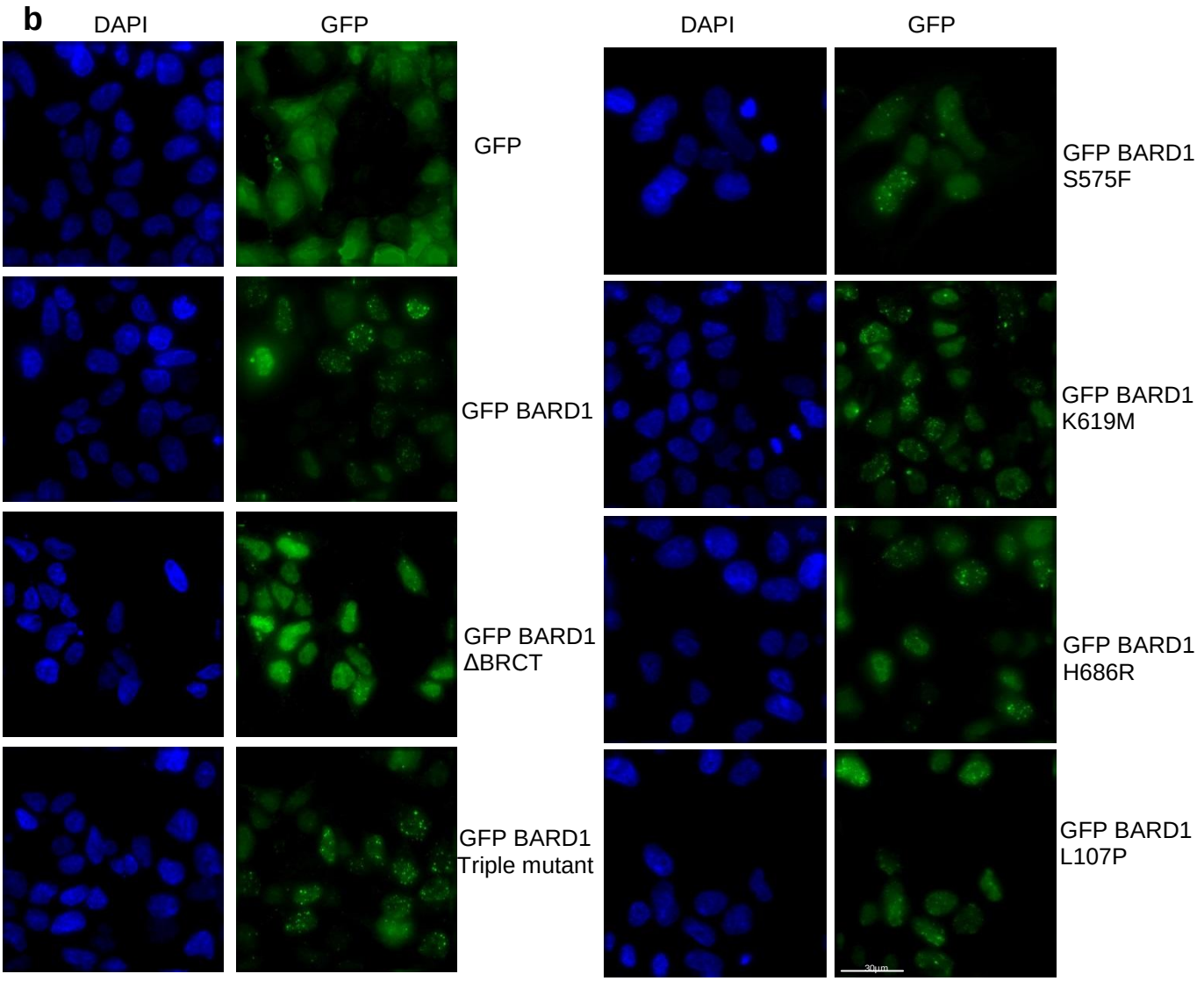
b
DAPI
GFP
DAPI
GFP
GFP
GFP BARD1 S575F
GFP BARD1
GFP BARD1 K619M
GFP BARD1 ΔBRCT
GFP BARD1 H686R
GFP BARD1 Triple mutant
GFP BARD1 L107P
30µm

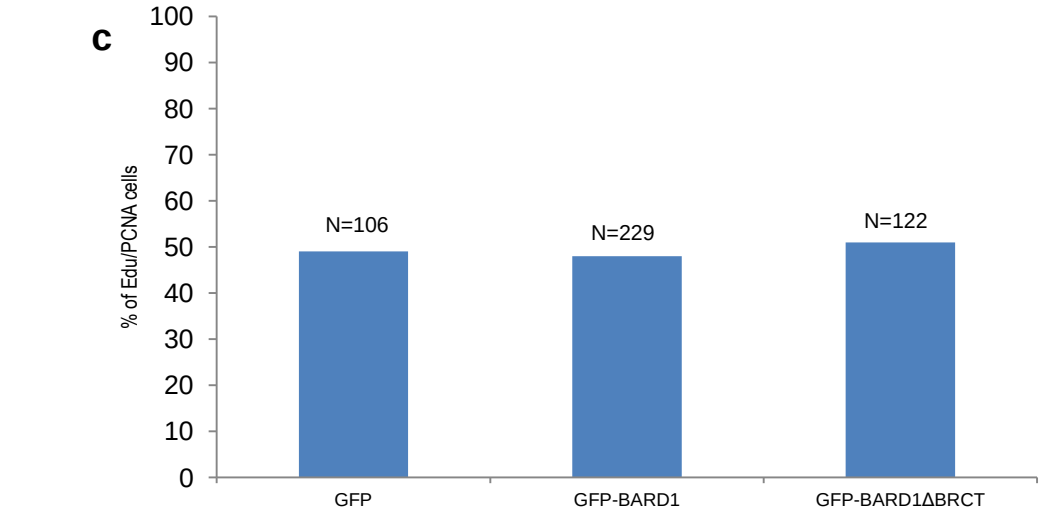

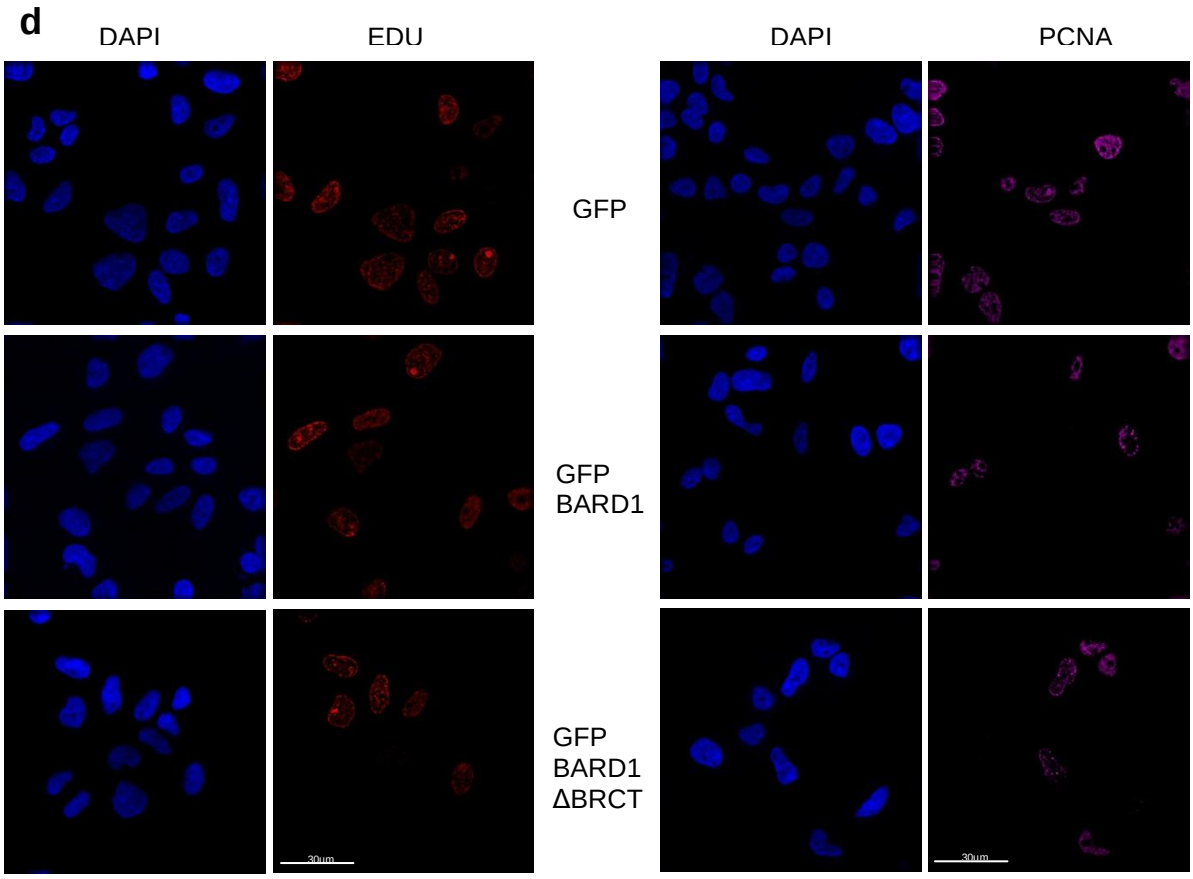

Figure 4,2 Ability of BARD1 and mutants to form S-phase foci.
(a) Graph illustrating the percentage of cells containing GFP-BARD1 foci. N represents the amount of cells counted.
(b) Representative microscopy images from figure (a). Supplementary image S2(a).
(c) Graph illustrating the percentage of GFP-BARD1 cells in S-phase according to PCNA and EDU positive cells.
(d) Representative microscopy images from figure (c). Supplementary image S2(b). Images were taken by DeltaVision Spectris Restoration Microscope using a 60X objective.

The presence of both EDU and PCNA are considered to be good indicators of cells in S-phase. Unfortunately colocalisation of EDU/PCNA with GFP-BARD1 was not possible as GFP-BARD1 bleaches during the staining process. Several different techniques were adapted, however no clear images could be taken. In relation to the EDU and PCNA staining, GFP-BARD1 and GFP-BARD1ΔBRCT were used as representative cell lines to indicate the average amount of HEK cells in S-phase. As seen in chapter 3, the number of cells in each stage of the cell cycle is not affected by the overexpression of GFP-BARD1.

4.2.3 GFP-BARD1 and GFP-BARD1ΔBRCT localise to DSBs

The BRCA1 BARD1 heterodimer localises to sites containing acute DNA damage and this localisation it believed to coordinate repair events [208]. The BARD1 BRCT domains are extremely important for the efficient repair of DNA DSBs as loss of the BRCT domains substantially reduces the ability of the cell to faithfully repair DSBs by HR. Loss of the BRCT domains of BARD1 also sensitises the cell to PARP inhibitors as shown in the previous chapter. As seen in figure 4.2, GFP-BARD1ΔBRCT appears to show defects in localising to S-phase foci under normal conditions. This phenomenon along with the knowledge that the BARD1 BRCT domains are important for HR begs the question of whether the BARD1 BRCT domains are required to localise BARD1 to DSBs.

To address this question, the localisation of GFP-BARD1 and GFP-BARD1ΔBRCT was visualised by microscopy after the induction of a laser DSB stripe. The use of a UV laser to generate a linear subnuclear DNA DSB stripe has been extensively used to investigate the DSB recruitment process [356-358]. Intriguingly both GFP-BARD1 and GFP-BARD1ΔBRCT localised to laser damage stripes (figure 4.3). Both BARD1 and BARD1ΔBRCT colocalised with the DNA damage marker γH2AX, whereas the GFP control did not localise to the site of damage. The laser

striped cells were fixed and stained with γH2AX 1hr after laser treatment to allow BARD1 and other repair proteins to accumulate to sites of damage.

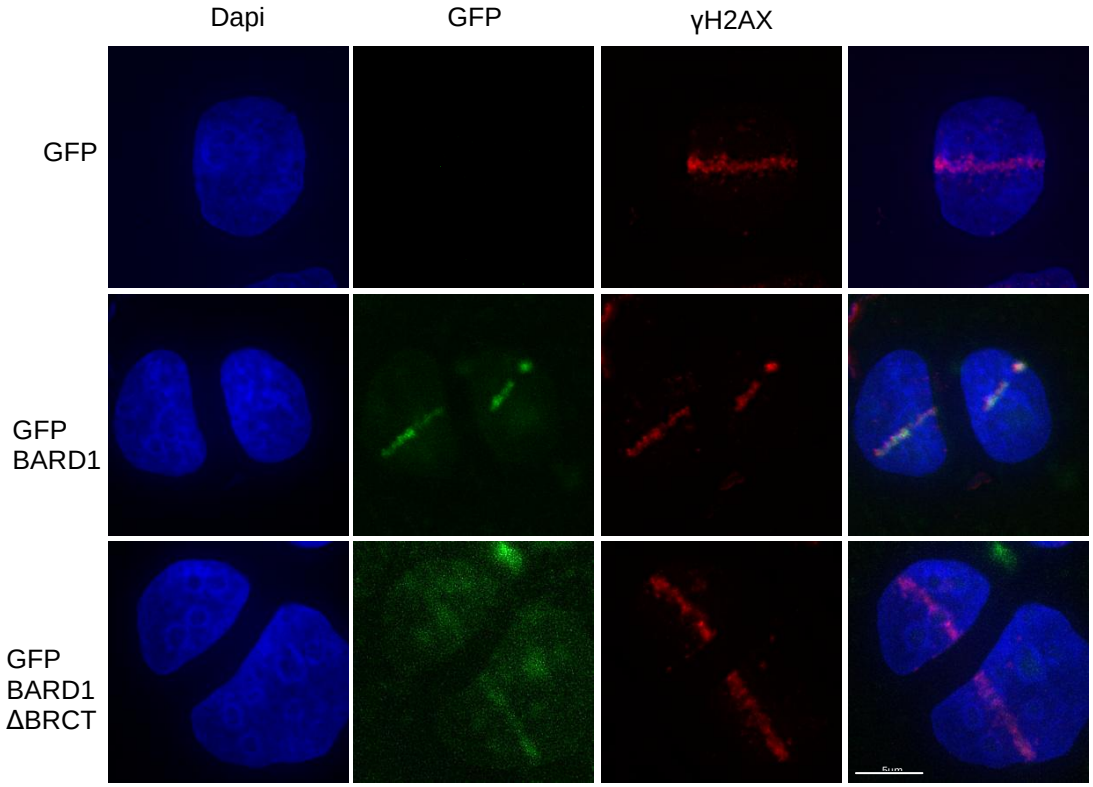

Figure 4.3 Localisation of GFP-BARD1 and GFP-BARD1ΔBRCT to DSBs
Representative images illustrating the localisation of GFP-BARD1 and GFP-BARD1ΔBRCT to γH2AX positive laser induced DSB stripes. Laser stripe was generated using a 405nm Leica UV laser and imaged by DeltaVision Spectris Restoration Microscope using a 100X objective. Cells were fixed and stained with α-γH2AX antibody 1hr after laser stripe. Experiment was repeated at least 3 times using 6 cells each time. Supplementary image S3.

It is evident from the images in figure 4.3 that although GFP-BARD1ΔBRCT does indeed localise to the stripe of damage, the amount of protein present appears to be less in comparison to GFP-BARD1. This may be due to the expression of GFP-BARD1ΔBRCT as all HEK BARD1 cell lines were induced with the maximum concentration of tetracycline for microscopy (10μg/ml) which could reflect different expression with different cell lines. It is also possible that GFP-BARD1ΔBRCT is less efficient at localising to damage stripes.

In order to confirm this result and to study the ability of the BARD1 BRCT point mutants, discussed in chapter 3, to localise to DSBs a U2OS cell line which allows the visualisation of a DSB by microscopy was utilised. The U2OS cell line contains a stably integrated reporter containing several hundred lac operator repeats upstream of a transgene [359]. As described by *Greenberg et al*. the expression of an mCherry tagged Fok1 nuclease domain fused to a Lac repressor results in the binding of this construct to the Lac operator repeats where the Fok1 nuclease creates a DSB *in vivo* [360]. The DSB is represented by a single mCherry foci within the cell. Transient co-transfection of GFP-BARD1 constructs with the mCherry-Fok1-LacI revealed that BARD1 containing point mutations in the BRCT domains appear to localise to DSB similar to full length BARD1. In agreement with figure 4.3, GFP-BARD1ΔBRCT also appears to efficiently localise to the DSB (figure 4.4 (b,c). As a control mCherry-Fok1-LacI containing a point mutation in the Fok1 nuclease (Fok1D450A) which renders the enzyme nuclease dead was used (both plasmids were a kind gift from Roger Greenberg).

a

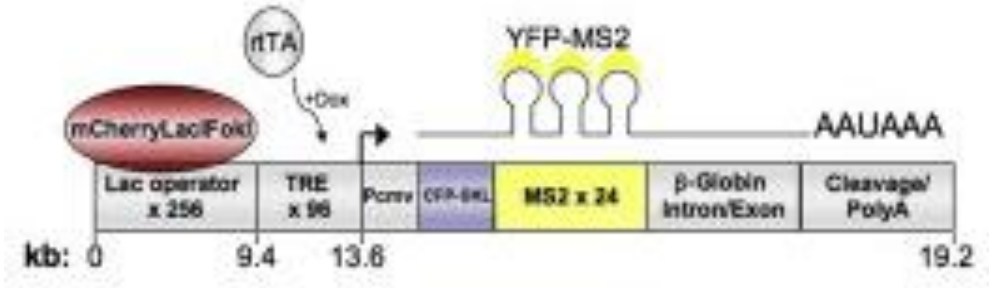
rtTA
+Dox
mCherryLacIFokI
YFP-MS2
AAUAAA
Lac operator x 256
TRE x 96
Pcmv
CFP-SKL
MS2 x 24
β-Globin Intron/Exon
Cleavage/ PolyA
kb: 0
9.4
13.6
19.2

b

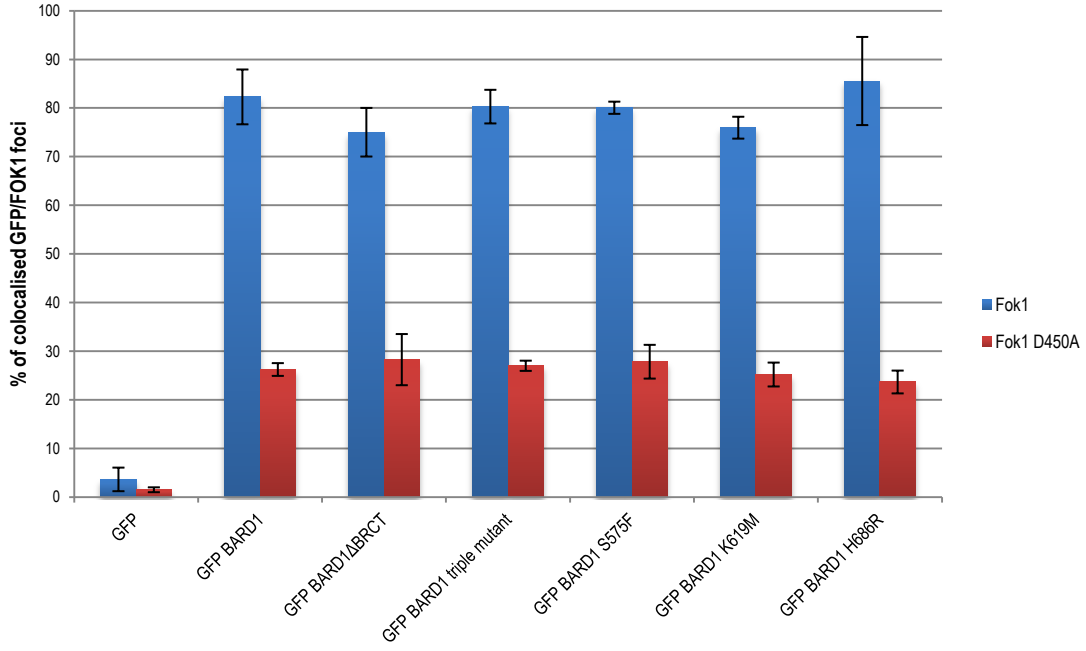
% of colocalised GFP/FOK1 foci
100
90
80
70
60
50
40
30
20
10
0
GFP
GFP BARD1
GFP BARD1ΔBRCT
GFP BARD1 triple mutant
GFP BARD1 S575F
GFP BARD1 K619M
GFP BARD1 H686R
Fok1
Fok1 D450A

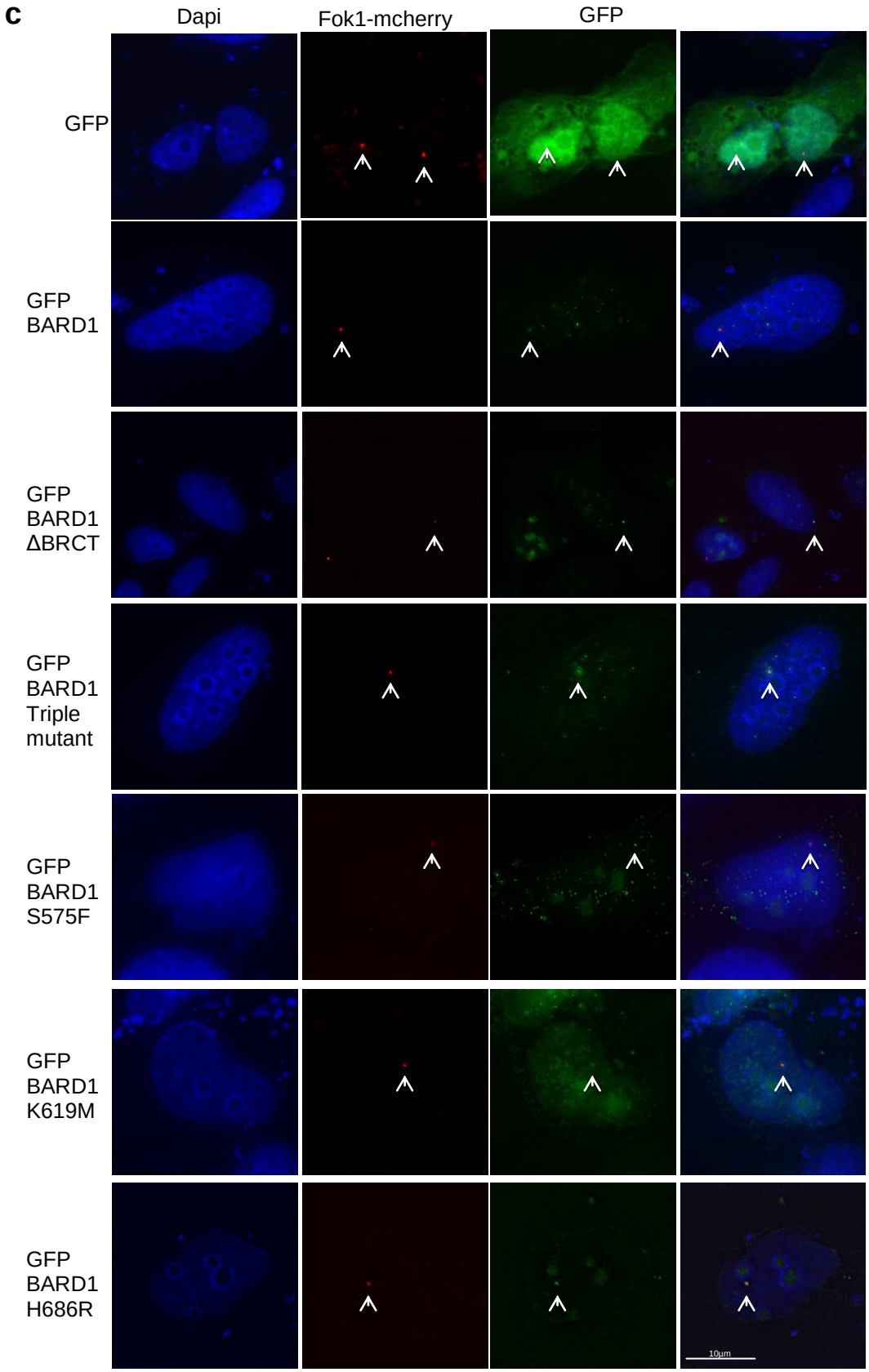
C
Dapi
Fok1-mcherry
GFP
GFP
GFP BARD1
GFP BARD1 ΔBRCT
GFP BARD1 Triple mutant
GFP BARD1 S575F
GFP BARD1 K619M
GFP BARD1 H686R
10μm

Figure 4.4 Localisation of BARD1 and mutants to Fok1 induced DSBs.
(a) Illustration of the Fok1 mCherry LacI binding to the Lac operator repeats. Adapted from *Greenberg et al, 2010.*
(b) Graph of the percentage of cells in which mCherry-Fok1-LacI colocalise with GFP-tagged BARD1. Blue bars represent cells transfected with the mCherry-Fok1-LacI, red bars indicate transfection with mCherry-Fok1d450a-LacI. Experiment was repeated 3 times, each time analysing 100 cells per transfection.
(c) Representative microscopy images from (b). Cells were pre-extracted, fixed and stained 24hrs after co-transfection. Images were taken by DeltaVision Spectris Restoration Microscope using a 60X objective. Supplementary image S4.

It is important to note that the high background level of GFP foci formed with the nuclease dead Fok1 (20-30%) is unlikely to be due to the nuclease activity of the Fok1D450A mutant and more likely to be due to naturally occurring DSB in the highly repetitive lac operator sequence. Extremely repetitive sequences are known to be very fragile and breaks are often associated with them.

4.2.4 BARD1ΔBRCT shows delayed kinetics in localising to DSB.

It has become clear that the loss of the BARD1 BRCT domains do not affect the ability of BARD1 to localise to DNA DSBs. However in a recent study, *Yu et al.* show that the loss of the BRCT domains of BARD1 appears to have a more subtle kinetic problem in localising to sites of damage. The BARD1 BRCT domains are important in the very early recruitment of BRCA1 to DSBs independent of γH2AX. This paper suggests that BARD1 is recruited to PAR at DSB via its BRCT domains in the first 20seconds after a break occurs. In the presence of PARP inhibitors GFP-BARD1 is only recruited later on. Functionally this does not affect the overall recruitment of BRCA1 to sites of damage, as in the absence of the BARD1 BRCT domains, BRCA1 is later recruited in a γH2AX dependent manner. The biological and functional relevance of this early recruitment remains unclear as BARD1ΔBRCT can also localise to DSB tethered to BRCA1 in the later recruitment stage involving γH2AX [287].

In the aforementioned paper, U2OS cells were transiently transfected with different GFP BARD1 constructs. To investigate whether the same results were observed in cell lines stably expressing GFP-BARD1 and GFP-BARD1ΔBRCT, the HEK cell lines ,previously described, were laser striped and the recruitment of GFP-BARD1 and GFP-BARD1ΔBRCT were monitored in real time in the presence or

absence of a PARP inhibitor. In agreement with *Yu et al,* GFP-BARD1 recruited to the damage stripes in under a minute whereas GFP-BARD1ΔBRCT only recruited to the DSB after well over 2 minutes (figure 4.5). The delayed kinetics of GFP-BARD1ΔBRCT appeared to be due to the inability of BARD1 to bind PAR at DSB as the presence of a PARP inhibitor showed the same delayed kinetics with the full length GFP-BARD1 protein. The inhibition of PARP only affected the kinetics of GFP-BARD1, as there is no PARP present for the BRCT domains to bind to and initiate the very early recruitment of BARD1 to sites of damage. PARP inhibitors had no effect on the recruitment of GFP-BARD1ΔBRCT.

As described earlier in the chapter, HEK GFP-BARD1 cells contain two distinctly different types of cells, in relation to the expression of GFP-BARD1. 50% of the population contain discrete S-phase associated nuclear foci, whereas the other half have a more uniform distribution of GFP-BARD1. Cells containing S-phase foci required over 5 minutes before any recruitment could be seen to stripes. Intriguingly there was no difference seen in recruitment of “S-phase foci” cells when treated with a PARP inhibitors. GFP-BARD1ΔBRCT only have one type of cell morphology as they appear not to form S-phase foci.

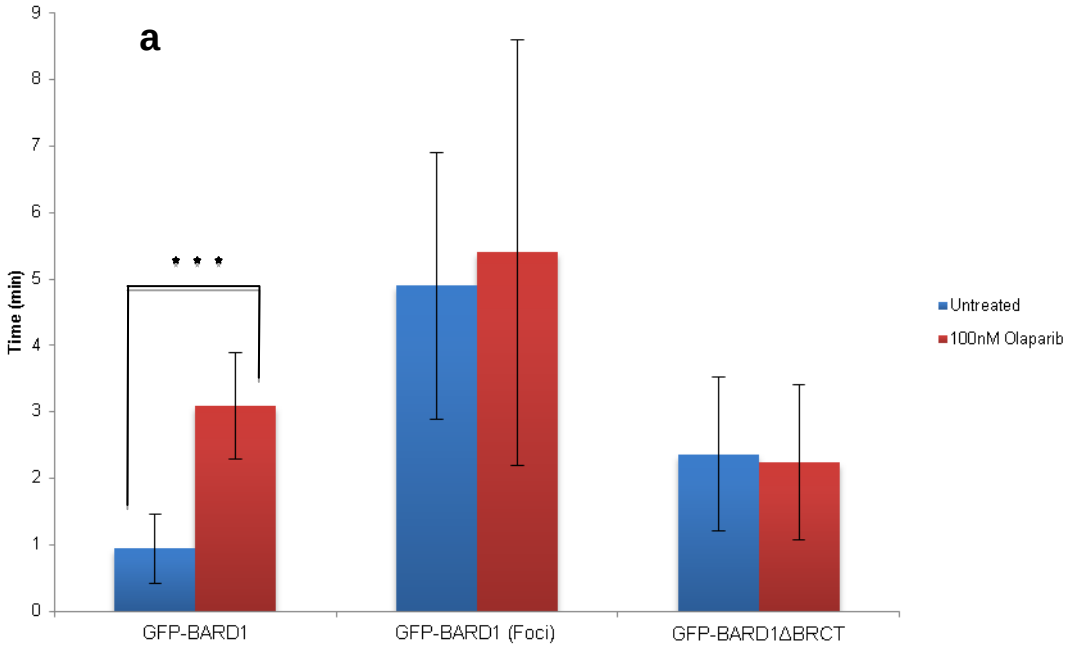

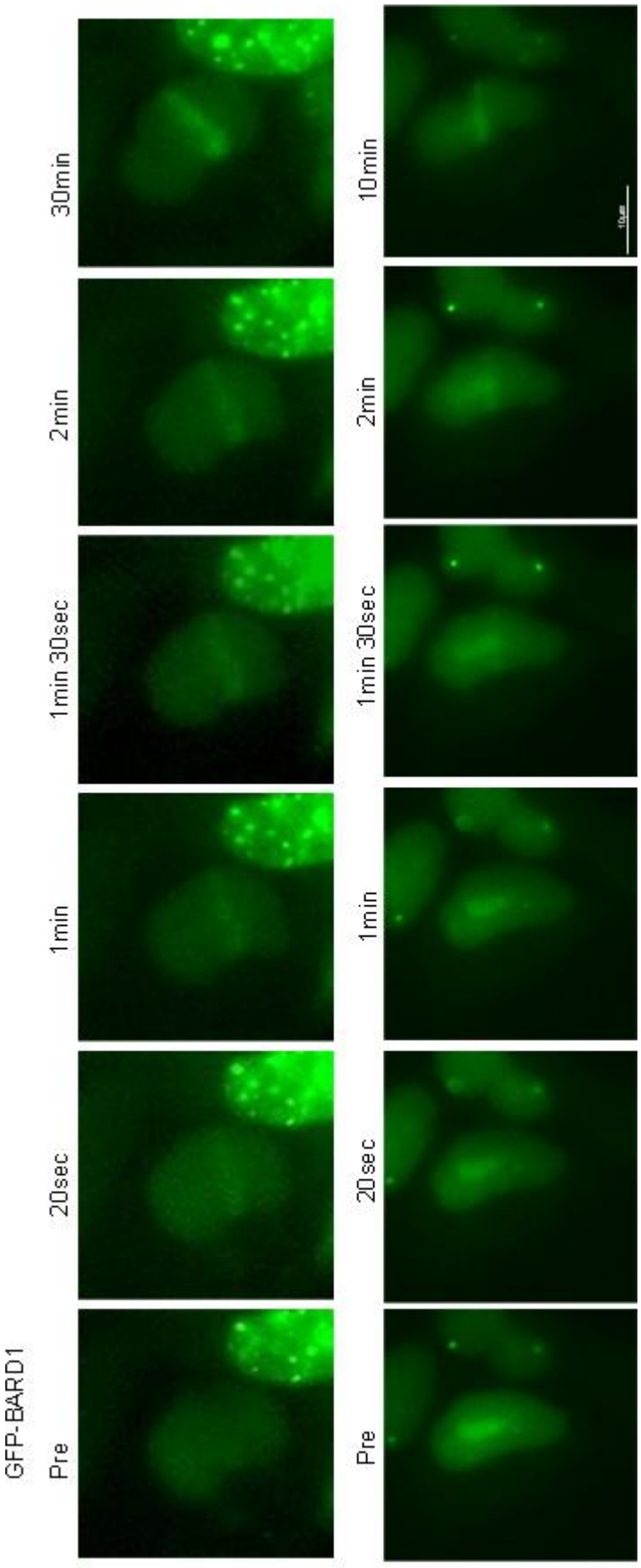
b
GFP-BARD1
Pre
20sec
1min
1min 30sec
2min
30min
0nM Olaparib
Pre
20sec
1min
1min 30sec
2min
10min
100nM Olaparib

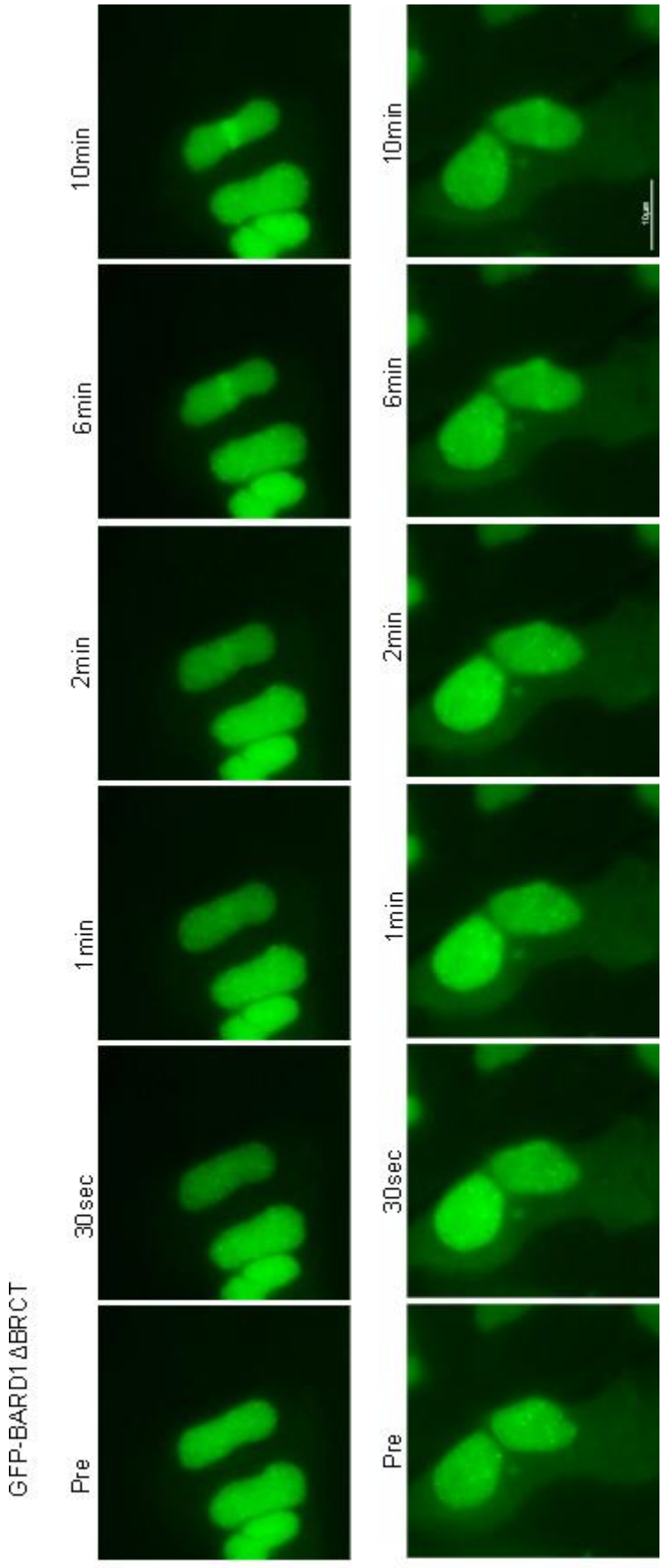
c
GFP-BARD1 ΔBRCT
0nM olaparib
100nM olaparib
Pre
30sec
1min
2min
6min
10min

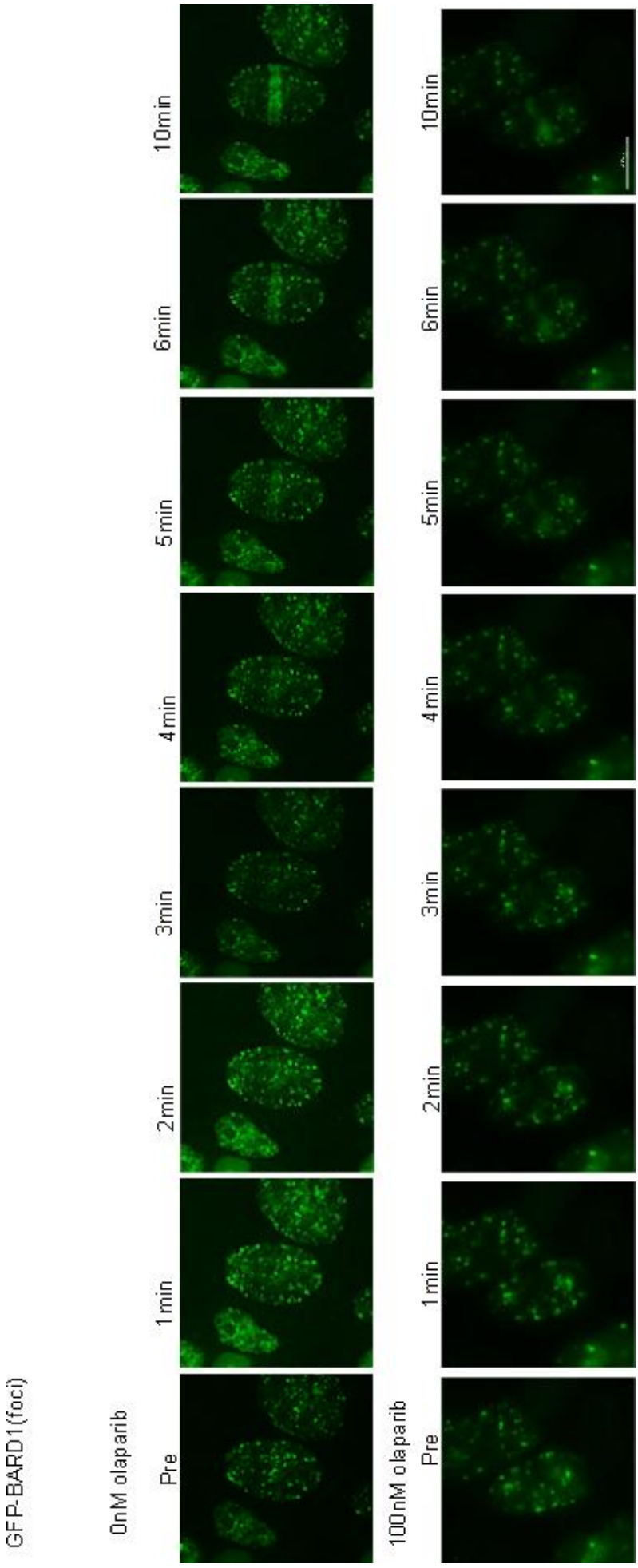
GFP-BARD1 (foci)
0nM olaparib
Pre
1 min
2 min
3min
4 min
5 min
6min
10min
100nM olaparib
Pre
1 min
2 min
3min
4 min
5min
6min
10min

d

Figure 4.5 Real time localisation of GFP-BARD1 and GFP-BARD1ΔBRCT to DSBs.
(a) Graph illustrating the time difference between GFP-BARD1 and GFP-BARD1ΔBRCT in localising to laser induced DSB stripes with and without PARP inhibitors. The experiment was repeated up to 6 times, each time with at least 6 cells.
(b,c,d) Representative images for the graph in figure (a). (b) GFP-BARD1, (c) GFP-BARD1ΔBRCT and (d) GFP-BARD1 cells containing S-phase foci. Live stripes and imaging was generated using a 405nm laser on a DeltaVision Spectris Restoration Microscope using a 60X objective. Supplementary figures S5(a,b,c)

4.2.5 Delayed recruitment kinetics of GFP-BARD1ΔBRCT does not appear to affect HR.

According to *Yu et al* the early recruitment of BARD1 to laser induced stripes is due to the BRCT domains binding PAR which is found at DSBs. Specifically the potential phospho-interacting amino acid K619. BARD1K619A was shown not to interact with PAR and to have the same delayed recruitment kinetics as the complete loss of the BRCT domains [287].

To address whether there is any functional relevance in the delayed recruitment of BARD1ΔBRCT in terms of faithful repair of DSBs, a HRE assay was used to determine the homologous recombination efficiency of cells treated with a PARP inhibitor. In chapter 3, DTDR17 cells containing point mutations in the BARD1 BRCT domains which are predicted to prevent the binding of a phospho-protein, were HR competent and showed no sensitivity to PARP inhibitors. As the role of PAR appears important for the early recruitment of BARD1*, Bard1* DTDR17 cells reconstituted with either HsBARD1, HsBARD1ΔBRCT or BARD1 BRCT point mutants (as described in chapter3) were treated with a low dose of a PARP inhibitor before measuring the HR efficiency of the cells via the HRE assay. The BARD1 point mutations suggested to be responsible for the early recruitment of BARD1 at DSB showed no defects in HR (figure 4.6) These results indicated that the early recruitment of BARD1 to sites of damage does not affect the ability of the cell to carry out faithful repair of DNA DSBs.

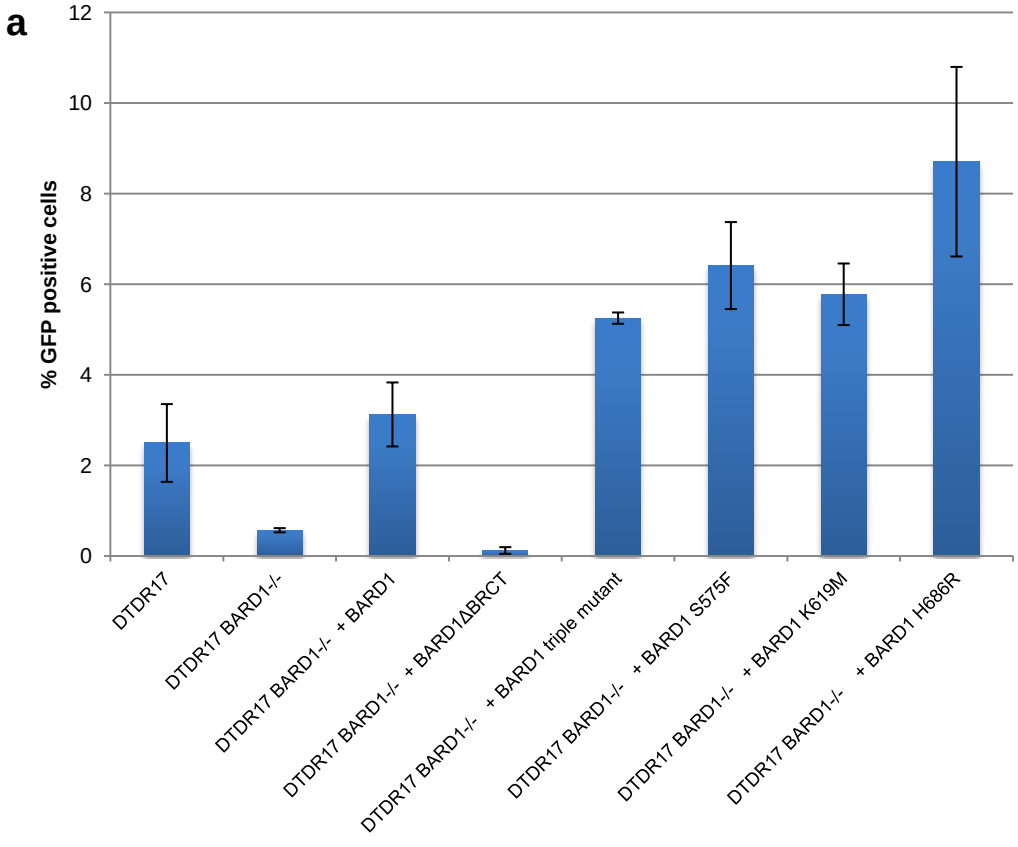
a
% GFP positive cells
12
10
8
6
4
2
0
DTDR17
DTDR17 BARD1-/-
DTDR17 BARD1-/- + BARD1
DTDR17 BARD1-/- + BARD1ΔBRCT
DTDR17 BARD1-/- + BARD1 triple mutant
DTDR17 BARD1-/- + BARD1 S575F
DTDR17 BARD1-/- + BARD1 K619M
DTDR17 BARD1-/- + BARD1 H686R

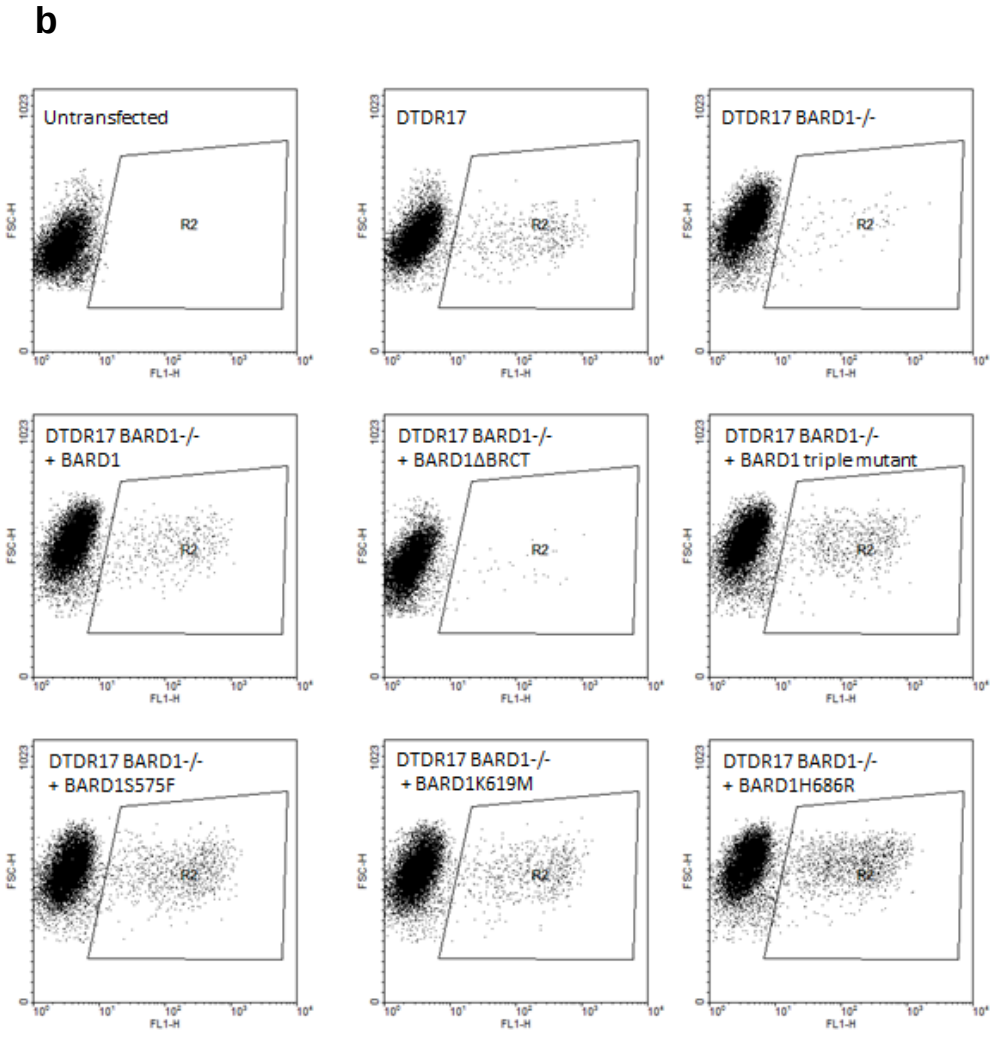
b
Untransfected
DTDR17
DTDR17 BARD1-/-
DTDR17 BARD1-/- + BARD1
DTDR17 BARD1-/- + BARD1ΔBRCT
DTDR17 BARD1-/- + BARD1 triple mutant
DTDR17 BARD1-/- + BARD1S575F
DTDR17 BARD1-/- + BARD1K619M
DTDR17 BARD1-/- + BARD1H686R
R2
FSC-H
FL1-H

Figure 4.6 BARD1 BRCT point mutant are HR proficient in the presence of a PARP inhibitor
(a) HRE assay illustrating the percentage of cells expressing GFP 24hrs after transfection with the Isce-I expressing plasmid and treatment with 100nM olaparib. Results were normalised to untransfected cells. Data shown are the mean of at least 3 independent experiments. Error bars, s.d.
(b) Representive dot plot of raw data from figure (a) Cells expressing GFP were identified by FACS analysis. GFP positive cells were gated for relative to their GFP status and size (FSC-H) and seen in the box R2.

4.2.6 The BRCT domains of BARD1 are important in the recruitment of RAD51 to DSBs.

The BRCT domains of BARD1 are important for the early recruitment of BARD1 and BRCA1 to DSBs. This early recruitment depends on the phospho-binding amino acids within the BARD1 BRCT domains according to *Li et al* [287]. However, as shown earlier and in chapter 3, the corresponding point mutations in the BARD1 BRCT domains do not appear to affect the ability of the cell to carry out HR. BARD1ΔBRCT cells retain the ability to localise to DNA DSBs more than likely due to the γH2AX dependent recruitment of the BRCA1 BARD1 heterodimer. The functional relevance of the BARD1 BRCT domains in recruitment to DSBs may lie in their ability to recruit downstream proteins involved in the repair of DSBs. In order to investigate this theory, the DTDR17 *Bard1* cell lines reconstituted with either full length HsBARD1 or HsBARD1ΔBRCT were treated with γ-irradiation and the recruitment of downstream repair proteins was analysed.

RAD51 has been shown to be vital for the repair of DSBs by HR. RAD51 is the main protein responsible for strand invasion of a homologous sister chromatid, the main event during HR repair [226]. Once a DSB occurs the DNA is first resected allowing RPA to bind, RPA is then displaced by RAD51 allowing repair to take place [361]. The recruitment of RAD51 to a DSB is dependent on the BRCA1 BARD1 heterodimer and loss of BRCA1 results in failure of RAD51 to localise to the DSB [362]. In order to assess whether the BRCT domains of BARD1 are important for the recruitment of RAD51 and RPA to DSBs, the aforementioned DTDR17 cell lines were

treated with 4GY γ-irradiation and stained for either RAD51 or RPA 4hrs after irradiation, allowing enough time to see the recruitment. Γ-irradiation is commonly used to study the recruitment of repair proteins to DSB.

Interestingly complete loss of BARD1 or just the BRCT domains of BARD1 resulted in a severe decrease in the amount of RAD51 foci detected after γ-irradiation, suggesting that the BRCT domains are indeed important for the ultimate recruitment of RAD51 (figure 4.7(a,b). Recruitment of RPA, however, was not hindered in the *Bard1* cells and only reduced by 2 fold in the *Bard1* cells reconstituted with either HsBARD1 or HsBARD1ΔBRCT (figure 4.7(c,d)

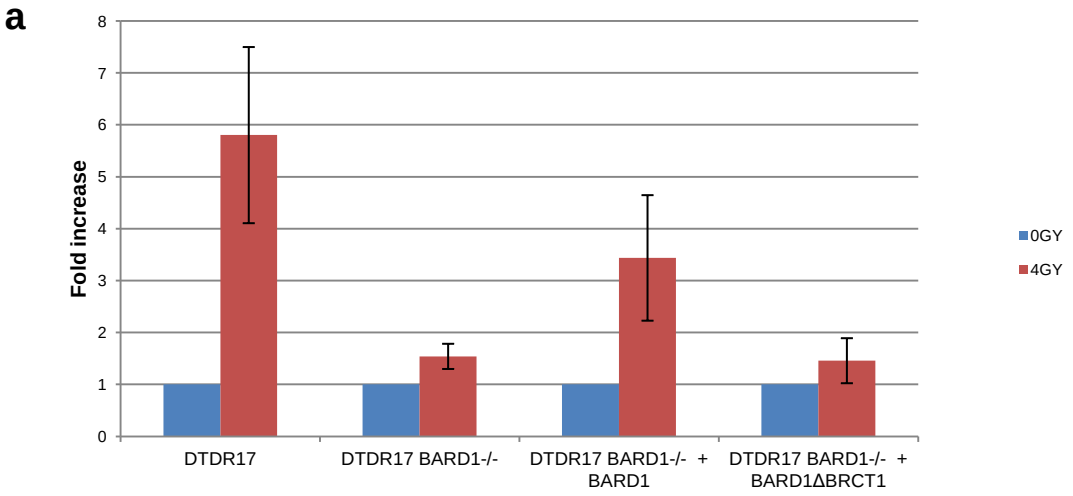

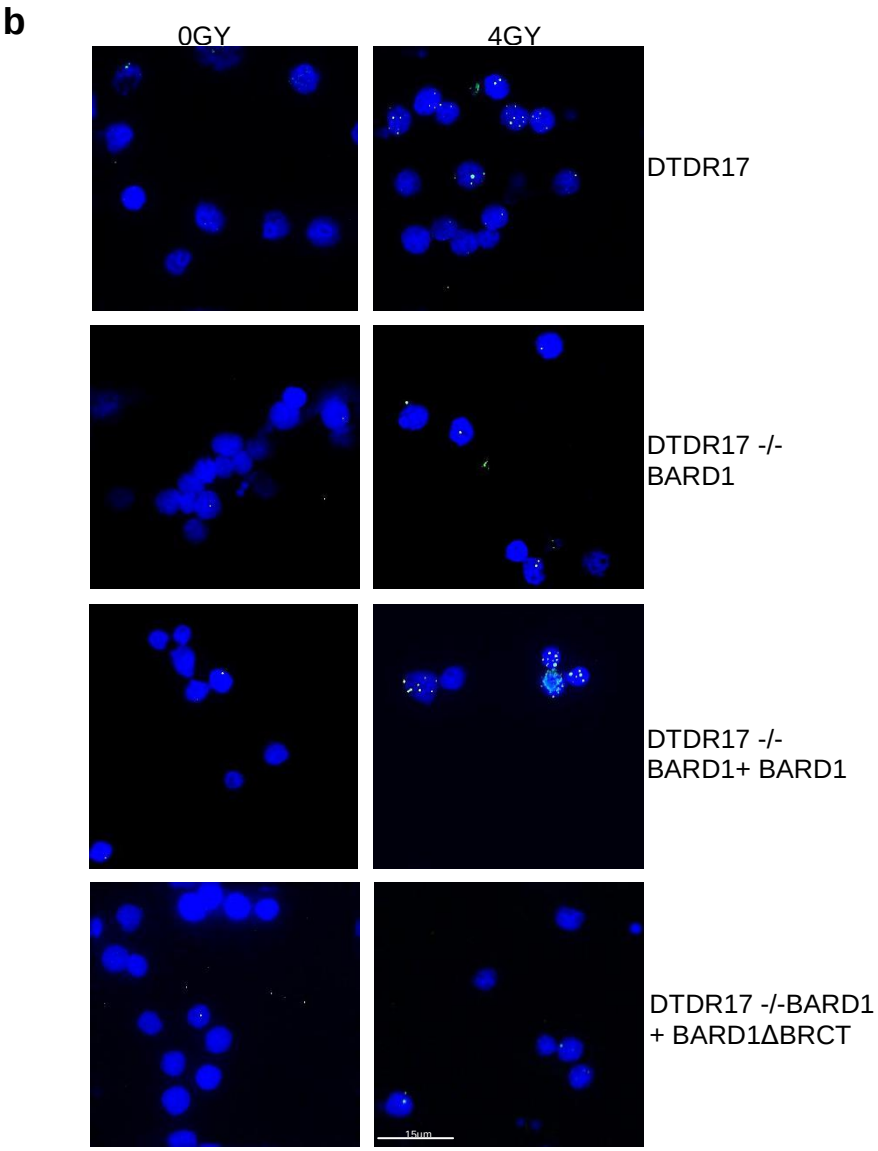
b
0GY
4GY
DTDR17
DTDR17 -/- BARD1
DTDR17 -/- BARD1+ BARD1
DTDR17 -/-BARD1 + BARD1ΔBRCT
15um

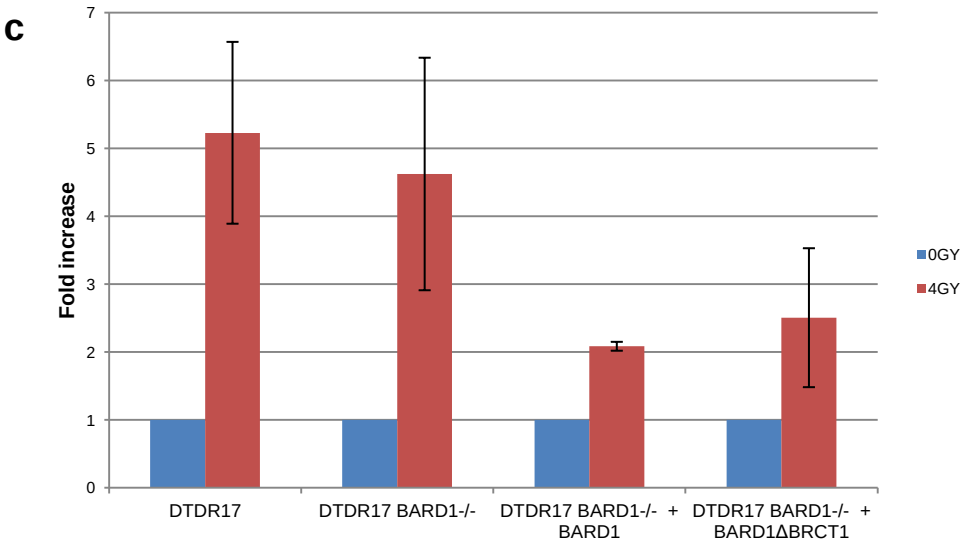
c
Fold increase
0
1
2
3
4
5
6
7
DTDR17
DTDR17 BARD1-/-
DTDR17 BARD1-/- + BARD1
DTDR17 BARD1-/- + BARD1ΔBRCT1
0GY
4GY

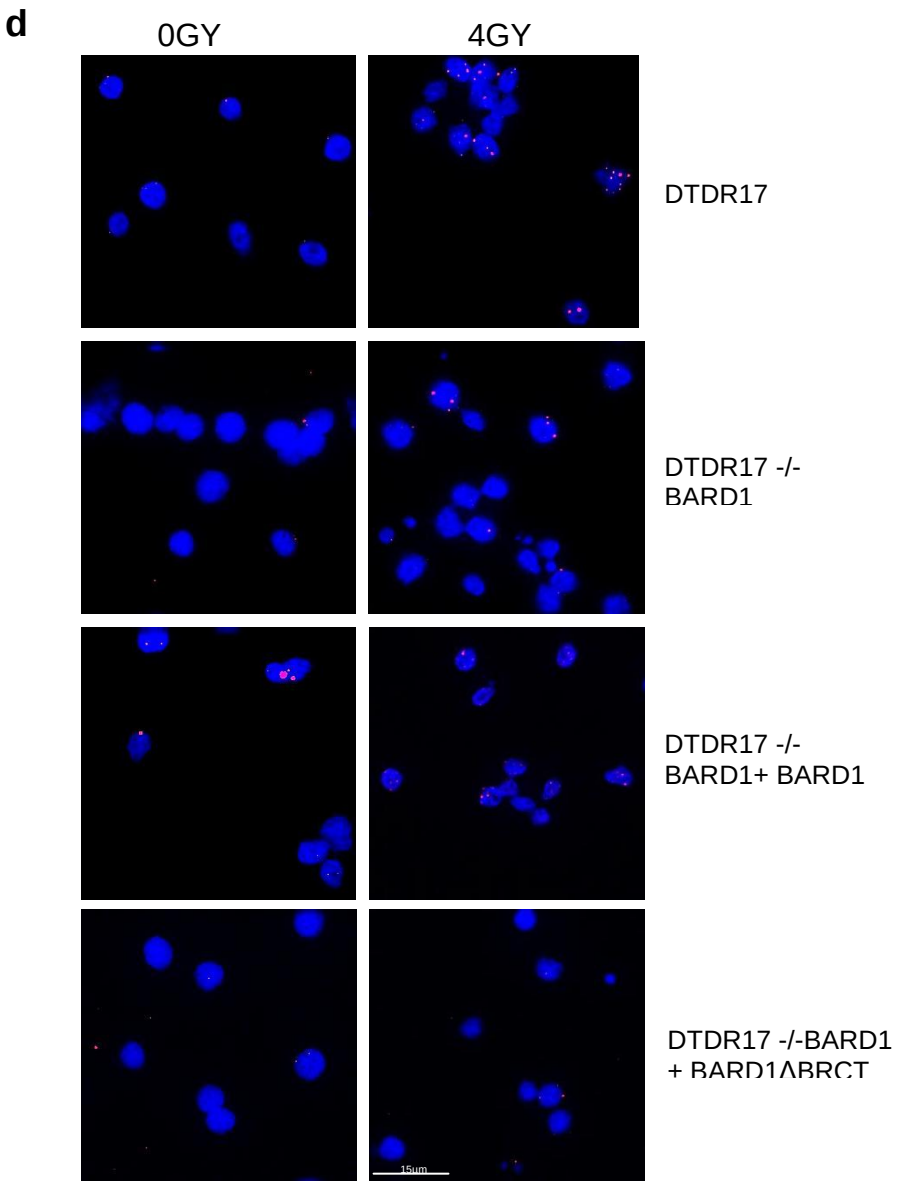

Figure 4.7 Recruitment of RAD51 and RPA to DSB after γ-irradiation.
(a) Bar chart reflecting the fold increase of RAD51 after 4 GY γ-irradiation in comparison to undamaged in DTDR17 cells with different BARD1 status. Data shown are the mean of at least 3 independent experiments. Error bars, s.d
(b) Representative microscopy images from figure (a). Cells were pre-extracted, stained and fixed with α-RAD51 4hrs after irradiation. Images were taken using a DeltaVision Spectris Restoration Microscope using a 60X objective. Supplementary image S6(a).
(c) Bar chart reflecting the fold increase of RPA after 4 GY γ-irradiation in comparison to undamaged in DTDR17 cells with different BARD1 status. Data shown are the mean of at least 3 independent experiments. Error bars, s.d.
(d) Representative microscopy images from figure (c). Cells were pre-extracted, stained and fixed with α-RPA 4hrs after irradiation. Images were taken using a DeltaVision Spectris Restoration Microscope using a 60X objective. Supplementary image S6(b)

Although the results obtained for the recruitment of RAD51 to DSB induced foci appear to be consistent for each experimental replica, the consistency of the RPA data is not as clear. The RAD51 antibody used has been previously used for similar experiments in DT40 [345, 363], indicating that this particular antibody does recognise chicken RAD51. Whereas there have been no similar studies carried out using the RPA antibody that was used in this experiment in DT40 cells.

4.2.7 Loss of the BRCT domains of BARD1 shows a slight decrease in CtIP recruitment to IR induced DSBs

From studies carried out in the previous chapter, the BARD1 BRCT domains appear to help stabilise the BRCA1-C complex involving CtIP. CtIP collaborates with the MRN complex to promote DNA end resection which is important for the initiation of repair of DSB by HR [55, 87]. CtIP is also required for the recruitment of RAD51 to DSB [345]. As RAD51 IR foci are reduced in the absence of the BARD1 BRCT domains, it is possible that it results from a defect in the ability of CtIP to recruit to sites of damage.

DTDR17 *Bard1* cells reconstituted with either HsBARD1 or HsBARD1ΔBRCT were treated with IR and the number of CtIP IR induced foci were analysed to study the effect that the BRCT domains of BARD1 has on the recruitment of CtIP to DSBs. There appears to be a slight reduction in the amount of IR induced CtIP foci formed in the absence of the BARD1 BRCT domains (figure 4.8). Cells were pre-extracted, fixed and stained 1hr after γ-irradiation. A shorter recovery time was used in this experiment in comparison to the RAD51 experiment as CtIP is recruited to DSBs much earlier than RAD51.

a

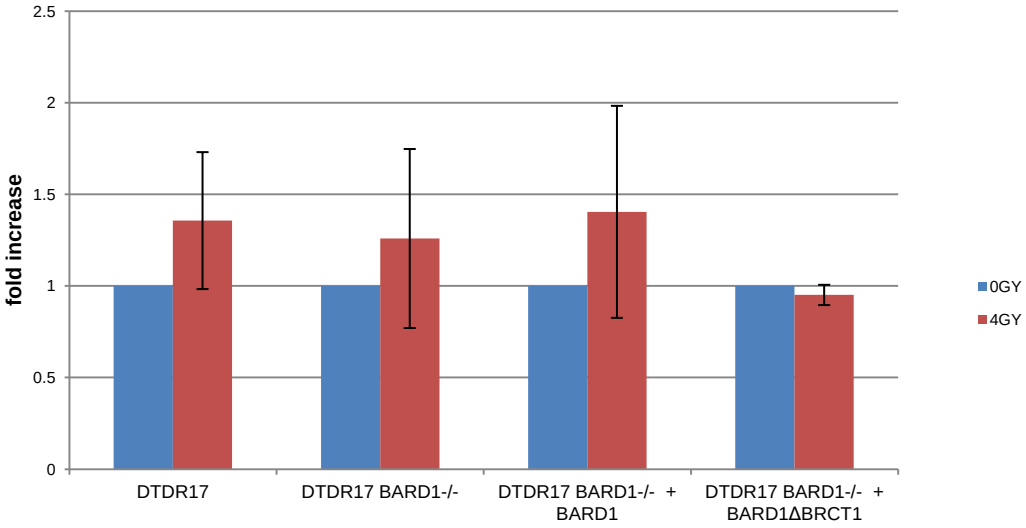
2.5
2
1.5
1
0.5
0
fold increase
DTDR17
DTDR17 BARD1-/-
DTDR17 BARD1-/- + BARD1
DTDR17 BARD1-/- + BARD1ΔBRCT1
0GY
4GY

b

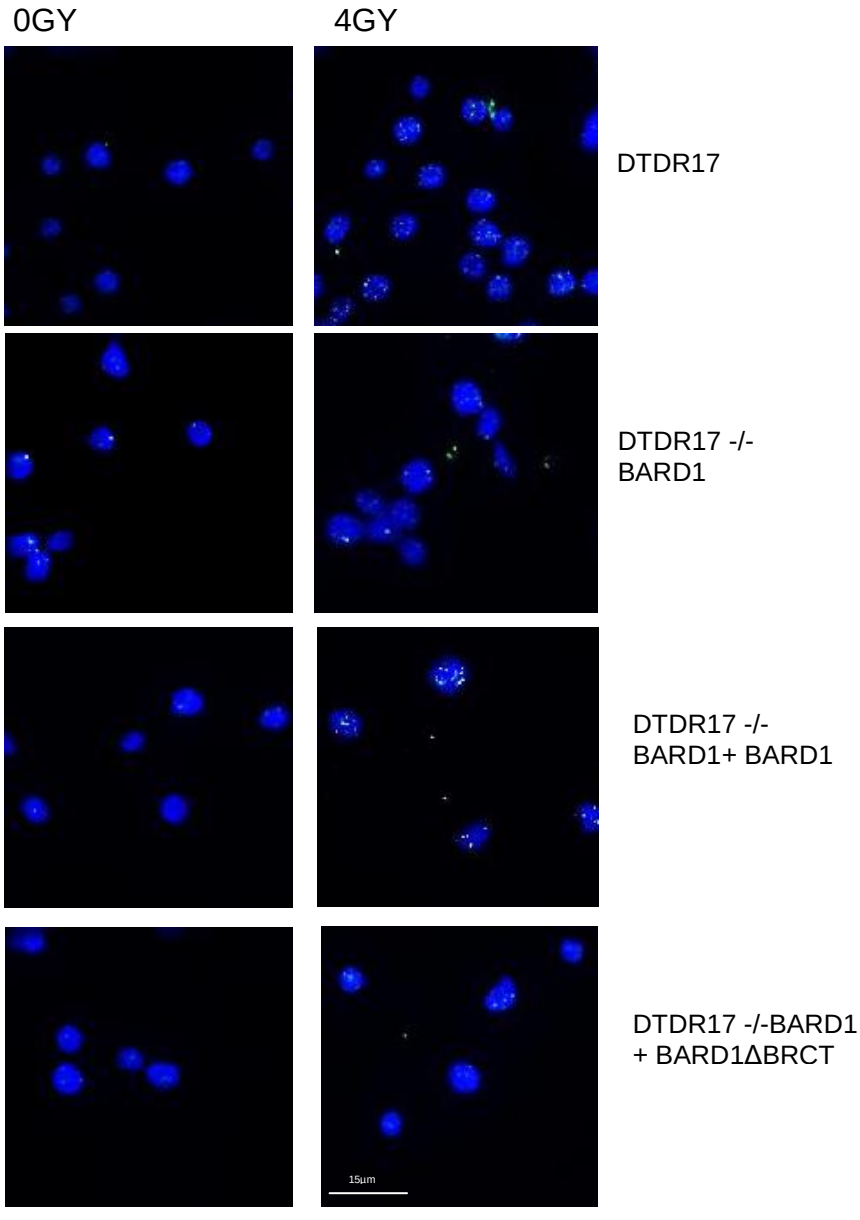
0GY
4GY
DTDR17
DTDR17 -/- BARD1
DTDR17 -/- BARD1+ BARD1
DTDR17 -/-BARD1 + BARD1ΔBRCT
15µm

Figure 4.8 Recruitment of CtIP to DSB after γ-irradiation.
(a) Bar chart reflecting the fold increase of CtIP after 4 GY γ-irradiation in comparison to undamaged in DTDR17 cells with different BARD1 status. Foci were counted using the Imaris software. Data shown are the mean of at least 3 independent experiments. Error bars, s.d
(b) Representative microscopy images from figure (a). Cells were pre-extracted, stained and fixed with α-CtIP 1hrs after irradiation. Images were taken using a DeltaVision Spectris Restoration Microscope using a 60X objective. Supplementary image S7.

Interestingly *Bard1* cells showed the same slight increase in IR induced CtIP foci as Wild type and reconstituted full length BARD1. However the results in figure 4.8 remain difficult to interpret as the fold increase of IR induced CtIP foci is very small compared to undamaged.

4.3 Summary

BARD1ΔBRCT cells do not form S-phase associated foci whereas full length BARD1 and the respective point mutants do.

The recruitment of BARD1 to the S-phase foci is not dependent on BRCA1.

BARD1ΔBRCT can localise to laser induced DSBs, however with slightly delayed kinetics in comparison to BARD1.

Point mutations in the BRCT domains do not prevent BARD1 from localising to DSBs.

Early recruitment of BARD1 via its BRCT domains appears not to have a functional role in HR.

Loss of the BRCT domains of BARD1 hinders the formation of IR induced RAD51 foci and potentially CtIP.

Note; Due to the potential poor quality of printed microscopy images, an electronic copy of the microscopy images can be found on the supplementary disc at the end of the appendix

Chapter 5 Novel interacters of the BARD1 BRCT domains.

5.1 Introduction

BARD1 plays an important role in maintaining genome stability. This is mainly through its binding with BRCA1. BARD1 is responsible for retaining BRCA1 in the nucleus, where it has its function, by masking the nuclear export signal of BRCA1. BRCA1 ubiquitin ligase activity is also greatly enhanced in the presence of BARD1.

The BARD1 BRCT domains are also important for HR. Along with its binding to BRCA1, BARD1 has also been shown to interact with CstF-50, a polyadenylation factor that is involved in specifying the processing site of mRNA [364]. This interaction is thought to inhibit polyadenylation and prevent inappropriate RNA processing during transcription at sites of DNA repair.

BARD1 has also been described as a NF-kB interactor and is thought to regulate its transcriptional activity [365]. To date there are no known BARD1 BRCT interactors apart from its ability to bind PAR [287], which is important for very early recruitment to DNA damage.

This chapter describes attempts to identify potential BARD1 BRCT interactors as well as novel BARD1 interactors which may contribute to the DNA Damage response.

5.2 Results

5.2.1 Optimisation of GFP-BARD1 pull down.

BRCT domains are highly conserved protein regions which bind phosphorylated proteins and are found in many DNA damage response proteins [300, 301, 346]. With the recent knowledge that the BARD1 BRCT domains are important for HR, it is plausible that the HR function of the BARD1 BRCT domains may depend on their interaction with another protein involved in DNA repair. In order to investigate this

possibility Mass Spectrometry was used to identify potential new BARD1 BRCT interactors.

HEK Flp In cells stably expressing either GFP-BARD1 or GFP-BARD1ΔBRCT, previously used in chapters 3 and 4, were used to analyse potential BARD1 and BARD1ΔBRCT interactors. By comparing the BARD1 interactors or complex members with the BARD1ΔBRCT interactors via Mass Spectrometry, it was possible to identify proteins which were dependent on the BARD1 BRCT domains. Pulling down the BARD1 BRCT domains alone was decided against as proteins which may indirectly interact with BARD1 or its BRCT domains, as part of a complex, may have been missed.

Before analysing the potential BARD1 interactors via Mass Spectrometry, the GFP pull down was optimised to assure it would have the capacity to pull down the majority of BARD1 complexes or interactors. GFP-trap beads were used for the pull down as the beads are covalently coated in a *Camelidae* V_HH domain which binds GFP. These V_HH domains are the smallest intact antigen binding fragments available and avoids the use of large conventional antibodies. GFP-trap beads are also extremely specific and do not require long incubation for binding. For this experiment it was important to maintain the expression of GFP-BARD1 and GFP-BARD1ΔBRCT as close to endogenous levels of BARD1 as possible. Expression levels greatly exceeding endogenous levels of BARD1 may have unwanted dominant negative effects. A variety of different tetracycline concentrations were used to induce BARD1 expression and it appeared that 2.5ng/ml was optimal for GFP-BARD1 expression whereas 7.5ng/ml was need to induce GFP-BARD1ΔBRCT to the same level. Using 2.5ng and 7.5ng tetracycline, GFP-BARD1 and GFP-BARD1ΔBRCT expression was maintained at around 3 fold over endogenous (figure 3.5(a). All tetracycline inducible cell lines were maintained in Tet-free media as normal media can contain different levels of Tetracycline.

In order to assess whether the conditions for pulling down GFP-BARD1 and GFP-BARD1ΔBRCT were optimal, a GFP-trap pull down was carried out and analysed by Western blot. Under the conditions used, as described in the materials and methods chapter, GFP-BARD1 was clearly pulled down. The BRCA1/BARD1 complex members such as Abraxas, FANCJ and CtIP also co-immunoprecipitated with both GFP-BARD1 and GFP-BARD1ΔBRCT (figure 5.1). The ability to pull down BRCA1 and the BRCA1 complex members clearly demonstrates the potential ability of this technique to identify BARD1 interactors, direct or indirect.

Mass Spectrometry analysis was carried out with lysates from both crosslinked and non-crosslinked pull down conditions. DSP was used as a crosslinking agent. DSP contains two reactive amine N-hydroxysuccinimide esters, one at each end of an 8-carbon linker arm, These reactive esters form a stable amine bond with primary amines. DSP is a reversible crosslinker, allowing the separation of complex proteins after immunoprecipitation. Using DSP, less stable interactions formed between BARD1 and potential interactors may be found. It is clear from figure 5.1 that the use of DSP does not affect the efficacy of the GFP-trap pull down as BRCA1 and the BRCA1 A, B and C complex members are still co-immunoprecipitated with both GFP-BARD1 and GFP-BARD1ΔBRCT.

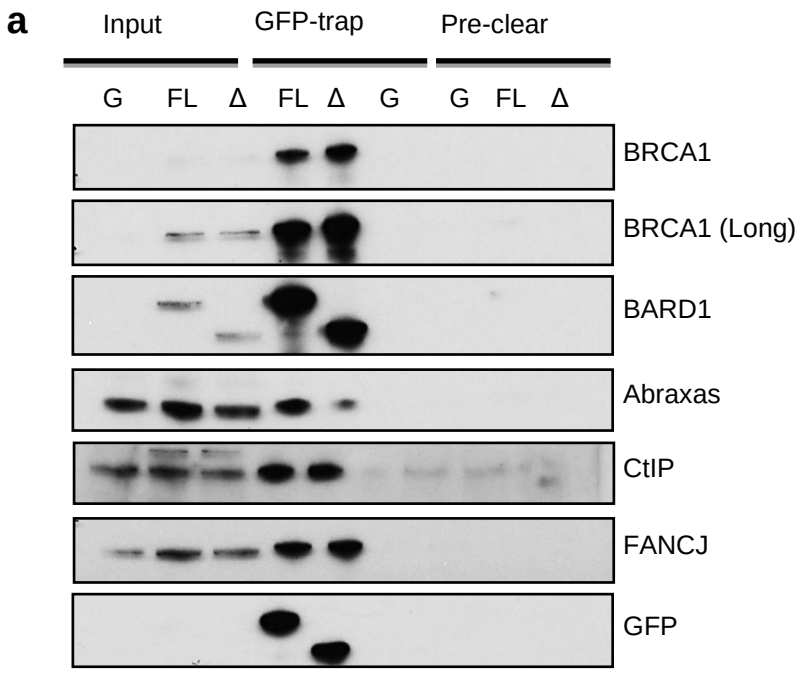

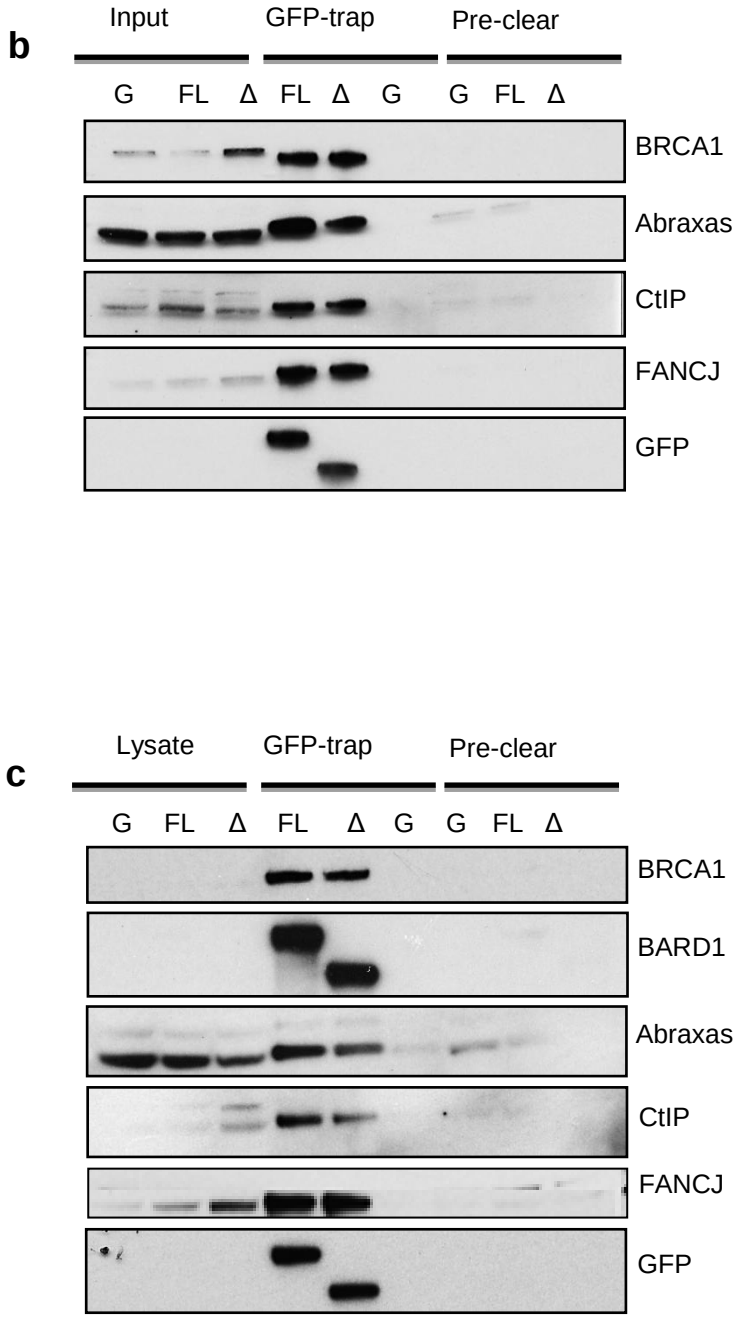

Figure 5.1 Crosslinking does not interfere with the efficacy of GFP-trap pull downs.
(a) Representative Western blot from a non-crosslinked GFP-BARD1 and GFP-BARD1ΔBRCT pull down. Input is 50µg of lysate. HEK-GFP (G), GFP-BARD1 (FL), GFP-BARD1ΔBRCT (Δ).
(b) Representative Western blot from a non-crosslinked GFP-BARD1 and GFP-BARD1ΔBRCT pull down. Lysates were quenched with 200mM Tris before adding to beads. Input is 50µg of lysate.
(c) Representative Western blot from a crosslinked GFP-BARD1 and GFP-BARD1ΔBRCT pull down. Lysates were quenched with 200mM Tris before adding to beads. Input is 50µg of lysate.

A HEK cell lines containing only GFP was used as a negative control for this experiment, and as seen in figure 5.1, GFP alone fails to pull down any of the proteins associated with the BRCA1 BARD1 complexes. As observed in chapter 3, loss of the BRCT domains of BARD1 does not prevent the binding of the BRCA1 complexes, however a decrease is often seen with CtIP and on occasion with Abraxas. Tris was used in figure 5.1 (b) as a control because after DSP treatment the reaction must be quenched with Tris. The addition of 200mM Tris also has no effect on the efficiency of the pull down.

5.2.2 Mass Spectrometry analysis of proteins co-immunoprecipitated with GFP-BARD1 and GFP-BARD1ΔBRCT.

Mass Spectrometry was initially used to identify proteins co-immunoprecipitated with both GFP-BARD1 and GFP-BARD1ΔBRCT under non-crosslinked conditions (figure 5.2). GFP-trap pull down was carried out using 40mg of either GFP-BARD1 or GFP-BARD1ΔBRCT cell lysates. The cells were treated with tetracycline to induce BARD1 expression over night before harvesting and lysis. The concentration of tetracycline used is described in figure 3.5(a). Immunoprecipitated proteins were then run on a pre-cast 4-12% Bis-Tris gel to minimise contamination. Once the proteins had run around 1cm into the gel, the gel was stained and the proteins were excised and digested with trypsin before Mass Spectrometry analysis, as described in the methods and materials chapter. This initial Mass Spectrometry was carried out using a Thermo Scientific LTQ Orbitrap and sample preparation was carried out in lab.

Mass Spectrometry analysis was carried out using PEAKs. In order to confidently identify proteins and peptides bound to either BARD1 or BARD1ΔBRCT, a stringent validation cut off was used. Only proteins containing at least two identified peptides with over 95% homology were taken as positive results. Non-specific or contaminating proteins were taken into account by deducting any proteins found in the GFP-only control sample. The higher the coverage and the number of unique peptides

associated with a protein, the more reliable the result is. There is also a direct correlation with the amount of that particular protein identified.

As expected, BRCA1 and BARD1 were the most common proteins identified by Mass Spectrometry. Both have over 30% coverage and large number of unique peptides. Interestingly FANCJ was also identified with high confidence. FANCJ is the only BRCA1 complex protein identified however both Abraxas and CtIP are known to be difficult to detect via Mass Spectrometry. Although Abraxas itself was not identified, other members of the BRCA1-A complex such as RAP80 and Merit40 were.

The following tables show a selection of Mass Spectrometry hits, found in both GFP-BARD1 and GFP-BARD1ΔBRCT samples or either one or the other. Several of the proteins identified have a function in DNA repair, stress response, transcription regulation and post-translational modification which will be discussed later. As seen in the Venn diagram in figure 5.3, 202 proteins were associated with only GFP-BARD1 and 239 with GFP-BARD1ΔBRCT. Only 35 proteins were identified in both samples.

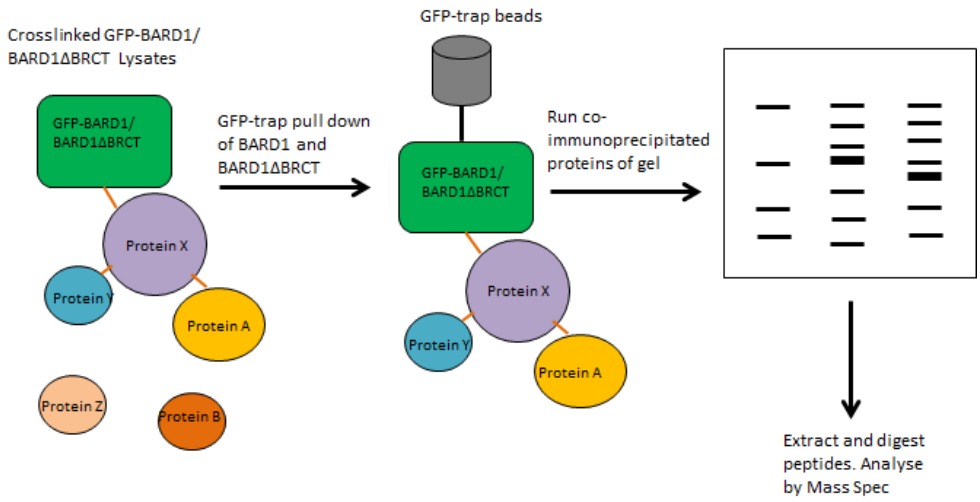

Figure 5.2 GFP-trap pull down and Mass Spectrometry
Illustration of the method used to identify potential BARD1 and BARD1ΔBRCT interactors. Cropssslinking was used in this diagram, however Mass Spectrometry was also permormed under non-crosslinkling conditions.

1	Accession Number	Protein Name	Coverage (%)	#Peptides (unique)
	IPI00017746	BARD1	59/44	45 (45)/ 31 (31)
	IPI00218982	BRCA1	28/38	33 (33)/ 48 (48)
	IPI00012500	FANCJ	9/22	5 (5)/ 18 (18)
	IPI01022339	DDX17	27/ 34	14 (8)/ 16 (10)
	IPI01015591	DHX15	9/ 4	4 (4)/ 2 (1)
	IPI00642944	PABPC4	17/ 24	7 (4)/ 8 (3)
	IPI00003886	SNORD19B	7/ 5	3 (3)/ 1 (1)
	IPI01013544	HSPA1B	32/ 47	15 (0)/ 24 (1)
	IPI00006702	PELP1	6/ 2	3 (3)/ 2 (2)
	IPI01022950	SLC25A3	4/ 4	1 (1)/ 1 (1)

2	Accession Number	Protein Name	Coverage (%)	#Peptides (unique)
	IPI00910607	BAT2D1	6	4 (1)
	IPI00646886	MOV10	14	5 (5)
	IPI00880119	PHF8	6	2 (2)
	IPI00941219	PRRC2C	3	5 (2)
	IPI00438230	TRIM28	20	8 (8)
	IPI00967719	RAP80	10	1 (1)
	IPI00893035	CAD	11	1 (1)
	IPI00006442	COIL Coilin	11	5 (5)
	IPI00894449	KIF3C	4	1 (1)
	IPI00292387	NOLC1	13	8 (8)

3	Accession Number	Protein Name	Coverage (%)	#Peptides (unique)
	IPI00101987	MERIT40	6	1 (1)
	IPI00979099	BCLAF1	2	1 (1)
	IPI00005711	HDAC6	3	1 (1)
	IPI00172559	PALB2	1	1 (1)
	IPI00749013	UBCH5C	14	1 (1)
	IPI00008524	PABPC1	29	13 (8)
	IPI01010638	PHGDH	5	2 (2)
	IPI00009104	RUVBL2	5	2 (2)

Table 5.1 Mass Spectrometry protein hits under normal conditions
(1) Proteins identified by Mass Spectrometry common to both GFP-BARD1 and GFP-BARD1ΔBRCT. Coverage represents the % coverage of peptides found in relation to the protein.
(2) Table of Mass Spectrometry hits associated with only GFP-BARD1.
(3) Table of identified protein only found in the GFP-BARD1ΔBRCT sample.
PINK; DNA Damage and repair
GREEN; Transcription regulation
PURPLE; Stress response
BLUE; Post-translational modifying enzymes (demethylases, Sumo-conjugating enzymes etc)
ORANGE; Associated or part of the NuRD complex.

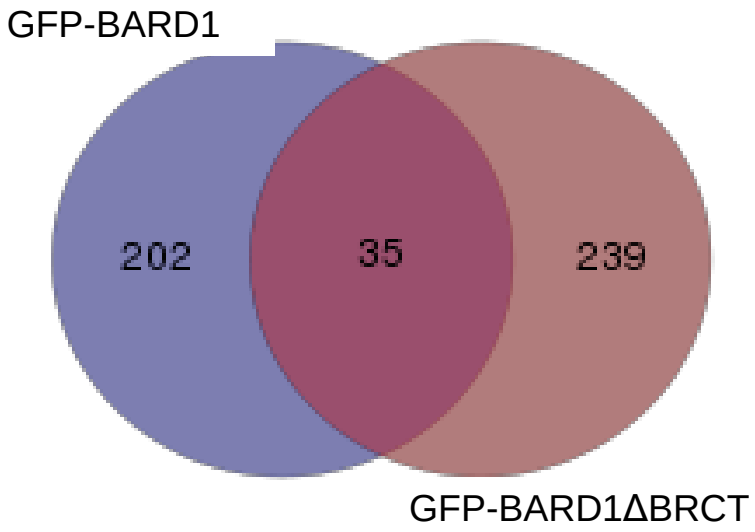

Figure 5.3 Venn Diagram of Mass Spectrometry hits
Venn diagram indicating the number of proteins found in either GFP-BARD1 or GFP-BARD1ΔBRCT. The overlap of the two spheres shows number of protein common in both samples.

5.2.3 Mass Spectrometry analysis of cross-linked proteins co-immunoprecipitated with GFP-BARD1 and GFP-BARD1ΔBRCT.

In order to identify more transient or indirect BARD1 interactors and more specifically proteins which interact with the BARD1 BRCT domains, a second Mass Spectrometry was carried out using a crosslinker. During the lysis of GFP-BARD1 and GFP-BARD1ΔBRCT cells, DSP was added to crosslink proteins, stabilising complexes and weaker more transient interactions. As stated previously, DSP is a reversible crosslinker containing two reactive NHS esters at either side of a spacer arm. These NHS esters stably bind primary amine groups often found in the side chain lysine residues of most proteins. DSP contains a disulphide bond in the spacer arm which can be easily cleaved in the presence of a reducing agent such as DTT. The reversibility of DSP made it an optimal crosslinker for this experiment as proteins which form complexes with BARD1 can be easily separated after immunoprecipitation and analysed by Mass Spectrometry.

GFP-trap pull down of GFP-BARD1 and GFP-BARD1ΔBRCT for analysis by Mass Spectrometry was carried out in the same way as in 5.2.2 apart from the addition of DSP. After immunoprecipitation the samples were processed and analysed by the Mass Spectrometry facility in the College of Life Sciences, Dundee whereas previously the Mass Spectrometry facility in Ninewells was used. Trypsin digestion and preparation of the samples was carried out as part of the service. Mass Spectrometry was accomplished using an Orbitrap. Analysis of Mass Spectrometry targets was performed using Scaffold software. The validation of results was achieved using the same exclusion principals used for the previous Mass Spectrometry and GFP-alone proteins were also subtracted from the GFP-BARD1 and GFP-BARD1ΔBRCT hits.

As in 5.2.2, BRCA1 and BARD1 were identified with the highest confidence from the list of potential Mass Spectrometry hits. As expected, the number of potentially interesting protein hits were dramatically increased in the presence of a crosslinker.

Several more proteins known to be involved in DNA damage repair were identified in this screen compared to the non-crosslinked pull down Mass Spectrometry. Intriguingly the number of proteins common to both GFP-BARD1 and GFP-BARD1ΔBRCT that were identified was far greater when crosslinked (figure 5.5).

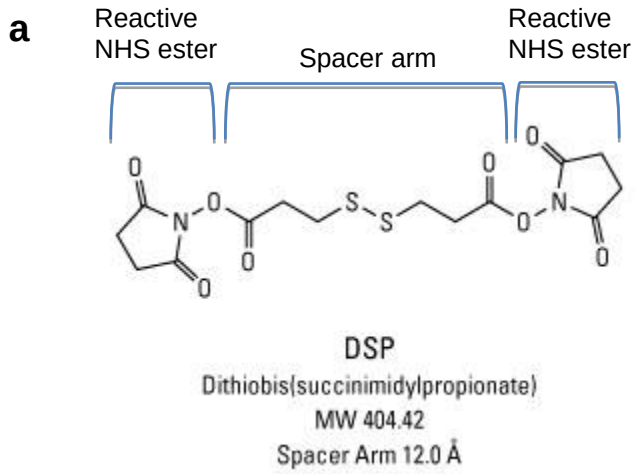

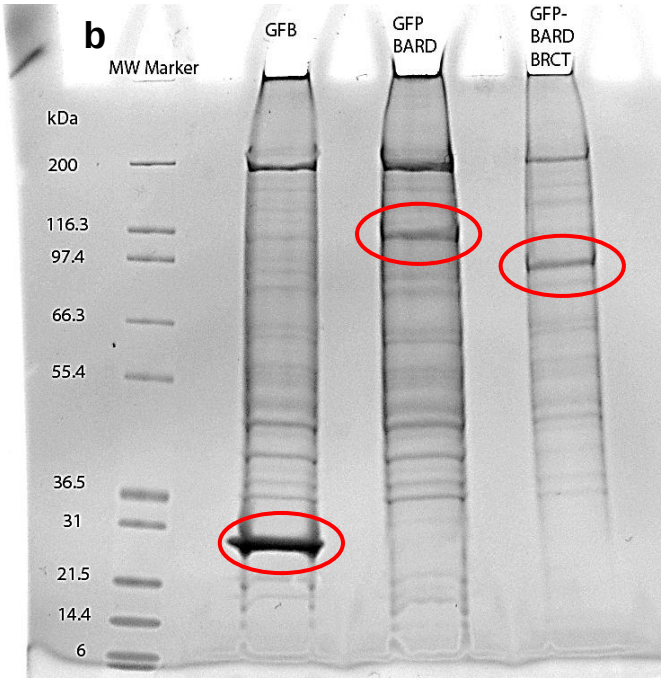

Figure 5.4 GFP-trap pull down samples for Mass Spectrometry
(a) Illustration of the DSP crosslinker, image adapted from *Piercenet.com*
Image of a coomassie stained gel containing the GFP GFP-BARD1 and GFP-BARD1ΔBRCT samples after immunoprecipitation. The proteins were then cut from the gel, digested and identified by Mass Spectrometry.

1	Accession Number	Protein Name	Coverage (%) FL/Δ	#Peptides unique FL/Δ
	IPI00017746	BARD1	59/46	45/42
	IPI00218982	BRCA1	38/48	51/69
	IPI00029754	MLH1	11/16	5/8
	IPI00396071	RAP80	11/14	6/5
	IPI00000846	CHD4	3.4/6	4/7
	IPI00017297	MATRIN3	9.7/5.4	4/2
	IPI00164724	BRE	7.3/7.3	3/3
	IPI00008531	CoREST	8.7/8.7	3/3
	IPI00171798	MTA2	5.4/12	1/4
	IPI00871617	BRCC36	8.9/12	2/3
	IPI00746337	PMS2	4.6/5.1	3/3
	IPI00101987	MERIT40	13/20	1/2
	IPI00012773	MTA1	7/7	4/4
	IPI00412408	BRCA2	.5/1	1/2
	IPI00017303	MSH2	4.1/1.5	2/1
	IPI00184330	MCM2	1.4/2.8	1/2
	IPI00172559	PALB2	1.3/3.4	1/2
	IPI00012500	FANCJ	40/49	34/48
	IPI00217540	LSD1	13/14	7/8
	IPI00445401	HUWE1	1.6/2.5	4/5
	IPI00395865	RBBP7	17/13	3/2
	IPI00013774	HDAC1	12/15	3/2

2	Accession Number	Protein Name	Coverage (%)	#Peptides unique
	IPI00032957	UBC9	28	9
	IPI00646779	TUBB6	27	2
	IPI00007927	SMC2	2	2
	IPI00219446	PEBP1	20	2
	IPI00215914	ARF1	22	2
	IPI00003309	RPABC3	13	2
	IPI00029159	MRE11	6.8	4

3	Accession Number	Protein Name	Coverage (%)	#Peptides unique
	IPI00947285	Suprabasin	9.2	3
	IPI00009342	IQGAP1	1.9	2
	IPI00396015	ACC1	1.2	2

Table 5.2 Crosslinked Mass Spectrometry protein hits.
(1) Proteins identified by Mass Spectrometry common to both GFP-BARD1 and GFP-BARD1ΔBRCT. Coverage represents the % coverage of peptides found in relation to the protein.
(2) Table of Mass Spectrometry hits associated with only GFP-BARD1.
(3) Table of identified protein only found in the GFP-BARD1ΔBRCT sample.
PINK; DNA Damage and repair
GREEN; Transcription regulation
BLUE; Post-translational modifying enzymes (demethylases, Sumo-conjugating enzymes etc)
ORANGE; Associated or part of the NuRD complex.

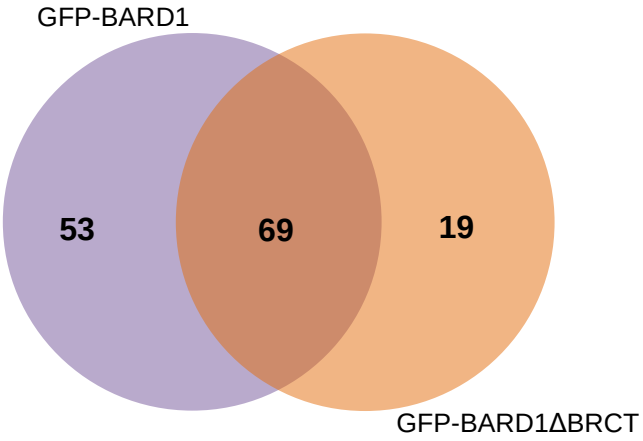

Figure 5.5 Venn Diagram of Crosslinked Mass Spectrometry hits
Venn diagram indicating the number of proteins found in either GFP-BARD1 or GFP-BARD1ΔBRCT. The overlap of the two spheres shows number of protein common in both samples.

5.2.4 Identification and validation of potential BARD1 and BARD1 BRCT domain interacting proteins.

After data analysis, six proteins, identified by Mass Spectrometry which potentially interact with either full length BARD1 or the BARD1 BRCT domains, were chosen for further validation and analysis. The following proteins were chosen for further analysis as they are known to localise to sites of damage. CHD4, HUWEI. LSD1, MTA2, RBBP7 and UBC9 have all been either shown to be involved in DNA repair or form complexes with proteins associated with the DDR. Interestingly several protein identified as potential BARD1 interactors are part of the NuRD complex, a chromatin remodelling complex. The involvement of chromatin remodelling factors in the repair of DNA damage is now beginning to emerge and the potential involvement of BARD1 would be very interesting in terms of the its function in the DDR.

CHD4 (chromodomain-helicase-DNA-binding 4) was first identified as an autoantigen in dermatitis often leading to malignancy [366-368]. CHD4 contains an ATPase/helicase domain which allows it to bind and mobilise nucleosomes on DNA [369]. CHD4 is also a core member of the NuRD complex which is a key chromatin remodelling complex. It is believed that the CHD4 PHD fingers preferentially bind unmodified lysine residue 4 on histone 3 and also to trimethylated lysine 9 on the same histone [370]. Chromatin remodelling proteins have long been known to be involved in the DDR. Interestingly CHD4 has been shown to be recruited to sites of DNA damage in two independent mechanisms. Firstly it has been shown to be recruited by binding to poly(ADP-ribosyl)ated proteins, including PARP1 [371] and secondly by the ubiquitin ligase RNF8 [372]. It is believed that CHD4, as part of the NuRD complex, creates a chromatin environment which allows the amplification of the DNA damage signal ultimately leading to the recruitment of repair proteins such as BRCA1. CHD4s involvement in DNA damage repair and its binding to poly(ADP-ribosyl)ated proteins makes it a very interesting potential BARD1 interactor. However it was only found in the crosslinked Mass Spectrometry pull down in both GFP-BARD1 and GFP-

BARD1ΔBRCT suggesting that the interaction is not dependent on the BRCT domains and may be transient or indirect.

MTA1 and MTA2 are also integral components of the NuRD complex [373] and were identified in the crosslinked pull down by Mass Spectrometry. Both MTA1 and MTA2 were common to both GFP-BARD1 and GFP-BARD1ΔBRCT. MTA1 has been suggested to be important in the efficient repair of DSBs as depletion of MAT1 renders cells sensitive to IR [374] and re-expression of MTA1 rectifies this defect.

HUWEI is a large HECT domain containing ubiquitin ligase protein. Several HUWEI substrates are involved in DNA damage responses and repair [375-378]. HuweI adds lysine 48 (k48) chains to its substrates targeting them for proteasomal degradation, however it has also been shown to add lysine 63 (k63) ubiquitin chains to C-Myc suggesting a signalling role [379]. Interestingly UBC9, a SUMO conjugating enzyme, was also identified as a potential BARD1 interactor.

It has become evident that SUMO modification plays an important role in DNA repair [380-385]. UBC9 is the only known SUMO conjugating enzyme in mammalian cells and it has been shown, along with other SUMO proteins, to localise to DSB [380, 382, 386]. SUMOylation is also important for recruitment of repair proteins to sites of damage [181].

Signalling involving posttranslational modifications such as ubiquitylation and sumoylation plays a fundamental role in the repair of DNA DSBs making a potential interaction between BARD1 and HUWEI and UBC9 very interesting. As with CHD4, HUWEI was only identified in the crosslinked pull down in both GFP-BARD1 and GFP-BARD1ΔBRCT. Intriguingly UBC9 was identified with high confidence in the crosslinked GFP-BARD1 sample only suggesting that if BARD1 and UBC9 interact it may be through the BARD1 BRCT domains.

RBBP7 was identified in both GFP-BARD1 and GFP-BARD1ΔBRCT crosslinked pull down samples. RBBP7 was highlighted as an interesting Mass

Spectrometry candidate as it is also suggested to be involved in the NuRD complex and interacts with BRCA1 [387]

LSD1 was the first human lysine specific demethylase discovered in 2004 [388, 389]. LSD1 removes one or two methyl groups from lysine 4 on histone 4. Work in Mosammaparast lab, suggests a direct role for LSD1 in DNA repair as LSD1 is directly recruited to laser induced DNA damage stripes [390]. As methylation plays an important role in recruiting some of the major DDR proteins such as 53BP1 to sites of damage, a potential interaction between LSD1 and BARD1 may shed some light on alternative functions of BARD1 in DNA damage repair. LSD1 was identified in both GFP-BARD1 and GFP-BARD1ΔBRCT pull down samples, however only when a crosslinker was used.

In order to confirm the selected Mass Spectrometry hits, a GFP-trap pull down was used. The pull down was carried out under the same conditions as used to identify BARD1 interactors by Mass Spectrometry. GFP-BARD1 and GFP-BARD1ΔBRCT were pulled down under crosslinking conditions and the respective Mass Spectrometry hit proteins were blotted for by Western blot. Unfortunately the proteins of interest were not detected by Western blot after co-immunoprecipitation with GFP-BARD1 and GFP-BARD1ΔBRCT (figure 5.6). BRCA1 and FANCJ were used as positive controls for the pull down.

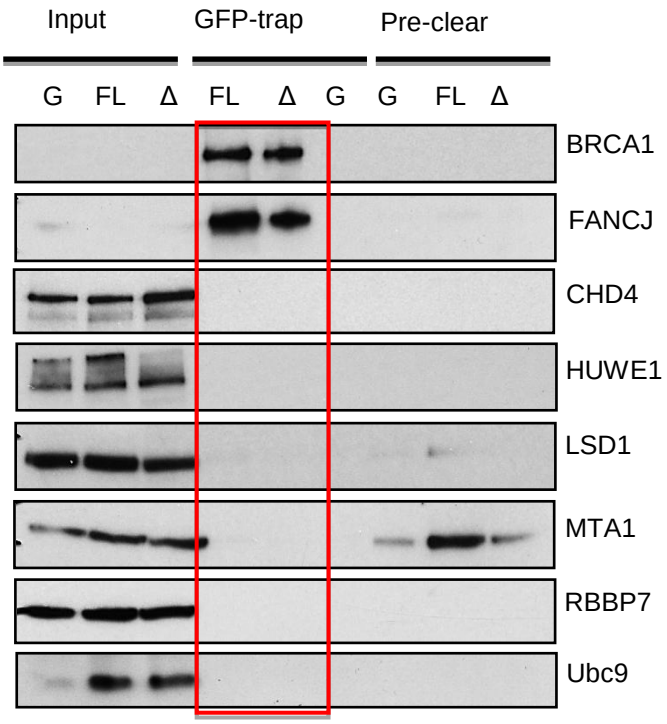

Figure 5.6 Confirming potential BARD1 interactors
Representative Western blot of Mass Spectrometry identified BARD1 interactors. HEK GFP-BARD1 and GFP-BARD1ΔBRCT cells were induced with tetracycline o/n before lysis and crosslinking. GFP-BARD1 and GFP-BARD1ΔBRCT lysates were pulled down and co-immunoprecipitated proteins were blotted for. Experiment was carried out at least 3 times.

It is clear from figure 5.6 that the antibodies used do indeed recognise their target proteins as a representative band can be seen in the input lane. It is possible that a Western blot is not sensitive enough to detect the amount of protein identified by Mass Spectrometry as less than 10 peptides from each protein were detected. It remains unclear if the chosen Mass Spectrometry candidates are indeed true BARD1 or BARD1 BRCT interactors. It is also important to keep in mind that these potential hits may not directly bind with BARD1 as BARD1 and BRCA1 form several complexes of which these proteins may interact with.

5.2.5 CHD4 localises to laser induced DNA DSBs.

Although the Mass Spectrometry target proteins could not be confirmed by Western blot, it is still possible that they are indeed true interactors. As BARD1 localises to laser induced DNA DSBs, the localisation of the potential BARD1 interactors to the same laser induced damage stripes, along with the Mass Spectrometry data, might indicate a possible function at DSB with BARD1.

This hypothesis was tested by inducing a laser stripe of damage in U2OS cells and evaluating whether the proteins of interest co-localised with γH2AX using the same antibodies as in figure 5.6. Surprisingly none of the Mass Spectrometry hits co-localised with γH2AX (figure 5.7 (a). However preliminary results suggest that CHD4 can localise to a laser induced damage stripe (figure 5.7 (b). The antibodies used to confirm the Mass Spectrometry targets were chosen specifically for their compatibility for Western blots but also for their suggested potential to be used for immunofluorescence. The negative results seen in figure 5.7(a) may be partly due to the antibodies not being suitable for immunofluorescence or *in-vivo* studies.

All the potential protein interactors chosen are known to be involved directly or indirectly with DNA damage repair and CHD4 in particular has been shown to localise to laser stripe induced damage [371, 391]. The results seen in figure 5.7 (b) suggest that CHD4 does localise to sites of damage, however this may be due to the fact that HEK cells were transiently transfected with a GFP-tagged HsCHD4 construct with no reliance on antibodies. This leads to the speculation that the other Mass Spectrometry hits may also localise to DNA damage under the correct experimental settings. Due to lack of time, no further evaluation could be carried out.

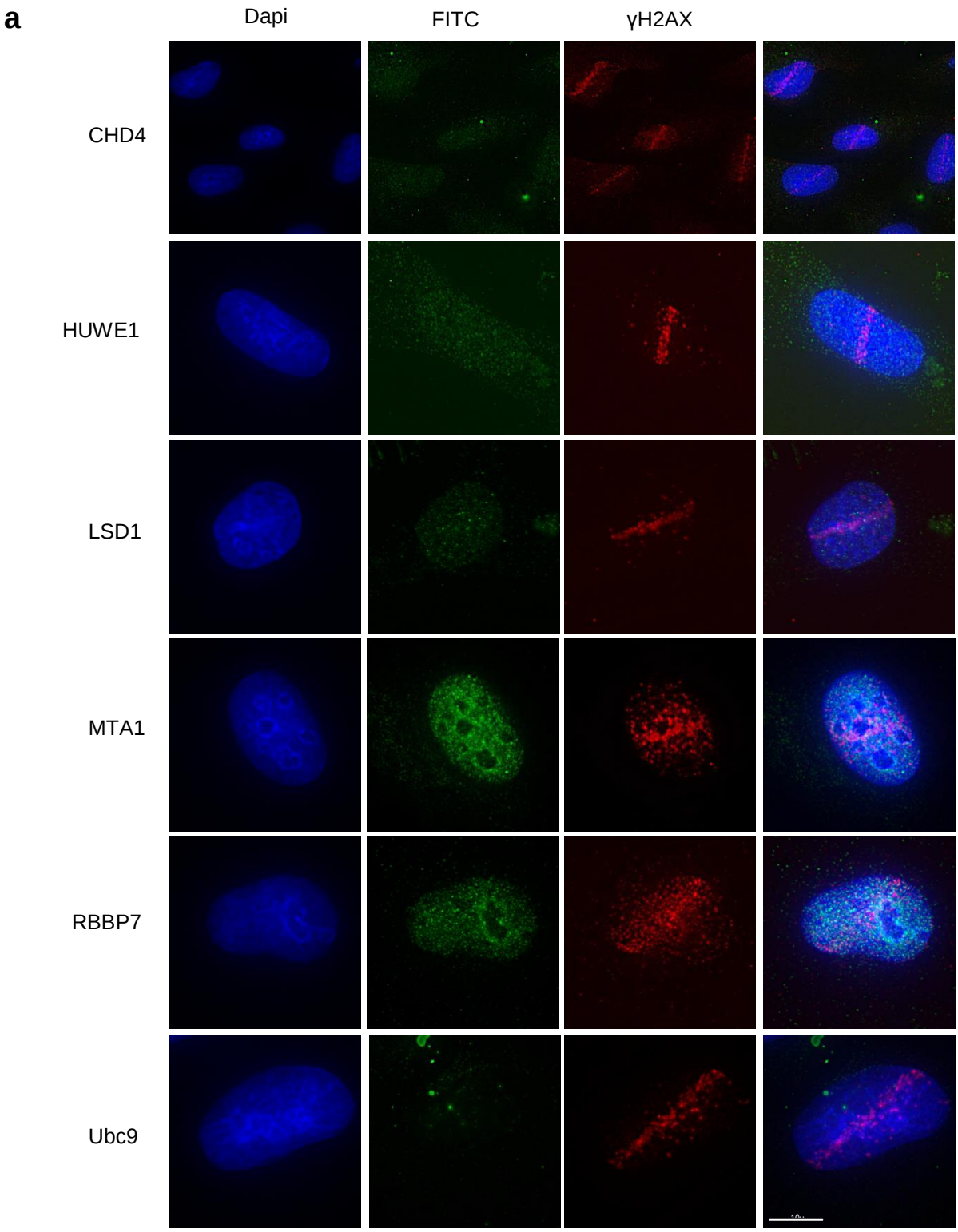
a
Dapi
FITC
γH2AX
CHD4
HUWE1
LSD1
MTA1
RBBP7
Ubc9

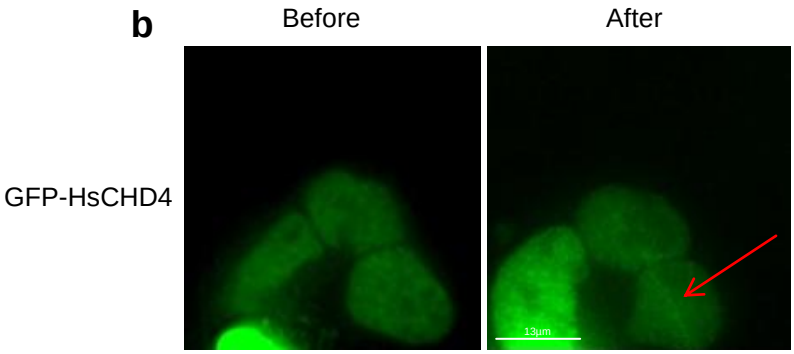

Figure 5.7 CHD4 localises to laser induced DNA damage stripe.
(a) Representative images illustrating the failure of the Mass Spectrometry target proteins to localise to γH2AX positive laser induced DSB stripes. Laser stripe was generated using a 405nm Leica UV laser and imaged by DeltaVision Spectris Restoration Microscope using a 100X objective. Cells were fixed and stained with antibodies against the respective proteins (green) and γH2AX (red) 1hr after laser stripe. Experiment was repeated at least 3 times using 6 cells each time. Supplementary figure S8(a)
(b) Preliminary results showing live imaging localisation of a transiently expressed GFP-CHD4 to Laser induced DNA damage stripe. HEK cells were transiently transfected with GFP-CHD4 24 hrs before laser striping. Cells were laser damaged using a 405nm laser on the DeltaVision Spectris Restoration Microscope. A 60X objective was used to capture the image. Images were taken before laser stripe and 5mins after. Supplementary figure S8(b)

5.3 Summary

2.5ng/ml and 7.5ng/ml tetracycline is needed to induce the expression of GFP-BARD1 and GFP-BARD1ΔBRCT to around 3 fold endogenous BARD1 levels in HEK inducible cell lines.

Abraxas, FANCJ and CtIP co-immunoprecipitate with both GFP-BARD1 and GFP-BARD1ΔBRCT under the conditions used with GFP-trap beads.

Mass Spectrometry analysis of proteins co-immunoprecipitated with both GFP-BARD1 and GFP-BARD1ΔBRCT revealed that the majority of proteins which may bind BARD1 are part of a complex or weak interactors as crosslinking is required.

Several proteins identified as potential BARD1 interactors have a role in transcription regulation, post-translational modification and DNA repair.

CHD4, HuwеI, LSD1, MTA1 and RBBP7 were found to interact with both BARD1 and BARD1ΔBRCT via Mass Spectrometry, however none of them could be confirmed.

UBC9 was found to interact only with BARD1, suggesting that it potentially requires the BARD1 BRCT domains for interaction, however this result was also not confirmed.

CHD4 localises to laser induced DNA damage stripes.

Chapter 6 Ubiquitin ligases and signalling at DNA DSBs.

The results in Chapter 6 are unrelated to the other results chapters and include the main findings of the original project of my PhD. Due to experimental difficulties in generating certain cell lines within this chapter and the publication of similar results by other groups on RNF8 and RNF168, a second project was initiated. This second project involved the investigation of the importance of the BARD1 BRCT domains in HR and the majority of the results in this thesis arise from this second project. Chapter 6 was included as a representation of a small piece of work carried out at the beginning of my PhD before the aims of the project changed.

6.1 Introduction

Signalling at DSBs is an early event in DSB repair that depends on protein ubiquitylation [136] along with various other posttranslational modifications. Signalling at DSBs ultimately leads to the recruitment of proteins involved in the repair of DSBs. Early on in the DSB response, phosphorylation-dependant protein-protein interactions are vital to coordinate both damage recognition and also signal amplification. The signalling cascade becomes highly dependent on the ubiquitin ligase activity of RNF8 and RNF168 which recruits other DDR proteins and also amplifies the damage signal.

Although there has been great advances in determining the mechanism and signalling involved at DSBs there are still many important questions that have yet to be answered. Some of the main questions that have yet to be addressed involve the interplay between different posttranslational modification within DNA damage signalling and their effects on chromatin structure. This chapter will address the function and biological relevance of RNF8 and RNF168 in the repair of DNA DSBs using biochemical and molecular biology techniques,

6.2 Results

6.2.1 Generation of ubiquitin ligase dead RNF8 and RNF168.

Signalling at DSB employs a variety of DDR proteins and various posttranslational modifications which form a subnuclear foci at the DSB site known as ionizing radiation induced foci (IRIF) [105]. The IRIF arise due to an accumulation of DDR proteins, which are paramount for mediating not only the signalling and repair of damaged DNA but also to activate cell cycle checkpoints or apoptosis.

Signalling at DNA DSBs ultimately serves to recruit repair proteins such as BRCA1 and 53BP1 to sites of damage. It has become evident that both RNF8 and RNF168 ubiquitin ligases are important mediators of DNA repair at DSBs, as shown in studies carried out with knock-out mice [178, 179, 392]. In order to investigate the effect that the ubiquitin ligase activity of RNF8 and RNF168 has on the repair of DNA damage, point mutations were generated in the RING domains of both proteins which rendered them ubiquitin ligase dead.

The RING finger motif is a cysteine rich sequence which adopts a 3D structure coordinating two zinc ions. Eight conserved amino acids, seven cysteines and one histidine, are responsible for binding the two zinc ions [393]. The RING domain E3 ubiquitin ligases function as a substrate adapter linking the ubiquitin charged E2 enzyme to the substrate.

The RING domains of RNF8 and RNF168 are very similar to those of BRCA1, another ubiquitin ligase important in DNA repair. Mutation of I26 in the BRCA1 RING domain has been shown to abrogate its ubiquitin ligase activity by preventing its binding to an E2 enzyme [170]. In order to generate point mutation in the RNF8 and RNF168 RING domains which would abrogate their ubiquitin ligase activity, they were compared to the BRCA1 RING domain (figure 6.1(a).

RNF8I405A and RNF168I18A plasmids were generated in order to assess the contribution of the RING domains and ubiquitin ligase activity of these proteins in DNA repair. By creating a point mutation in the RING domain of RNF8 and RNF168 which is predicted to render the proteins ubiquitin ligase dead, cells harbouring these mutated proteins could be analysed in relation to their sensitivity to DNA damaging agents. Both WT and mutant counterparts were tagged with His in order to facilitate purification of these proteins.

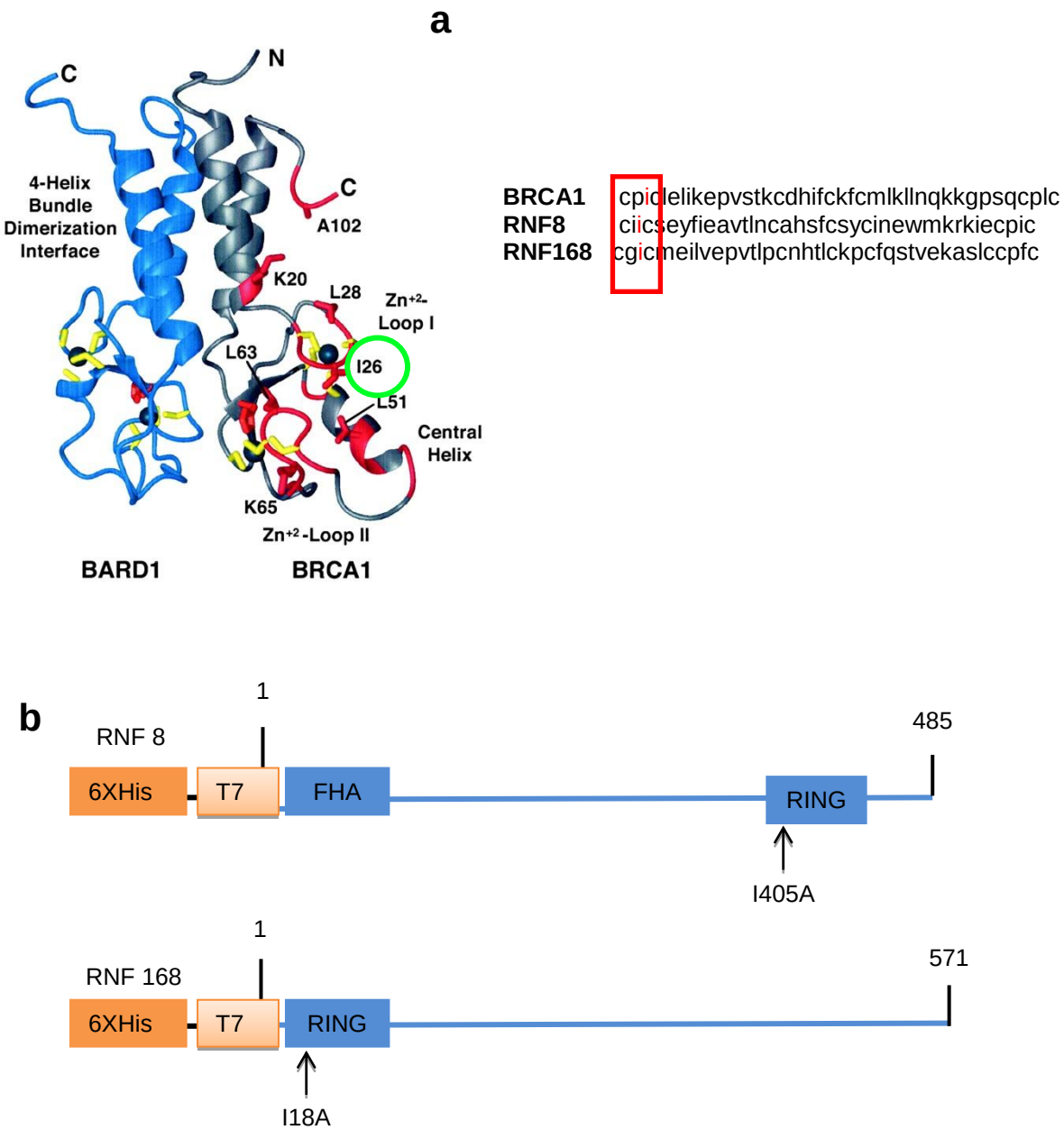

Figure 6.1 Generation of RNF8 and RNF168 ubiquitin ligase dead point mutant.
(a) Schematic representation of the BRCA1 BARD1 RING domains. The residue responsible for binding E2 enzymes in BRCA1 is circled in green. Mutation of i26 results in loss of ubiquitin ligase function. Sequence alignment of the BRCA1 RING domain with the RNF8 and RNF168 RING domain. BRCA1 i26 is circled in red and the corresponding lysine residues in the RNF proteins are also circled. Figure adapted from *Brzovic et al. (2003)*
(b) Illustration of RNF plasmids generated. Both WT and point mutant RNF proteins have been tagged with His to allow for His tag protein purification.

6.2.2 Optimising the expression and solubility of His tagged RNF8, RNF168 and mutant proteins.

RNF8I405A and RNF168I18A are predicted to lack their E3 ubiquitin ligase activity. In order to confirm that these point mutations do indeed disrupt the enzymatic ability of the RING domain, RNF8, RNF168 and their respective RING mutants were purified and biochemically analysed for ubiquitin ligase activity.

Before purification, the expression and solubility of the proteins were optimised. The mutant and WT RNF8 and RNF168 gene sequences were cloned into the pOPTH vector in order to tag them with 6xHis. His tags combine the advantages of small size and relatively high binding affinity. In addition, elution conditions for His-tagged proteins are mild allowing recovery of native proteins. However a His-tag does not enhance the solubility of the recombinant protein.

BL21(DE3) Lys competent *E-coli* cells were used as a host cells for the expression of the recombinant RNF8 and RNF168 proteins as they have two important attributes which makes them ideal for protein expression. BL21(DE3) Lys have key genetic markers which allows recombinant protein to be expressed with minimal basal expression and they are also inducible which can help minimise the toxic effect of certain proteins. The expression of the recombinant protein is induced by adding IPTG.

Initially His-RNF8, His-RNF8I405A, His-RNF168 and His-RNF168I18A BL21(DE3) Lys cells were induced with 1mM IPTG and the cells were harvested between 30mins and 3hrs after induction to identify the optimal time to induce

expression. His-RNF8 and His-RNF8I405A appeared to be maximally induced after 1hr whereas His-RNF168 and His-RNF168I18A required 2-3hrs (figure 6.2)

Although the expression of His-RNF8 and His-RNF8I405A is clearly visible via coomasie stained gels, His-RNF168 and His-RNF168I18A expression required a Western blot using an α-His antibody for detection. From this point on, optimisation of His-RNF168 and His-RNF168I18A will be analysed by Western blot as opposed to coomasie staining.

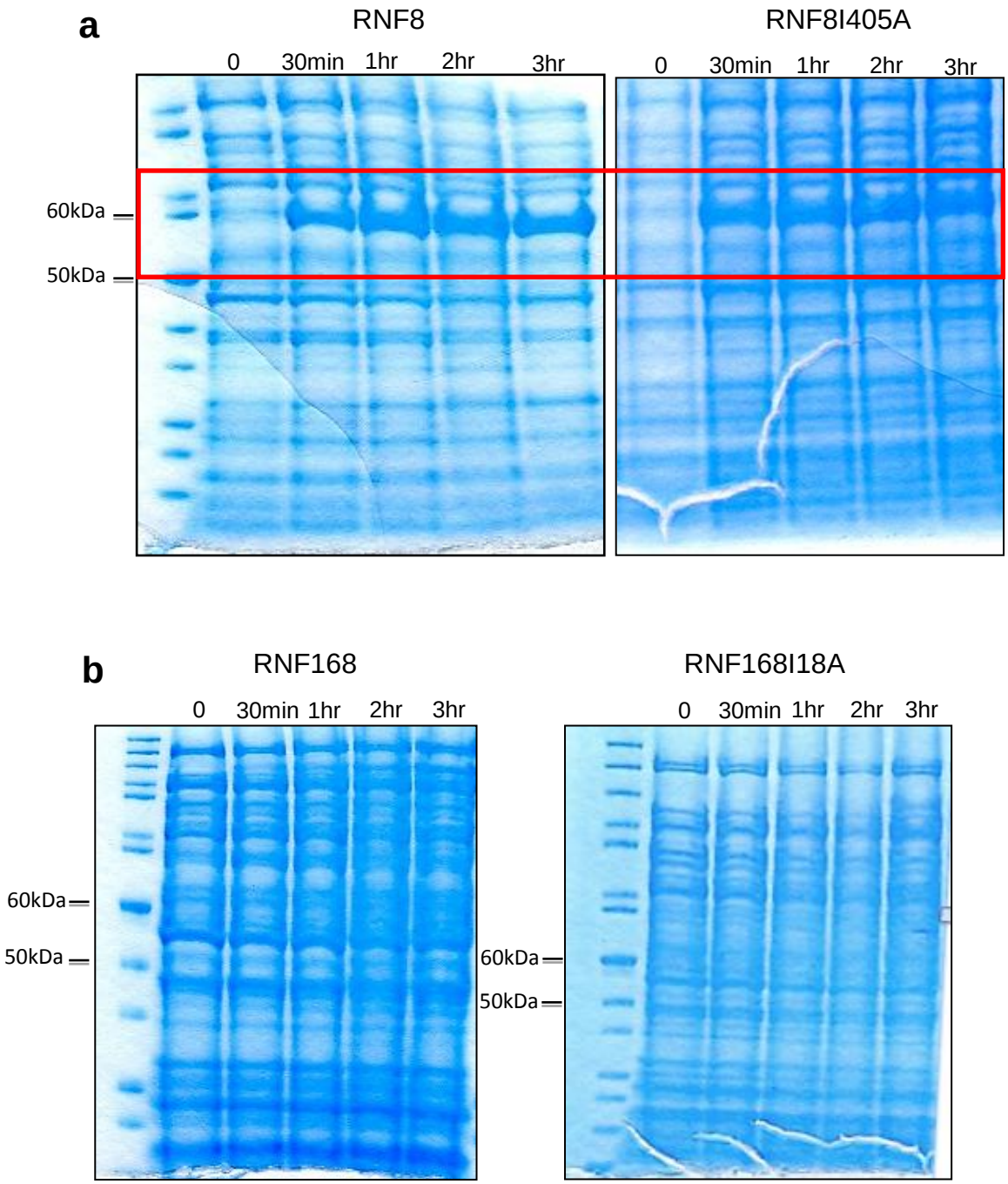

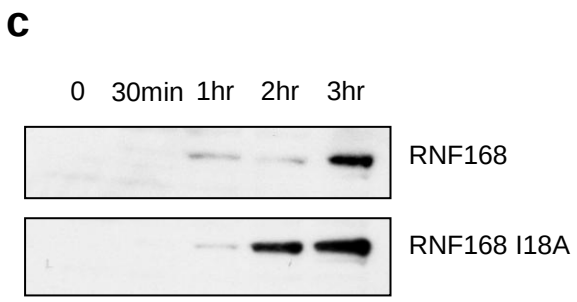

Figure 6.2 Timed induction of RNF proteins.
(a) Coomasie stained gel of BL21(DE3) Lys bacterial pellet after IPTG induction. Bacteria expressing either His-RNF8 or His-RNF8I405A were harvested before induction and up to 3hrs after 1mM induction with IPTG. Bacterial pellets were boiled in sample buffer and run on a 4-12% Bis-Tris gel before staining with simply Blue coomasie stain.
(b) Coomasie stained gel of BL21 bacterial pellet after IPTG induction of His-RNF168 and His-RNF168I18A. Experiment was carried out in the same way as in (a).
(c) Western blot of samples from figure (b). Bacterial pellets were boiled in sample buffer and run on a 4-12% Bis-Tris gel before Western blotting. α-His antibody was used to detect His-RNF168 and His-RNF168I18A.

Once the correct amount of time needed to induce the expression of the RNF proteins was defined (2hrs), the solubility of the protein was optimised. The solubility of His-RNF8, His-RNF8I405A, His-RNF168 and His-RNF168I18A was carefully evaluated by comparing the supernatant (soluble) and pellet (insoluble) fractions of IPTG induced BL21(DE3) Lys cells after lysis.

BL21(DE3) Lys cells were induced with 0.4mM or 1mM IPTG and harvested 2hrs after induction. The cells were then lysed, as described in the methods and materials section, and the soluble and insoluble fractions were separated by centrifugation before analysis by either coomasie stained gels or Western blot. Both His-RNF8 and His-RNF8I405A showed reasonable solubility after induction with both 0.4mM and 1mM IPTG (figure 6.3 (a,b), although the amount of insoluble His-RNF8 and His-RNF8I405A was greater when induced with 1mM IPTG, the overall soluble fraction remained the same with both concentrations of IPTG. This indicates that the use of 0.4mM IPTG is sufficient as higher concentrations do not increase the solubility.

The soluble fraction of both His-RNF168 and His-RNF168I18A was poor after induction with either 0.4mM and 1mM IPTG (figure 6.3 (c). The yield and solubility of

proteins can be greatly affected by the concentration and time of induction as well as the incubation temperature. In order to optimise the solubility of His-RNF168 and His-RNF168I18A, a longer induction time as well as a lower incubation temperature was used. Inducing His-RNF168 and His-RNF168I18A with 0.4mM IPTG overnight at 18°C appeared to increase the solubility of both proteins (figure 6.3 (d).

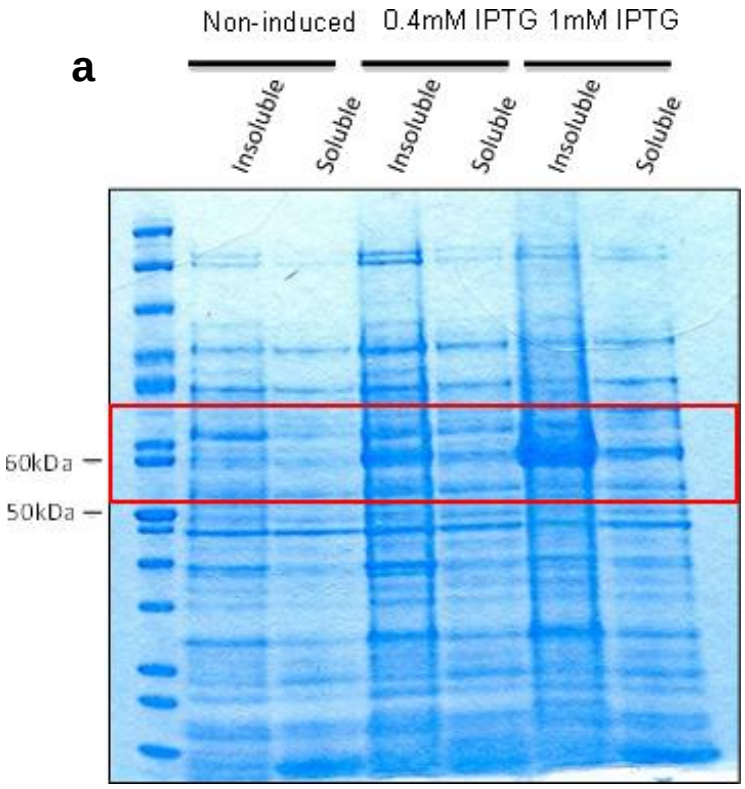

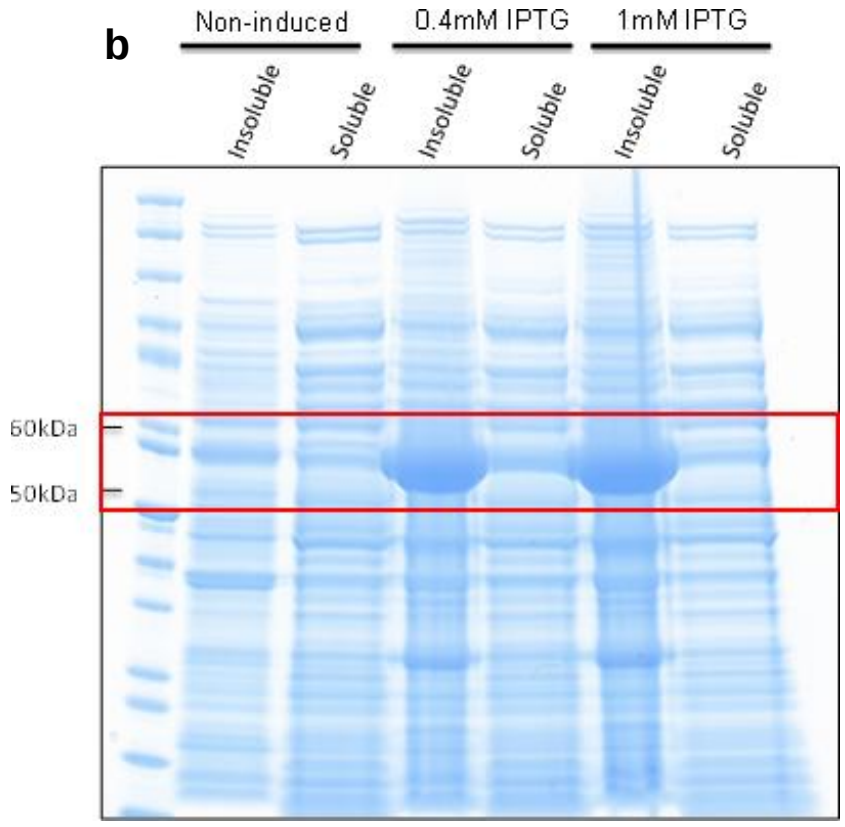
b
Non-induced
0.4mM IPTG
1mM IPTG
Insoluble
Soluble
Insoluble
Soluble
Insoluble
Soluble
60kDa
50kDa

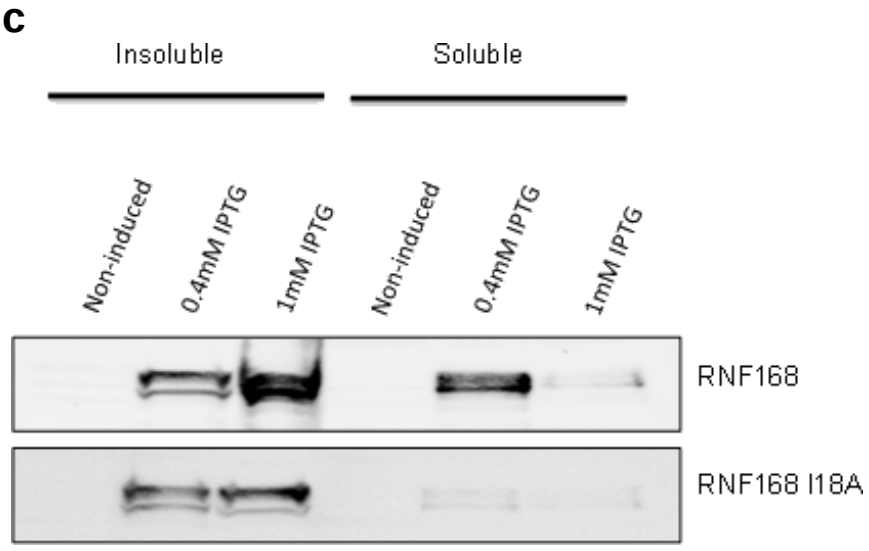
c
Insoluble
Soluble
Non-induced
0.4mM IPTG
1mM IPTG
Non-induced
0.4mM IPTG
1mM IPTG
RNF168
RNF168 I18A

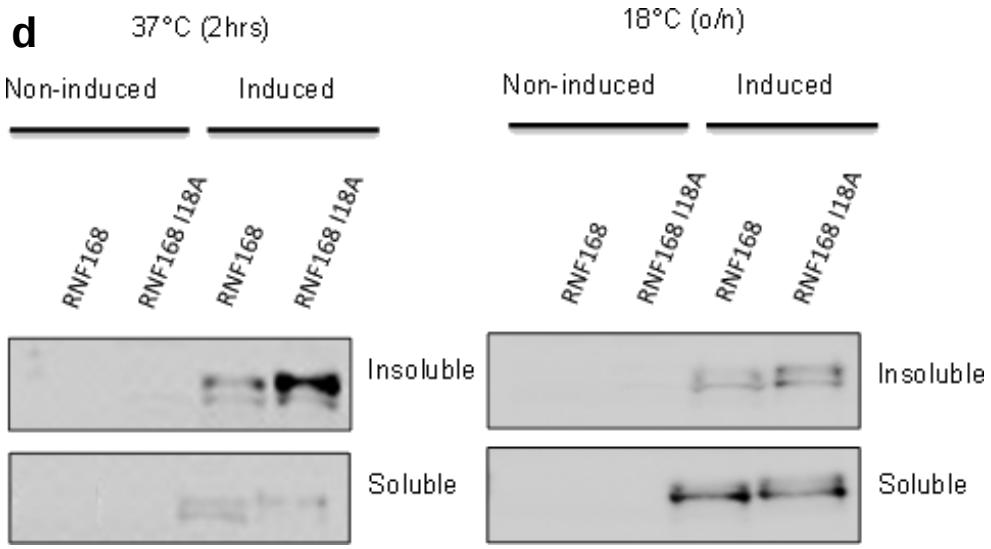

Figure 6.3 Solubility of RNF proteins
(a) Coomasie stained gel of BL21(DE3) Lys His-RNF8 bacterial pellet after IPTG induction. Bacteria were harvested before induction and 2hrs after 0.4mM/1mM induction with IPTG. Bacterial pellets were lysed and separated into soluable and insoluable fractions via centrifugation and run on a 4-12% Bis-Tris gel before staining with simply Blue coomasie stain.
(b) Coomasie stained gel of induced His-RNF8I405A. Sample prepared as in figure (a)
(c) Western blot of IPTG induced His-RNF168 and His-RNF168I18A. Samples were prepared as if figure (a) and blotted for using α-His antibody.
(d) Western blot of His-RNF168 and His-RNF168I18A induced with 0.4mM IPTG either for 2hrs at 37°C or o/n at 18°C. Bacterial pellets were lysed and separated into soluable and insoluable fractions via centrifugation and run on a 4-12% Bis-Tris gel before blotting with α-His antibody.

6.2.3 Purification of His-RNF8, His-RNF8I405A, His-RNF168 and His-RNF168I18A.

Once the expression and solubility of the His-tagged RNF proteins was optimised, the system was scaled up and the proteins were purified. The purification of the ubiquitin ligases involved in the DDR allowed the biochemical characterisation of RNF8 and RNF168.

The expression of His-RNF8 and His-RNF8I405A was induced with 0.4mM IPTG at 37°C for 2hrs before lysis and purification whereas His-RNF168 and His-RNF168I18A was induced with 0.4mM IPTG overnight at 18°C to increase the solubility of the protein. After lysis and sonication the soluble sample fractions were loaded onto the HisTrap FF column to allow the His-tagged proteins to bind to the Ni2+ charged sepharose. A low concentration of imidazole (40mM) was included in the binding/wash buffer to prevent unspecific His-cluster binding to the column. A higher concentration of imidazole (500mM) was used to elute the His-tagged RNF8 and RNF168 proteins. Imidazole is a competitive binder of Ni and displaces the His-tagged proteins from the column.

Eluted samples were collected and dialysed to reduce the concentration of imidazole and other potentially contaminating molecules. Using Dialysis, the concentration of NaCl was also lowered, as high salt may interfere with the biochemical assay in which the purified proteins will be used for. It is evident from figure 6.4, that the His-tagged proteins have been purified. Although there are some non-specific proteins contaminating the sample, this is unlikely to interfere with the biochemical assays as the *E-coli* bacterial host do not contain any ubiquitin ligases indicating that any ubiquitin ligase activity seen is completely due to the activity of RNF8 and RNF168.

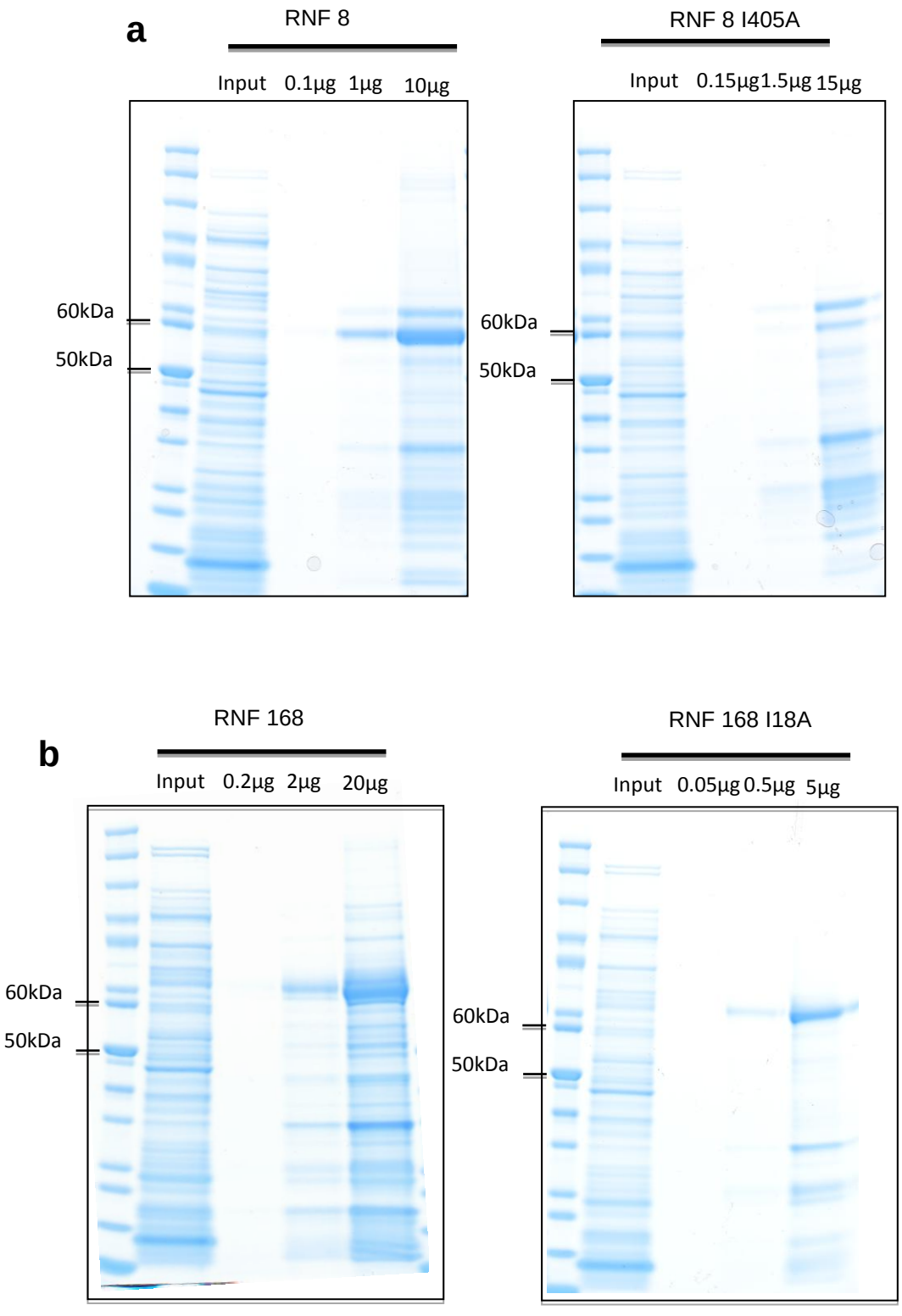

Figure 6.4 Purification of His-RNF8, His-RNF8I405A, His-RNF168 and His-RNF168I18A.
(a) Coomasie stained gel of purified His-RNF8 and His-RNF8I405A. Input represents sample prior to HisTrap FF column purification. Purified sample concentration was increased to highlight purity of sample.
(b) Coomasie stained gel of purified His-RNF168 and His-RNF168I18A. Input represents sample prior to HisTrap FF column purification. Purified sample concentration was increased to highlight purity of sample. Input and purified samples contain only soluable fraction.

6.2.4 Purified His-RNF8I405A and His-RNF168I18A are inactive ubiquitin ligases.

To assess the ubiquitin ligase activity of purified His-tagged RNF8 and RNF168 proteins an *in vitro* ubiquitin ligase activity assay was carried out. The ubiquitin ligase activity assay using BRCA1/BARD1 as the E3 ubiquitin ligase has been previously described by our laboratory [394]. Details of this assay can be found in the methods and materials chapter.

This assay relies on the principle that in the presence of ubiquitin, ATP, an E1 and E2 enzyme, an active E3 ubiquitin ligase enzyme monoubiquitylates free Histone H2A. Using both free ubiquitin and radioactive ^{125}I labelled ubiquitin, ubiquitylation of H2A can be clearly seen by PAGE analysis.

Mel18 is part of the PRC1-like polycomb repressor complexes and a heterodimer containing Mel18 and RING1B has been shown to be an efficient E3 ligase, ubiquitylating free histones *in vitro* and specifically H2A in a nucleosomal context [395]. Mel18/RING1B (b) was used as a positive control for the ubiquitin ligase activity assays as it appeared to be the most competent at ubiquitylating H2A *in vitro* (figure6.5 (a). Mel18/RING1B (b) seemed to have increased E3 activity in comparison to other batches (a,c) of the purified protein and also in comparison to different BRCA1/BARD1 RING domain purified proteins.

By optimizing the *in vitro* ubiquitin ligase activity assay the correct concentrations of all the components was elucidated (figure 6.5 (b). Maximal H2A ubiquitylation was observed in lane 4, containing 1µl of all the reagents used at the indicated concentration. The concentrations of the reagents highlighted in figure 6.5 (b) were then used in all subsequent assays. Reassuringly no ubiquitylation was seen in the absence of the E3 ligase (lane 9) and only autoubiquitylation of Mel18 can be seen in the absence of H2A (lane 8). The large lowest band seen in all the gels is

unconjugated ^{125}I labelled ubiquitin as, more often than not, the majority of ^{125}I labelled ubiquitin is not fully used up in the reaction.

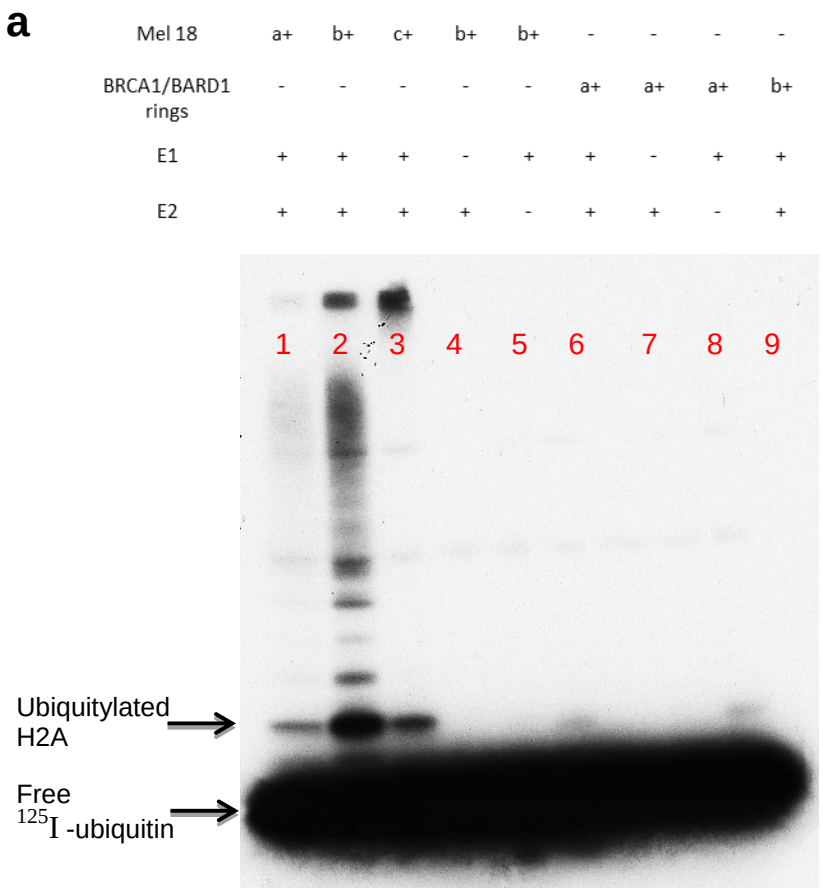

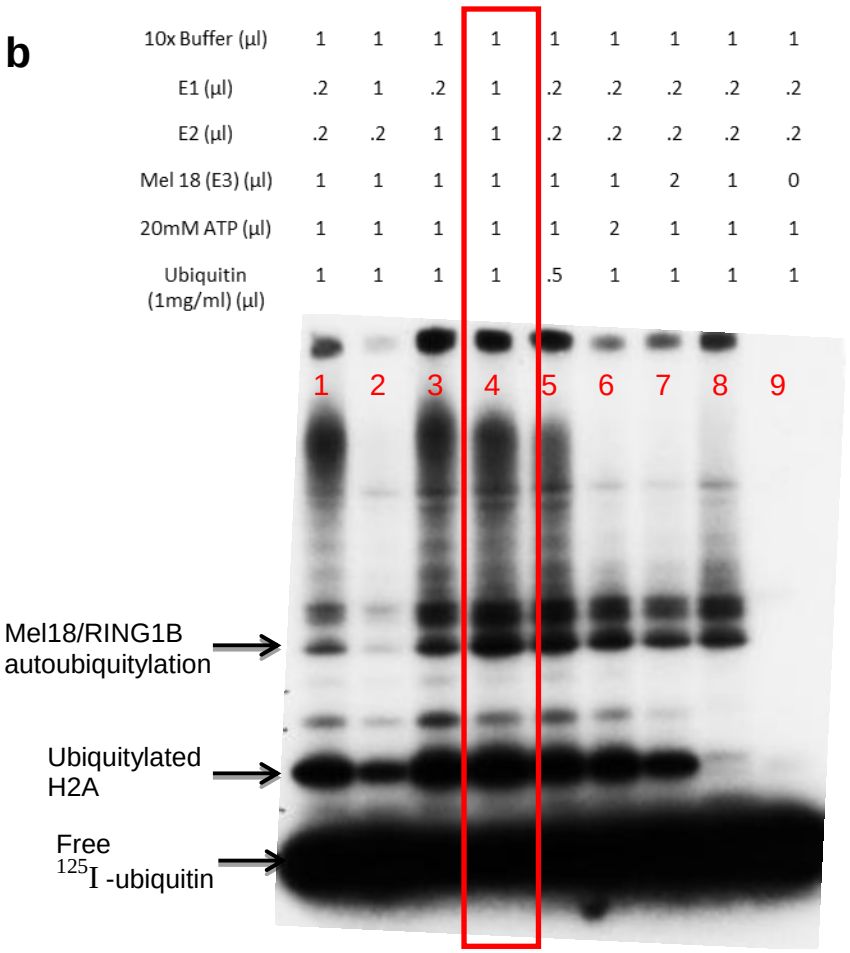

Figure 6.5 Optimisation of the *in vitro* ubiquitin ligase activity assay
(a) Ubiquitin ligase activity assay showing Mel18/RING1B and BRCA1/BARD1 ring domains display E3 ligase activity in the presence of H2A and UBCH5a E2 enzyme. Reagent were pre-incubated for 1hr with ubiquitin before incubation for a further hour with I_{125} labelled ubiquitin and H2A at 37°C. ^{125}I labelled products were analysed by PAGE and visualised using X-ray film or a phosphoimager. Ubiquitylated H2A and free ^{125}I labelled ubiquitin are labelled.
(b) Ubiquitin ligase activity assay illustrating the optimal conditions for the activity of Mel18/RING1B seen in the highlighted lane 4. Lane 8 contains no H2A substrate. Reagent were pre-incubated for 1hr with ubiquitin before incubation for a further hour with I_{125} labelled ubiquitin and H2A at 37°C. ^{125}I labelled products were analysed by PAGE and visualised using X-ray film or a phosphoimager. Ubiquitylated substrates and free ^{125}I labelled ubiquitin are labelled.

Both purified His-RNF8 and His-RNF168 show E3 ligase activity *in vitro* by ubiquitylating free histone H2A whereas the RING mutants do not appear to have any E3 activity (figure 6.6). The lack of ubiquitylated products formed by either His-RNF8I405A or His-RNF168I18A suggests that the point mutations generated in the RING domains does prevent the E3 ligase activity of the proteins. Both His-RNF8 and His-RNF168 appear to be autoubiquitylated and seem to be involved in the formation of polyubiquitylated products.

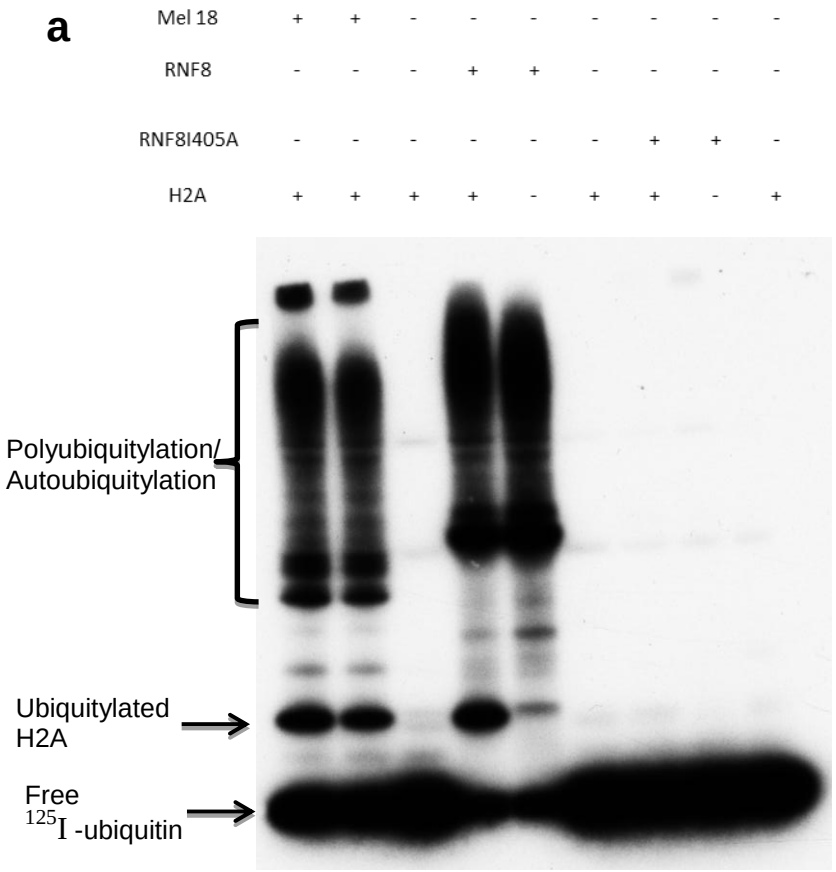

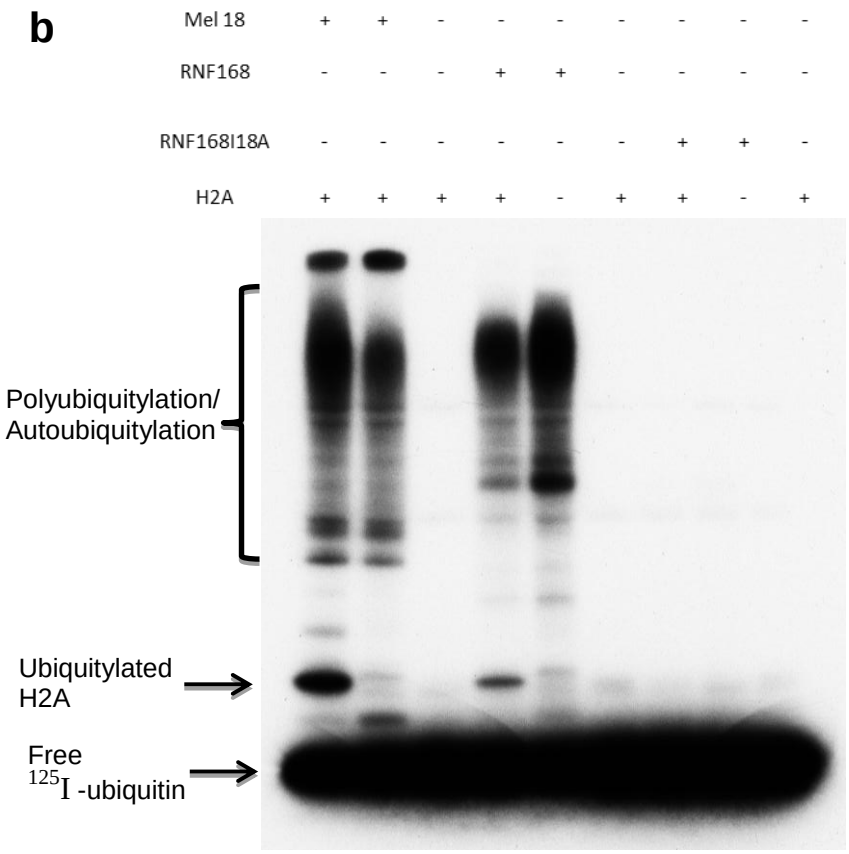

Figure 6.6 His-RNF8 and His-RNF168 are active E3 ligases, His-RNF8i405a or His-RNF168i18a show no E3 ligase activity.
(a) Ubiquitin ligase activity assay showing His-RNF8 displays E3 ligase activity in the presence of H2A and UBCH5a E2 enzyme. His-RNF8i405a shows no E3 ligase activity. Reagent were pre-incubated for 1hr with ubiquitin before incubation for a further hour with ^{125}I labelled ubiquitin and H2A at 37°C. ^{125}I labelled products were analysed by PAGE and visualised using X-ray film or a phosphoimager. Ubiquitylated products and free ^{125}I labelled ubiquitin are labelled.
(b) Ubiquitin ligase activity assay showing His-RNF168 displays E3 ligase activity in the presence of H2A and UBCH5a E2 enzyme. His-RNF168i18a shows no E3 ligase activity. Experimental procedure carried out as in (a).

6.2.5 His-RNF8 and His-RNF168 ubiquitylate all free histones *in vitro*.

Very little is known about the ubiquitylation substrates of both RNF8 and RNF168, so far the main targets are H2A and H2AX where the ubiquitin ligases are proposed to form K63 linked-ubiquitin chains [119-122, 125, 126]. In order to assess the ubiquitin ligase capabilities of RNF8 and RNF168 on a variety of free histone substrates, a ubiquitin ligase activity assay was carried out. Both RNF8 and RNF168 appear to be able to ubiquitylate all free tested histones *in vitro* whereas their mutant counterparts are not (figure 6.7).

The ability of RNF168 to ubiquitylate H2AX in comparison to RNF8 appears to be weaker in figure 6.7 (b). This is believed to be due to an overall weaker signal obtained with purified RNF168 in comparison to the activity of RNF8, overexposure of the same PAGE gel indicate that RNF168 can also ubiquitylate H2AX. It is important to note that although RNF8 and RNF168 were able to ubiquitylate all free histones tested, this does not directly implicate that RNF8 and RNF168 can ubiquitylate all histones in a nucleosomal context.

a

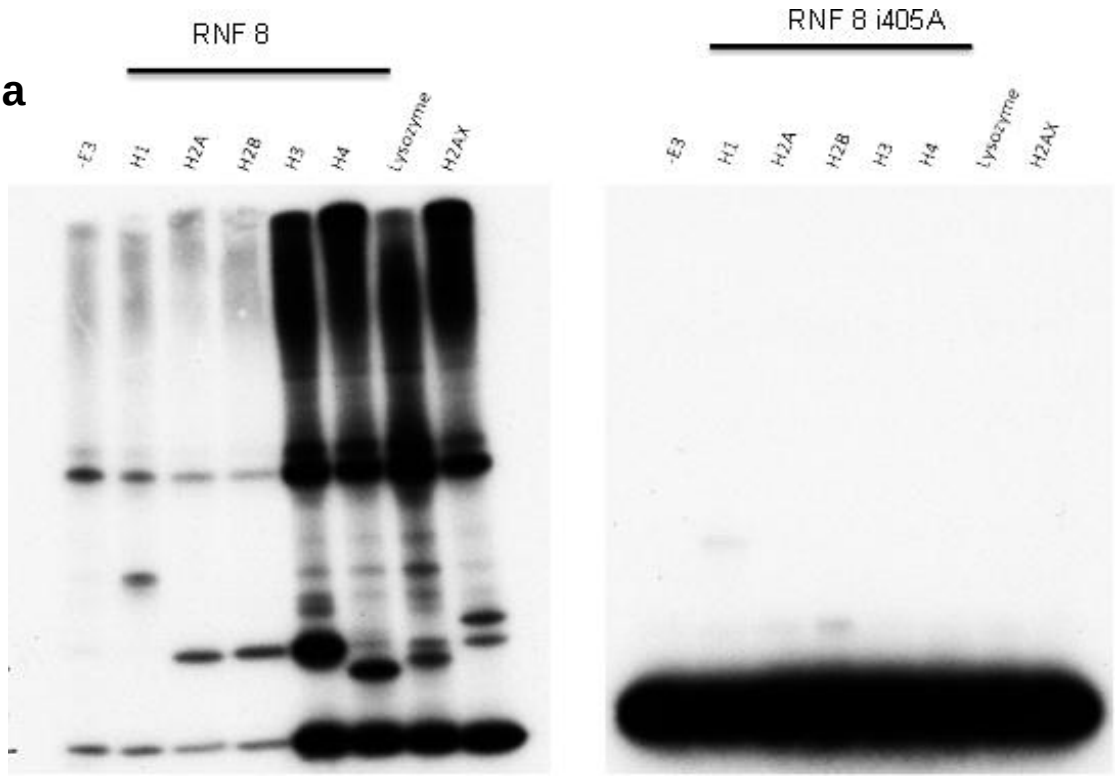

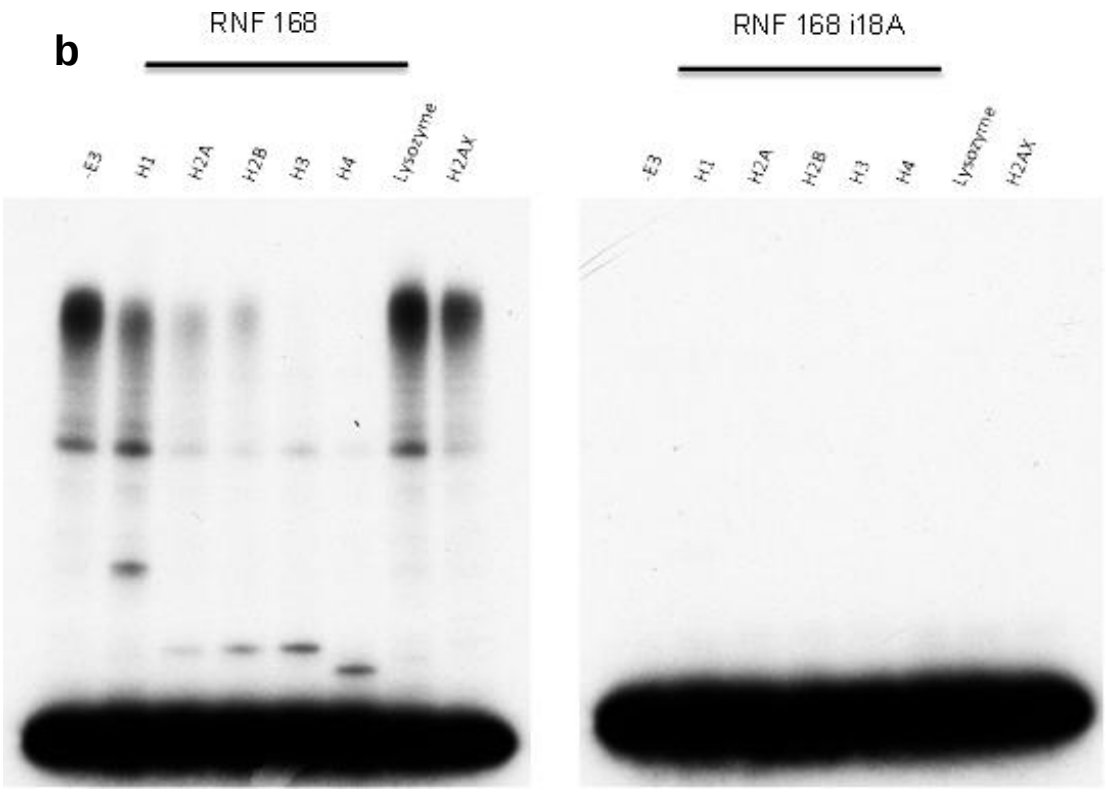

Figure 6.7 RNF8 and RNF168 ubiquitylate free histones *in vitro*
(a) His-RNF8 but not His-RNF8i405a can ubiquitylate all tested free histones *in vitro.* Reagents were pre-incubated for 1hr with ubiquitin before incubation for a further hour with ^{125}I labelled ubiquitin and indicated histones at 37°C. ^{125}I labelled products were analysed by PAGE and visualised using X-ray film or a phosphoimager.Lysozyme was used as a positive control.
(b) Ubiquitin ligase activity assay illustrating that His-RNF168 but not His-RNFi18a can ubiquitylate the majority of free histones. Experimental procedure carried out as in (a).

The higher intensity of the signal on the right hand side in the RNF8 figure 6.7(a) is due to the use of an older batch of ^{125}I labelled ubiquitin in the first four samples in the figure whereas a newer batch was used in the second half of the gel.

6.2.6 *Rnf8* DT40 cells are sensitive to Parp inhibitors while *Rnf168* DT40 cells show sensitivity to HU.

Both RNF8 and RNF168 localise to DNA damage foci after IR treatment [119]. A reduction in the level of RNF8 protein has been shown to decrease cell survival after IR and sensitise cells to UV and CPT [121, 177, 396]. *Rnf168* cells are also sensitive to CTP and mutations in RNF168 are associated with the RIDDLE syndrome disease which is characterised by defects in DSB repair [126, 177]. Collectively this evidence suggests that both RNF 8 and RNF168 play an important role in the repair of DNA damage.

To understand the contribution of RNF8 and RNF168 in repairing DNA damage in our systems, colony survival assays were carried out to assess the sensitivity of DT40 *Rnf8* and *Rnf168* knockout cells lines to DNA damaging agents (HU and Parp inhibitors). *Rnf8* and *Rnf168* knockout cells lines were treated with HU and PARP inhibitors and the percentage of surviving colonies were counted 10 days after treatment. Cells sensitive to either HU or PARP Inhibitors indicate defects in their ability to repair DNA damage (replication errors and DNA DSBs). *Rnf8* cells showed a slight sensitivity to PARP inhibitors while *Rnf168* cells showed a decrease in survival when treated with HU (Figure 6.9).

The DT40 *Rnf8* and *Rnf168* cell lines were a kind gift from Vibe H. Oestergaard and details regarding the generation of the cell lines can be found in *Oestergaard et al. 2012* [177]. Before assessing the biological relevance of RNF8 and RNF168 in the repair of DNA damage, the knockout cell lines were first confirmed as true knockouts. Using primers, designed by *Oestergaard et al,* specific to the genomic region knocked out in either the RNF8 or RNF168 cell lines, a PCR was carried out confirming the knock out status of the RNF8 and RNF168 cell lines (figure 6.8). Knock out had to be confirmed by genomic PCR as there are no commercial antibodies available which recognise chicken RNF8 or RNF168.

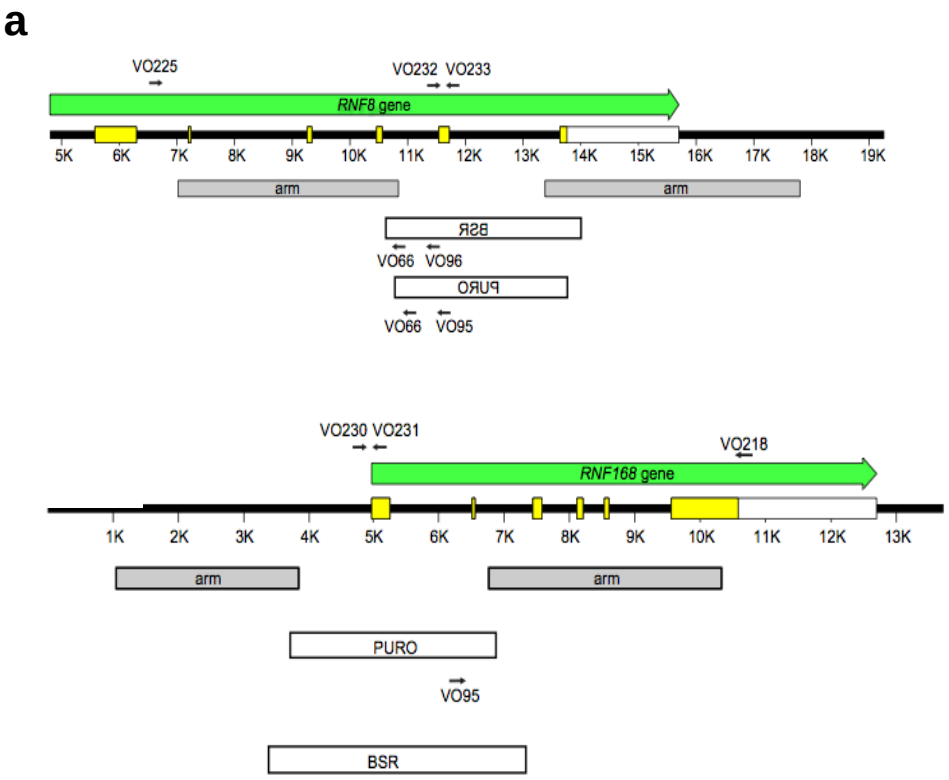

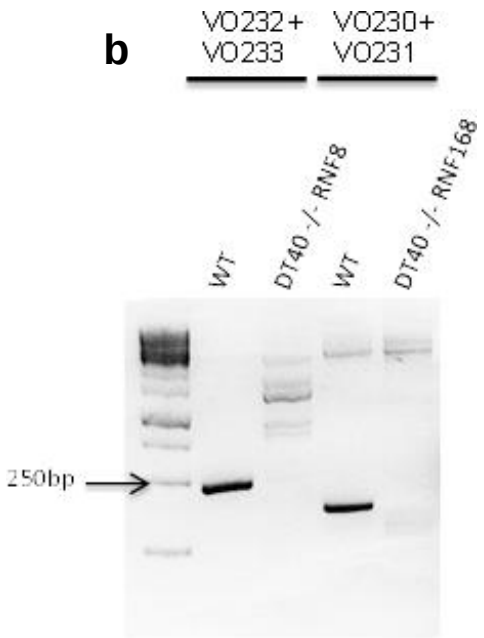

Figure 6.8 Confirmation of the RNF8 and RNF168 knockout status of DT40 cell lines.
(a) Confirmation of the knockout status of RNF8 and RNF168 cell lines. A PCR using the indicated primers shows a positive product band for RNF8 and RNF168 only in the WT genomic DNA and not in the Knock out cell lines. The RNF8 PCR product is expected to be around 250bp and >250bp for RNF168.
(b) Illustration of the design of the PCR primers used to amplify a region of the RNF8 and RNF168 gene, subsequently knocked out. The PURO gene replaced the area of the RNF genes above it. VO232 and VO233 primers were designed to amplify the region of the RNF8 gene replaced by PURO whereas VO230 and VO231 was designed similarly for the RNF168 gene. Figures adapted from *Oestergaard et al. 2012.*

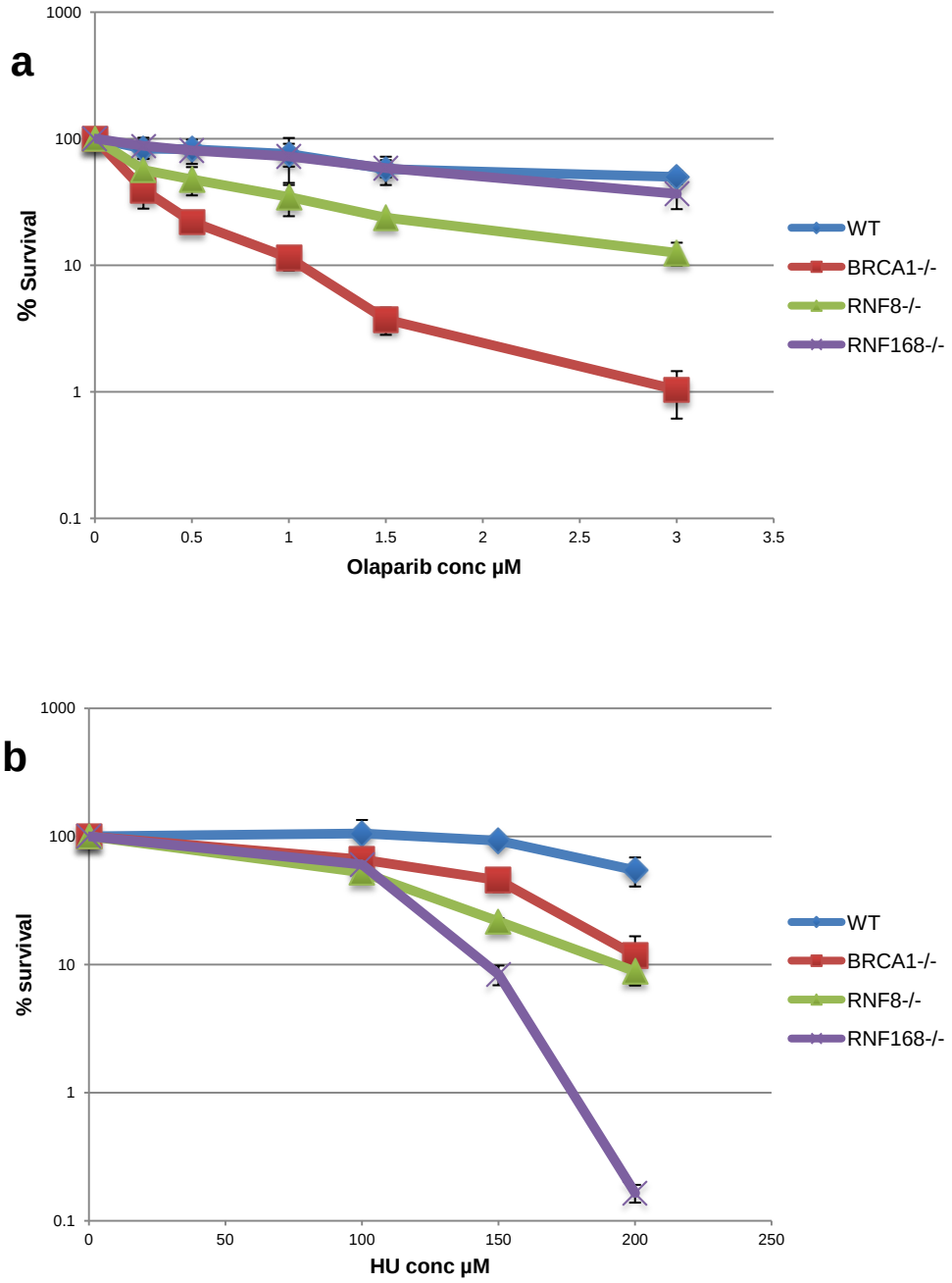

Figure 6.9 Sensitivity of *Rnf8* and *Rnf168* cells to DNA damaging agent.
(a) Colony survival assay illustrating the sensitivity of *Rnf8* cells to PARP inhibitor, Olaparib. Cells were treated for 24hrs with 0-3µM Olaparib before being plated on methylcellulose cellulose media, as described in the Methods and materials section. Surviving colonies were counted 9-12 days after plating and plotted relative to untreated cells. Data shown are the mean of at least 3 independent experiments. Error bars, s.d.
(b) Colony survival assay illustrating the sensitivity of *Rnf168* cells to HU. Cells chronically treated with 0-200µM HU as described in the Methods and materials section. Surviving colonies were counted 9-12 days after plating and plotted relative to untreated cells. Data shown are the mean of at least 3 independent experiments. Error bars, s.d.

Brca1 DT40 cells were used a positive control in figure 6.9 (a). Although *Rnf8* cells showed an 8 fold lower survival percentage in comparison to WT cells when treated with a PARP inhibitor, *Rnf168* cells showed negligible sensitivity. On the other hand, the survival of *Rnf168* cells was greatly impaired after treatment with HU whereas *Rnf8* cells similar sensitivity to HU as *Brca1* cells. Collectively these results indicate a potential function of the RNF8 and RNF168 proteins in the repair of damaged DNA.

6.2.7 RNF8I405A cells are not sensitive to PARP inhibitors. The survival of RNF168I18A cells are compromised in the presence of HU.

Results shown in figure 6.9 indicate a functional role for RNF8 and RNF168 in the repair of DNA damage. In order to elucidate whether the ubiquitin ligase activity of the RNF8 and RNF168 proteins are responsible for their functional role in DNA repair, *Rnf8* and *Rnf168* DT40 cells were reconstituted with ubiquitin ligase dead RNF8 and RNF168 and analysed for their sensitivity to DNA damaging agents. According to data previously shown in this chapter, the point mutations generated in the RING domains of RNF8 and RNF168 prevents their ubiquitin ligase activity *in vitro*. *Rnf8* DT40 cells were reconstituted with either HsGFP-RNF8 or HsGFP-RNF8I405A. *Rnf168* cells were reconstituted with either GgYFP-RNF168 or GgYFP-RNF168I18A.

Rnf8 cells reconstituted with HsGFP-RNF8I405A were not sensitive to PARP inhibitors whereas complete knockout of RNF8 was sensitive. The expression of full length GFP-HsRNF8 in *Rnf8* cells fully restored their resistance to PARP inhibitors. This may suggest that the function of RNF8 in DNA repair is not dependent on it E3 ligase activity, at least not the type of damage created by PARP inhibitors.

Rnf168 cells reconstituted with YFP-GgRNF168I18A appeared to be more sensitive than complete *Rnf168* knockout cells. Reconstitution of *Rnf168* cells with full

length YFP-GgRNF168 only partially rescued the cell line from HU sensitivity. As the endogenous expression of the RNF8 and RNF168 proteins could not be analysed due to a lack of chicken antibodies against these proteins, it is difficult to conclude if the expression of the reconstituted proteins may interfere with the outcome of these results. However it seems that the ubiquitin ligase activity of RNF168 is indeed required for its function in DNA repair when treated with HU.

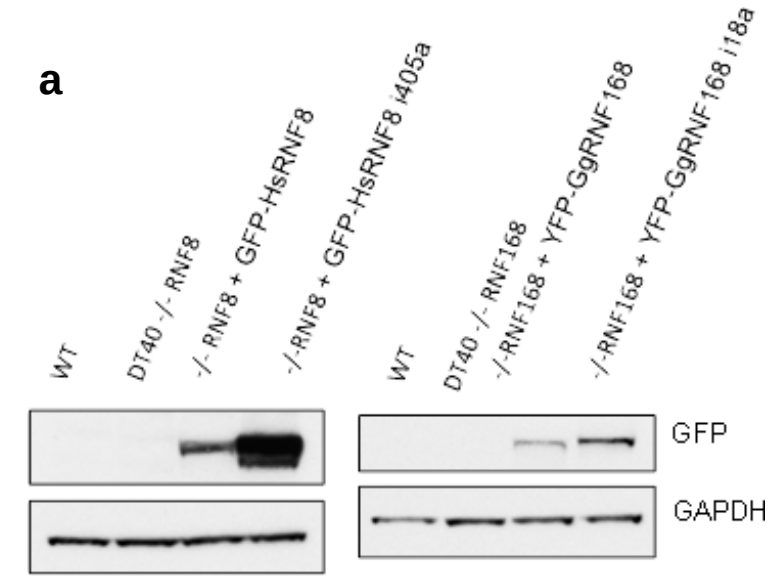

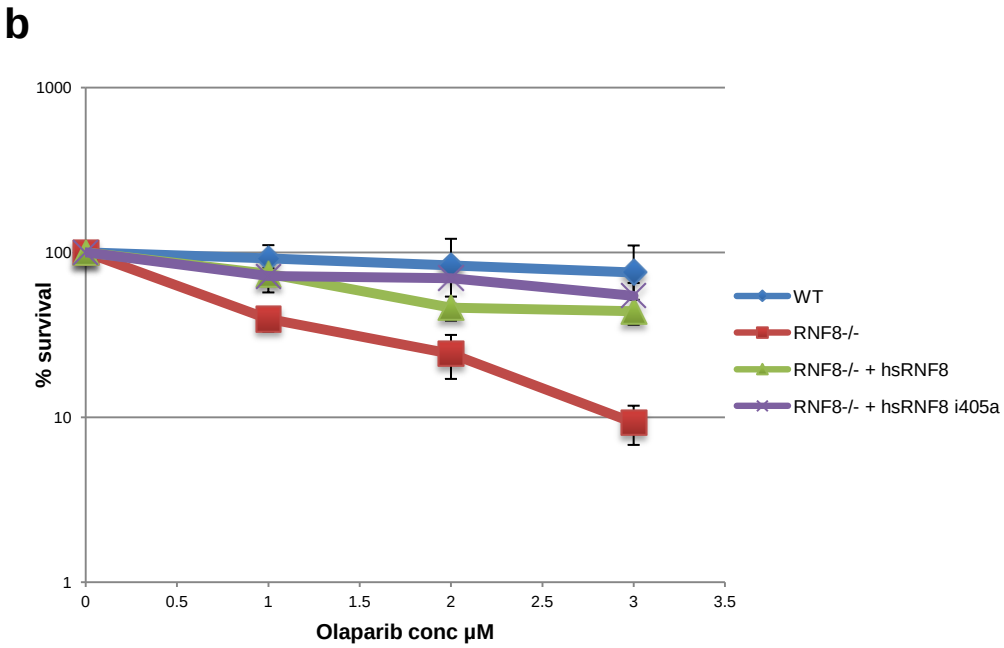

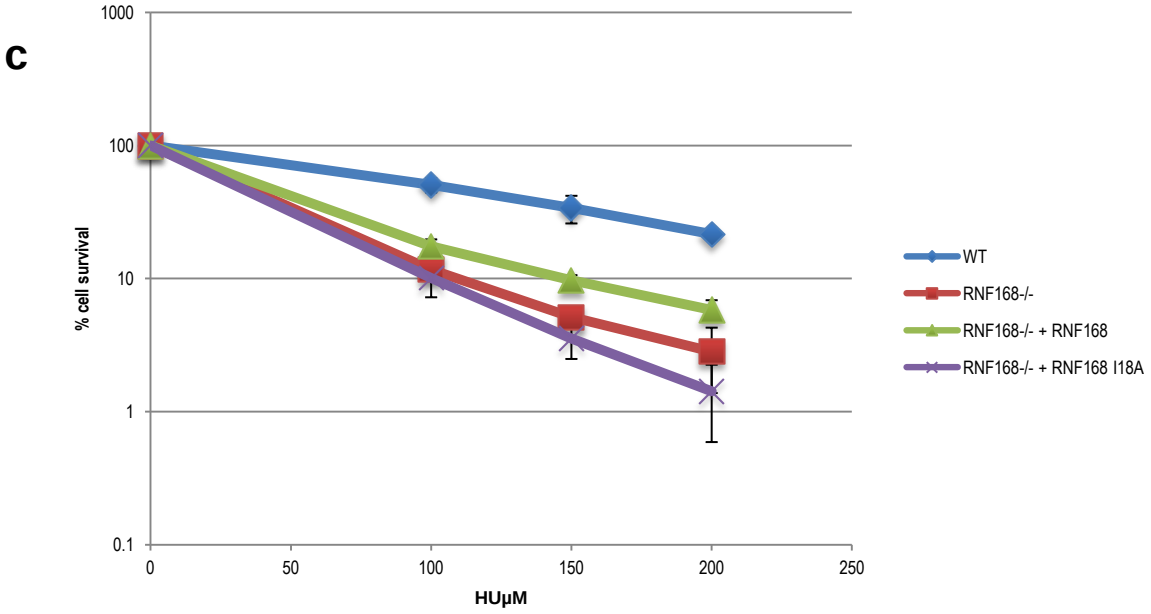

Figure 6.10 Sensitivity of RNF8i405A and RNF168i18A cells to DNA damaging agent.
(a) Western blot of the expression of reconstituted RNF8 and RNF168 cell line. A-GFP antibody was used to detect the expression of all reconstituted RNF proteins and α-GAPDH was used a loading control.
(b) Colony survival assay illustrating that *Rnf8* cells reconstituted with GFP_hsRNF8i405A does not appear to be sensitive to PARP inhibitor, Olaparib. Cells were treated for 24hrs with 0-3μM Olaparib before being plated on methylcellulose cellulose media, as described in the Methods and materials section. Surviving colonies were counted 9-12 days after plating and plotted relative to untreated cells. Data shown are the mean of at least 3 independent experiments. Error bars, s.d.
(c) Colony survival assay illustrating the sensitivity of *Rnf168* cells reconstituted with YFP-GgRNF168i18A to HU. Cells chronically treated with 0-200μM HU as described in the Methods and materials section. Surviving colonies were counted 9-12 days after plating and plotted relative to untreated cells. Data shown are the mean of at least 3 independent experiments. Error bars, s.d.

Any sensitivity seen to either PARP inhibitors or HU seems to be independent of localisation of the reconstituted RNF proteins as they all localise to the nucleus as seen in figure 6.11.

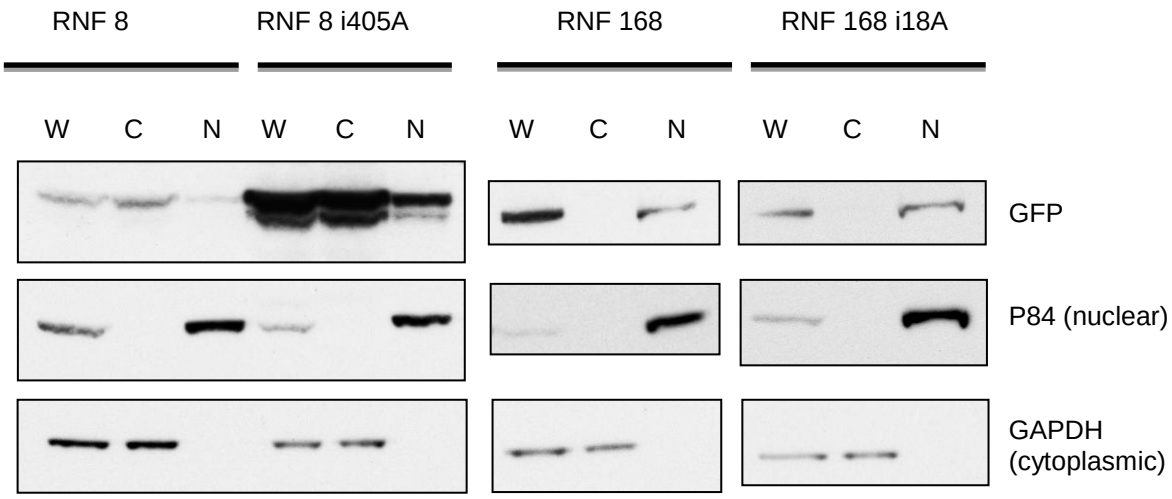

Figure 6.11 Nuclear localisation of reconstituted RNF proteins
Cell lysates were fractioned into their cytoplasmic and nuclear fractions as described in the Methods and Materials chapter. W(whole), C(cytoplasmic) and N(nuclear) Fractions were analysed by Western blotting. The majority of all the RNF proteins, full length and mutant, are located in the nuclear fractions.

Both RNF8 and RNF168 are believed to contribute to the ubiquitylation of histone H2A and H2AX in response to DNA damage, H2A and ubH2A was blotted for by Western blot using lysates from reconstituted *Rnf8* and *Rnf168* cells. Intriguingly an increase in ubH2A was seen in the *Rnf8* cell line reconstituted with full length GFP-HsRNF8 and not with YFP-GgRNF168. Neither of the ubiquitin ligase dead reconstituted cells showed an increase in ubH2A levels by Western blot. This result suggests that RNF8 is necessary for mono-ubiquitylation of H2A which is in agreement with the literature. Interestingly RNF168 cells reconstituted with YFP-GgRNF168 and also WT cells did not show an increase in mono-ubiquitylated H2A. As RNF168 is proposed to be responsible for mono-ubiquitylation of H2A [123] you would expect to see an increase of mono-ubiquitylated H2A in the presence of RNF168 in comparison to its ubiquitin ligase dead counterpart. It is possible that RNF8 is the limiting factor involved in this

process and only with the overexpression of RNF8 is an increase of ubiquitylated H2A observed.

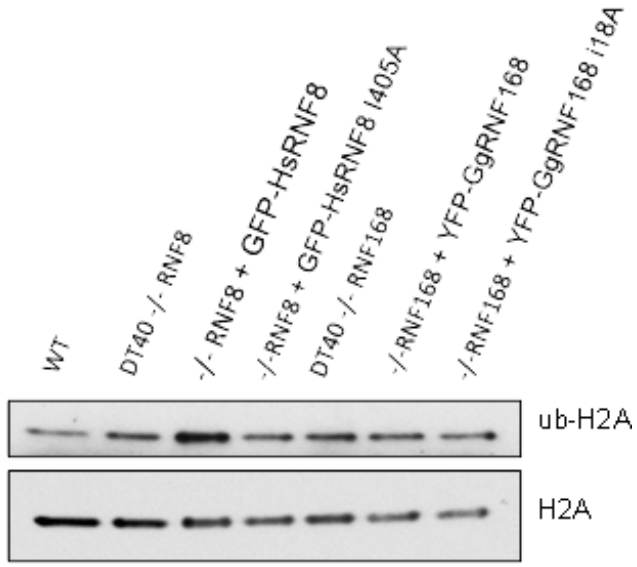

Figure 6.12 ub-H2A levels in the RNF reconstituted cell lines.
Western blot of the H2A and ub-H2A levels from the indicated cell lines. Cells were harvested and a histone extraction was carried out as described in the methods and materials. Samples were analysed by PAGE and Western blotting. A H2A antibody was used to detect both H2A and ub-H2A.

6.3 Summary

RNF8 and RNF168 are active ubiquitin ligases and ubiquitylate free histone substrates *in vitro*.

RNF8I405A and RNF168I18A are ubiquitin ligase dead mutants unable to ubiquitylate free histone substrates *in vitro*.

Rnf8 DT40 cells are sensitive to PARP inhibitors suggesting that RNF8 is important in repairing DSB. This function of RNF8 is not dependent on its ubiquitin ligase activity.

Rnf168 DT40 cells are not sensitive to PARP inhibitors but show sensitivity to DNA damaging agent HU. The ubiquitin ligase function of RNF168 is required to overcome HU sensitivity.

Overexpression of RNF8 increases the amount of mono-ubiquitylated H2A *in vivo* whereas its ubiquitin ligase dead mutant does not. Whereas no increase of mono-ubiquitylated H2A was observed with the re-expression of RNF168 or RNF168I18A.

Chapter 7 Discussion

The work carried out in this dissertation highlights the contribution of the BARD1 BRCT domains to the repair of DNA DSBs by HR. My results suggest that the BARD1 BRCT domains promote the stability of the BRCA1-C complex and that this is not dependent on the potential phospho-peptide binding ability of the BARD1 BRCT domains. My results indicate that the BRCT domains of BARD1 are important in the localisation of BARD1 to sites of damage and also to S-phase "BRCA1 nuclear dots". These findings together with the identification of potential interactions of BARD1 with proteins identified with Mass Spectrometry, lead to a model whereby the BARD1 BRCT domains contribute to the DDR by stabilising CtIP to the BRCA1-C complex and potentially ensure correct localisation of BARD1 at sites of damage. These roles of the BARD1 BRCT domains may function independently of other proteins or more likely, involve the interaction with another protein important for repair.

BARD1 is known to play an important role in DNA repair as a regulator of BRCA1 function and tumour suppressor activity. BARD1 and BRCA1 form a heterodimer through α-helices adjacent to their RING domains. BARD1 masks a nuclear export signal in BRCA1, promoting retention of BRCA1 in the nucleus where it carries out its functions in the DDR [397]. The binding of BARD1 to BRCA1 also greatly enhances the ubiquitin ligase activity of BRCA1 [169, 233]. Initial clues that BARD1 is important in genome stability came from the study of *Bard1* null mice which are embryonic lethal and cells from these mice exhibited genetic instability [194, 207]. More recently, there has been evidence that the BRCT domains of BARD1 are important in DSB repair. Loss of the BRCT domains severely impaired the ability of the cells to carry out HR repair of DSBs according to *Westermark et al*. and *Baer et al.*[266, 269]. Interestingly a frame shift mutation in the BARD1 gene has also recently been identified in hereditary breast cancer patients. The frame shift mutation in BARD1 results in the loss of the second BRCT domain of BARD1 [213]. These patients do not carry either *Brca1* or

Brca2 mutations which are more frequently associated with inherited breast and ovarian cancers. A similar study carried out by *Ratajska et al.* identified a novel truncation mutation in non-BRCA1/BRCA2 breast cancer patients resulting in the loss of both BRCT domains of BARD1 [214]. The work described in this thesis confirms the importance of the BARD1 BRCT domains in DNA DSB repair by HR. Spectrometry ifically, DT40 *Bard1* cells expressing human BARD1ΔBRCT showed a marked decrease in their ability to carry out homology directed repair of DSB and were also sensitive to PARP inhibitors in comparison to WT cells.

The domain structure of BARD1 and BRCA1 are very similar. Both proteins contain RING finger domains in their N-terminus and tandem BRCT domain repeats in their C-terminus. The BRCA1 BRCT domains serve as phospho-protein interaction domains and interact with Abraxas, FANCJ and CtIP. The interaction of BRCA1 with these proteins is important for the maintenance of genome stability. The mechanism and function of the BARD1 BRCT domains in the DDR is still unclear, however as the BRCA1 BRCT domains mediate important interactions required for DNA damage repair it is possible that the BARD1 BRCT domains also carry out similar functions in the DDR. The three main questions which will be addressed in this thesis, regarding how the BRCT domains of BARD1 may contribute to the DDR, are as follows; Do the BRCT domains of BARD1 contribute to the stabilisation of the BRCA1 complexes? Do the BRCT domains affect the localisation of BARD1? And do the BRCT domains potentially interact with any proteins that may be important for DNA repair? These questions will be addressed in relation to how they might explain the importance of the BARD1 BRCT in genome stability and prevention of cancer.

7.1 The importance of BRCT domains in the DDR.

BRCT domains are versatile protein interacting domains first discovered in the C-terminus of the tumour suppressor gene, BRCA1 [193]. BRCT domains are found in over 20 proteins in the human genome and can be found as a single unit or in multiple copies [193, 289, 290, 304]. The majority of BRCT domain containing proteins are

involved in the DNA damage response and DNA repair [289, 290, 300, 301, 346]. The importance of BRCT domains in DNA repair and maintenance of genome integrity is demonstrated by the fact that mutations in the BRCT domains of proteins such as BRCA1, NBN and MCPH1 lead to an increase susceptibility to cancer [183, 184, 398]. In agreement with this, *Shakya et al.* has shown that mutations in the BRCT domains of BRCA1 results in a decrease in efficient HR [298]. I have also shown that point mutations in the BRCA1 BRCT domains, responsible for binding phosphorylated peptides, results in decreased efficiency in HR. In contrast to these studies, *Dever et al* proposed that mutations in the BRCT binding site of BRCA1 results in hyper-recombination [321], however analysis of breast cancers which often contain mutation in the BRCA1 BRCT domains suggest that the BRCT domains are indeed important in the DDR. Interestingly, as previously mentioned, mutations in the BARD1 BRCT domains have been associated with a small number of breast cancers further strengthening the hypothesis that the BRCT domains play a vital role in the repair of damaged DNA.

The DDR involves the recognition of damaged DNA which initiates a complex signalling pathway that has several functional consequences. Signalling at DNA damage sites marks the damage site for repair, recruits proteins involved in the repair and also creates a chromatin environment whereby repair can take place before the cell progresses through the cell cycle [399]. Phosphorylation plays a major role in the signalling at sites of DNA damage [400-402] and BRCT domains have been shown to bind phospho-proteins important for DNA repair [291, 300, 301, 314, 315, 346, 354]. The general fold of a BRCT domain involves a central 4-stranded β-sheet with a single α-helix on one side and a pair of α-helices on the other [299]. Phospho-peptides have been shown to bind tandem BRCT domains via conserved bipartite recognition of two distinct binding pockets. The first binding pocket recognises pSer in the N-terminal BRCT domain whereas a hydrophobic pocket found in the interface of the two BRCT domains binds the amino acid of the phospho-peptide at residue +3 from the pSer

[291]. Analysis of several BRCT domains indicate that both the hydrophobic core and residues involved in the binding of phosphorylated peptides are well conserved and the majority of variation in structure and sequence between different BRCT domains is found in connecting loops between BRCT domains [291, 305].

Crystallography analysis of BARD1 BRCT domains revealed that they share a very similar structural formation to other tandem BRCT domain containing proteins involved in the DDR such as those found in BRCA1 and MDC1 [311]. The BARD1 BRCT domains also have a pSer binding pocket and a hydrophobic pocket which are believed to be involved in the binding of phospho-peptides. It has been suggested that the hydrophobic pocket responsible for binding the ligand at the +3 position determines the Spectrometry ificity of the ligand [304]. Intriguingly *Birrane et al.* found that the interaction between His686, which is responsible for potential ligand binding at the +3 position, and a ligand may be dynamically regulated by its protonation in response to a change in pH. This suggests that an interaction between the BARD1 BRCT domains and a phospho-peptide may be dependent on a shift in the cellular microenvironment [311]. Although the BARD1 BRCT domains appear to be important in the repair of DNA DSBs via HR, the mechanism and exact function of the BARD1 BRCT domains in HR remain unclear and there are no known proteins which interact with the BARD1 BRCT domains.

7.1.1 Do the BRCT domains contribute to the formation of the BRCA1-A, -B or -C complexes.

Although there is no evidence that the BARD1 BRCT domains interact with Abraxas, CtIP or FANCJ it is still possible that they directly or indirectly help stabilise the BRCA1-A ,-B and -C complexes. The results in this dissertation suggest that the BARD1 BRCT domains help stabilise CtIP but not Abraxas or FANCJ in the BRCA-A, -B and -C complexes. The BRCA1 complexes have been shown to be important in the repair of damaged DNA (reviewed in [353]) and the role that the BARD1 BRCT

domains play in the repair of DSBs may be attributed to their ability to stabilise CtIP to the BRCA1-C complex.

Germ line mutations of BRCA1 are associated with familiar breast and ovarian cancer [185, 403] and several of these mutations are found in the BRCT domains of BRCA1 disrupting their ability to bind phospho-peptides [404]. Although it remains largely unknown how the BRCA1 complexes contribute to cancer prevention, it is evident that the formation of these complexes are essential for BRCA1 tumour suppressor function.

The BRCA1-A complex contains at least five different components; RAP80, Abraxas, MERIT40, BRE and BRCC36 [128-130, 132, 133, 303]. Abraxas serves as a central adapter protein in this complex binding to the BRCA1 BRCT domains. RAP80 binds to ubiquitylated H2A surrounding the DNA break via its ubiquitin interacting motifs. This tethers the BRCA1-A complex to the site of damage and is mainly responsible for the recruitment of BRCA1 and other key repair proteins to damaged DNA. The signalling and recruitment of the BRCA1-A complex at DNA damage sites is believed to have a repressive role in homology directed repair as the loss of Abraxas or RAP80 leads to a hyper-recombination phenotype in cells [224]. Interestingly the BARD1 BRCT domains did not appear to contribute to the stabilisation of the BRCA1-A complex and loss of the BARD1 BRCT domains showed a decrease in HR efficiency which would not correlate with the hyper-recombination phenotype seen by *Hu et al.* [224] if the BARD1 BRCT domains are involved in the stabilisation of the BRCA1-A complex.

According to evidence in this dissertation, the BARD1 BRCT domains do not contribute to the stabilisation of the BRCA1-B complex involving FANCJ. FANCJ is a DEAH helicase domain containing protein that binds to the BRCA1 BRCT domains [294]. FANCJ is required for progression through S phase [332] and it has also been shown to be required after DNA damage for the checkpoint that accumulates cells in

the G2 phase of the cell cycle [86, 301]. FANCJ is also known as a Fanconi anemia group J protein. Patients with Fanconi anemia (FA) develop several malignancies and also suffer with various developmental defects [334, 335]. As FA patients are extremely sensitive to DNA interstrand crosslinking agents [334, 335], FANCJ is considered to play a role in DNA interstrand crosslink repair. Similar to BRCA1, FANCJ mutations are also associated with hereditary breast cancer [294, 405] and FANCJ has been shown to be important in the repair of DSB by HR [406]. Evidence suggests that repair of DSB by HR is critical if interstrand crosslinks are not repaired correctly by the Fanconi anemia proteins hence the interaction of BRCA1 and FANCJ is essential for DNA DSB repair. As expected *Brca1* cells are extremely sensitive to crosslinking agents such as MMC and cisplatin [200], however loss of the C-terminus of BARD1 including the BRCT domains does not sensitise cells to MMC treatment to the same extent as *Brca1* cells [269]. According to *Westermark et al.* there is no statistical significance in the sensitivity of cells which do not have the BRCT domains of BARD1to MMC compared to WT cells at a concentration where BRCA1 cells are extremely sensitive. This evidence is in line with the results in this dissertation which show that the BARD1 BRCT domains do not contribute to the formation or stabilisation of the BRCA1-B complex and although the BRCT domains of BARD1 appear to be crucial for HR, it is not due to a function in the BRCA1-B complex.

Results in this dissertations suggest that the BARD1 BRCT domains play a role in stabilising CtIP in the BRCA1-C complex and a model can been seen in figure 7.1. In the absence of the BARD1 BRCT domains the amount of CtIP co-immunoprecipitated with BARD1 is severely reduced in comparison to the level of CtIP pulled down with full length BARD1. The number of CtIP foci formed in the absence of the BARD1 BRCT after cells were treated with γ-irridation was also observed to be less compared with WT cells. However the result of this experiment may be questionable as complete loss of BARD1 did not illustrate the same decrease in the number of IR induced CtIP foci as the loss of the BARD1 BRCT domains demonstrated. The BRCA1-C complex is

composed of CtIP, the MRN complex and BRCA1/BARD1 heterodimer. It is believed that the formation BRCA1-C complex is cell cycle dependent and only forms during S and G2 phase when cells can carry out HR [87]. BRCA1 has been shown to interact with CtIP through its BRCT domains in a phosphorylation dependent manner [86]. CtIP is a DNA endonuclease and is required for DNA end resection at the very early stages of DSB repair by HR [55, 222]. The interaction of CtIP with the MRN complex is thought to stimulate the nuclease activity of the MRN complex and promote DNA end resection. It is worth noting that the tumour suppressor function of BRCA1 and its role in homology directed repair depends on the BRCT domains of BRCA1 [298] and that all three phospho-proteins known to interact with BRCA1 via its BRCT domains are important in HR [353]. In agreement with these results, I have shown that point mutations in the BRCT domains of BRCA1 which abrogate phospho-protein binding, severely decrease the ability of the cell to carry out HR and shows sensitivity to PARP inhibitors. As BARD1 is an important regulator of BRCA1 function, and is almost always found bound to BRCA1 in the nucleus where BRCA1 forms the BRCA1-A, -B, and –C complexes, it is possible that BARD1 BRCT domains may also be important in the BRCA1 complexes. There have been several opposing studies regarding the importance of the BRCA1-CtIP interaction in the repair of DNA DSB by HR. However it remains clear that both BRCA1 and CtIP are required for efficient HR. The involvement of BRCA1 in DNA resection remains contradictory. On one hand, *Schlegel et al.* show that cells treated with a BRCA1 siRNA abolished the formation of ssDNA focus in response to ionising radiation suggesting a role for BRCA1 in DNA end resection however they conclude that this is not dependent on the BRCT domains of BRCA1 [407]. *Chen et al* also found that the assembly of nuclear ssDNA/RPA foci after ionising radiation was impaired in the HCC1937 cell line which contains a truncated version of BRCA1 lacking its BRCT domains [87]. On the other hand, Zhao et al. showed no reduction in IR induced RPA foci in siRNA BRCA1 depleted HeLa cell [166]. It remains unclear if BRCA1, Spectrometry ifically the BRCT domains, play a role in end resection.

The importance of the BRCA1-CtIP interaction in DNA resection and HR repair of DNA DSB is also controversial. Previous studies in our lab suggested that the interaction between CtIP and BRCA1 is crucial for the repair of DNA DSB by HR. DT40 $CtIP^{-/-/-}$ cells were reconstituted with either WT human CtIP or with a phospho-mutant CtIP (HsCtIPS372A), which prevents CtIP binding to BRCA1, and the CtIP cell line expressing HsCtIPS372A showed a marked defect in the ability to carry out HR [344]. The repair of DSB by HR requires extensive DNA end resection implicating the importance of the BRCA1-CtIP interaction in end resection prior to repair of DSB by HR. Contrary to this, *Nakamura et al.* reported that homology directed repair was proficient in DT40 ($CtIP^{S332A/-/-}$) cells expressing endogenous chicken CtIP with the equivalent phospho-point mutant as used by our lab [345]. Very recently *Reczek et al.* showed that the BRCA1-CtIP interaction is not required for the major resection dependent pathways of DSB repair including HR in mouse ES cells [225]. Although the relevance of the BRCA1-CtIP interaction in the repair of DNA DSB by HR remains unclear, *Nakamura et al.* suggested that they function in the nuclease mediated removal of covalently bound oligonucleotides to peptides at DNA DSBs [345]. This would be consistent with the observed sensitivity seen to topoisomerase inhibitors in cell lines in which BRCA1 and CtIP cannot interact.

If the interaction between BRCA1 and CtIP is not essential for HR, what are the cellular functions of this conserved interaction and how might the potential function of the BARD1 BRCT domains in stabilising the BRCA1-C complex be important for HR and tumour suppression? Previous studies have implicated this interaction to be important for activation of the G_2/M cell cycle checkpoint [86], and unpublished results in our lab show that the BARD1 BRCT domains are required for the progression of the cells through the cell cycle after cisplatin treatment. Although these potential activities are likely to facilitate cellular responses to DNA damage, it doesn't explain the defects seen in HR with the loss of the BARD1 BRCT domains or indeed with the loss of the BRCA1 BRCT domains. Interestingly, what does remain clear is that according to my

results, the contribution of the BARD1 BRCT domains to the stabilisation of the BRCA1-C complex is independent of the potential phospho-binding ability of the BARD1 BRCT domains as point mutations predicted to abrogate potential phospho-peptide interaction did not show a decrease in the amount of CtIP pulled down in comparison to full length BARD1. However the contribution of the BRCT domains of BARD1 to the stabilisation of the BRCA1-C complex is completely dependent on the interaction of BRCA1 and BARD1, as I have shown that the L107P BARD1 mutant which cannot interact with BRCA1, does not form part of the BRCA1-C complex. Also BARD1 fails to interact with CtIP in the absence of BRCA1 as shown by mammalian-two hybrid. Extensive further work is required to assess the contribution of the BARD1 BRCT domains in the stabilisation of the BRCA1-C complex.

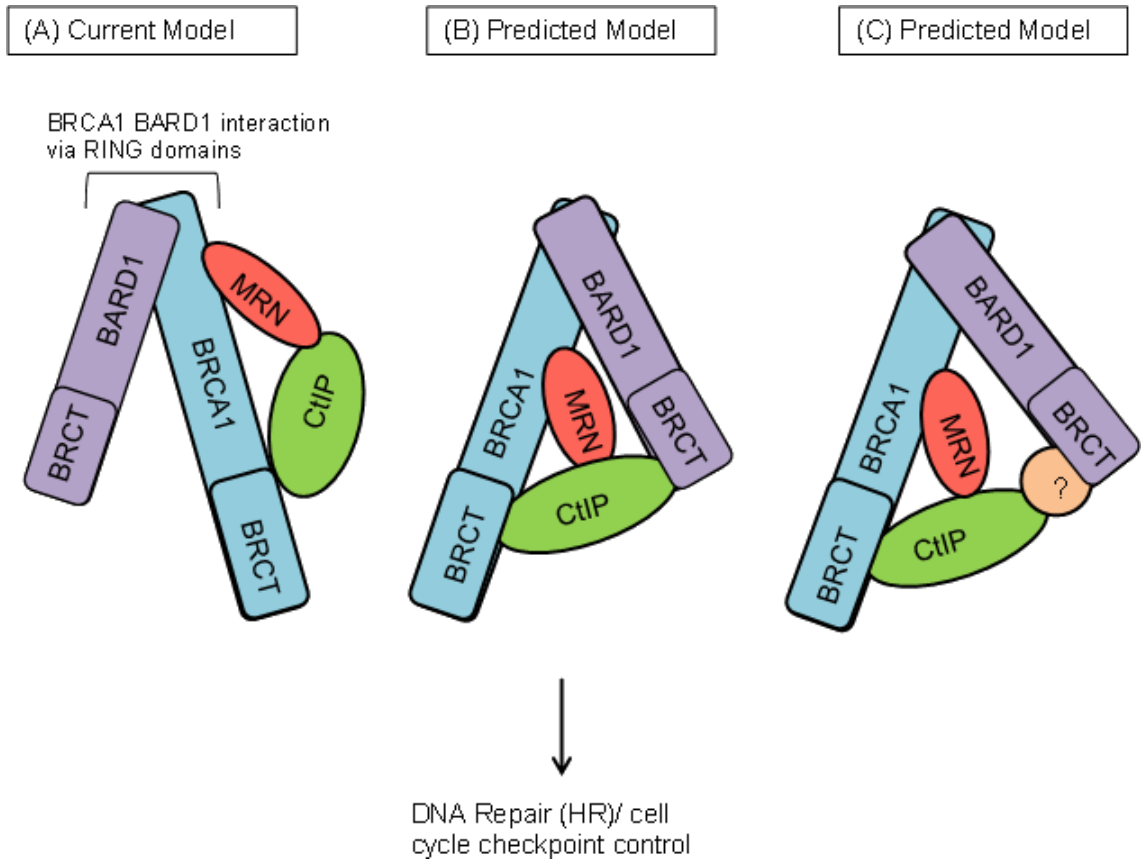

Figure 7.1 Current and predicted model for the BRCA1-C complex.
Previous evidence from the literature has suggested that the BRCA1 BRCT domains interact with CtIP and the MRN complex (A). My results suggest that the BARD1 BRCT domains contribute to the stabilisation of the BRCA1-C complex by directly or indirectly interacting with CtIP (B,C). BRCA1 and BARD1 interact via their RING domains. Potentially, an indirect interaction between BARD1 and CtIP may require an intermediate protein termed (?).

7.1.2 Are the BARD1 BRCT domains involved in the localisation of BARD1/BRCA1 to sites of damage.

The mechanism and function of BRCA1 in the repair of DNA DSB remains unclear however BRCA1 is a bona fide player in DNA DSB repair by HR as *Brca1* cells show extreme sensitivity to ionizing radiation and drugs which induce DSB [208, 408]. BRCA1 is a mediator between the sensor of damage and repair and is required for the efficient repair of DSB by HR [217, 353]. My results confirm the requirement of BRCA1 in HR as loss of BRCA1 results in defects in HR and also sensitises cells to PARP inhibitors. Localisation of BRCA1 to DNA DSB is required for repair by HR, as *Greenberg et al.* showed the loss of RAD51 to laser induced DNA DSB in the absence

of a fully functional BRCA1 [228]. RAD51 is important in strand exchange vital to HR and defects in RAD51 function severely impedes the repair of DSBs [409-411]. BRCA1 is also required for the sub nuclear assembly of RAD51 following DNA damage by the crosslinking agent cisplatin [362].

The interaction of BARD1 with BRCA1 is crucial to BRCA1 function in HR as BARD1 stabilises and allows nuclear retention of BRCA1. Due to the importance of this interaction it is possible that the BARD1 BRCT domains play a role in the localisation of BRCA1 to sites of damage. Loss of the BARD1 BRCT domains leads to defects in the repair of DNA DSBs by HR as shown in my results and by *Westermark et al*. and *Baer et al.* [266, 269]. It is possible that the BRCT domains of BARD1 may contribute to HR and genome stability by facilitating the correct localisation of BRCA1 to DNA damage.

Phosphorylation of H2AX (γH2AX), mediated by ATM and ATR, has been shown to facilitate the recruitment of BRCA1 to sites of DNA damage [323]. However BRCA1 can still be recruited to sites of damage in the absence of γH2AX but it cannot be stably retained suggesting that γH2AX is required for the sustained recruitment of BRCA1/BARD1 [357]. The phosphorylation of H2AX initiates a signalling cascade which ultimately recruits repair proteins such as BRCA1 and 53BP1 to sites of damage. The degree of H2AX phosphorylation correlates with the level of DNA DSBs [356]. Recently, studies have shown that ubiquitylation during the signalling cascade at DSBs is responsible for the recruitment of BRCA1 through its interaction with RAP80 [128, 130, 133]. RAP80 is part of the BRCA1-A complex and binds to ubiquitin chains on H2AX after H2AX phosphorylation. RAP80 cannot be solely responsible for BRCA1 recruitment as the loss of RAP80 does not completely abolish IR induced BRCA1 foci according *to Hu et al* [224].

Recently *Li et al.* made a substantial contribution to the understanding of how BRCA1/BARD1 is recruited to DSBs. They suggested that BRCA1 is recruited to DNA damage in two waves, the initial early recruitment is suggested to be dependent on the

BARD1 BRCT domains and independent of γH2AX, whereas the second wave of recruitment depends on γH2AX [287]. This piece of work demonstrated that the BARD1 BRCT domains are capable of localising to laser stripe induced DSB within 20 seconds after damage in the absence of γH2AX and is responsible for the very early recruitment of BRCA1/BARD1 to DSBs. In the absence of the BARD1 BRCT domains, BRCA1 failed to recruit early to DSBs and only localised to the DNA damage stripe after 2 minutes. This later recruitment of BRCA1 in the absence of the BARD1 BRCT domains was dependent on γH2AX. Although BARD1 failed to recruit early to the site of damage in the absence of its BRCT domains, it localised with BRCA1 in a γH2AX dependent manner later. In agreement with my results, the early recruitment of BRCA/BARD1 to laser induced damage stripes is believed to be due to the binding of the BARD1 BRCT domains to PAR. Cells treated with PARP inhibitors failed to recruit BRCA1/BARD1 in the early recruitment phase to DNA damage. My results also indicate that in the absence of the BRCT domains of BARD1 or with the treatment of PARP inhibitors, BARD1 requires longer to localise to laser induced damage stripes indicating the importance of the BARD1 BRCT domains in the early recruitment of BARD1 to DSBs. Although the trends seen by *Li et at* are very similar to those I observed in the recruitment of BARD1 with the loss of the BRCT domains or with the treatment of PARP inhibitors, the exact timings were delayed in my experiments. *Li et al.* shows early recruitment after 20 seconds and γH2AX recruitment after 2minutes, whereas I observed early recruitment after 1min and the later recruitment after 3minutes. This may be partially explained by the use of different wave length lasers to induce damage. A 405nm UV laser was used in my experiments to induce damage, whereas Li et al. availed of 337.1nm laser. Regardless of the slight time difference, the results indicate the same outcome suggesting a role for the BARD1 BRCT domains in the very early recruitment of the BARD1 to DSBs.

Li et al. extended their finding by demonstrating that it is the phospho-binding ability of the BARD1 BRCT domains that are responsible for the early recruitment of

BRCA1/BARD1. They generated a point mutation in the BARD1 BRCT domain predicted to bind phosphorylated proteins (BARD1K619A) and this protein showed the same delayed kinetics in localising to sites of damage as the complete loss of the BARD1 BRCT domains did. In this study, the BARD1 BRCT domains bind ADP-ribose, the basic unit of PAR [287]. This is believed to be in a phosphorylation dependent manner as there are two phosphate groups in ADP-ribose and BARD1K619A failed to interact with PAR. Although poly(ADP-ribose) polymerases (PARPs) have been shown to be important for SSB repair [412-414], recent structural analysis has also indicated that PARP1 recognises DSBs [286].

I have shown that loss of the BRCT domains of BARD1 does not prevent BARD1 recruitment to laser induced DNA DSBs, however in agreement with the work carried out by *Li et al.* the BARD1 BRCT domains appear to play a more intricate role in the timing of recruitment. The observation that the BRCT domains of BARD1, particularly the potential phospho-interacting amino acids in the BARD1 BRCT domains, are important in the early recruitment of BRCA1/BARD1 to DNA damage does not explain their biological relevance in HR or tumour suppression. My results suggest that although the BRCT domains of BARD1 are important for HR, as loss of the BRCT domains of BARD1 results in defects in HR and sensitises cells to PARP inhibitors, the potential phospho-binding ability of the BARD1 BRCT domains are dispensable in HR. *Bard1* DT40 cells reconstituted with BARD1S575F, BARD1K619M and BARD1H686R and a triple mutant containing all three point mutations showed no defects in the repair of HR and were not sensitive to PARP inhibitors. These cells were also competent in HR even after treatment with PARP inhibitors. *Laufer et al.* also presented similar results indicating that the potential phospho-peptdide interaction of the BRCT domains of BARD1 was not required for its function in HR [266]. This evidence suggests that the early recruitment of BRCA1/BARD1 to DSBs by the BARD1 BRCT domains does not appear to affect the cells ability to carry out efficient HR.

An interesting observation was made in this dissertation which suggested that in the absence of the BARD1 BRCT domains, BARD1 localisation to “BRCA1 nuclear dots” is impaired. In 1996, *Scully et al*. reported the discrete localisation of BRCA1 into nuclear foci [415]. As suggested by *Chen et al.* [416] and confirmed by *Scully et al.* the “BRCA1 nuclear dots” appear in the S-phase of the cell cycle [208]. BRCA1 expression is cell cycle dependent and elevated levels of BRCA1 expression are seen in S-phase [416-419] which correlates with a hyper-phosphorylated form of the protein [416]. Subsequently both RAD51 and BARD1 were shown to co-localise with “BRCA1 nuclear dots” in a S-phase dependent manner in the absence of DNA damage [215, 355]. I have also shown that the accumulation of BARD1 at discrete nuclear foci is S-Phase related as the number of cells with BARD1 nuclear foci directly correlated to the amount of cells in S-phase according to both EDU and PCNA immunostaining and FACs analysis of BrdU and PI stained cells. This evidence strongly suggested a role for BRCA1/BARD1 heterodimer in the maintenance of genome stability and potentially in the processing of replicated DNA. To date, the exact function of the BRCA1 nuclear foci is still unknown, however it does appear to be important in the availability of BRCA1/BARD1 for recruitment to sites of damage. After DNA damage these BRCA1 foci largely disperse and form larger foci containing repair proteins important in the repair of DNA damage [215, 356, 420]. Also after DNA damage the BRCA1 nuclear foci co-localise with PCNA replication structures, whereas prior to damage co-localisation was not observed [208].

There is no evidence suggesting that these S-phase BRCA1 nuclear foci are important in the actual repair of DSBs, however it is intriguing that in the absence of the BARD1 BRCT domains, BARD1 shows defects in its ability to localise to these foci. It would be very interesting to study the effects of BRCA1 recruitment to these S-phase associated nuclear foci in the absence of the BARD1 BRCT domains. *Jin et al.* suggested that the formation of the BRCA1 nuclear foci may require BRCA1 [355] however my results suggest that at least the recruitment of BARD1 to these nuclear

foci does not require its interaction with BRCA1. BARD1L107P which cannot interact with BRCA1 was fully competent in forming discrete nuclear foci similar to WT BARD1. Interestingly although loss of the BRCT domains of BARD1 compromised BARD1 localisation to S-phase nuclear foci, point mutation that are predicted to abrogate phospho-protein interaction were also competent in forming S-phase nuclear foci.

The contribution of the BARD1 BRCT domains to the formation of the BRCA1 nuclear foci requires much more investigation, as does the function and biological relevance of these structures. The defects seen in the localisation of BARD1 to nuclear foci do not appear to impede on the recruitment of BARD1 to sites of damage as BARD1ΔBRCT is proficient in localising to laser stripe induced damage. However it is clear from my results that the interaction of BRCA1 with BARD1 is not required for the BARD1 localisation to these S-phase nuclear foci which leads to the Spectrometry ulation that potentially it is BARD1 that allows BRCA1 to be recruited to the BRCA1 nuclear foci.

Another interesting observation I made in this dissertation was the extremely delayed kinetics of cells exhibiting BARD1 nuclear foci to recruit to laser induced DNA damage stripes. Cells which exhibited uniformly dispersed BARD1 in the nucleus localised to laser stripes within 1 minute of damage whereas S-phase cells which showed discrete nuclear foci formation of BARD1 required at least 4 to 5 minutes to accumulate at sites of damage. There were no observable nuclear foci formation in cells lacking the BARD1 BRCT domains and the slight delayed kinetics seen with the localisation of these cells is believed to be due to the inability of BARD1 to be recruited in the absence of the BRCT domains as discussed earlier. The importance of the increased delayed kinetics seen in cells expressing full length BARD1 which formed discrete nuclear foci, believed to be S-phase BRCA1 nuclear foci, remains unclear.

7.1.3 How do novel interactors of BARD1 and its BRCT domains contribute to its role in DNA DSB repair.

Mass Spectrometry analysis of BARD1 interacting proteins in this dissertation revealed several proteins involved in the NuRD complex which may interact with BARD1. The NuRD complex is a nucleosome remodelling and histone deacetylation complex. Given that the role of chromatin remodelling in response to DNA DSBs is just beginning to emerge, the potential association of BARD1 with members of the NuRD complex is very intriguing.

In eukaryotic cells, the tight packaging of DNA into highly structured and condensed chromatin poses a significant impediment to DNA based processes such as transcription, replication and repair. To overcome these regulatory boundaries, cells have evolved two major processes to modify chromatin structure. The first is by post translational modification of histone tails and the second by ATP-dependent remodelling of chromatin. Emerging evidence suggests that DNA signalling and repair processes act in an integrated fashion with chromatin structures at sites of DNA damage [421-426]. While it appears intuitive that condensed chromatin protects the DNA from damage, a more open and relaxed chromatin state is required for loading repair proteins onto chromatin at sites of damage [424].

CHD4, MTA1/2, HDAC1, LSD1 and RBBP7 are all core components of the NuRD complex [427, 428] and were found to co-immunoprecipitate with BARD1 by Mass Spectrometry in this dissertation. Although none of these proteins could be confirmed to interact with BARD1 by western blot, their identification by Mass Spectrometry remains very interesting and may provide an insight into the importance of BARD1 in the repair of DSB with future work. It is possible that these proteins could not be confirmed by western blot due to the small quantities that were identified by Mass Spectrometry. Only a small number of peptides were identified for each NuRD protein by Mass Spectrometry in comparison to BRCA1 which identified over 50 unique

peptides in the analysis and confirmation of BARD1 interacting proteins. It is also important to note that the NuRD complex members identified as potential BARD1 interactors where only seen when a crosslinker was used to stabilise potential BARD1 complex members. This suggests that any interaction between BARD1 and the NuRD complex may be very distant or transient making it more difficult to confirm. Further study is needed to confirm that the Mass Spectrometry candidates identified as BARD1 interactors are indeed true interactors however the current evidence of the role of the NuRD complex in DSB repair is intriquiging and could potentially involve BARD1.

Smeenk et al. have proposed that the NuRD complex is a novel regulator of DSB repair as the NuRD complex is rapidly recruited to DSBs and promotes histone ubiquitylation via RNF8/RNF168. They have also reported that the NuRD complex is important for the ubiquitin dependent accumulation of RNF168 and BRCA1 to sites of damage. Consequently the loss of certain components of the NuRD complex is implicated in defects in DNA repair and checkpoint activation [429]. CHD4 localises to laser induced DNA damage stripes [429]. Preliminary data from my dissertation also suggests that CHD4 localises to DNA damage stripes. An increase in γH2AX, a marker for DNA damage, was observed by *Pegoraro et al.* in the absence of CHD4 [430] which is consistent with the idea that CHD4 and the NuRD complex play a role in DNA repair. Loss of CHD4 also sensitises cells to IR [371]. CHD4 has been shown to be recruited to DNA damage by two separate mechanisms, first of all by binding to poly(ADP-ribosyl)ated proteins, including PARP1 [371], which then mediates the PARP-dependent recruitment of NuRD proteins MTA2 and HDAC1. The second method is dependent on the ubiquitin ligase RNF8 [372]. Upon recruitment by RNF8, the chromatin remodelling activity of CHD4 is proposed to decondense the chromatin surrounding a DSB allowing the formation of ubiquitin conjugates by both RNF8 and RNF168 [372]. The amplification of the ubiquitin signal at DSB is prerequisite for the DNA damage repair signal and downstream recruitment of repair proteins such as BRCA1 and 53BP1 [429]. In agreement with these results, knockdown of CHD4 results

in a decrease of ubiquitylation at DSBs which corresponds to the reduced accumulation of BRCA1 and RNF168 at DSBs [372]. The potential interaction of BARD1 and CHD4 is very interesting especially as both proteins are recruited to DSB very early after damage in a PARP dependent manner. It would be intriguing to explore the connection between BARD1 and CHD4 in relation to their PARP dependent recruitment to DSBs. Both proteins are recruited to DSB in a PARP-dependent manner independent of γH2AX [287, 371] As *Li et al* proposed that the BARD1 BRCT domains bind PAR directly, it is possible that BARD1 may play a role in recruiting CHD4. However both CHD4 and BARD1 can also be recruited to DSB by RNF8 and BRCA1 suggesting that the early recruitment may function as a failsafe rather than being pivotal to their recruitment.

MTA1 is an integral component of the NuRD complex [373] and is one of the most commonly overexpressed gene products in human cancers. The levels of MTA1 have been shown to be greatly increased in metastatic and aggressive cancers [431-433]. Given MTA1s role in cancer it was not surprising to find that it also played a role in the DNA damage response to ionizing radiation [374]. Depletion of MTA1 renders cells extremely sensitive to ionizing radiation suggesting a role for MTA1 in DSB repair [374]. Similarly to CHD4, *Chou et al*. have shown that MTA1 is also recruited to sites of DNA damage in a PARP-dependent fashion [288]. MTA1 protein is stabilised in response to ionizing radiation [374]. Under normal conditions MTA1 is targeted for degradation by COP1 ubiquitin ligase, however after DNA damage ATM phosphorylates COP1 which promotes its auto-degradation and therefore stabilises MTA1 in response to DNA damage [374]. The exact role of MTA1 in the repair of DSBs remains unclear however it would appear from experimental evidence that MTA1 contributes to the efficient repair of DSBs.

Another NuRD complex protein shown to interact with BARD1 by Mass Spectrometry was MTA2. A biochemical study indicated that MTA2 is responsible for modulating the histone deactylation activity of the NuRD complex [434]. Initial

indications that MTA2 is important for DSB repair came from a study carried out in worms. *van Haaften et al.* showed that the loss of EGR1, the worm MTA2 homolog, sensitised cells to IR [435]. Since then, it has been shown that MTA2 is also recruited to DSB breaks and human cells lacking MTA2 are also sensitive to IR [429].

Histone deactylase 1 (HDAC1) is another core component of the NuRD complex and is believed to be involved in transcriptional repression by removing acetyl groups from histone tails, condensing chromatin [373]. *Bhaskara et al.* have suggested a role for HDAC1 in DNA replication fork progression as loss of HDAC1/2 results in a reduction of the replication fork velocity and also increases replication stress leading to DNA damage [436]. A connection between HDAC1 and the DNA damage response was seen in 2009 by *Pegoraro et al.* as loss of many NuRD complex members including HDAC1 resulted in an increase in γH2AX signal. HDAC1 has also been shown to be recruited to laser induced DNA damage stripes [437] in a manner that is dependent on CHD4 and PARP [371]. The function of HDAC1 in DSB repair remains unclear as very little research has been carried out in this field so far.

As mentioned previously, BARD1 was shown to interact with many proteins associated with the NuRD complex by Mass Spectrometry in this dissertation. It has become evident from research carried out that the NuRD complex appears to have a functional role in the repair of DSBs. As this is a very novel area of research it is difficult to predict the potential role that the interaction of BARD1 may have with members of the NuRD complex. It is possible that BARD1 may be involved in the recruitment of CHD4 to sites of damage as CHD4 can be recruited in a PARP dependent manner and BARD1 has been shown to interact with PAR at DSBs. The functional and biological relevance of these potential interactions is uncertain and whether the NuRD complex functions mainly to remodel chromatin allowing access of repair proteins or whether it has a more involved role in the actual repair of damage has yet to be discovered. However a potential interaction between BARD1 and

components of the NuRD complex may contribute to our understanding of the importance of BARD1 in DSB repair in the future.

RBBP7 is another component of the NuRD complex which was found to co-immunoprecipitate with BARD1 by Mass Spectrometry. RBBP7 is an evolutionary conserved histone binding protein [438] proposed to be important for establishing heterochromatin. Very little is known about the function of this protein however RBBP7 is believed to be a structural protein that provides an interactive interface for other components of the NuRD complex [427, 434]. RBBP7 is a subunit of the CAF1 complex which assembles chromatin during DNA replication and repair [439]. It has also been shown that RBBP7 interacts with the BRCA1 BRCT domains and this interaction is disrupted in the presence of DNA damaging agents [262]. As RBBP7 has already been shown to interact with BRCA1, it is possible that it was pulled down with BARD1 as part of a larger complex with BRCA1. The functional role of RBBP7 in repair of DSB is unclear as is the relevance of a potential interaction with BARD1.

The final NuRD complex protein which was seen to associate with BARD1 in this dissertation was LSD1. LSD1 is a histone demethylase that mediates H3K4me1/2 demethylation involved in transcriptional repression [388]. It has also been shown to be part of the NuRD complex [428]. A very recent study carried out by *Mosammaparast et al.* has discovered a novel function of LSD1 in the repair of DNA DSBs. This study showed that LSD1 localises to laser induced DNA DSB stripes which coincided with H3K4me2 demethylation. The recruitment of LSD1 to DSB was dependent on its interaction with ubiquitin ligase RNF168 which is very reminiscent of the CHD4-RNF8 recruitment [390]. Interestingly, *Mosammaparast et al.* suggested that LSD1 is important in the recruitment of 53BP1 to sites of damage as loss of LSD1 in cells results in a decrease in 53BP1 foci formation after damage. As HR efficiency is observed to increase slightly in the absence of LSD1 it is proposed that LSD1 may play an important role in repressing or limiting the amount of HR which occurs after a DSB is sensed. I have shown that BARD1 is important for HR and loss of BARD1 results in

a decrease in HR efficiency. The potential interaction between BARD1 and LSD1 may be involved in the repair choice of DSB, whether it be by HR or NHEJ and would allow a greater understanding of the functional relevance of BARD1 in the repair of DSBs.

Post translational modifications such as phosphorylation, ubiquitylation, methylation and sumoylation are extremely important in the DDR and also for the recruitment of repair proteins to sites of damage. Not only do post translational modifications remodel chromatin allowing access of repair proteins to the site of damage and repress transcription they are also responsible for a complex signalling pathway at DSBs which serves to recruit repair proteins. Histones surrounding DNA DSB are vastly ubiquitylated and amplify the DNA damage signal. Ubiquitylation of histones is also responsible for the ultimate recruitment of BRCA1 to sites of damage. Methylation of H4K20 has been shown to recruit the repair protein 53BP1 to DSBs [440]. The importance of PTMs at DSBs makes the potential interaction between BARD1 and members of the NuRD complex, especially the lysine demethylase LSD1, very intriguing. It is also important to note that HUWE1, a ubiquitin ligase, was also identified as a potential BARD1 interactor.

In relation to post translational modifying enzymes involved in DSB repair and signalling, UBC9, a SUMO E2 conjugating enzyme was the only DDR protein identified that interacted with the BARD1 BRCT domains Spectrometry ifically according to Mass Spectrometry data in this dissertation. In contrast to the ubiquitylation pathway which utilises several E2 conjugating enzymes, UBC9 is the only SUMO E2 enzyme hence a vital regulator of the sumoylation pathway. Interestingly UBC9 has been shown to interact with RAD51 [441-443], a key component of the HR machinery and loss of nuclear UBC9 correlated with a decrease in the RAD51 foci formation after DNA damage [444]. In correlation with this, I have also seen a reduction in the formation of IR induced RAD51 foci in the absence of both full length BARD1 and just the BARD1 BRCT domains. An intriguing similarity between BARD1 BRCT domains and UBC9 is their ability to interact with PARP, UBC9 was discovered as a PARP interactor in a

yeast-two hybrid screen [445] however the function of this interaction in relation to DNA repair is still unknown. As further evidence of the importance of UBC9 in the repair of DNA DSBs, a study carried out on samples derived from breast cancer patients which contained a polymorphism in UBC9 showed a decrease in efficient HR in comparison to samples containing WT UBC9. This body of evidence highly suggests that UBC9 is an important player in the repair of DNA DSBs however much more work is needed to determine its function and the relevance of a potential interaction between UBC9 and the BARD1 BRCT domains.

7.1.4 Conclusions and future work.

The work presented in this dissertation suggests an important role for the BARD1 BRCT domains in the repair of DNA DSB by HR. Proteins containing BRCT domains have been shown to be integral to the DDR and the importance of the BARD1 BRCT domains only strengthen this observation. Very little is understood about the function and relevance of the BARD1 BRCT domains in DNA repair however the work I have presented here suggests that they may contribute to the stabilisation of the BRCA1-C complex by directly or indirectly binding CtIP. Future research into the relevance of the stabilisation of the BRCA1-C complex by the BARD1 BRCT domains is needed to elucidate if this stabilisation does indeed contribute to the ability of the cell to carry out efficient HR. Results that indicate that BARD1 BRCT domains stabilise the BRCA1-C complex were carried out in normal non-damaging conditions. It would be very interesting to study the effect of this finding in a damage context. Also it is not clear if BARD1 stabilises CtIP in the BRCA1-C complex by interacting directly with CtIP or through a scaffold protein which may bind both BARD1 and CtIP. Further work will be required to analyse this theory. Although results from this thesis suggest that the potential phospho-interacting ability of the BARD1 BRCT domains do not contribute to the HR function of the BARD1 BRCT domains, *Birrane et al.* suggested that the interaction of BARD1 BRCT with a phospho-protein may depend on the pH of the surrounding environment [311]. A potential phosphorylation dependent interaction

between the BARD1 BRCT domains and a repair protein may be important for HR under certain microenvironmental conditions, therefore I believe that future work should also concentrate on investigating the conditions of the microenvironment surrounding a DSB. A change in the pH at DSBs may uncover BARD1 BRCT interactors which remain hidden under normal conditions.

The BARD1 BRCT domains also appear to be important for the localisation of BARD1 to BRCA1 nuclear foci during S-phase however the functional importance of these foci remains unclear. The BARD1 BRCT domains are responsible for the early recruitment of BRCA1 to DSB however the ultimate recruitment of BARD1 to sites of damage is not perturbed in the absence of the BRCT domains. Interestingly the HR defects seen in the absence of the BARD1 BRCT domains is functionally unrelated to the predicted phospho-peptide interaction sites of the BARD1 BRCT domains. In future work, I believe it is important to investigate the functional role of “BRCA1 nuclear foci” and if they contribute to the DDR. It would also be interesting to assess if the BARD1 BRCT domains are needed to recruit BRCA1 to the S-phase foci. Although the BARD1 BRCT domains have been shown to be important for the early recruitment of BRCA1/BARD1 to sites of damage, it remains unclear how this may contribute to HR. Further work is needed to fully investigate the functional outcome and requirements of this early recruitment of proteins to DSB.

Mass Spectrometry analysis of BARD1 interactors highlighted a variety of potential BARD1 interactors that play a role in the DDR. Interestingly the majority of these proteins are associated with the chromatin remodelling complex NuRD. Although none of these protein targets were verified, further research into the potential involvement of BARD1 with the NuRD complex may prove very interesting in relation to the repair of DNA especially as the role of chromatin remodelling proteins in DNA repair is a novel and exciting field of research at the moment. Although not much is known about the function of sumoylation in the DDR, results indicating that BARD1 may interact with the SUMO E2 conjugating enzyme UBC9 in a BRCT dependent

manner may provide a greater insight into the importance of the BARD1 BRCT domains in HR uncovering a novel role for BARD1 and potentially BRCA1 in the repair of DNA.

7.2 The role of ubiquitin ligases RNF8 and RNF168 in DSB repair

DNA DSBs are considered to be one of the most dangerous types of lesions a cell can incur [446], which can arise during normal cellular process such as metabolism or replication or by exogenous agents such as IR or mutagenic chemicals [2]. DNA DSBs are repaired by either NHEJ or HR as discussed in the introduction and if they are not repaired properly it can lead a Spectrometry trum of mutations which can in turn lead to cancer [446]. The cellular response to DSBs is defined by the rapid accumulation of proteins involved in repair and also signalling factors at the site of damage [2, 165, 423]. An efficient response to DNA damage involves a complex signalling cascade which avails of PTM such as phosphorylation, actylation and ubiquitylation which leads to the ultimate recruitment of DNA repair proteins. Over the past few years an expanding view of the importance of ubiquitin signalling as a means to modulate the timing and efficient repair of DSBs has emerged.

Studies carried out in knockout mice illustrate the importance of RNF8 and RNF168 ubiquitin ligases in the DNA damage induced ubiquitylation cascade and DSB repair [178, 179, 392]. Mutations in RNF168 are also associated with the human RIDDLE syndrome which is characterised by radiosensitivity and immunodeficiency among other clinical features [126]. K63, non-degrading, ubiquitin chains are essential for the recruitment of repair proteins BRCA1 and 53BP1 to DSBs [2, 181, 182], Both RNF8 and RNF168 are required for ubiquitylation at sites of damage and loss of either proteins severely impedes the recruitment of BRCA1 and 53BP1 to DSBs [122, 124, 126, 177]. I have shown that both RNF8 and RNF168 are active ubiquitin ligases and ubiquitylate most free histones *in vitro*. In agreement with the importance of RNF8/168

in DNA damage repair, I have shown that loss of either *RNF8* or *RNF168* in DT40 cells sensitises them to DNA damaging agents. *Oestergaard et al*, showed a similar sensitivity of *Rnf8* and *Rnf168* DT40 cells to DNA damaging agents IR and CPP [177]. Although it is evident that ubiquitin ligases RNF8 and RNF168 are important for the repair of DSB the mechanism and exact functions of these proteins are only now beginning to emerge.

One of the earliest events in DSB repair is the recruitment of ATM which is responsible for the phosphorylation of H2AX [220]. γH2AX is a common marker associated with DNA damage. Recent evidence suggests that the ubiquitin ligase RNF2 and its interacting partner BMI1 are involved in the recruitment of ATM, initiating the signalling cascade at damage sites. RNF2/BMI1 catalyses the monubiquitination of H2AX at K119 and K120 in response to DNA damage and is required for the formation of γH2AX [447-450]. Based on the observation that loss of either RNF2 or BMI1 leads to sensitization of cells to IR and delays the DDR response, RNF2/BMI1 are predicted to play an important role in DNA repair. Although mono-ubiquitylation is an important step early in the DDR, it is the formation of K63 linked ubiquitin chains that are most persistent at sites of damage and are vital to the downstream recruitment of repair proteins BRCA1 and 53BP1 [2, 181, 182]. Interestingly, it has been shown that the concerted action of RNF8 and RNF168 are responsible for catalysing the conjugation of K63 linked ubiquitin chains on H2AX at position K13 and K15 [123, 451]. Intriguingly, K63 polyubiquitin chain formation crucial to the recruitment of repair proteins is found on the opposite side of histone H2A in respect to the monoubiquitination of H2AX by RNF2/BMI1.

There has been a lot of research dedicated to investigating whether RNF8 or RNF168 is responsible for the initial priming monoubiquitylation of histone H2AX and its subsequent polyubiquitylation. RNF8 is recruited to DSBs in a λH2AX and MDC1 dependent manner by its FHA domain [119, 121], whereas RNF168 is recruited to damage by its UIMs dependent on RNF8 [124, 126]. Due to the recruitment order, it

was suggested that RNF8 was responsible for the monoubiquitylation of histones and RNF168 amplified the DNA damage signal by extending the ubiquitin chains. Despite the initial *in vitro* analysis that RNF8 can monoubiquitylate H2A and that both the catalytic activity of RNF8 as well as the UIMs of RNF168 are required for RNF168 recruitment, recent observation indicate that H2A is a substrate for RNF168 and cannot be modified by RNF8 [123, 124, 126, 451]. This evidence suggests that RNF168 monoubiquitylates H2AX at K13 and K15 and RNF8 extends K63 linked ubiquitin chains [123]. *Mattiroli et al.* propose a model whereby RNF8 ubiquitylates non-nucleosomal proteins at DSBs which in turn recruits RNF168 and may explain the necessity of its ligase activity for the recruitment of RNF168. In concurrence with the proposed model, my results also indicate that RNF168 is responsible for the monoubiquitylation of H2A as only DT40 *Rnf8* cells overexpressing full length RNF8 showed an increase in monoubiquitylated H2A whereas a ubiquitin ligase dead mutant RNF8 and RNF168 did not. However re-expression of RNF168 in a RNF168 DT40 knockout cell line did not indicate an increase in H2A mono-ubiquitylation. This may be due to the fact that endogenous levels of RNF8 in the cell may not be sufficient to see an overall increase in H2A mono-ubiquitylation explaining why an increase is only seen when RNF8 is overexpressed.

The non-proteolytic polyubiquitin chains catalyzed by RNF8 and RNF168 DSBs in response to damage serve as docking sites which ultimately recruit BRCA1 and 53BP1 [120-122, 124]. The relative dynamics with which these two proteins localise to DNA damage is believed to be very important in regulating the choice of repair of DNA DSBs. The two main pathways used in mammalian cells to repair DNA DSBs are NHEJ, which is considered to be error prone, and HR, a faithful method of repair [25, 446]. BRCA1 and 53BP1 have collective roles in DSB repair, BRCA1 is required for efficient repair by HR while 53BP1 promotes NHEJ [344, 452-454]. Although both RNF8 and RNF168 are required to recruit both BRCA1 and 53BP1, the overall function of the signalling pathway at DSBs is believed to repress HR preventing over resection

at sites of damage which may prove deleterious to the cell. Recruitment of 53BP1 antagonises HR, however the recruitment of BRCA1 by RNF8 and RNF168 also appears to suppress HR as loss of Abraxas or RAP80, which tethers BRCA1 to the DSB, results in an increase in HR (unpublished results in the lab)[224, 232]. Loss of RNF168 has also been shown to affect NHEJ while RNF8 appears to be important for both HR and NHEJ [455, 456]. These findings support a model in which RNF8 and RNF168 are vital to the delicate choice between HR and NHEJ which may ultimately decide the outcome of the cell after damage.

The recruitment of BRCA1 to DSBs directly involves the ubiquitin ligase activity of RNF8 and RNF168, however the mechanism of 53BP1 recruitment requires more study. 53BP1 is recruited to dimethylated histone H4 on K20 at DSBs via its tudor domains [457, 458]. Although it does not contain any ubiquitin recognising domains, it is suggested that RNF8 and RNF168 ubiquitylation is required to remove factors that bind to H4K20me2 sites thus unmasking the binding sites for 53BP1 [455, 459]. However the exact mechanism responsible for the recruitment of 53BP1 by RNF8 and RNF168 is still not fully understood. Keeping in mind that the main function of RNF8 and RNF168 is to closely regulate the amount of HR at DSBs, it was interesting to discover that DT40 *Rnf8* cells were sensitive to PARP inhibitors suggesting a direct role in HR and according to my results this defect was not due to the ubiquitin ligase activity of RNF8 as a ubiquitin ligase dead mutant RNF8 was able to fully complement the initial sensitivity to PARP inhibitors. DT40 *Rnf168* cells showed sensitivity to HU which could not be corrected by the re-expression of a ubiquitin ligase dead mutant. These results suggest that RNF8 and RNF168 are required for efficient repair of DNA damage however only RNF168 ubiquitin ligase activity appears to be necessary for repair. Interestingly, as suggested previously by *Oestergaard et al.* it seems that RNF8 and RNF168 may not act in a strictly linear manner [177] as both proteins are sensitive to different types of damaging agents which result in different types of damage. It would be very interesting to study the contribution of both RNF8 and RNF168 to the repair of

different types of damage to gain a greater understanding of the role they play in the DDR.

7.2.1 Conclusions and Future Work

It is evident from the literature that both RNF8 and RNF168 are extremely important for the signalling response to DNA damage and the recruitment of repair proteins 53BP1 and BRCA1 to sites of damage. In the absence of either of the proteins, cells become sensitive to a variety of DNA damaging agents suggesting that they are important for repair. Recent evidence has demonstrated that RNF168 is required for mono-ubiquitylation of histone H2A whereas RNF8 is required to extend the ubiquitin chains after damage. My results indicate that although RNF8 and RNF168 are both important for DNA damage repair, the RNF8 ubiquitin ligase activity is not required for the repair of DSBs generated by PARP inhibitor. Whereas *Rnf168* cells are not sensitive to PARP inhibitors in the first place and instead show sensitivity to HU which is dependent of the ubiquitin ligase activity of RNF168. This leads to some very interesting questions which I believe should be addressed in the future. If RNF8 is important for the repair of DSB predicted to be generated by PARP inhibitors but does not require the ubiquitin ligase function of the protein, then how does RNF8 contribute to the repair? It would also be interesting to identify the suspected non-nucleosomal protein ubiquitylation targets of RNF8 which are predicted to be important for the recruitment of RNF168. By investigating the different repair pathways which require either RNF8 or RNF168, I believe we may gain a greater understanding of the individual contributions of these proteins in the DDR.

1. Jackson, S.P. and J. Bartek, *The DNA-damage response in human biology and disease.* Nature, 2009. **461**(7267): p. 1071-8.
2. Ciccia, A. and S.J. Elledge, *The DNA damage response: making it safe to play with knives.* Mol Cell, 2010. **40**(2): p. 179-204.
3. Giglia-Mari, G., A. Zotter, and W. Vermeulen, *DNA damage response.* Cold Spring Harb Perspect Biol, 2011. **3**(1): p. a000745.
4. Rich, T., R.L. Allen, and A.H. Wyllie, *Defying death after DNA damage.* Nature, 2000. **407**(6805): p. 777-83.
5. van Gent, D.C., J.H. Hoeijmakers, and R. Kanaar, *Chromosomal stability and the DNA double-stranded break connection.* Nat Rev Genet, 2001. **2**(3): p. 196-206.
6. Lu, C.Y., et al., *Oxidative DNA damage estimated by urinary 8-hydroxydeoxyguanosine and indoor air pollution among non-smoking office employees.* Environ Res, 2007. **103**(3): p. 331-7.
7. Pfeiffer, P., W. Goedecke, and G. Obe, *Mechanisms of DNA double-strand break repair and their potential to induce chromosomal aberrations.* Mutagenesis, 2000. **15**(4): p. 289-302.
8. Hoeijmakers, J.H., *Genome maintenance mechanisms for preventing cancer.* Nature, 2001. **411**(6835): p. 366-74.
9. Khanna, K.K. and S.P. Jackson, *DNA double-strand breaks: signaling, repair and the cancer connection.* Nat Genet, 2001. **27**(3): p. 247-54.
10. Cartagena-Lirola, H., et al., *Budding Yeast Sae2 is an In Vivo Target of the Mec1 and Tel1 Checkpoint Kinases During Meiosis.* Cell Cycle, 2006. **5**(14): p. 1549-59.
11. Soulas-Sprauel, P., et al., *V(D)J and immunoglobulin class switch recombinations: a paradigm to study the regulation of DNA end-joining.* Oncogene, 2007. **26**(56): p. 7780-91.
12. Lieber, M.R., *The mechanism of double-strand DNA break repair by the nonhomologous DNA end-joining pathway.* Annu Rev Biochem, 2010. **79**: p. 181-211.
13. Aravind, L. and E.V. Koonin, *SAP - a putative DNA-binding motif involved in chromosomal organization.* Trends Biochem Sci, 2000. **25**(3): p. 112-4.
14. Aravind, L. and E.V. Koonin, *Prokaryotic homologs of the eukaryotic DNA-end-binding protein Ku, novel domains in the Ku protein and prediction of a prokaryotic double-strand break repair system.* Genome Res, 2001. **11**(8): p. 1365-74.
15. Gu, J. and M.R. Lieber, *Mechanistic flexibility as a conserved theme across 3 billion years of nonhomologous DNA end-joining.* Genes Dev, 2008. **22**(4): p. 411-5.
16. Rothkamm, K. and M. Lobrich, *Evidence for a lack of DNA double-strand break repair in human cells exposed to very low x-ray doses.* Proc Natl Acad Sci U S A, 2003. **100**(9): p. 5057-62.
17. Schwarz, K., et al., *Human severe combined immune deficiency and DNA repair.* Bioessays, 2003. **25**(11): p. 1061-70.
18. Critchlow, S.E. and S.P. Jackson, *DNA end-joining: from yeast to man.* Trends Biochem Sci, 1998. **23**(10): p. 394-8.
19. Boulton, S.J. and S.P. Jackson, *Saccharomyces cerevisiae Ku70 potentiates illegitimate DNA double-strand break repair and serves as a barrier to error-prone DNA repair pathways.* EMBO J, 1996. **15**(18): p. 5093-103.
20. Yu, X. and A. Gabriel, *Ku-dependent and Ku-independent end-joining pathways lead to chromosomal rearrangements during double-strand break repair in Saccharomyces cerevisiae.* Genetics, 2003. **163**(3): p. 843-56.
21. Perrault, R., et al., *Backup pathways of NHEJ are suppressed by DNA-PK.* J Cell Biochem, 2004. **92**(4): p. 781-94.

22. Falzon, M., J.W. Fewell, and E.L. Kuff, *EBP-80, a transcription factor closely resembling the human autoantigen Ku, recognizes single- to double-strand transitions in DNA.* J Biol Chem, 1993. **268**(14): p. 10546-52.
23. Walker, J.R., R.A. Corpina, and J. Goldberg, *Structure of the Ku heterodimer bound to DNA and its implications for double-strand break repair.* Nature, 2001. **412**(6847): p. 607-14.
24. de Vries, E., et al., *HeLa nuclear protein recognizing DNA termini and translocating on DNA forming a regular DNA-multimeric protein complex.* J Mol Biol, 1989. **208**(1): p. 65-78.
25. Lieber, M.R., *The mechanism of human nonhomologous DNA end joining.* J Biol Chem, 2008. **283**(1): p. 1-5.
26. Meek, K., *New targets to translate DNA-PK signals.* Cell Cycle, 2009. **8**(23): p. 3809.
27. Chen, L., et al., *Interactions of the DNA ligase IV-XRCC4 complex with DNA ends and the DNA-dependent protein kinase.* J Biol Chem, 2000. **275**(34): p. 26196-205.
28. Soubeyrand, S., et al., *Artemis phosphorylated by DNA-dependent protein kinase associates preferentially with discrete regions of chromatin.* J Mol Biol, 2006. **358**(5): p. 1200-11.
29. Cruet-Hennequart, S., et al., *Enhanced DNA-PK-mediated RPA2 hyperphosphorylation in DNA polymerase eta-deficient human cells treated with cisplatin and oxaliplatin.* DNA Repair (Amst), 2008. **7**(4): p. 582-96.
30. Yu, Y., et al., *DNA-PK and ATM phosphorylation sites in XLF/Cernunnos are not required for repair of DNA double strand breaks.* DNA Repair (Amst), 2008. **7**(10): p. 1680-92.
31. Ma, Y., et al., *Hairpin opening and overhang processing by an Artemis/DNA-dependent protein kinase complex in nonhomologous end joining and V(D)J recombination.* Cell, 2002. **108**(6): p. 781-94.
32. Ma, Y., et al., *A biochemically defined system for mammalian nonhomologous DNA end joining.* Mol Cell, 2004. **16**(5): p. 701-13.
33. Povirk, L.F., *Biochemical mechanisms of chromosomal translocations resulting from DNA double-strand breaks.* DNA Repair (Amst), 2006. **5**(9-10): p. 1199-212.
34. Ahnesorg, P., P. Smith, and S.P. Jackson, *XLF interacts with the XRCC4-DNA ligase IV complex to promote DNA nonhomologous end-joining.* Cell, 2006. **124**(2): p. 301-13.
35. Buck, D., et al., *Cernunnos, a novel nonhomologous end-joining factor, is mutated in human immunodeficiency with microcephaly.* Cell, 2006. **124**(2): p. 287-99.
36. Chen, C., K. Umezu, and R.D. Kolodner, *Chromosomal rearrangements occur in S. cerevisiae rfa1 mutator mutants due to mutagenic lesions processed by double-strand-break repair.* Mol Cell, 1998. **2**(1): p. 9-22.
37. Welcker, A.J., et al., *Involvement of very short DNA tandem repeats and the influence of the RAD52 gene on the occurrence of deletions in Saccharomyces cerevisiae.* Genetics, 2000. **156**(2): p. 549-57.
38. Weinstock, D.M., E. Brunet, and M. Jasin, *Formation of NHEJ-derived reciprocal chromosomal translocations does not require Ku70.* Nat Cell Biol, 2007. **9**(8): p. 978-81.
39. Bentley, J., et al., *DNA double strand break repair in human bladder cancer is error prone and involves microhomology-associated end-joining.* Nucleic Acids Res, 2004. **32**(17): p. 5249-59.
40. Heacock, M., et al., *Molecular analysis of telomere fusions in Arabidopsis: multiple pathways for chromosome end-joining.* EMBO J, 2004. **23**(11): p. 2304-13.
41. Ma, J.L., et al., *Yeast Mre11 and Rad1 proteins define a Ku-independent mechanism to repair double-strand breaks lacking overlapping end sequences.* Mol Cell Biol, 2003. **23**(23): p. 8820-8.

42. Bennardo, N., et al., *Alternative-NHEJ is a mechanistically distinct pathway of mammalian chromosome break repair.* PLoS Genet, 2008. **4**(6): p. e1000110.
43. Lee, K. and S.E. Lee, *Saccharomyces cerevisiae Sae2- and Tel1-dependent single-strand DNA formation at DNA break promotes microhomology-mediated end joining.* Genetics, 2007. **176**(4): p. 2003-14.
44. Ahmad, A., et al., *ERCC1-XPF endonuclease facilitates DNA double-strand break repair.* Mol Cell Biol, 2008. **28**(16): p. 5082-92.
45. Liang, L., et al., *Human DNA ligases I and III, but not ligase IV, are required for microhomology-mediated end joining of DNA double-strand breaks.* Nucleic Acids Res, 2008. **36**(10): p. 3297-310.
46. Holliday, R., *The Induction of Mitotic Recombination by Mitomycin C in Ustilago and Saccharomyces.* Genetics, 1964. **50**: p. 323-35.
47. Liu, Y. and S.C. West, *Happy Hollidays: 40th anniversary of the Holliday junction.* Nat Rev Mol Cell Biol, 2004. **5**(11): p. 937-44.
48. Haber, J.E., *Exploring the pathways of homologous recombination.* Curr Opin Cell Biol, 1992. **4**(3): p. 401-12.
49. Nassif, N., et al., *Efficient copying of nonhomologous sequences from ectopic sites via P-element-induced gap repair.* Mol Cell Biol, 1994. **14**(3): p. 1613-25.
50. Szostak, J.W., et al., *The double-strand-break repair model for recombination.* Cell, 1983. **33**(1): p. 25-35.
51. Kreuzer, K.N., et al., *Recombination-dependent DNA replication stimulated by double-strand breaks in bacteriophage T4.* J Bacteriol, 1995. **177**(23): p. 6844-53.
52. D'Amours, D. and S.P. Jackson, *The Mre11 complex: at the crossroads of dna repair and checkpoint signalling.* Nat Rev Mol Cell Biol, 2002. **3**(5): p. 317-27.
53. Hopfner, K.P., et al., *The Rad50 zinc-hook is a structure joining Mre11 complexes in DNA recombination and repair.* Nature, 2002. **418**(6897): p. 562-6.
54. Paull, T.T. and M. Gellert, *Nbs1 potentiates ATP-driven DNA unwinding and endonuclease cleavage by the Mre11/Rad50 complex.* Genes Dev, 1999. **13**(10): p. 1276-88.
55. Sartori, A.A., et al., *Human CtIP promotes DNA end resection.* Nature, 2007. **450**(7169): p. 509-14.
56. Iftode, C., Y. Daniely, and J.A. Borowiec, *Replication protein A (RPA): the eukaryotic SSB.* Crit Rev Biochem Mol Biol, 1999. **34**(3): p. 141-80.
57. Sung, P., *Yeast Rad55 and Rad57 proteins form a heterodimer that functions with replication protein A to promote DNA strand exchange by Rad51 recombinase.* Genes Dev, 1997. **11**(9): p. 1111-21.
58. New, J.H., et al., *Rad52 protein stimulates DNA strand exchange by Rad51 and replication protein A.* Nature, 1998. **391**(6665): p. 407-10.
59. Shinohara, A., et al., *Rad52 forms ring structures and co-operates with RPA in single-strand DNA annealing.* Genes Cells, 1998. **3**(3): p. 145-56.
60. Wolner, B., et al., *Recruitment of the recombinational repair machinery to a DNA double-strand break in yeast.* Mol Cell, 2003. **12**(1): p. 221-32.
61. Pellegrini, L., et al., *Insights into DNA recombination from the structure of a RAD51-BRCA2 complex.* Nature, 2002. **420**(6913): p. 287-93.
62. Symington, L.S., *Role of RAD52 epistasis group genes in homologous recombination and double-strand break repair.* Microbiol Mol Biol Rev, 2002. **66**(4): p. 630-70, table of contents.
63. Klapstein, K., T. Chou, and R. Bruinsma, *Physics of RecA-mediated homologous recognition.* Biophys J, 2004. **87**(3): p. 1466-77.
64. Chen, Z., H. Yang, and N.P. Pavletich, *Mechanism of homologous recombination from the RecA-ssDNA/dsDNA structures.* Nature, 2008. **453**(7194): p. 489-4.
65. Sugiyama, T., et al., *Rad52-mediated DNA annealing after Rad51-mediated DNA strand exchange promotes second ssDNA capture.* EMBO J, 2006. **25**(23): p. 5539-48.

66. Liu, Y., et al., *RAD51C is required for Holliday junction processing in mammalian cells.* Science, 2004. **303**(5655): p. 243-6.
67. Wu, L. and I.D. Hickson, *The Bloom's syndrome helicase suppresses crossing over during homologous recombination.* Nature, 2003. **426**(6968): p. 870-4.
68. Plank, J.L., J. Wu, and T.S. Hsieh, *Topoisomerase IIIalpha and Bloom's helicase can resolve a mobile double Holliday junction substrate through convergent branch migration.* Proc Natl Acad Sci U S A, 2006. **103**(30): p. 11118-23.
69. Wu, L., et al., *BLAP75/RMI1 promotes the BLM-dependent dissolution of homologous recombination intermediates.* Proc Natl Acad Sci U S A, 2006. **103**(11): p. 4068-73.
70. Lundblad, V. and E.H. Blackburn, *An alternative pathway for yeast telomere maintenance rescues est1- senescence.* Cell, 1993. **73**(2): p. 347-60.
71. Haber, J.E., *DNA recombination: the replication connection.* Trends Biochem Sci, 1999. **24**(7): p. 271-5.
72. Paques, F. and J.E. Haber, *Multiple pathways of recombination induced by double-strand breaks in Saccharomyces cerevisiae.* Microbiol Mol Biol Rev, 1999. **63**(2): p. 349-404.
73. Fishman-Lobell, J., N. Rudin, and J.E. Haber, *Two alternative pathways of double-strand break repair that are kinetically separable and independently modulated.* Mol Cell Biol, 1992. **12**(3): p. 1292-303.
74. Stark, J.M., et al., *Genetic steps of mammalian homologous repair with distinct mutagenic consequences.* Mol Cell Biol, 2004. **24**(21): p. 9305-16.
75. Ivanov, E.L., et al., *Genetic requirements for the single-strand annealing pathway of double-strand break repair in Saccharomyces cerevisiae.* Genetics, 1996. **142**(3): p. 693-704.
76. Sargent, R.G., et al., *Role of the nucleotide excision repair gene ERCC1 in formation of recombination-dependent rearrangements in mammalian cells.* Nucleic Acids Res, 2000. **28**(19): p. 3771-8.
77. Liang, F., et al., *Homology-directed repair is a major double-strand break repair pathway in mammalian cells.* Proc Natl Acad Sci U S A, 1998. **95**(9): p. 5172-7.
78. Gangloff, S., C. Soustelle, and F. Fabre, *Homologous recombination is responsible for cell death in the absence of the Sgs1 and Srs2 helicases.* Nat Genet, 2000. **25**(2): p. 192-4.
79. Pellicioli, A., et al., *Regulation of Saccharomyces Rad53 checkpoint kinase during adaptation from DNA damage-induced G2/M arrest.* Mol Cell, 2001. **7**(2): p. 293-300.
80. Branzei, D. and M. Foiani, *The checkpoint response to replication stress.* DNA Repair (Amst), 2009. **8**(9): p. 1038-46.
81. Esashi, F., et al., *CDK-dependent phosphorylation of BRCA2 as a regulatory mechanism for recombinational repair.* Nature, 2005. **434**(7033): p. 598-604.
82. Huertas, P. and S.P. Jackson, *Human CtIP mediates cell cycle control of DNA end resection and double strand break repair.* J Biol Chem, 2009. **284**(14): p. 9558-65.
83. Buis, J., et al., *Mre11 regulates CtIP-dependent double-strand break repair by interaction with CDK2.* Nat Struct Mol Biol, 2012. **19**(2): p. 246-52.
84. Frank-Vaillant, M. and S. Marcand, *Transient stability of DNA ends allows nonhomologous end joining to precede homologous recombination.* Mol Cell, 2002. **10**(5): p. 1189-99.
85. Symington, L.S. and J. Gautier, *Double-strand break end resection and repair pathway choice.* Annu Rev Genet, 2011. **45**: p. 247-71.
86. Yu, X. and J. Chen, *DNA damage-induced cell cycle checkpoint control requires CtIP, a phosphorylation-dependent binding partner of BRCA1 C-terminal domains.* Mol Cell Biol, 2004. **24**(21): p. 9478-86.
87. Chen, L., et al., *Cell cycle-dependent complex formation of BRCA1.CtIP.MRN is important for DNA double-strand break repair.* J Biol Chem, 2008. **283**(12): p. 7713-20.

88. You, Z., et al., *CtIP links DNA double-strand break sensing to resection.* Mol Cell, 2009. **36**(6): p. 954-69.
89. Kaidi, A., et al., *Human SIRT6 promotes DNA end resection through CtIP deacetylation.* Science, 2010. **329**(5997): p. 1348-53.
90. Garcia, V., et al., *Bidirectional resection of DNA double-strand breaks by Mre11 and Exo1.* Nature, 2011. **479**(7372): p. 241-4.
91. Neale, M.J., J. Pan, and S. Keeney, *Endonucleolytic processing of covalent protein-linked DNA double-strand breaks.* Nature, 2005. **436**(7053): p. 1053-7.
92. Langerak, P., et al., *Release of Ku and MRN from DNA ends by Mre11 nuclease activity and Ctp1 is required for homologous recombination repair of double-strand breaks.* PLoS Genet, 2011. **7**(9): p. e1002271.
93. Krejci, L., et al., *DNA helicase Srs2 disrupts the Rad51 presynaptic filament.* Nature, 2003. **423**(6937): p. 305-9.
94. Veaute, X., et al., *The Srs2 helicase prevents recombination by disrupting Rad51 nucleoprotein filaments.* Nature, 2003. **423**(6937): p. 309-12.
95. Krejci, L., et al., *Role of ATP hydrolysis in the antirecombinase function of Saccharomyces cerevisiae Srs2 protein.* J Biol Chem, 2004. **279**(22): p. 23193-9.
96. Colavito, S., et al., *Functional significance of the Rad51-Srs2 complex in Rad51 presynaptic filament disruption.* Nucleic Acids Res, 2009. **37**(20): p. 6754-64.
97. Seong, C., et al., *Regulation of Rad51 recombinase presynaptic filament assembly via interactions with the Rad52 mediator and the Srs2 anti-recombinase.* J Biol Chem, 2009. **284**(36): p. 24363-71.
98. Antony, E., et al., *Srs2 disassembles Rad51 filaments by a protein-protein interaction triggering ATP turnover and dissociation of Rad51 from DNA.* Mol Cell, 2009. **35**(1): p. 105-15.
99. Liu, J., et al., *Rad51 paralogues Rad55-Rad57 balance the antirecombinase Srs2 in Rad51 filament formation.* Nature, 2011. **479**(7372): p. 245-8.
100. Bugreev, D.V., et al., *Novel pro- and anti-recombination activities of the Bloom's syndrome helicase.* Genes Dev, 2007. **21**(23): p. 3085-94.
101. Sommers, J.A., et al., *FANCJ uses its motor ATPase to destabilize protein-DNA complexes, unwind triplexes, and inhibit RAD51 strand exchange.* J Biol Chem, 2009. **284**(12): p. 7505-17.
102. Adams, M.D., M. McVey, and J.J. Sekelsky, *Drosophila BLM in double-strand break repair by synthesis-dependent strand annealing.* Science, 2003. **299**(5604): p. 265-7.
103. McVey, M., et al., *Formation of deletions during double-strand break repair in Drosophila DmBlm mutants occurs after strand invasion.* Proc Natl Acad Sci U S A, 2004. **101**(44): p. 15694-9.
104. Gari, K., et al., *The Fanconi anemia protein FANCM can promote branch migration of Holliday junctions and replication forks.* Mol Cell, 2008. **29**(1): p. 141-8.
105. Wood, J.L. and J. Chen, *DNA-damage checkpoints: location, location, location.* Trends Cell Biol, 2008. **18**(10): p. 451-5.
106. Hakem, R., *DNA-damage repair; the good, the bad, and the ugly.* EMBO J, 2008. **27**(4): p. 589-605.
107. Hoeijmakers, J.H., *DNA damage, aging, and cancer.* N Engl J Med, 2009. **361**(15): p. 1475-85.
108. O'Driscoll, M. and P.A. Jeggo, *The role of double-strand break repair - insights from human genetics.* Nat Rev Genet, 2006. **7**(1): p. 45-54.
109. Bassing, C.H., et al., *Histone H2AX: a dosage-dependent suppressor of oncogenic translocations and tumors.* Cell, 2003. **114**(3): p. 359-70.
110. Celeste, A., et al., *H2AX haploinsufficiency modifies genomic stability and tumor susceptibility.* Cell, 2003. **114**(3): p. 371-83.
111. Carson, C.T., et al., *The Mre11 complex is required for ATM activation and the G2/M checkpoint.* EMBO J, 2003. **22**(24): p. 6610-20.

112. Uziel, T., et al., *Requirement of the MRN complex for ATM activation by DNA damage.* EMBO J, 2003. **22**(20): p. 5612-21.
113. Rogakou, E.P., et al., *DNA double-stranded breaks induce histone H2AX phosphorylation on serine 139.* J Biol Chem, 1998. **273**(10): p. 5858-68.
114. Celeste, A., et al., *Genomic instability in mice lacking histone H2AX.* Science, 2002. **296**(5569): p. 922-7.
115. Lou, Z., et al., *MDC1 maintains genomic stability by participating in the amplification of ATM-dependent DNA damage signals.* Mol Cell, 2006. **21**(2): p. 187-200.
116. Stucki, M., et al., *MDC1 directly binds phosphorylated histone H2AX to regulate cellular responses to DNA double-strand breaks.* Cell, 2005. **123**(7): p. 1213-26.
117. Stewart, G.S., et al., *MDC1 is a mediator of the mammalian DNA damage checkpoint.* Nature, 2003. **421**(6926): p. 961-966.
118. Lukas, C., et al., *Mdc1 couples DNA double-strand break recognition by Nbs1 with its H2AX-dependent chromatin retention.* EMBO J, 2004. **23**(13): p. 2674-83.
119. Huen, M.S., et al., *RNF8 transduces the DNA-damage signal via histone ubiquitylation and checkpoint protein assembly.* Cell, 2007. **131**(5): p. 901-14.
120. Kolas, N.K., et al., *Orchestration of the DNA-damage response by the RNF8 ubiquitin ligase.* Science, 2007. **318**(5856): p. 1637-40.
121. Mailand, N., et al., *RNF8 ubiquitylates histones at DNA double-strand breaks and promotes assembly of repair proteins.* Cell, 2007. **131**(5): p. 887-900.
122. Wang, B. and S.J. Elledge, *Ubc13/Rnf8 ubiquitin ligases control foci formation of the Rap80/Abraxas/Brca1/Brcc36 complex in response to DNA damage.* Proc Natl Acad Sci U S A, 2007. **104**(52): p. 20759-63.
123. Mattiroli, F., et al., *RNF168 ubiquitinates K13-15 on H2A/H2AX to drive DNA damage signaling.* Cell, 2012. **150**(6): p. 1182-95.
124. Doil, C., et al., *RNF168 binds and amplifies ubiquitin conjugates on damaged chromosomes to allow accumulation of repair proteins.* Cell, 2009. **136**(3): p. 435-46.
125. Pinato, S., et al., *RNF168, a new RING finger, MIU-containing protein that modifies chromatin by ubiquitination of histones H2A and H2AX.* BMC Mol Biol, 2009. **10**: p. 55.
126. Stewart, G.S., et al., *The RIDDLE syndrome protein mediates a ubiquitin-dependent signaling cascade at sites of DNA damage.* Cell, 2009. **136**(3): p. 420-34.
127. Noon, A.T., et al., *53BP1-dependent robust localized KAP-1 phosphorylation is essential for heterochromatic DNA double-strand break repair.* Nat Cell Biol. **12**(2): p. 177-84.
128. Sobhian, B., et al., *RAP80 targets BRCA1 to specific ubiquitin structures at DNA damage sites.* Science, 2007. **316**(5828): p. 1198-202.
129. Feng, L., J. Huang, and J. Chen, *MERIT40 facilitates BRCA1 localization and DNA damage repair.* Genes Dev, 2009. **23**(6): p. 719-28.
130. Kim, H., J. Chen, and X. Yu, *Ubiquitin-binding protein RAP80 mediates BRCA1-dependent DNA damage response.* Science, 2007. **316**(5828): p. 1202-5.
131. Shao, G., et al., *MERIT40 controls BRCA1-Rap80 complex integrity and recruitment to DNA double-strand breaks.* Genes Dev, 2009. **23**(6): p. 740-54.
132. Wang, B., et al., *NBA1, a new player in the Brca1 A complex, is required for DNA damage resistance and checkpoint control.* Genes Dev, 2009. **23**(6): p. 729-39.
133. Wang, B., et al., *Abraxas and RAP80 form a BRCA1 protein complex required for the DNA damage response.* Science, 2007. **316**(5828): p. 1194-8.
134. Xu, B., S. Kim, and M.B. Kastan, *Involvement of Brca1 in S-phase and G(2)-phase checkpoints after ionizing irradiation.* Mol Cell Biol, 2001. **21**(10): p. 3445-50.

135. Xu, B., et al., *Phosphorylation of serine 1387 in Brca1 is specifically required for the Atm-mediated S-phase checkpoint after ionizing irradiation.* Cancer Res, 2002. **62**(16): p. 4588-91.
136. Panier, S. and D. Durocher, *Regulatory ubiquitylation in response to DNA double-strand breaks.* DNA Repair (Amst), 2009. **8**(4): p. 436-43.
137. Wang, B., et al., *53BP1, a mediator of the DNA damage checkpoint.* Science, 2002. **298**(5597): p. 1435-8.
138. Evers, B. and J. Jonkers, *Mouse models of BRCA1 and BRCA2 deficiency: past lessons, current understanding and future prospects.* Oncogene, 2006. **25**(43): p. 5885-97.
139. Xu, X., et al., *Genetic interactions between tumor suppressors Brca1 and p53 in apoptosis, cell cycle and tumorigenesis.* Nat Genet, 2001. **28**(3): p. 266-71.
140. Bouwman, P., et al., *53BP1 loss rescues BRCA1 deficiency and is associated with triple-negative and BRCA-mutated breast cancers.* Nat Struct Mol Biol. **17**(6): p. 688-95.
141. Gelato, K.A. and W. Fischle, *Role of histone modifications in defining chromatin structure and function.* Biol Chem, 2008. **389**(4): p. 353-63.
142. Groth, A., et al., *Chromatin challenges during DNA replication and repair.* Cell, 2007. **128**(4): p. 721-33.
143. Li, B., M. Carey, and J.L. Workman, *The role of chromatin during transcription.* Cell, 2007. **128**(4): p. 707-19.
144. Costelloe, T., et al., *Chromatin modulation and the DNA damage response.* Exp Cell Res, 2006. **312**(14): p. 2677-86.
145. Ciehanover, A., Y. Hod, and A. Hershko, *A heat-stable polypeptide component of an ATP-dependent proteolytic system from reticulocytes.* Biochem Biophys Res Commun, 1978. **81**(4): p. 1100-5.
146. Hershko, A. and A. Ciechanover, *The ubiquitin system.* Annu Rev Biochem, 1998. **67**: p. 425-79.
147. Xu, P., et al., *Quantitative proteomics reveals the function of unconventional ubiquitin chains in proteasomal degradation.* Cell, 2009. **137**(1): p. 133-45.
148. Ikeda, F. and I. Dikic, *Atypical ubiquitin chains: new molecular signals. 'Protein Modifications: Beyond the Usual Suspects' review series.* EMBO Rep, 2008. **9**(6): p. 536-42.
149. Chen, Z.J. and L.J. Sun, *Nonproteolytic functions of ubiquitin in cell signaling.* Mol Cell, 2009. **33**(3): p. 275-86.
150. Komander, D., et al., *Molecular discrimination of structurally equivalent Lys 63-linked and linear polyubiquitin chains.* EMBO Rep, 2009. **10**(5): p. 466-73.
151. Kulathu, Y., et al., *Two-sided ubiquitin binding explains specificity of the TAB2 NZF domain.* Nat Struct Mol Biol, 2009. **16**(12): p. 1328-30.
152. Sato, Y., et al., *Structural basis for specific recognition of Lys 63-linked polyubiquitin chains by tandem UIMs of RAP80.* EMBO J, 2009. **28**(16): p. 2461-8.
153. Wilkinson, K.D., M.K. Urban, and A.L. Haas, *Ubiquitin is the ATP-dependent proteolysis factor I of rabbit reticulocytes.* J Biol Chem, 1980. **255**(16): p. 7529-32.
154. Ciechanover, A., et al., *Activation of the heat-stable polypeptide of the ATP-dependent proteolytic system.* Proc Natl Acad Sci U S A, 1981. **78**(2): p. 761-5.
155. Haas, A.L. and I.A. Rose, *The mechanism of ubiquitin activating enzyme. A kinetic and equilibrium analysis.* J Biol Chem, 1982. **257**(17): p. 10329-37.
156. Haas, A.L., et al., *Ubiquitin-activating enzyme. Mechanism and role in protein-ubiquitin conjugation.* J Biol Chem, 1982. **257**(5): p. 2543-8.
157. Ciechanover, A., *The ubiquitin-mediated system for intracellular protein degradation.* J Basic Clin Physiol Pharmacol, 1991. **2**(3): p. 141-59.
158. Li, W., et al., *Genome-wide and functional annotation of human E3 ubiquitin ligases identifies MULAN, a mitochondrial E3 that regulates the organelle's dynamics and signaling.* PLoS One, 2008. **3**(1): p. e1487.

159. Rotin, D. and S. Kumar, *Physiological functions of the HECT family of ubiquitin ligases.* Nat Rev Mol Cell Biol, 2009. **10**(6): p. 398-409.
160. Pickart, C.M., *Ubiquitin enters the new millennium.* Mol Cell, 2001. **8**(3): p. 499-504.
161. Kussie, P.H., et al., *Structure of the MDM2 oncoprotein bound to the p53 tumor suppressor transactivation domain.* Science, 1996. **274**(5289): p. 948-53.
162. Hao, B., et al., *Structure of a Fbw7-Skp1-cyclin E complex: multisite-phosphorylated substrate recognition by SCF ubiquitin ligases.* Mol Cell, 2007. **26**(1): p. 131-43.
163. Liu, J. and R. Nussinov, *The mechanism of ubiquitination in the cullin-RING E3 ligase machinery: conformational control of substrate orientation.* PLoS Comput Biol, 2009. **5**(10): p. e1000527.
164. Bergink, S. and S. Jentsch, *Principles of ubiquitin and SUMO modifications in DNA repair.* Nature, 2009. **458**(7237): p. 461-7.
165. Bekker-Jensen, S. and N. Mailand, *Assembly and function of DNA double-strand break repair foci in mammalian cells.* DNA Repair (Amst), 2010. **9**(12): p. 1219-28.
166. Zhao, G.Y., et al., *A critical role for the ubiquitin-conjugating enzyme Ubc13 in initiating homologous recombination.* Mol Cell, 2007. **25**(5): p. 663-75.
167. Watanabe, K., et al., *RAD18 promotes DNA double-strand break repair during G1 phase through chromatin retention of 53BP1.* Nucleic Acids Res, 2009. **37**(7): p. 2176-93.
168. Bekker-Jensen, S., et al., *HERC2 coordinates ubiquitin-dependent assembly of DNA repair factors on damaged chromosomes.* Nat Cell Biol, 2010. **12**(1): p. 80-6; sup pp 1-12.
169. Hashizume, R., et al., *The RING heterodimer BRCA1-BARD1 is a ubiquitin ligase inactivated by a breast cancer-derived mutation.* J Biol Chem, 2001. **276**(18): p. 14537-40.
170. Brzovic, P.S., et al., *Binding and recognition in the assembly of an active BRCA1/BARD1 ubiquitin-ligase complex.* Proc Natl Acad Sci U S A, 2003. **100**(10): p. 5646-51.
171. Ruffner, H., et al., *Cancer-predisposing mutations within the RING domain of BRCA1: loss of ubiquitin protein ligase activity and protection from radiation hypersensitivity.* Proc Natl Acad Sci U S A, 2001. **98**(9): p. 5134-9.
172. Reid, L.J., et al., *E3 ligase activity of BRCA1 is not essential for mammalian cell viability or homology-directed repair of double-strand DNA breaks.* Proc Natl Acad Sci U S A, 2008. **105**(52): p. 20876-81.
173. Seki, N., et al., *Isolation, tissue expression, and chromosomal assignment of a novel human gene which encodes a protein with RING finger motif.* J Hum Genet, 1998. **43**(4): p. 272-4.
174. Durocher, D. and S.P. Jackson, *The FHA domain.* FEBS Lett, 2002. **513**(1): p. 58-66.
175. Plans, V., et al., *The RING finger protein RNF8 recruits UBC13 for lysine 63-based self polyubiquitylation.* J Cell Biochem, 2006. **97**(3): p. 572-82.
176. Noon, A.T., et al., *53BP1-dependent robust localized KAP-1 phosphorylation is essential for heterochromatic DNA double-strand break repair.* Nat Cell Biol, 2010. **12**(2): p. 177-84.
177. Oestergaard, V.H., et al., *RNF8 and RNF168 but not HERC2 are required for DNA damage-induced ubiquitylation in chicken DT40 cells.* DNA Repair (Amst), 2012. **11**(11): p. 892-905.
178. Li, L., et al., *Rnf8 deficiency impairs class switch recombination, spermatogenesis, and genomic integrity and predisposes for cancer.* J Exp Med, 2010. **207**(5): p. 983-97.
179. Santos, M.A., et al., *Class switching and meiotic defects in mice lacking the E3 ubiquitin ligase RNF8.* J Exp Med, 2010. **207**(5): p. 973-81.
180. Lu, L.Y., et al., *RNF8-dependent histone modifications regulate nucleosome removal during spermatogenesis.* Dev Cell, 2010. **18**(3): p. 371-84.

181. Polo, S.E. and S.P. Jackson, *Dynamics of DNA damage response proteins at DNA breaks: a focus on protein modifications.* Genes Dev, 2011. **25**(5): p. 409-33.
182. Hu, X., A. Paul, and B. Wang, *Rap80 protein recruitment to DNA double-strand breaks requires binding to both small ubiquitin-like modifier (SUMO) and ubiquitin conjugates.* J Biol Chem, 2012. **287**(30): p. 25510-9.
183. Futreal, P.A., et al., *BRCA1 mutations in primary breast and ovarian carcinomas.* Science, 1994. **266**(5182): p. 120-2.
184. Miki, Y., et al., *A strong candidate for the breast and ovarian cancer susceptibility gene BRCA1.* Science, 1994. **266**(5182): p. 66-71.
185. Venkitaraman, A.R., *Cancer susceptibility and the functions of BRCA1 and BRCA2.* Cell, 2002. **108**(2): p. 171-82.
186. Alberg, A.J. and K.J. Helzlsouer, *Epidemiology, prevention, and early detection of breast cancer.* Curr Opin Oncol, 1997. **9**(6): p. 505-11.
187. Staff, S., J. Isola, and M. Tanner, *Haplo-insufficiency of BRCA1 in sporadic breast cancer.* Cancer Res, 2003. **63**(16): p. 4978-83.
188. King, M.C., et al., *Breast and ovarian cancer risks due to inherited mutations in BRCA1 and BRCA2.* Science, 2003. **302**(5645): p. 643-6.
189. Hall, J.M., et al., *Linkage of early-onset familial breast cancer to chromosome 17q21.* Science, 1990. **250**(4988): p. 1684-9.
190. Lafarge, S. and M.H. Montane, *Characterization of Arabidopsis thaliana ortholog of the human breast cancer susceptibility gene 1: AtBRCA1, strongly induced by gamma rays.* Nucleic Acids Res, 2003. **31**(4): p. 1148-55.
191. Siaud, N., et al., *Brca2 is involved in meiosis in Arabidopsis thaliana as suggested by its interaction with Dmc1.* EMBO J, 2004. **23**(6): p. 1392-401.
192. Abe, K., et al., *Inefficient double-strand DNA break repair is associated with increased fasciation in Arabidopsis BRCA2 mutants.* J Exp Bot, 2009. **60**(9): p. 2751-61.
193. Koonin, E.V., S.F. Altschul, and P. Bork, *BRCA1 protein products ... Functional motifs.* Nat Genet, 1996. **13**(3): p. 266-8.
194. Wu, L.C., et al., *Identification of a RING protein that can interact in vivo with the BRCA1 gene product.* Nat Genet, 1996. **14**(4): p. 430-40.
195. Rodriguez, J.A. and B.R. Henderson, *Identification of a functional nuclear export sequence in BRCA1.* J Biol Chem, 2000. **275**(49): p. 38589-96.
196. Deng, C.X. and S.G. Brodie, *Roles of BRCA1 and its interacting proteins.* Bioessays, 2000. **22**(8): p. 728-37.
197. Tutt, A. and A. Ashworth, *The relationship between the roles of BRCA genes in DNA repair and cancer predisposition.* Trends Mol Med, 2002. **8**(12): p. 571-6.
198. Meza, J.E., et al., *Mapping the functional domains of BRCA1. Interaction of the ring finger domains of BRCA1 and BARD1.* J Biol Chem, 1999. **274**(9): p. 5659-65.
199. Ayi, T.C., et al., *Conservation of function and primary structure in the BRCA1-associated RING domain (BARD1) protein.* Oncogene, 1998. **17**(16): p. 2143-8.
200. Moynahan, M.E., T.Y. Cui, and M. Jasin, *Homology-directed dna repair, mitomycin-c resistance, and chromosome stability is restored with correction of a Brca1 mutation.* Cancer Res, 2001. **61**(12): p. 4842-50.
201. Shen, S.X., et al., *A targeted disruption of the murine Brca1 gene causes gamma-irradiation hypersensitivity and genetic instability.* Oncogene, 1998. **17**(24): p. 3115-24.
202. Xu, X., et al., *Centrosome amplification and a defective G2-M cell cycle checkpoint induce genetic instability in BRCA1 exon 11 isoform-deficient cells.* Mol Cell, 1999. **3**(3): p. 389-95.
203. Mankouri, H.W. and I.D. Hickson, *Understanding the roles of RecQ helicases in the maintenance of genome integrity and suppression of tumorigenesis.* Biochem Soc Trans, 2004. **32**(Pt 6): p. 957-8.
204. Kennedy, R.D. and A.D. D'Andrea, *The Fanconi Anemia/BRCA pathway: new faces in the crowd.* Genes Dev, 2005. **19**(24): p. 2925-40.

205. van Attikum, H. and S.M. Gasser, *Crosstalk between histone modifications during the DNA damage response.* Trends Cell Biol, 2009. **19**(5): p. 207-17.
206. Brzovic, P.S., et al., *Structure of a BRCA1-BARD1 heterodimeric RING-RING complex.* Nat Struct Biol, 2001. **8**(10): p. 833-7.
207. McCarthy, E.E., et al., *Loss of Bard1, the heterodimeric partner of the Brca1 tumor suppressor, results in early embryonic lethality and chromosomal instability.* Mol Cell Biol, 2003. **23**(14): p. 5056-63.
208. Scully, R., et al., *Dynamic changes of BRCA1 subnuclear location and phosphorylation state are initiated by DNA damage.* Cell, 1997. **90**(3): p. 425-35.
209. Joukov, V., et al., *Functional communication between endogenous BRCA1 and its partner, BARD1, during Xenopus laevis development.* Proc Natl Acad Sci U S A, 2001. **98**(21): p. 12078-83.
210. Deng, C.X., *Tumor formation in Brca1 conditional mutant mice.* Environ Mol Mutagen, 2002. **39**(2-3): p. 171-7.
211. Jasin, M., *Homologous repair of DNA damage and tumorigenesis: the BRCA connection.* Oncogene, 2002. **21**(58): p. 8981-93.
212. Thai, T.H., et al., *Mutations in the BRCA1-associated RING domain (BARD1) gene in primary breast, ovarian and uterine cancers.* Hum Mol Genet, 1998. **7**(2): p. 195-202.
213. De Brakeleer, S., et al., *Cancer predisposing missense and protein truncating BARD1 mutations in non-BRCA1 or BRCA2 breast cancer families.* Hum Mutat, 2010. **31**(3): p. E1175-85.
214. Ratajska, M., et al., *Cancer predisposing BARD1 mutations in breast-ovarian cancer families.* Breast Cancer Res Treat, 2012. **131**(1): p. 89-97.
215. Scully, R., et al., *Association of BRCA1 with Rad51 in mitotic and meiotic cells.* Cell, 1997. **88**(2): p. 265-75.
216. Huber, L.J., et al., *Impaired DNA damage response in cells expressing an exon 11-deleted murine Brca1 variant that localizes to nuclear foci.* Mol Cell Biol, 2001. **21**(12): p. 4005-15.
217. Moynahan, M.E., et al., *Brca1 controls homology-directed DNA repair.* Mol Cell, 1999. **4**(4): p. 511-8.
218. Scully, R., et al., *Genetic analysis of BRCA1 function in a defined tumor cell line.* Mol Cell, 1999. **4**(6): p. 1093-9.
219. Farmer, H., et al., *Targeting the DNA repair defect in BRCA mutant cells as a therapeutic strategy.* Nature, 2005. **434**(7035): p. 917-21.
220. Burma, S., et al., *ATM phosphorylates histone H2AX in response to DNA double-strand breaks.* J Biol Chem, 2001. **276**(45): p. 42462-7.
221. Williams, R.S., et al., *Nbs1 flexibly tethers Ctp1 and Mre11-Rad50 to coordinate DNA double-strand break processing and repair.* Cell, 2009. **139**(1): p. 87-99.
222. Limbo, O., et al., *Ctp1 is a cell-cycle-regulated protein that functions with Mre11 complex to control double-strand break repair by homologous recombination.* Mol Cell, 2007. **28**(1): p. 134-46.
223. Bunting, S.F., et al., *53BP1 inhibits homologous recombination in Brca1-deficient cells by blocking resection of DNA breaks.* Cell, 2010. **141**(2): p. 243-54.
224. Hu, Y., et al., *RAP80-directed tuning of BRCA1 homologous recombination function at ionizing radiation-induced nuclear foci.* Genes Dev, 2011. **25**(7): p. 685-700.
225. Reczek, C.R., et al., *The interaction between CtIP and BRCA1 is not essential for resection-mediated DNA repair or tumor suppression.* J Cell Biol, 2013. **201**(5): p. 693-707.
226. Shinohara, A., H. Ogawa, and T. Ogawa, *Rad51 protein involved in repair and recombination in S. cerevisiae is a RecA-like protein.* Cell, 1992. **69**(3): p. 457-70.
227. Davies, A.A., et al., *Role of BRCA2 in control of the RAD51 recombination and DNA repair protein.* Mol Cell, 2001. **7**(2): p. 273-82.

228. Greenberg, R.A., et al., *Multifactorial contributions to an acute DNA damage response by BRCA1/BARD1-containing complexes.* Genes Dev, 2006. **20**(1): p. 34-46.
229. Sy, S.M., M.S. Huen, and J. Chen, *PALB2 is an integral component of the BRCA complex required for homologous recombination repair.* Proc Natl Acad Sci U S A, 2009. **106**(17): p. 7155-60.
230. Zhang, F., et al., *PALB2 links BRCA1 and BRCA2 in the DNA-damage response.* Curr Biol, 2009. **19**(6): p. 524-9.
231. Wei, L., et al., *Rapid recruitment of BRCA1 to DNA double-strand breaks is dependent on its association with Ku80.* Mol Cell Biol, 2008. **28**(24): p. 7380-93.
232. Coleman, K.A. and R.A. Greenberg, *The BRCA1-RAP80 complex regulates DNA repair mechanism utilization by restricting end resection.* J Biol Chem, 2011. **286**(15): p. 13669-80.
233. Chen, A., et al., *Autoubiquitination of the BRCA1*BARD1 RING ubiquitin ligase.* J Biol Chem, 2002. **277**(24): p. 22085-92.
234. Thakar, A., J. Parvin, and J. Zlatanova, *BRCA1/BARD1 E3 ubiquitin ligase can modify histones H2A and H2B in the nucleosome particle.* J Biomol Struct Dyn, 2010. **27**(4): p. 399-406.
235. Zhu, Q., et al., *BRCA1 tumour suppression occurs via heterochromatin-mediated silencing.* Nature, 2011. **477**(7363): p. 179-84.
236. Yu, X., et al., *BRCA1 ubiquitinates its phosphorylation-dependent binding partner CtIP.* Genes Dev, 2006. **20**(13): p. 1721-6.
237. Hartwell, L.H. and T.A. Weinert, *Checkpoints: controls that ensure the order of cell cycle events.* Science, 1989. **246**(4930): p. 629-34.
238. Hartwell, L.H. and M.B. Kastan, *Cell cycle control and cancer.* Science, 1994. **266**(5192): p. 1821-8.
239. Lobrich, M. and P.A. Jeggo, *The impact of a negligent G2/M checkpoint on genomic instability and cancer induction.* Nat Rev Cancer, 2007. **7**(11): p. 861-9.
240. Fabbro, M., et al., *BRCA1-BARD1 complexes are required for p53Ser-15 phosphorylation and a G1/S arrest following ionizing radiation-induced DNA damage.* J Biol Chem, 2004. **279**(30): p. 31251-8.
241. Kuerbitz, S.J., et al., *Wild-type p53 is a cell cycle checkpoint determinant following irradiation.* Proc Natl Acad Sci U S A, 1992. **89**(16): p. 7491-5.
242. Dulic, V., et al., *p53-dependent inhibition of cyclin-dependent kinase activities in human fibroblasts during radiation-induced G1 arrest.* Cell, 1994. **76**(6): p. 1013-23.
243. Reed, S.I., et al., *G1 control in mammalian cells.* J Cell Sci Suppl, 1994. **18**: p. 69-73.
244. Thompson, M.E., et al., *Decreased expression of BRCA1 accelerates growth and is often present during sporadic breast cancer progression.* Nat Genet, 1995. **9**(4): p. 444-50.
245. Aprelikova, O.N., et al., *BRCA1-associated growth arrest is RB-dependent.* Proc Natl Acad Sci U S A, 1999. **96**(21): p. 11866-71.
246. Larner, J.M., H. Lee, and J.L. Hamlin, *S phase damage sensing checkpoints in mammalian cells.* Cancer Surv, 1997. **29**: p. 25-45.
247. Painter, R.B., *Radioresistant DNA synthesis: an intrinsic feature of ataxia telangiectasia.* Mutat Res, 1981. **84**(1): p. 183-90.
248. Lim, D.S., et al., *ATM phosphorylates p95/nbs1 in an S-phase checkpoint pathway.* Nature, 2000. **404**(6778): p. 613-7.
249. Falck, J., et al., *The ATM-Chk2-Cdc25A checkpoint pathway guards against radioresistant DNA synthesis.* Nature, 2001. **410**(6830): p. 842-7.
250. Yazdi, P.T., et al., *SMC1 is a downstream effector in the ATM/NBS1 branch of the human S-phase checkpoint.* Genes Dev, 2002. **16**(5): p. 571-82.
251. Zhao, H., J.L. Watkins, and H. Piwnica-Worms, *Disruption of the checkpoint kinase 1/cell division cycle 25A pathway abrogates ionizing radiation-induced S and G2 checkpoints.* Proc Natl Acad Sci U S A, 2002. **99**(23): p. 14795-800.

252. Yarden, R.I., et al., *BRCA1 regulates the G2/M checkpoint by activating Chk1 kinase upon DNA damage.* Nat Genet, 2002. **30**(3): p. 285-9.
253. O'Connell, M.J., et al., *Chk1 is a wee1 kinase in the G2 DNA damage checkpoint inhibiting cdc2 by Y15 phosphorylation.* EMBO J, 1997. **16**(3): p. 545-54.
254. Rhind, N., B. Furnari, and P. Russell, *Cdc2 tyrosine phosphorylation is required for the DNA damage checkpoint in fission yeast.* Genes Dev, 1997. **11**(4): p. 504-11.
255. O'Connell, M.J., N.C. Walworth, and A.M. Carr, *The G2-phase DNA-damage checkpoint.* Trends Cell Biol, 2000. **10**(7): p. 296-303.
256. Cuddihy, A.R. and M.J. O'Connell, *Cell-cycle responses to DNA damage in G2.* Int Rev Cytol, 2003. **222**: p. 99-140.
257. Monteiro, A.N., A. August, and H. Hanafusa, *Evidence for a transcriptional activation function of BRCA1 C-terminal region.* Proc Natl Acad Sci U S A, 1996. **93**(24): p. 13595-9.
258. Humphrey, J.S., et al., *Human BRCA1 inhibits growth in yeast: potential use in diagnostic testing.* Proc Natl Acad Sci U S A, 1997. **94**(11): p. 5820-5.
259. Anderson, S.F., et al., *BRCA1 protein is linked to the RNA polymerase II holoenzyme complex via RNA helicase A.* Nat Genet, 1998. **19**(3): p. 254-6.
260. Scully, R., et al., *BRCA1 is a component of the RNA polymerase II holoenzyme.* Proc Natl Acad Sci U S A, 1997. **94**(11): p. 5605-10.
261. Moisan, A., et al., *BRCA1 can modulate RNA polymerase II carboxy-terminal domain phosphorylation levels.* Mol Cell Biol, 2004. **24**(16): p. 6947-56.
262. Chen, G.C., et al., *Rb-associated protein 46 (RbAp46) inhibits transcriptional transactivation mediated by BRCA1.* Biochem Biophys Res Commun, 2001. **284**(2): p. 507-14.
263. Fan, S., et al., *BRCA1 inhibition of estrogen receptor signaling in transfected cells.* Science, 1999. **284**(5418): p. 1354-6.
264. Ouchi, T., et al., *Collaboration of signal transducer and activator of transcription 1 (STAT1) and BRCA1 in differential regulation of IFN-gamma target genes.* Proc Natl Acad Sci U S A, 2000. **97**(10): p. 5208-13.
265. Zhang, H., et al., *BRCA1 physically associates with p53 and stimulates its transcriptional activity.* Oncogene, 1998. **16**(13): p. 1713-21.
266. Laufer, M., et al., *Structural requirements for the BARD1 tumor suppressor in chromosomal stability and homology-directed DNA repair.* J Biol Chem, 2007. **282**(47): p. 34325-33.
267. Kleiman, F.E. and J.L. Manley, *The BARD1-CstF-50 interaction links mRNA 3' end formation to DNA damage and tumor suppression.* Cell, 2001. **104**(5): p. 743-53.
268. Baer, R. and T. Ludwig, *The BRCA1/BARD1 heterodimer, a tumor suppressor complex with ubiquitin E3 ligase activity.* Curr Opin Genet Dev, 2002. **12**(1): p. 86-91.
269. Westermark, U.K., et al., *BARD1 participates with BRCA1 in homology-directed repair of chromosome breaks.* Mol Cell Biol, 2003. **23**(21): p. 7926-36.
270. Bryant, H.E., et al., *Specific killing of BRCA2-deficient tumours with inhibitors of poly(ADP-ribose) polymerase.* Nature, 2005. **434**(7035): p. 913-7.
271. McCabe, N., et al., *BRCA2-deficient CAPAN-1 cells are extremely sensitive to the inhibition of Poly (ADP-Ribose) polymerase: an issue of potency.* Cancer Biol Ther, 2005. **4**(9): p. 934-6.
272. Shaheen, M., et al., *Synthetic lethality: exploiting the addiction of cancer to DNA repair.* Blood, 2011. **117**(23): p. 6074-82.
273. Banerjee, S., S.B. Kaye, and A. Ashworth, *Making the best of PARP inhibitors in ovarian cancer.* Nat Rev Clin Oncol, 2010. **7**(9): p. 508-19.
274. D'Amours, D., et al., *Poly(ADP-ribosyl)ation reactions in the regulation of nuclear functions.* Biochem J, 1999. **342 (Pt 2)**: p. 249-68.

275. Hassa, P.O. and M.O. Hottiger, *The diverse biological roles of mammalian PARPS, a small but powerful family of poly-ADP-ribose polymerases.* Front Biosci, 2008. **13**: p. 3046-82.
276. Min, W. and Z.Q. Wang, *Poly (ADP-ribose) glycohydrolase (PARG) and its therapeutic potential.* Front Biosci (Landmark Ed), 2009. **14**: p. 1619-26.
277. de Murcia, G., et al., *Structure and function of poly(ADP-ribose) polymerase.* Mol Cell Biochem, 1994. **138**(1-2): p. 15-24.
278. El-Khamisy, S.F., et al., *A requirement for PARP-1 for the assembly or stability of XRCC1 nuclear foci at sites of oxidative DNA damage.* Nucleic Acids Res, 2003. **31**(19): p. 5526-33.
279. Ariumi, Y., et al., *Suppression of the poly(ADP-ribose) polymerase activity by DNA-dependent protein kinase in vitro.* Oncogene, 1999. **18**(32): p. 4616-25.
280. Galande, S. and T. Kohwi-Shigematsu, *Poly(ADP-ribose) polymerase and Ku autoantigen form a complex and synergistically bind to matrix attachment sequences.* J Biol Chem, 1999. **274**(29): p. 20521-8.
281. Haince, J.F., et al., *Ataxia telangiectasia mutated (ATM) signaling network is modulated by a novel poly(ADP-ribose)-dependent pathway in the early response to DNA-damaging agents.* J Biol Chem, 2007. **282**(22): p. 16441-53.
282. Haince, J.F., et al., *PARP1-dependent kinetics of recruitment of MRE11 and NBS1 proteins to multiple DNA damage sites.* J Biol Chem, 2008. **283**(2): p. 1197-208.
283. de Murcia, J.M., et al., *Requirement of poly(ADP-ribose) polymerase in recovery from DNA damage in mice and in cells.* Proc Natl Acad Sci U S A, 1997. **94**(14): p. 7303-7.
284. Meyer, R., et al., *Negative regulation of alkylation-induced sister-chromatid exchange by poly(ADP-ribose) polymerase-1 activity.* Int J Cancer, 2000. **88**(3): p. 351-5.
285. Bryant, H.E., et al., *PARP is activated at stalled forks to mediate Mre11-dependent replication restart and recombination.* EMBO J, 2009. **28**(17): p. 2601-15.
286. Ali, A.A., et al., *The zinc-finger domains of PARP1 cooperate to recognize DNA strand breaks.* Nat Struct Mol Biol, 2012. **19**(7): p. 685-92.
287. Li, M. and X. Yu, *Function of BRCA1 in the DNA damage response is mediated by ADP-ribosylation.* Cancer Cell, 2013. **23**(5): p. 693-704.
288. Chou, D.M., et al., *A chromatin localization screen reveals poly (ADP ribose)-regulated recruitment of the repressive polycomb and NuRD complexes to sites of DNA damage.* Proc Natl Acad Sci U S A, 2010. **107**(43): p. 18475-80.
289. Bork, P., et al., *A superfamily of conserved domains in DNA damage-responsive cell cycle checkpoint proteins.* FASEB J, 1997. **11**(1): p. 68-76.
290. Callebaut, I. and J.P. Mornon, *From BRCA1 to RAP1: a widespread BRCT module closely associated with DNA repair.* FEBS Lett, 1997. **400**(1): p. 25-30.
291. Glover, J.N., R.S. Williams, and M.S. Lee, *Interactions between BRCT repeats and phosphoproteins: tangled up in two.* Trends Biochem Sci, 2004. **29**(11): p. 579-85.
292. di Masi, A. and A. Antoccia, *NBS1 Heterozygosity and Cancer Risk.* Curr Genomics, 2008. **9**(4): p. 275-81.
293. Gullotta, F., et al., *Targeting the DNA double strand breaks repair for cancer therapy.* Curr Med Chem, 2010. **17**(19): p. 2017-48.
294. Cantor, S.B., et al., *BACH1, a novel helicase-like protein, interacts directly with BRCA1 and contributes to its DNA repair function.* Cell, 2001. **105**(1): p. 149-60.
295. Goldberg, M., et al., *MDC1 is required for the intra-S-phase DNA damage checkpoint.* Nature, 2003. **421**(6926): p. 952-6.
296. Kim, J.E., D.D. Billadeau, and J. Chen, *The tandem BRCT domains of Ect2 are required for both negative and positive regulation of Ect2 in cytokinesis.* J Biol Chem, 2005. **280**(7): p. 5733-9.

297. Dore, A.S., et al., *Structure of an Xrcc4-DNA ligase IV yeast ortholog complex reveals a novel BRCT interaction mode.* DNA Repair (Amst), 2006. **5**(3): p. 362-8.
298. Shakya, R., et al., *BRCA1 tumor suppression depends on BRCT phosphoprotein binding, but not its E3 ligase activity.* Science, 2011. **334**(6055): p. 525-8.
299. Zhang, X., et al., *Structure of an XRCC1 BRCT domain: a new protein-protein interaction module.* EMBO J, 1998. **17**(21): p. 6404-11.
300. Manke, I.A., et al., *BRCT repeats as phosphopeptide-binding modules involved in protein targeting.* Science, 2003. **302**(5645): p. 636-9.
301. Yu, X., et al., *The BRCT domain is a phospho-protein binding domain.* Science, 2003. **302**(5645): p. 639-42.
302. Kim, H., J. Huang, and J. Chen, *CCDC98 is a BRCA1-BRCT domain-binding protein involved in the DNA damage response.* Nat Struct Mol Biol, 2007. **14**(8): p. 710-5.
303. Liu, Z., J. Wu, and X. Yu, *CCDC98 targets BRCA1 to DNA damage sites.* Nat Struct Mol Biol, 2007. **14**(8): p. 716-20.
304. Leung, C.C. and J.N. Glover, *BRCT domains: easy as one, two, three.* Cell Cycle, 2011. **10**(15): p. 2461-70.
305. Rodriguez, M.C. and Z. Songyang, *BRCT domains: phosphopeptide binding and signaling modules.* Front Biosci, 2008. **13**: p. 5905-15.
306. Leung, C.C., et al., *Insights from the crystal structure of the sixth BRCT domain of topoisomerase IIbeta binding protein 1.* Protein Sci, 2010. **19**(1): p. 162-7.
307. Williams, R.S., R. Green, and J.N. Glover, *Crystal structure of the BRCT repeat region from the breast cancer-associated protein BRCA1.* Nat Struct Biol, 2001. **8**(10): p. 838-42.
308. Lee, M.S., et al., *Structure of the BRCT repeat domain of MDC1 and its specificity for the free COOH-terminal end of the gamma-H2AX histone tail.* J Biol Chem, 2005. **280**(37): p. 32053-6.
309. Edwards, R.A., et al., *The BARD1 C-terminal domain structure and interactions with polyadenylation factor CstF-50.* Biochemistry, 2008. **47**(44): p. 11446-56.
310. Kilkenny, M.L., et al., *Structural and functional analysis of the Crb2-BRCT2 domain reveals distinct roles in checkpoint signaling and DNA damage repair.* Genes Dev, 2008. **22**(15): p. 2034-47.
311. Birrane, G., et al., *Crystal structure of the BARD1 BRCT domains.* Biochemistry, 2007. **46**(26): p. 7706-12.
312. Wu, P.Y., et al., *Structural and functional interaction between the human DNA repair proteins DNA ligase IV and XRCC4.* Mol Cell Biol, 2009. **29**(11): p. 3163-72.
313. Lloyd, J., et al., *A supramodular FHA/BRCT-repeat architecture mediates Nbs1 adaptor function in response to DNA damage.* Cell, 2009. **139**(1): p. 100-11.
314. Clapperton, J.A., et al., *Structure and mechanism of BRCA1 BRCT domain recognition of phosphorylated BACH1 with implications for cancer.* Nat Struct Mol Biol, 2004. **11**(6): p. 512-8.
315. Shiozaki, E.N., et al., *Structure of the BRCT repeats of BRCA1 bound to a BACH1 phosphopeptide: implications for signaling.* Mol Cell, 2004. **14**(3): p. 405-12.
316. Campbell, S.J., R.A. Edwards, and J.N. Glover, *Comparison of the structures and peptide binding specificities of the BRCT domains of MDC1 and BRCA1.* Structure, 2010. **18**(2): p. 167-76.
317. Yamane, K. and T. Tsuruo, *Conserved BRCT regions of TopBP1 and of the tumor suppressor BRCA1 bind strand breaks and termini of DNA.* Oncogene, 1999. **18**(37): p. 5194-203.
318. Yamane, K., E. Katayama, and T. Tsuruo, *The BRCT regions of tumor suppressor BRCA1 and of XRCC1 show DNA end binding activity with a multimerizing feature.* Biochem Biophys Res Commun, 2000. **279**(2): p. 678-84.

319. Huyton, T., et al., *The BRCA1 C-terminal domain: structure and function.* Mutat Res, 2000. **460**(3-4): p. 319-32.
320. Joo, W.S., et al., *Structure of the 53BP1 BRCT region bound to p53 and its comparison to the Brca1 BRCT structure.* Genes Dev, 2002. **16**(5): p. 583-93.
321. Dever, S.M., et al., *Mutations in the BRCT binding site of BRCA1 result in hyper-recombination.* Aging (Albany NY), 2011. **3**(5): p. 515-32.
322. Hu, X., et al., *NBA1/MERIT40 and BRE interaction is required for the integrity of two distinct deubiquitinating enzyme BRCC36-containing complexes.* J Biol Chem, 2011. **286**(13): p. 11734-45.
323. Harper, J.W. and S.J. Elledge, *The DNA damage response: ten years after.* Mol Cell, 2007. **28**(5): p. 739-45.
324. Sun, L. and Z.J. Chen, *The novel functions of ubiquitination in signaling.* Curr Opin Cell Biol, 2004. **16**(2): p. 119-26.
325. Haglund, K. and I. Dikic, *Ubiquitylation and cell signaling.* EMBO J, 2005. **24**(19): p. 3353-9.
326. Love, K.R., et al., *Mechanisms, biology and inhibitors of deubiquitinating enzymes.* Nat Chem Biol, 2007. **3**(11): p. 697-705.
327. Song, L. and M. Rape, *Reverse the curse--the role of deubiquitination in cell cycle control.* Curr Opin Cell Biol, 2008. **20**(2): p. 156-63.
328. Ventii, K.H. and K.D. Wilkinson, *Protein partners of deubiquitinating enzymes.* Biochem J, 2008. **414**(2): p. 161-75.
329. Reyes-Turcu, F.E., K.H. Ventii, and K.D. Wilkinson, *Regulation and cellular roles of ubiquitin-specific deubiquitinating enzymes.* Annu Rev Biochem, 2009. **78**: p. 363-97.
330. Cooper, E.M., et al., *K63-specific deubiquitination by two JAMM/MPN+ complexes: BRISC-associated Brcc36 and proteasomal Poh1.* EMBO J, 2009. **28**(6): p. 621-31.
331. Litman, R., et al., *BACH1 is critical for homologous recombination and appears to be the Fanconi anemia gene product FANCJ.* Cancer Cell, 2005. **8**(3): p. 255-65.
332. Kumaraswamy, E. and R. Shiekhattar, *Activation of BRCA1/BRCA2-associated helicase BACH1 is required for timely progression through S phase.* Mol Cell Biol, 2007. **27**(19): p. 6733-41.
333. Gong, Z., et al., *BACH1/FANCJ acts with TopBP1 and participates early in DNA replication checkpoint control.* Mol Cell, 2010. **37**(3): p. 438-46.
334. Moldovan, G.L. and A.D. D'Andrea, *How the fanconi anemia pathway guards the genome.* Annu Rev Genet, 2009. **43**: p. 223-49.
335. Wang, W., *Emergence of a DNA-damage response network consisting of Fanconi anaemia and BRCA proteins.* Nat Rev Genet, 2007. **8**(10): p. 735-48.
336. Bridge, W.L., et al., *The BRIP1 helicase functions independently of BRCA1 in the Fanconi anemia pathway for DNA crosslink repair.* Nat Genet, 2005. **37**(9): p. 953-7.
337. Levitus, M., et al., *The DNA helicase BRIP1 is defective in Fanconi anemia complementation group J.* Nat Genet, 2005. **37**(9): p. 934-5.
338. Levran, O., et al., *The BRCA1-interacting helicase BRIP1 is deficient in Fanconi anemia.* Nat Genet, 2005. **37**(9): p. 931-3.
339. Cantor, S., et al., *The BRCA1-associated protein BACH1 is a DNA helicase targeted by clinically relevant inactivating mutations.* Proc Natl Acad Sci U S A, 2004. **101**(8): p. 2357-62.
340. Gupta, R., et al., *Analysis of the DNA substrate specificity of the human BACH1 helicase associated with breast cancer.* J Biol Chem, 2005. **280**(27): p. 25450-60.
341. Youds, J.L., et al., *DOG-1 is the Caenorhabditis elegans BRIP1/FANCJ homologue and functions in interstrand cross-link repair.* Mol Cell Biol, 2008. **28**(5): p. 1470-9.

342. Xie, J., et al., *Targeting the FANCJ-BRCA1 interaction promotes a switch from recombination to poleta-dependent bypass.* Oncogene, 2010. **29**(17): p. 2499-508.
343. Cantor, S.B. and S. Guillemette, *Hereditary breast cancer and the BRCA1-associated FANCJ/BACH1/BRIP1.* Future Oncol, 2011. **7**(2): p. 253-61.
344. Yun, M.H. and K. Hiom, *CtIP-BRCA1 modulates the choice of DNA double-strand-break repair pathway throughout the cell cycle.* Nature, 2009. **459**(7245): p. 460-3.
345. Nakamura, K., et al., *Collaborative action of Brca1 and CtIP in elimination of covalent modifications from double-strand breaks to facilitate subsequent break repair.* PLoS Genet, 2010. **6**(1): p. e1000828.
346. Rodriguez, M., et al., *Phosphopeptide binding specificities of BRCA1 COOH-terminal (BRCT) domains.* J Biol Chem, 2003. **278**(52): p. 52914-8.
347. Xia, Y., et al., *Enhancement of BRCA1 E3 ubiquitin ligase activity through direct interaction with the BARD1 protein.* J Biol Chem, 2003. **278**(7): p. 5255-63.
348. Sonoda, E., et al., *Reverse genetic studies of homologous DNA recombination using the chicken B-lymphocyte line, DT40.* Philos Trans R Soc Lond B Biol Sci, 2001. **356**(1405): p. 111-7.
349. Dhar, P.K., et al., *DNA repair studies: experimental evidence in support of chicken DT40 cell line as a unique model.* J Environ Pathol Toxicol Oncol, 2001. **20**(4): p. 273-83.
350. Pierce, A.J., et al., *XRCC3 promotes homology-directed repair of DNA damage in mammalian cells.* Genes Dev, 1999. **13**(20): p. 2633-8.
351. Fong, P.C., et al., *Inhibition of poly(ADP-ribose) polymerase in tumors from BRCA mutation carriers.* N Engl J Med, 2009. **361**(2): p. 123-34.
352. Rouleau, M., et al., *PARP inhibition: PARP1 and beyond.* Nat Rev Cancer, 2010. **10**(4): p. 293-301.
353. Wang, B., *BRCA1 tumor suppressor network: focusing on its tail.* Cell Biosci, 2012. **2**(1): p. 6.
354. Williams, R.S., et al., *Structural basis of phosphopeptide recognition by the BRCT domain of BRCA1.* Nat Struct Mol Biol, 2004. **11**(6): p. 519-25.
355. Jin, Y., et al., *Cell cycle-dependent colocalization of BARD1 and BRCA1 proteins in discrete nuclear domains.* Proc Natl Acad Sci U S A, 1997. **94**(22): p. 12075-80.
356. Rogakou, E.P., et al., *Megabase chromatin domains involved in DNA double-strand breaks in vivo.* J Cell Biol, 1999. **146**(5): p. 905-16.
357. Celeste, A., et al., *Histone H2AX phosphorylation is dispensable for the initial recognition of DNA breaks.* Nat Cell Biol, 2003. **5**(7): p. 675-9.
358. Lukas, C., et al., *Distinct spatiotemporal dynamics of mammalian checkpoint regulators induced by DNA damage.* Nat Cell Biol, 2003. **5**(3): p. 255-60.
359. Janicki, S.M., et al., *From silencing to gene expression: real-time analysis in single cells.* Cell, 2004. **116**(5): p. 683-98.
360. Shanbhag, N.M., et al., *ATM-dependent chromatin changes silence transcription in cis to DNA double-strand breaks.* Cell, 2010. **141**(6): p. 970-81.
361. Sugiyama, T., E.M. Zaitseva, and S.C. Kowalczykowski, *A single-stranded DNA-binding protein is needed for efficient presynaptic complex formation by the Saccharomyces cerevisiae Rad51 protein.* J Biol Chem, 1997. **272**(12): p. 7940-5.
362. Bhattacharyya, A., et al., *The breast cancer susceptibility gene BRCA1 is required for subnuclear assembly of Rad51 and survival following treatment with the DNA cross-linking agent cisplatin.* J Biol Chem, 2000. **275**(31): p. 23899-903.
363. Takizawa, Y., et al., *GEMIN2 promotes accumulation of RAD51 at double-strand breaks in homologous recombination.* Nucleic Acids Res, 2010. **38**(15): p. 5059-74.

364. Kleiman, F.E. and J.L. Manley, *Functional interaction of BRCA1-associated BARD1 with polyadenylation factor CstF-50.* Science, 1999. **285**(5433): p. 1576-9.
365. Dechend, R., et al., *The Bcl-3 oncoprotein acts as a bridging factor between NF-kappaB/Rel and nuclear co-regulators.* Oncogene, 1999. **18**(22): p. 3316-23.
366. Ge, Q., et al., *Molecular analysis of a major antigenic region of the 240-kD protein of Mi-2 autoantigen.* J Clin Invest, 1995. **96**(4): p. 1730-7.
367. Seelig, H.P., et al., *The major dermatomyositis-specific Mi-2 autoantigen is a presumed helicase involved in transcriptional activation.* Arthritis Rheum, 1995. **38**(10): p. 1389-99.
368. Brehm, A., et al., *dMi-2 and ISWI chromatin remodelling factors have distinct nucleosome binding and mobilization properties.* EMBO J, 2000. **19**(16): p. 4332-41.
369. Wang, H.B. and Y. Zhang, *Mi2, an auto-antigen for dermatomyositis, is an ATP-dependent nucleosome remodeling factor.* Nucleic Acids Res, 2001. **29**(12): p. 2517-21.
370. Mansfield, R.E., et al., *Plant homeodomain (PHD) fingers of CHD4 are histone H3-binding modules with preference for unmodified H3K4 and methylated H3K9.* J Biol Chem, 2011. **286**(13): p. 11779-91.
371. Polo, S.E., et al., *Regulation of DNA-damage responses and cell-cycle progression by the chromatin remodelling factor CHD4.* EMBO J, 2010. **29**(18): p. 3130-9.
372. Luijsterburg, M.S., et al., *A new non-catalytic role for ubiquitin ligase RNF8 in unfolding higher-order chromatin structure.* EMBO J, 2012. **31**(11): p. 2511-27.
373. Xue, Y., et al., *NURD, a novel complex with both ATP-dependent chromatin-remodeling and histone deacetylase activities.* Mol Cell, 1998. **2**(6): p. 851-61.
374. Li, D.Q., et al., *E3 ubiquitin ligase COP1 regulates the stability and functions of MTA1.* Proc Natl Acad Sci U S A, 2009. **106**(41): p. 17493-8.
375. Hall, J.R., et al., *Cdc6 stability is regulated by the Huwe1 ubiquitin ligase after DNA damage.* Mol Biol Cell, 2007. **18**(9): p. 3340-50.
376. Herold, S., et al., *Miz1 and HectH9 regulate the stability of the checkpoint protein, TopBP1.* EMBO J, 2008. **27**(21): p. 2851-61.
377. Parsons, J.L., et al., *Ubiquitin ligase ARF-BP1/Mule modulates base excision repair.* EMBO J, 2009. **28**(20): p. 3207-15.
378. Markkanen, E., et al., *Regulation of oxidative DNA damage repair by DNA polymerase lambda and MutYH by cross-talk of phosphorylation and ubiquitination.* Proc Natl Acad Sci U S A, 2012. **109**(2): p. 437-42.
379. Adhikary, S., et al., *The ubiquitin ligase HectH9 regulates transcriptional activation by Myc and is essential for tumor cell proliferation.* Cell, 2005. **123**(3): p. 409-21.
380. Galanty, Y., et al., *Mammalian SUMO E3-ligases PIAS1 and PIAS4 promote responses to DNA double-strand breaks.* Nature, 2009. **462**(7275): p. 935-9.
381. Kalocsay, M., N.J. Hiller, and S. Jentsch, *Chromosome-wide Rad51 spreading and SUMO-H2A.Z-dependent chromosome fixation in response to a persistent DNA double-strand break.* Mol Cell, 2009. **33**(3): p. 335-43.
382. Morris, J.R., et al., *The SUMO modification pathway is involved in the BRCA1 response to genotoxic stress.* Nature, 2009. **462**(7275): p. 886-90.
383. Nagai, S., N. Davoodi, and S.M. Gasser, *Nuclear organization in genome stability: SUMO connections.* Cell Res, 2011. **21**(3): p. 474-85.
384. Ulrich, H.D., *Ubiquitin and SUMO in DNA repair at a glance.* J Cell Sci, 2012. **125**(Pt 2): p. 249-54.
385. Jackson, S.P. and D. Durocher, *Regulation of DNA damage responses by ubiquitin and SUMO.* Mol Cell, 2013. **49**(5): p. 795-807.
386. Pinder, J.B., K.M. Attwood, and G. Dellaire, *Reading, writing, and repair: the role of ubiquitin and the ubiquitin-like proteins in DNA damage signaling and repair.* Front Genet, 2013. **4**: p. 45.

387. Yarden, R.I. and L.C. Brody, *BRCA1 interacts with components of the histone deacetylase complex.* Proc Natl Acad Sci U S A, 1999. **96**(9): p. 4983-8.
388. Shi, Y., et al., *Histone demethylation mediated by the nuclear amine oxidase homolog LSD1.* Cell, 2004. **119**(7): p. 941-53.
389. Forneris, F., et al., *Histone demethylation catalysed by LSD1 is a flavin-dependent oxidative process.* FEBS Lett, 2005. **579**(10): p. 2203-7.
390. Mosammaparast, N., et al., *The histone demethylase LSD1/KDM1A promotes the DNA damage response.* J Cell Biol, 2013. **203**(3): p. 457-70.
391. Larsen, D.H., et al., *The chromatin-remodeling factor CHD4 coordinates signaling and repair after DNA damage.* J Cell Biol, 2010. **190**(5): p. 731-40.
392. Bohgaki, T., et al., *Genomic instability, defective spermatogenesis, immunodeficiency, and cancer in a mouse model of the RIDDLE syndrome.* PLoS Genet, 2011. **7**(4): p. e1001381.
393. Saurin, A.J., et al., *Does this have a familiar RING?* Trends Biochem Sci, 1996. **21**(6): p. 208-14.
394. Mallery, D.L., C.J. Vandenberg, and K. Hiom, *Activation of the E3 ligase function of the BRCA1/BARD1 complex by polyubiquitin chains.* EMBO J, 2002. **21**(24): p. 6755-62.
395. Elderkin, S., et al., *A phosphorylated form of Mel-18 targets the Ring1B histone H2A ubiquitin ligase to chromatin.* Mol Cell, 2007. **28**(1): p. 107-20.
396. Marteijn, J.A., et al., *Nucleotide excision repair-induced H2A ubiquitination is dependent on MDC1 and RNF8 and reveals a universal DNA damage response.* J Cell Biol, 2009. **186**(6): p. 835-47.
397. Fabbro, M., et al., *BARD1 induces BRCA1 intranuclear foci formation by increasing RING-dependent BRCA1 nuclear import and inhibiting BRCA1 nuclear export.* J Biol Chem, 2002. **277**(24): p. 21315-24.
398. di Masi, A., et al., *Cancer predisposing mutations in BRCT domains.* IUBMB Life, 2011. **63**(7): p. 503-12.
399. Rouse, J. and S.P. Jackson, *Interfaces between the detection, signaling, and repair of DNA damage.* Science, 2002. **297**(5581): p. 547-51.
400. Bakkenist, C.J. and M.B. Kastan, *Initiating cellular stress responses.* Cell, 2004. **118**(1): p. 9-17.
401. Matsuoka, S., et al., *ATM and ATR substrate analysis reveals extensive protein networks responsive to DNA damage.* Science, 2007. **316**(5828): p. 1160-6.
402. Bensimon, A., et al., *ATM-dependent and -independent dynamics of the nuclear phosphoproteome after DNA damage.* Sci Signal, 2010. **3**(151): p. rs3.
403. Narod, S.A. and W.D. Foulkes, *BRCA1 and BRCA2: 1994 and beyond.* Nat Rev Cancer, 2004. **4**(9): p. 665-76.
404. Glover, J.N., *Insights into the molecular basis of human hereditary breast cancer from studies of the BRCA1 BRCT domain.* Fam Cancer, 2006. **5**(1): p. 89-93.
405. Seal, S., et al., *Truncating mutations in the Fanconi anemia J gene BRIP1 are low-penetrance breast cancer susceptibility alleles.* Nat Genet, 2006. **38**(11): p. 1239-41.
406. Niedernhofer, L.J., A.S. Lalai, and J.H. Hoeijmakers, *Fanconi anemia (cross)linked to DNA repair.* Cell, 2005. **123**(7): p. 1191-8.
407. Schlegel, B.P., F.M. Jodelka, and R. Nunez, *BRCA1 promotes induction of ssDNA by ionizing radiation.* Cancer Res, 2006. **66**(10): p. 5181-9.
408. Foray, N., et al., *Gamma-rays-induced death of human cells carrying mutations of BRCA1 or BRCA2.* Oncogene, 1999. **18**(51): p. 7334-42.
409. Lim, D.S. and P. Hasty, *A mutation in mouse rad51 results in an early embryonic lethal that is suppressed by a mutation in p53.* Mol Cell Biol, 1996. **16**(12): p. 7133-43.
410. Tsuzuki, T., et al., *Targeted disruption of the Rad51 gene leads to lethality in embryonic mice.* Proc Natl Acad Sci U S A, 1996. **93**(13): p. 6236-40.
411. Sonoda, E., et al., *Rad51-deficient vertebrate cells accumulate chromosomal breaks prior to cell death.* EMBO J, 1998. **17**(2): p. 598-608.

412. Burkle, A., *Physiology and pathophysiology of poly(ADP-ribosyl)ation.* Bioessays, 2001. **23**(9): p. 795-806.
413. Okano, S., et al., *Spatial and temporal cellular responses to single-strand breaks in human cells.* Mol Cell Biol, 2003. **23**(11): p. 3974-81.
414. Fisher, A.E., et al., *Poly(ADP-ribose) polymerase 1 accelerates single-strand break repair in concert with poly(ADP-ribose) glycohydrolase.* Mol Cell Biol, 2007. **27**(15): p. 5597-605.
415. Scully, R., et al., *Location of BRCA1 in human breast and ovarian cancer cells.* Science, 1996. **272**(5258): p. 123-6.
416. Chen, Y., et al., *BRCA1 is a 220-kDa nuclear phosphoprotein that is expressed and phosphorylated in a cell cycle-dependent manner.* Cancer Res, 1996. **56**(14): p. 3168-72.
417. Gudas, J.M., et al., *Cell cycle regulation of BRCA1 messenger RNA in human breast epithelial cells.* Cell Growth Differ, 1996. **7**(6): p. 717-23.
418. Rajan, J.V., et al., *Brca2 is coordinately regulated with Brca1 during proliferation and differentiation in mammary epithelial cells.* Proc Natl Acad Sci U S A, 1996. **93**(23): p. 13078-83.
419. Vaughn, J.P., et al., *BRCA1 expression is induced before DNA synthesis in both normal and tumor-derived breast cells.* Cell Growth Differ, 1996. **7**(6): p. 711-5.
420. Chen, J., et al., *Stable interaction between the products of the BRCA1 and BRCA2 tumor suppressor genes in mitotic and meiotic cells.* Mol Cell, 1998. **2**(3): p. 317-28.
421. Bao, Y., *Chromatin response to DNA double-strand break damage.* Epigenomics, 2011. **3**(3): p. 307-21.
422. Luijsterburg, M.S. and H. van Attikum, *Chromatin and the DNA damage response: the cancer connection.* Mol Oncol, 2011. **5**(4): p. 349-67.
423. Lukas, J., C. Lukas, and J. Bartek, *More than just a focus: The chromatin response to DNA damage and its role in genome integrity maintenance.* Nat Cell Biol, 2011. **13**(10): p. 1161-9.
424. Xu, Y. and B.D. Price, *Chromatin dynamics and the repair of DNA double strand breaks.* Cell Cycle, 2011. **10**(2): p. 261-7.
425. Miller, K.M. and S.P. Jackson, *Histone marks: repairing DNA breaks within the context of chromatin.* Biochem Soc Trans, 2012. **40**(2): p. 370-6.
426. Soria, G., S.E. Polo, and G. Almouzni, *Prime, repair, restore: the active role of chromatin in the DNA damage response.* Mol Cell, 2012. **46**(6): p. 722-34.
427. Denslow, S.A. and P.A. Wade, *The human Mi-2/NuRD complex and gene regulation.* Oncogene, 2007. **26**(37): p. 5433-8.
428. Wang, Y., et al., *LSD1 is a subunit of the NuRD complex and targets the metastasis programs in breast cancer.* Cell, 2009. **138**(4): p. 660-72.
429. Smeenk, G., et al., *The NuRD chromatin-remodeling complex regulates signaling and repair of DNA damage.* J Cell Biol, 2010. **190**(5): p. 741-9.
430. Pegoraro, G., et al., *Ageing-related chromatin defects through loss of the NURD complex.* Nat Cell Biol, 2009. **11**(10): p. 1261-7.
431. Toh, Y., S.D. Pencil, and G.L. Nicolson, *A novel candidate metastasis-associated gene, mta1, differentially expressed in highly metastatic mammary adenocarcinoma cell lines. cDNA cloning, expression, and protein analyses.* J Biol Chem, 1994. **269**(37): p. 22958-63.
432. Kumar, R., et al., *A naturally occurring MTA1 variant sequesters oestrogen receptor-alpha in the cytoplasm.* Nature, 2002. **418**(6898): p. 654-7.
433. Toh, Y. and G.L. Nicolson, *The role of the MTA family and their encoded proteins in human cancers: molecular functions and clinical implications.* Clin Exp Metastasis, 2009. **26**(3): p. 215-27.
434. Zhang, Y., et al., *Analysis of the NuRD subunits reveals a histone deacetylase core complex and a connection with DNA methylation.* Genes Dev, 1999. **13**(15): p. 1924-35.

435. van Haaften, G., et al., *Identification of conserved pathways of DNA-damage response and radiation protection by genome-wide RNAi.* Curr Biol, 2006. **16**(13): p. 1344-50.
436. Bhaskara, S., et al., *Histone deacetylases 1 and 2 maintain S-phase chromatin and DNA replication fork progression.* Epigenetics Chromatin, 2013. **6**(1): p. 27.
437. Miller, K.M., et al., *Human HDAC1 and HDAC2 function in the DNA-damage response to promote DNA nonhomologous end-joining.* Nat Struct Mol Biol, 2010. **17**(9): p. 1144-51.
438. Verreault, A., et al., *Nucleosomal DNA regulates the core-histone-binding subunit of the human Hat1 acetyltransferase.* Curr Biol, 1998. **8**(2): p. 96-108.
439. Verreault, A., et al., *Nucleosome assembly by a complex of CAF-1 and acetylated histones H3/H4.* Cell, 1996. **87**(1): p. 95-104.
440. FitzGerald, J.E., M. Grenon, and N.F. Lowndes, *53BP1: function and mechanisms of focal recruitment.* Biochem Soc Trans, 2009. **37**(Pt 4): p. 897-904.
441. Kovalenko, O.V., et al., *Mammalian ubiquitin-conjugating enzyme Ubc9 interacts with Rad51 recombination protein and localizes in synaptonemal complexes.* Proc Natl Acad Sci U S A, 1996. **93**(7): p. 2958-63.
442. Shen, Z., et al., *Associations of UBE2I with RAD52, UBL1, p53, and RAD51 proteins in a yeast two-hybrid system.* Genomics, 1996. **37**(2): p. 183-6.
443. Shen, Z., et al., *UBL1, a human ubiquitin-like protein associating with human RAD51/RAD52 proteins.* Genomics, 1996. **36**(2): p. 271-9.
444. Saitoh, H., M.D. Pizzi, and J. Wang, *Perturbation of SUMOlation enzyme Ubc9 by distinct domain within nucleoporin RanBP2/Nup358.* J Biol Chem, 2002. **277**(7): p. 4755-63.
445. Masson, M., et al., *Poly(ADP-ribose) polymerase interacts with a novel human ubiquitin conjugating enzyme: hUbc9.* Gene, 1997. **190**(2): p. 287-96.
446. Wyman, C. and R. Kanaar, *DNA double-strand break repair: all's well that ends well.* Annu Rev Genet, 2006. **40**: p. 363-83.
447. Bergink, S., et al., *DNA damage triggers nucleotide excision repair-dependent monoubiquitylation of histone H2A.* Genes Dev, 2006. **20**(10): p. 1343-52.
448. Ginjala, V., et al., *BMI1 is recruited to DNA breaks and contributes to DNA damage-induced H2A ubiquitination and repair.* Mol Cell Biol, 2011. **31**(10): p. 1972-82.
449. Pan, M.R., et al., *Monoubiquitination of H2AX protein regulates DNA damage response signaling.* J Biol Chem, 2011. **286**(32): p. 28599-607.
450. Wu, C.Y., et al., *Critical role of monoubiquitination of histone H2AX protein in histone H2AX phosphorylation and DNA damage response.* J Biol Chem, 2011. **286**(35): p. 30806-15.
451. Gatti, M., et al., *A novel ubiquitin mark at the N-terminal tail of histone H2As targeted by RNF168 ubiquitin ligase.* Cell Cycle, 2012. **11**(13): p. 2538-44.
452. Nakamura, K., et al., *Genetic dissection of vertebrate 53BP1: a major role in non-homologous end joining of DNA double strand breaks.* DNA Repair (Amst), 2006. **5**(6): p. 741-9.
453. Xie, A., et al., *Distinct roles of chromatin-associated proteins MDC1 and 53BP1 in mammalian double-strand break repair.* Mol Cell, 2007. **28**(6): p. 1045-57.
454. Difilippantonio, S., et al., *53BP1 facilitates long-range DNA end-joining during V(D)J recombination.* Nature, 2008. **456**(7221): p. 529-33.
455. Meerang, M., et al., *The ubiquitin-selective segregase VCP/p97 orchestrates the response to DNA double-strand breaks.* Nat Cell Biol, 2011. **13**(11): p. 1376-82.
456. Poulsen, M., et al., *Human RNF169 is a negative regulator of the ubiquitin-dependent response to DNA double-strand breaks.* J Cell Biol, 2012. **197**(2): p. 189-99.
457. Sanders, S.L., et al., *Methylation of histone H4 lysine 20 controls recruitment of Crb2 to sites of DNA damage.* Cell, 2004. **119**(5): p. 603-14.

458. Botuyan, M.V., et al., *Structural basis for the methylation state-specific recognition of histone H4-K20 by 53BP1 and Crb2 in DNA repair.* Cell, 2006. **127**(7): p. 1361-73.
459. Mallette, F.A., et al., *RNF8- and RNF168-dependent degradation of KDM4A/JMJD2A triggers 53BP1 recruitment to DNA damage sites.* EMBO J, 2012. **31**(8): p. 1865-78.

Appendix

All appendix documents can be found on a disc at the end of the thesis.

A complete list of the non-crosslinked Mass Spectrometry results can be found in PDFs in the appendix.

A complete list of the results of the crosslinked Mass Spectrometry can be found in the disc appendix at the rear of the thesis. The document is in a Scaffold format and it is called "Mass spec BARD1". in order to view this, a free version of Scaffold 3 must first be downloaded.

The appendix disc also contains supplementary microscopy images mentioned within the results chapters.